

**Cell-to-cell Communication Mechanisms:
Understanding and Targeting Pathways of Disease Pathogenesis
and Resistance in *Pseudomonas aeruginosa* Infections
and Human Prostate Cancer**

DISSERTATION

zur Erlangung des Grades
des Doktors der Naturwissenschaften
der Naturwissenschaftlich-Technischen Fakultäten
der Universität des Saarlandes

von

Antonio Gurdjieff Gomes de Mello Martins, M.Sc.

Saarbrücken

2017

Day of Colloquium: 09. October 2017
Dean: Prof. Dr. Guido Kickelbick
Chairman: Prof. Dr. Claus Jacob
Commission: Prof. Dr. Rolf W. Hartmann
Prof. Dr. Claus-Michael Lehr
Acad. Colleague: Dr. Stefan Böttcher

Die vorliegende Arbeit wurde von Februar 2014 bis Juli 2017 unter Anleitung von Herrn Univ.-Prof. Dr. Rolf W. Hartmann in der Fachrichtung Pharmazie der Naturwissenschaftlich-Technischen Fakultät der Universität des Saarlandes sowie am Helmholtz-Institut für Pharmazeutische Forschung Saarland (HIPS) – Department of Drug Design and Optimization angefertigt.

*to my wife, Tanja, and my mother
in memory of my father*

*“In the long history of humankind
those who learned to collaborate
and improvise most effectively
have prevailed”.*

– Charles Darwin

TABLE OF CONTENTS

1	Summary	VIII
2	Zusammenfassung	IX
3	Paper included in this Thesis	X
4	Contribution Report	XI
5	List of Abbreviations	XII
6	Introduction	1
6.1	Cell-to-cell Communication Mechanisms and Resistance to Treatment	1
6.2	<i>Pseudomonas aeruginosa</i> – An End to Traditional Antibiotics?	4
6.2.1	The Antivirulence Approach Against <i>Pseudomonas aeruginosa</i> Quorum Sensing	6
6.2.2	<i>Pseudomonas aeruginosa</i> <i>pqs</i> QS System and the Synthesis of HAQs	8
6.2.3	Silencing the <i>pqs</i> QS System with Quorum Sensing Inhibitors (QSIs).....	10
6.3	Steroid Cell-to-Cell Communication – The Complex Micro “Talk” of Multicellular Organisms	11
6.3.1	Endocrine Signalling of Androgens in the Human Prostate	12
6.3.2	Prostate Cancer and the Role of the AR in Disease.....	14
6.3.3	Disrupting Cancer Intercellular Communication and Resistance to Treatment ..	16
7	Aim of the Thesis	19
8	Results	20
8.1	Chapter 1 – Application of Dual Inhibition Concept within Looped Autoregulatory Systems toward Antivirulence Agents against <i>Pseudomonas aeruginosa</i> Infections	20
8.2	Chapter 2 – Effects of Next Generation PqsR-targeting Anti-infectives against Biofilm and Virulence of <i>Pseudomonas aeruginosa</i>	29
8.3	Chapter 3 – CYP17A1-independent Production of the Neurosteroid-derived 5 α -pregnan-3 β ,6 α -diol-20-one in Androgen-responsive Prostate Cancer Cell Lines under Serum Starvation and Inhibition by Abiraterone	51
9	Final Discussion	72
9.1	Biological Evaluation of PqsD and PqsR Dual-Inhibitor in <i>Pseudomonas aeruginosa</i>	72

9.1.1 Synergistic Effects of PqsD Inhibition and PqsR Antagonism in Virulence Factor Pyocyanin Production	72
9.1.2 The Favourable Pleiotropic Effects of a Dual-Inhibitor Compound in Targeting <i>pqs</i> QS Communication	74
9.1.2.1 <i>Effects on Virulence Factor (PCN) and Siderophore Production</i>	74
9.1.2.2 <i>Effects of QSIs on Biofilm Formation and Extracellular Polymeric Substance Constitution</i>	76
9.1.2.3 <i>Dual-Inhibition Efficacy in the <u>Galleria mellonella</u> Acute Infection Model</i>	78
9.1.3 Conclusion and Outlook – Synergistic Interference of <i>pqs</i> QS Communication System	79
9.2 Layering the Intercellular Communication of Prostate Cancer Cell Lines – Androgens and Beyond	80
9.2.1 Assessing Primordial Precursor Metabolism	81
9.2.1.1 <i>The Pregnenolone Precursor-Specific Metabolism in Prostate Carcinoma Cell Lines</i>	81
9.2.1.2 <i>Immunoassay-Based Quantification of Total Steroids</i>	82
9.2.2 Alternative Steroidogenic Pathways in AR-Driven Autocrine Signalling	83
9.2.3 The CYP17A1-Independent Hindrance of Steroidogenesis with Abiraterone	84
9.2.3.1 <i>Formation of Δ^4-Abi and 3β-HSD Inhibition on 5α,3β,6α-P Formation</i>	84
9.2.3.2 <i>Immunological Assays Hint at a Neuroendocrine Phenotype Transition of Prostate Epithelial Cells in a CYP17A1-Independent Microenvironment</i>	85
9.2.4 Conclusion and Outlook – Mis-Regulation of Steroid Signalling in Prostate Cancer	87
10 References	89
11 Appendix	XIV
11.1 Supporting Information	XIV
11.1.1 Chapter 1	XIV
11.1.2 Chapter 2	XXXIII
11.1.3 Chapter 3	LI
11.2 Conference Contributions	LVII
11.3 Curriculum Vitæ	LIX
12 Acknowledgments	LXI

1 SUMMARY

In disease, communication networks are responsible for phenotypic behaviours that may overcome immune responses and sustain unfavourable cellular developments, ultimately leading to treatment resistance. Innovative approaches and a broader understanding of these pathways are necessary to capitalize therapeutic strategies and increase therapy efficacy. In this work, I focus on the prospective clinical benefit of interfering with cell-to-cell signalling in *Pseudomonas* infections and prostate cancer. Potent signal receptor (PqsR) antagonists and first-in-class dual-inhibitor (also targeting signal synthase PqsD) potentiated favourable antivirulence outcomes within the cell density-dependent *Pseudomonas* quinolone signal (PQS) quorum sensing. Best compounds significantly reduced acute and chronic (biofilm) pathogenicity-related molecules and protected *G. mellonella* larvae without a selective pressure on growth. Timely antivirulence approach is a promising strategy with potential for lower therapy resistance development.

In mammals, misregulation of steroid signalling axes can lead to cancer initiation and metastases. Using diverse prostate carcinoma cell lines, we demonstrated the potential of androgen-responsive cells in generating mitogenic neurosteroid 5 α -pregnan-3 β ,6 α -diol-20-one in a CYP17-independent manner. Currently the central target for therapy, suppression of CYP17 activity also led to androgen precursor formation in a neuroendocrine fashion, untargeted by the current therapeutic armamentarium against the disease.

2 ZUSAMMENFASSUNG

Während des Verlaufs verschiedenster Krankheiten spielen molekulare Kommunikationsnetzwerke eine wichtige Rolle. Innovative Strategien und ein besseres Verständnis dieser Netzwerke sind notwendig, um neue therapeutische Ansätze zu entwickeln und die Effizienz bestehender Therapien zu verbessern. Diese Arbeit ist darauf fokussiert, gezielt in solche definierten Signalwege einzugreifen: in das Zell-Zell-Signalling bei Infektionen durch Pseudomonaden einerseits, und bei Prostata-Krebserkrankungen andererseits.

So zeigten potente Signalrezeptor (PqsR) - Antagonisten und die ersten dualen Hemmstoffe (die neben PqsR auch PqsD hemmen) vielversprechende anti-Virulenz Aktivitäten innerhalb eines von der Zelldichte abhängigen, sogenannten „*Pseudomonas* quinolone signal (PQS) quorum sensing“ Netzwerks. Die besten Verbindungen reduzierten die akuten und chronischen (Biofilm) mit der Pathogenität in Beziehung stehenden Moleküle signifikant. Zudem schützten diese Hemmstoffe *G. mellonella* - Larven, ohne auf diese einen Selektionsdruck auszuüben. Ein solcher anti-Virulenz-Ansatz ist eine vielversprechende Strategie mit dem Potential, die Resistenzentwicklung im Therapieverlauf zu minimieren.

In Säugern kann eine Fehlregulation der Steroid-Signalwege zu einer Krebsentstehung und Metastasen führen. Im Rahmen dieser Arbeit wurden diverse Prostata-Karzinom-Zellen untersucht. Hier konnte gezeigt werden, dass es möglich ist, dass Zellen, die auf Androgene ansprechen, das mitogene Neurosteroid 5 α -pregnan-3 β ,6 α -diol-20-one auf CYP17-unabhängige Weise bilden können. Eine Hemmung von CYP17, dem derzeit zentralen Therapie-Target, führte auch zu der Bildung von Androgen-Vorläufern auf eine neuroendokrine Art und Weise, was bei heutigen Therapieversuchen bislang nicht berücksichtigt wird.

3 PAPER INCLUDED IN THIS THESIS

This thesis is divided into three chapters. The first composed of the following publication:

Application of Dual Inhibition Concept within Looped Autoregulatory Systems toward Antivirulence Agents against *Pseudomonas aeruginosa* Infections

Andreas Thomann*, Antonio G. G. de Mello Martins*, Christian Brengel, Martin Empting, and Rolf W. Hartmann

ACS Chem Biol **2016**, 11(5):1279-86 – doi: 10.1021/acscchembio.6b00117.

* These authors contributed equally to this work.

4 CONTRIBUTION REPORT

The author would like to declare his contributions to the paper included in this thesis.

The author developed and performed *in vitro* and *in vivo* assays. *In vitro*, he measured growth curves of *P. aeruginosa*, pyocyanin and pyoverdine inhibition levels, and helped in the assessment of antibiotic rescue upon combination treatment. *In vivo*, he performed *G. mellonella* acute infection survival assay. He was involved in the conception, writing and reviewing of the manuscript.

5 LIST OF ABBREVIATIONS

2-AA	2-aminoacetophenone
2-ABA	2-aminobenzoylacetate
2-ABA-CoA	2-aminobenzoylacetate-CoA
5 α ,3 β ,6 α -P	5 α -pregnane-3 β ,6 α -diol-20-one
Abi	Abiraterone
ADT	Androgen deprivation therapy
AHL	<i>N</i> -Acyl-L-homoserine lactone
AI	Autoinducer
AKR	Aldo-keto reductase
Akt	Protein kinase B
AR	Androgen receptor
AR-V	Androgen receptor splice variant
ARE	Androgen response element
cAMP	Cyclic adenosine monophosphate
CNS	Central nervous system
CoA	Coenzyme A
CRPC	Castration-resistant prostate cancer
CV	Crystal violet
CYP	Cytochrome P450
D4A	Δ^4 -abiraterone
DHEA	Dehydroepiandrosterone
DHQ	Dihydroxyquinoline
DHT	Dihydrotestosterone
DSF	Diffusible Signal Factor
eDNA	Extracellular DNA
ELISA	Enzyme-linked immunosorbent assay
EPS	Extracellular polymeric substance
ERK	Extracellular signal-regulated kinases
ESI-ToF-MS	Electrospray ionization – time-of-flight – mass spectrometry
GJIC	Gap junctional intercellular communication
HAQ	4-hydroxy-2-alkylquinolines

HHQ	2-heptyl-4(1H)-hydroxyquinoline
HPLC	High-pressure liquid chromatography
HQNO	4-hydroxy-2-heptyl-quinoline- <i>N</i> -oxide
HSD	Hydroxysteroid dehydrogenase
HSL	Homoserine lactone
ID-NTD	Intrinsically disordered N-terminal binding domain
IQS	Integrating QS signal
LBD	Ligand binding domain
LDL	Low-density lipoprotein
LTTR	LysR-type transcriptional regulator
MDR	Multidrug-resistant
mTOR	Mechanistic target of rapamycin
NE	Neuroendocrine
NMR	Nuclear magnetic resonance (spectroscopy)
PA	<i>Pseudomonas aeruginosa</i>
PC	Prostate cancer
PCN	Pyocyanin
PI3K	Phosphatidylinositol-3-kinase
PQS	<i>Pseudomonas</i> Quinolone Signal
PVD	Pyoverdine
qPCR	Quantitative polymerase chain reaction
QS	Quorum sensing
QSI	Quorum sensing inhibitor
ROS	Reactive oxygen species
SHBG	Sex hormone-binding globulin
SHR	Steroid hormone receptor
SRD	Steroid reductase
STS	Steroid sulfatase
UGT	UDP-glucuronyltransferases

6 INTRODUCTION

6.1 Cell-to-cell Communication Mechanisms and Resistance to Treatment

The origins of cell-to-cell (or intercellular) communication in the ancient unicellular world have remained elusive to the scientific community for centuries (1). Reliance on patchy fossil records and the often contradictory findings of modern computer modelling (2,3) are likely to intrigue evolution experts for many more years to come. It is evident, however, that the ability to effectively communicate has conferred unicellular and multicellular organisms significant survival benefits that were readily and successively selected over time (4–7), constituting today the abundant and often complex mechanisms of intercellular signalling networks. At its simplest, intercellular communication functions as an optimal tool for cooperation, specialization/differentiation, and environmental adaptation (8). Illustrating Darwin’s seminal work, cells, by “talking” to each other, ensure the survival of the fittest (9).

The concept of “major evolutionary transitions” (10) hypothesises that previously independent individuals cooperate to form new, more complex systems with some ecological or efficiency benefit (Figure 1) (i.e. genes became genomes, archaea and eubacteria formed eukaryotic cells, and unicellular eukaryotes formed multicellular organisms) through the storage and transmission of heritable information. The rationale between intra- and interspecies cooperation involve predation evasion, facilitation of reproduction, and increased efficiency in the use and production of resources for metabolism and survival, ultimately benefiting overall fitness of the organisms involved (11,12).

The chemical languages used in cell-to-cell communication mechanisms are almost as diverse as the number and nature of individuals involved in these microscopic conferences. Broadly, they include the synthesis, release, and detection of communication-relevant molecules, which are generally termed signalling molecules (13,14). In prokaryotes, signalling molecules exert their communicative function by diffusion to the extracellular environment and across cell membranes. These compounds are defined by their 1) involvement as a reaction to environmental changes, 2) perception or recognition by a specific receptor, and 3) ensuing concerted response that 4) extends beyond any physiological changes required simply to metabolize or detoxify it (15). More specifically, the most studied signalling molecules involved in bacterial intraspecies communication to date include *N*-Acyl-L-homoserine lactones (AHLs) (16) – most widely found in Gram-negative pathogens; Autoinducer-2 (AI-2) (17) –

INTRODUCTION

shared among Gram-negative and Gram-positive bacteria; Autoinducer-3 (AI-3) (18) – bacterial response to eukaryotic hormones; Autoinducing peptide (AIP) (19) – regulating virulence and competence of Gram-positive organisms; Diffusible (Signal) Factors (DSFs) (20,21) – colonization and infection of eukaryotic hosts; and Indoles (22,23) – influencing quorum sensing (QS) phenotypes in population density-sensitive microorganisms such as *Escherichia coli* and *Pseudomonas aeruginosa* (PA). In addition, bacteria have also developed interspecies communication methods to ensure survival during the course of evolution. Notably, peptidoglycans – involved in symbiotic and pathogenic interactions with animals and plants (24) – and antibiotics such as erythromycin and streptomycin, whose synthetic pathways predate human clinical use by 500 million years (25), have been shown to regulate homeostasis and competition strategies in microbial communities (26). The (extracellular) factors described above are of paramount importance for microbial populations and constitute some of the precursors of multicellularity (9). The ever-increasing synergy of clustered individual cells to maximize the efficiency of their cooperation, by sharing energetically costly “public goods”, evolved into large, well-integrated, and highly cooperative communities of specialized (differentiated) individuals (Figure 1).

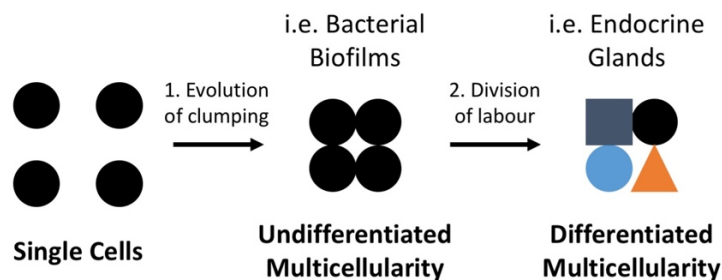


Figure 1. Major steps in the transition to multicellularity and cellular specialization/differentiation. Individual cells initially formed cooperative groups with increased efficiencies (i.e., microbial communities) that later evolved into synergistic, more complex systems or organisms (i.e., mammalian endocrine glands). Modified from ref. (9).

These ultimately resulted in the independent appearance of complex multicellular organisms multiple times from a variety of ancestral unicellular lineages in the history of observable evolution (5). Progressive growth, spatial segregation, and temporal specialization of multiple cell types (with some eventually losing their reproductive capacity) led to differential gene expression at defined time points and within varied regions of the same organism (27). This allowed a remarkable plasticity of biological innovations that would be impossible for single cells, which is particularly true in their intricate cross-talk mechanisms (28). These coordinated societies of interacting partners demanded signalling units many times more complex than those found in unicellular exocrine systems (29). Broadly speaking, multicellular organisms display three distinct mechanisms (14) of cell-to-cell communication namely, 1) extracellular

pathways, which include the secretion and effector functions of hormones, growth factors, cytokines and neurotransmitters; 2) intracellular metabolic pathways, triggered by extracellular effectors and initiated by a variety of second messengers such as cyclic adenosine monophosphate (cAMP), Ca^{++} , reactive oxygen species (ROS), nitric oxide, ceramide, and (mitogen-activated) protein kinases; and 3) gap junctional intercellular communication (GJIC), constituted of direct cytoplasmic continuity between adjacent cells through densely packed membrane channels, which is a hallmark and an absolute requirement for multicellular life, intimately related to embryonic development and overall tissue homeostasis (30,31).

Knowing the different languages used in cell-to-cell communication mechanisms is the first step in unravelling the complexity of signalling pathways taking place in different systems but, in addition, it is crucial to understand the means through which these networks take place in orchestrating the coexistence of the many cell types and the high level of coordination they demand. Fundamentally, the communication or transfer of information from one cell to another is categorized by a recipient/target cell responding to the signal from a secreting/donor cell, a process taking place by the highly specific binding of the signalling molecule to its cognate receptor (32). Cell-to-cell interactions are regulated via different methods depending on the distances between the donor and the target cells. Locally-borne signals include autocrine/autonomic inputs – target and secreting cells are identical, and paracrine – target cell is in the vicinity of the secreting zone, while distantly-borne messages, exclusive to multicellular organisms, are termed endocrine – target and secreting cells are distant and secreted factors typically depend on a contiguous specialized media, such as the blood or lymph (30,33,34). Most biologic phenomena are under the overlapping influence of two or more of these systems.

Apart from maintaining cellular/tissue integrity and homeostasis, and ensuring adequate cell growth and development, signalling molecules and associated pathways in cell-to-cell communication mechanisms are also closely associated with the protection and survival of uni- and multicellular organisms against biotic or abiotic stressors. From a clinical and medicinal standpoint, the latter translates (in the case of pathophysiological processes) in the development of one of humanity's greatest healthcare challenges: resistance to treatment. That is antibiotic resistance in bacterial infections that depend on quorum-sensing (9,35,36) and abrogation of therapeutic antitumour activity in the complex microenvironment of endocrine cancers that possess mis-regulated signalling circuits (30,31,34,37).

The focus of this work has two fronts: to explore the auto- and paracrine signalling pathways of the population density-dependent quorum sensing phenomenon of the Gram-negative

INTRODUCTION

bacterium PA in driving virulence, biofilm formation and innate/adaptive antibiotic resistance against clinically relevant therapeutics. Thus, highlighting the relevance and promising outcomes of hampering bacterial communication by the inhibition of synthesis and binding of signalling molecules (autoinducers – AIs) to cognate receptors that result in highly detrimental, coordinated group behaviours. And increase the understanding of the endocrine mechanisms that initiate and propagate tumour cell development, conferring immune- and therapeutic evasion of metastatic, drug-resistant human prostate cancer (PC) cells]. Hopefully, paving the way to developing novel, more robust and long-lasting approaches that are needed to treat affected patients effectively. While it is important to note that correlations exist between bacterial infections and cancers in humans, as in the cases of infection-driven cytokine production leading to uncontrolled stimulation and proliferation and tumour cells (38), as well as steroid hormones modulating bacterial phenotypes by promiscuous receptors (39), this work will address QS and PC separately.

6.2 *Pseudomonas aeruginosa* – An End to Traditional Antibiotics?

PA is a ubiquitous Gram-negative bacterium highly adaptive to changes in environmental conditions and able to colonize a variety of mammalian tissues (40) and medical devices (41,42), causing both acute and chronic infections (43). Commonly found in ventilator-associated pneumonia, sputum of cystic fibrosis (CF) patients, meningitis, abscesses, soft tissue, urinary, catheter-associated, and corneal infections, as well as conjunctival erythema (44), the healthcare-associated cost load and clinical relevance of PA infections to immunocompromised individuals and global societies, cannot be overstated. The successful treatment and eradication of *Pseudomonas* infections are severely hampered by the ready acquisition of resistance (45) to commonly used antibiotics such as ciprofloxacin, imipenem, tobramycin, and aztreonam (46). In addition, the appearance of multidrug-resistant (MDR) phenotypes in 13% of PA-associated colonisations (in the US alone) highlights the serious threat of such infections (44). Colistin, a cyclic amphipathic antibiotic, is currently the last resort of treatment left against MDR PA (47) and already shows signs of resistance development (48). The high incidence, severity, and recalcitrance of this “superbug” are made possible by multifaceted contributing factors, including PA’s multi-factorial arsenal of virulence factors at its disposal, as well as the ability to form highly complex microbial communities, called biofilms (43,44,49–51).

The co-evolutionary battle between bacterial infections and antimicrobial compounds has been extensively studied, and resistance mechanisms can be broadly classified as occurring via either: 1) innate (52), 2) acquired (53,54), and 3) adaptive (55,56) resistances. Specifically to PA, innate or intrinsic resistance is largely based on the semi-permeable outer membrane of Gram-negative bacteria that acts as a significant physical barrier to the penetration of antibiotics (57), narrowing antimicrobial treatments to small hydrophilic compounds such as β -lactams and quinolones. This fact synergizes with another innate mechanism: the prevalence of efflux pumps and periplasmic extended-spectrum β -lactamases (58), making PA infections naturally challenging to treat. In addition, exposure to selective pressures, such as antibiotics, leads to acquired resistance insofar the occurrence and selection of a broad array of chromosomal mutations (59) and horizontal transfer of resistance-containing plasmids (60). Often, the effects of intrinsic resistance can be further potentiated by such mutations, as seen in the case of increased expression of MexEF-OprN and AmpC genes, responsible for the formation and activity of multidrug efflux pumps and β -lactamases, respectively (61,62). Finally, adaptive resistance, rapidly triggered by variations in environmental growth circumstances such as pH, heat shock, DNA stress (SOS response), and nutrient deficiencies (43) are becoming increasingly appreciated for its contribution in MDR phenotypes and the shifts between planktonic and sessile life cycles (63). The onset of adaptive resistance involves the expression and interaction of a plethora of genes (termed “resistomes”) and is exemplified in social behaviour changes, such as the formation of biofilm and swarming motility in PA (56,64).

Overall, antibiotic resistance in microbial infections results from the contribution of intrinsic, acquired and adaptive mechanisms intertwined in complex genetic networks and metabolic heterogeneity of bacterial subpopulations *in vivo*. This already precarious scenario is made worse by the prevalence of MDR species vastly outpacing the advent of new antibiotic classes or the successful administration of currently available antibiotic combinations that do not possess some degree of cross-resistance mechanisms (65). Ultimately, addressing multidrug resistance demands a paradigm shift in therapy focus and strategy, ensuring successful clearance of pathogens while protecting the symbiotic host-microbial balance.

Some of the emerging strategies to circumvent the global threat of antibiotic resistance include the inhibition of bacterial adherence capabilities (66,67), the employment of viral therapies (bacteriophages) (68), and efflux pump inhibitors (69). However, while the first does not directly address acute or systemic infections, the latter two are still amenable to resistance development (70,71), rendering treatments ineffective due to selective pressure responses by the bacteria.

INTRODUCTION

Alternatively, the increasing comprehension of bacterial reliance on highly conserved cell-to-cell QS communication mechanisms (35) implicated in invasion abilities, adaptation, and development of escape mechanisms as well as virulence factor expression (pathogenicity) (72,73) represents a promising and attractive target as an alternative to classical antibiotic treatment. This approach, coined as antivirulence therapy (74), depends on the activity of quorum quenchers, or pathoblockers, that hinder the production, release and/or perception of small diffusible bacterial signalling molecules (AIs). These accumulate with increasing cell density and trigger coordinated responses, achieving outcomes that would otherwise be impossible as single individuals. The rationale behind the effective use of pathoblockers is the avoidance of the enormous selective pressure of bactericidal (targeting cell viability) and bacteriostatic (targeting cell growth) drugs (75) aiming at essential biochemical processes such as cell wall integrity and protein/nucleic biosynthesis (76) – the central strategy of current antibiotics. Rather, antivirulence compounds supposedly apply less evolutionary pressures, and thereby promote less drug resistance, as most virulence traits are not essential for survival (50). In addition, QS, albeit non-essential, is linked to a variety of physiological processes in bacteria (77) namely, bioluminescence, competence, antibiotic biosynthesis, motility, biofilm maturation and antibiotic susceptibility (increased tolerance of biofilms and upregulation of resistance-associated genes) (78,79). Therefore, QS inhibition not only holds the potential to reduce bacterial virulence but may also restore antibiotic efficacy in patients.

6.2.1 The Antivirulence Approach Against *Pseudomonas aeruginosa* Quorum Sensing

Fortuitously, PA has been extensively studied as a model organism for bacterial quorum sensing, and while the complexity of bacterial “molecular languages” is far from complete elucidation, significant progress has been made in understanding this pathogen’s intricate communication mechanisms (80,81). In general, Gram-negative bacteria rely on AHL-based signalling systems typically constituted of synthases and cognate receptors homologous to LuxI and LuxR, first described in the bioluminescent marine bacterium *Vibrio fischeri* in the early 1970’s (82). The length and saturation state of the acyl chain translate into receptor affinity and fidelity of different quorum sensing-capable species. In PA, two of at least four hierarchically interconnected QS circuits (81) (Figure 2) depend on AHLs in order to trigger their cell density-dependent gene expression programme, namely the superordinate *las* (by *N*-(3-oxododecanoyl)-L-homoserine lactone: 3-oxo-C12-HSL) and *rhl* (*N*-butanoyl-L-homoserine lactone: C4-HSL) (83) systems. Briefly, the diffusible 3-oxo-C12-HSL molecule, synthesised

by LasI, binds and activates the transcription factor LasR upon reaching a putative threshold concentration in the cellular microenvironment, driving the production of virulence factors such as LasB elastase, LasA and Apr proteases, and exotoxin A (64), as well as the increased expression of *lasI* itself (thus the term autoinducers) (44). Analogously, in the *rhl* system, C4-HSL targets gene promoters upon binding and activation of RhIR responsible for pyocyanin (and other phenazines), rhamnolipids, siderophores, hydrogen cyanide, and cytotoxic lectin production (36).

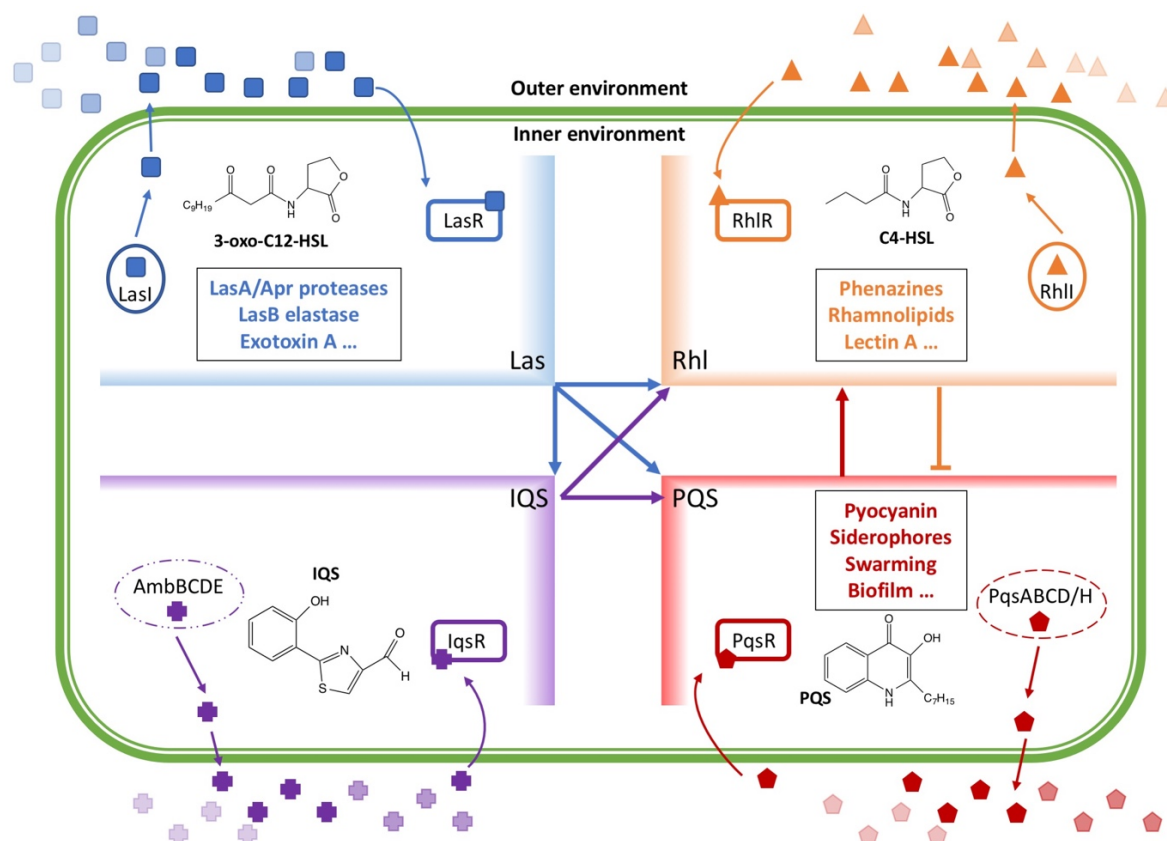


Figure 2. Schematic representation of the four QS signalling networks *las*, *rhl*, *pqs*, and *iqs* in *P. aeruginosa*, with respective regulons. Arrows indicate a stimulatory effect and flat lines represent a negative regulation. Text boxes highlight physiological phenomena and production of virulence factors intimately related to the effects of corresponding QS systems. Abbreviations: 3-oxo-C12-HSL, *N*-(3-oxododecanoyl)-*L*-homoserine lactone; C4-HSL, *N*-butanoyl-*L*-homoserine lactone; PQS, *Pseudomonas* quinolone signal; IQS, integrating QS signal. Modified from ref. (81).

Increasing the level of complexity of *Pseudomonas aeruginosa* QS networks, a third system, dependent on a different class of signalling molecules, the 4-hydroxy-2-alkylquinolines (HAQs) (84), was described in the late 1990's and termed the *Pseudomonas* quinolone signal system (*pqs*) (85). Contrary to the canonical AHL production and signalling found in a variety of Gram-negative organisms, HAQ biosynthesis has been restricted to *Pseudomonas* and *Burkholderia* genera. While the intermediate 2-heptyl-4(1H)-hydroxyquinoline (HHQ) is likely involved in promiscuous interspecies signalling (86) (especially important for interactions in microbial communities such as biofilms), the final product of the *pqs* pathway, 2-heptyl-3-

INTRODUCTION

hydroxy-4(1H)-quinolone (PQS), is exclusive to PA. Both molecules wield signalling capabilities, albeit with different affinities, by binding to the PQS receptor (PqsR), as known as multiple virulence factor receptor (Mvfr). These facts highlight the particularity of the *pqs* network, discussed in more detail in the next section, and its attractiveness as an antivirulence target. As shown in Figure 2, *pqs* signalling is partially modulated by the activities of *las* and *rhl*, and itself regulates the expression of the *rhl* system in a positive feedforward loop (87). In addition, Lee and colleagues (88) have recently reported a stress response-mediated mechanism that plays a role in integrating PA's environmental responses to stress with its complex QS network, named integrating QS signal (IQS), which uses 2-(2-hydroxyphenyl)-thiazole-4-carbaldehyde as its signalling molecule.

Taken together, the QS systems in *Pseudomonas* are true master switches of bacterial behaviour and survival. Quorum sensing mechanisms have been shown to ultimately regulate more than 300 genes across PA's genome (89), with PqsR alone controlling 141 genes (86) and indirectly modulating 18% of the bacterium's total genome (90), underlining its role in global genomic regulation.

6.2.2 *Pseudomonas aeruginosa pqs* QS System and the Synthesis of HAQs

The leading actor in the *pqs* signalling network is PqsR, and unlike the AHL-dependent QS systems that rely on LuxR-type of transcriptional regulators, it belongs to the distinctive evolutionary family of LysR-type transcriptional regulators (LTTRs) (91). The LysR group is most abundant in proteobacteria, and its uniqueness lies in the dual function (autoregulation of activation and repression of specific genomic promoters) of its members, as opposed to the single type receiver-response mechanism of LuxR regulators (92).

Briefly, the biosynthesis of HHQ and PQS start with the sequential metabolism of anthranilic acid (derived from tryptophan or chorismic acid (93)) by enzymes located in the *pqs* polycistronic operon *pqsABCDE*, regulated by PqsR activity, and *pqsH* (94,95) (Figure 3). Initially, PqsA ligase and Coenzyme A (CoA) convert anthranilic acid into anthraniloyl-CoA (96). Upon binding to the active site of PqsD, the thioester is converted into 2-aminobenzoylacetate-CoA (2-ABA-CoA) with the help of malonyl-CoA (97). The thioesterase PqsE catalyses the cleavage of the thioester bond of 2-ABA-CoA resulting in the formation of 2-aminobenzoylacetate (2-ABA) (98). In turn, 2-ABA is transformed into HHQ after condensation with octanoic acid accomplished by the activity of the heterodimeric enzyme PqsBC (97). Finally, oxidation of HHQ by the flavin monooxygenase PqsH in the presence of NADH results in the formation of PQS (99), with 100-fold higher affinity to binding and activating PqsR than its HHQ precursor (100). Activation of PqsR reignites the system in a

positive forward feedback loop (autoinduction) as well as the concomitant expression of PqsR-dependent physiological changes, resulting in the production of the arsenal of virulence- and biofilm-associated factors (44). In addition to PQS and HHQ, the biosynthetic pathway described above is also implicated in the production of important but less appreciated intermediates, namely dihydroxyquinoline (DHQ), 4-hydroxy-2-heptyl-quinoline-*N*-oxide (HQNO), and 2-aminoacetophenone (2-AA). DHQ and HQNO are pathogen-derived toxins with significant cytotoxic effects to eukaryotic (pathogenicity) (101) and prokaryotic (competition and biofilm formation through the release of DNA into the extracellular space – eDNA) (102) cells respectively, layering *Pseudomonas* niches of infection. In turn, 2-AA, a small volatile molecule, appears to be involved in the generation of persistence in PA infections by regulating the switch between acute and chronic phenotypes (103).

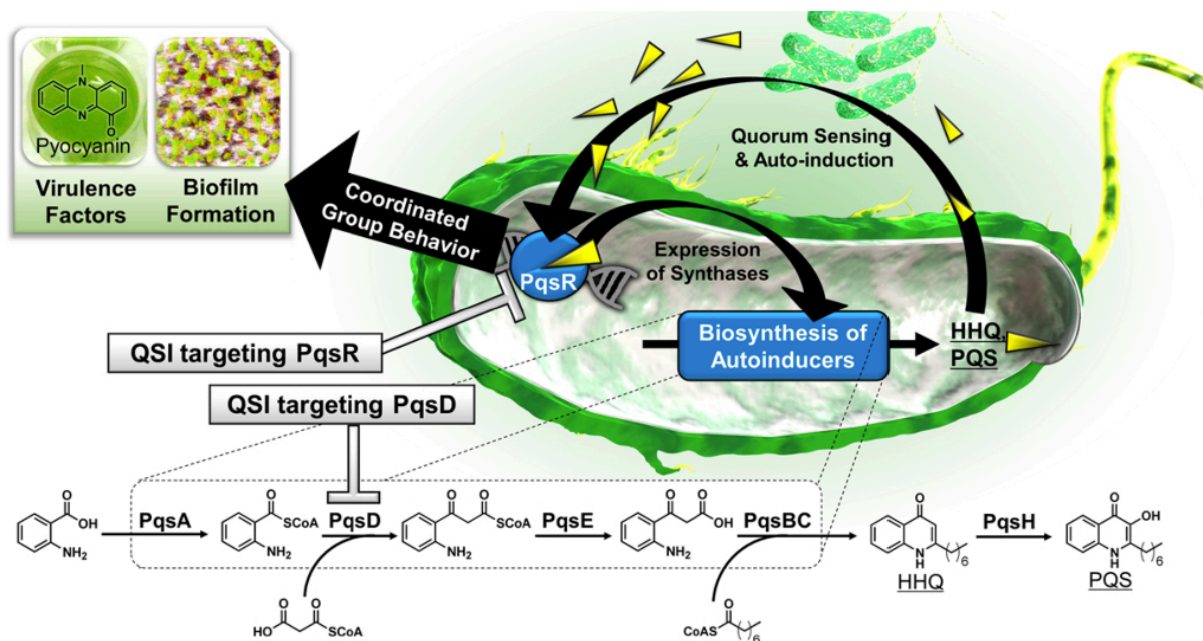


Figure 3. Schematic representation of signalling molecule biosynthesis and dual quorum sensing inhibition strategy in the *Pseudomonas* quinolone signal QS biosynthetic system. Simultaneous inhibition of signal synthesis and sensing is a promising approach to the reduction of virulence factor and biofilm formation. Abbreviations: CoA, Coenzyme A; HHQ, 2-heptyl-4-quinolone; PQS, *Pseudomonas* quinolone signal; QSI, quorum sensing inhibitor. Reprinted with permission from (104), p. 1280. Copyright © 2016, American Chemical Society.

The diverse chemical nature and biological effects of the different signalling molecules in the *pqs* QS system shown above illustrate the complexity of this network. Notably, PQS and related intermediates are fundamental in *Pseudomonas* ubiquitous signalling language, blurring the line between the autocrine and paracrine communication routes, shifting between the two or using them simultaneously (105). The first, as cells that produce a signalling molecule and its cognate receptor – self-communication – and the latter, designed for cells to communicate with others in the vicinity – neighbour communication. Moreover, the *pqs* QS system also facilitates

INTRODUCTION

paracrine signalling in PA's sessile, biofilm phenotype typical of chronic infections (49,106). As previously mentioned, biofilms occur in a form of adaptive resistance, developed in order to promote horizontal gene transfer between microbial populations, limit antibiotic/stressor penetration through thick, viscous extracellular polymeric substance (EPS) (107), and generate unique environmental niches that modulate physiological activity within the biofilm. This can be accomplished, for example, by restricting oxygenation or nutrient distribution and stimulating the formation of tolerant and persistent cells with decreased growth and metabolism (49). Biofilms, however, are far from being static communities, active dispersal of planktonic individuals (thereby propagating infection), differential gene expression, and immune invasion are tightly controlled mechanisms (106). This control is partially performed by the *pqs* QS network, insofar the production of cytotoxic compound HQNO that generates significant amounts of eDNA from lysed organisms (including PA itself) (102). Extracellular DNA not only partakes in the structural architecture of biofilms but also facilitates cell migration and shuttling of exosomes and QS molecules through a complex, interconnected network of furrows and trails within the community (108).

6.2.3 Silencing the *pqs* QS System with Quorum Sensing Inhibitors (QSIs)

Quorum quenching strategies rely on three broad mechanisms that target QS-mediated bacterial cell-to-cell communication structures, namely 1) inhibition of signalling molecule biosynthesis, 2) the availability of the signal itself, and 3) the sensing/reception of the signalling molecule by sensor cells (76). Although AHL-based quorum quenching has been the most investigated as an alternative to antibiotic therapy (64,76), inhibition of the *pqs* system has additional advantages based on its restricted phylogenetic distribution as previously mentioned, allowing for highly selective therapies that would spare beneficial symbionts and commensals of the human microbiome. As shown in Figure 3, the *pqs* system has a number of possible theoretical targets, including the AI synthases (PqsA, PqsD, PqsE, PqsBC, and PqsH) and the AI cognate receptor PqsR. Not all synthases are equally suitable for appropriate drug targeting, however. Inhibition of the catalytic activity of downstream enzymes such as PqsBC and PqsH would eventually result in the accumulation of PQS precursors still bearing detrimental biological activity shown in murine models such as DHQ and 2-AA, and HHQ, respectively (109). Additionally, the thioesterase function of PqsE has been shown to be non-essential, with redundant activity by non-specific enzymes (i.e., TesB) still leading to the production of HHQ and PQS in mutants (98). Finally, from the upstream synthases involved in PQS biosynthesis, PqsD stands out as the most promising drug target in this pathway due to the lack of available PqsA crystal structure to date and attenuated virulent phenotypes observed in *pqsD* mutants

(94,110). Since the first reported PqsD inhibitors (111), significant progress has been made yielding potent and selective compounds (112–115) with no bactericidal or bacteriostatic properties.

The arrest of signal synthesis is but one approach to silence bacterial communication. Another, perhaps even more relevant strategy, is to avoid the activation of cognate receptors responsible for eliciting the downstream signal transduction cascade. Due to the redundancy of bacterial communication mechanisms, QS systems also integrate information from metabolic and environmental stimuli (63,76). Therefore, efficient antivirulence approaches that address receptor activation (by cognate AIs or otherwise) hold even greater promise. In that regard, targeting PqsR is pivotal in hampering *Pseudomonas*' virulence and pathogenicity (64). *PqsR* mutants resulted in the absence of HAQs and pyocyanin production (91,94) as well as reduced biofilm-forming capabilities of adherence-related lectin A and constituents of the complex extracellular matrix such as eDNA(116). In addition, these mutants were also deficient in producing the persistence-related molecule 2-AA, highlighting the role of the *pqs* system in acute, sessile, and resistant infections. Furthermore, PqsR activity is an absolute requirement for full virulence phenotypes against plants (117), nematodes (94), and mice (118). Successful discovery and optimization of PqsR antagonists based on natural ligands (119,120), small fragment approaches (121,122), and high-throughput screening (91) have already shown the remarkable achievements made possible when silencing the *pqs* system.

As indicated above, addressing AI synthases do hold great potential as antivirulence therapy candidates to treat PA infections as well as blockage of cognate receptors demonstrated by the successes in *in vitro* and animal studies of these proposed treatments. However, due to the complexity and plasticity of the PQS QS system, a combination of inhibition/antagonism strategies may be necessary to silence communication and prevent pathogenesis fully. This fact prompted us to investigate a dual-target approach addressing both ends of the PQS QS pathway spectrum (Figure 3). In this work, the suitability and relevant cumulative benefits of addressing signal synthesis and sensing (dual inhibition) are explored and highlighted on Chapter 1 (104).

6.3 Steroid Cell-to-Cell Communication – The Complex Micro “Talk” of Multicellular Organisms

Steroid hormones are true masters of intercellular communication in vertebrates and under normal physiological conditions coordinate and control the correct development and function of a variety of tissues, organs, and glands from early embryonic development through to adult life (123). Broadly speaking, these cholesterol-derived compounds can be classified as

INTRODUCTION

progestogens (early steroid precursors), corticosteroids, oestrogens, and androgens (124) all of which target specific steroid hormone receptors (SHRs) in the organism. SHRs are ligand-activated, tissue- and cell type-specific receptors mostly located in the cytosol (125) with some also found in the membrane of eukaryotic cells (126), initiating the downstream signalling cascade of tyrosine kinases. SHRs regulate numerous biological processes by interacting with specific response elements in the cellular DNA and various coregulatory proteins (activators or repressors of gene expression) (125). This cross-talk, achieved by such genomic and non-genomic interactions, adds immense complexity to hormonal responses and provide precise, robust, and versatile intercellular signalling (127).

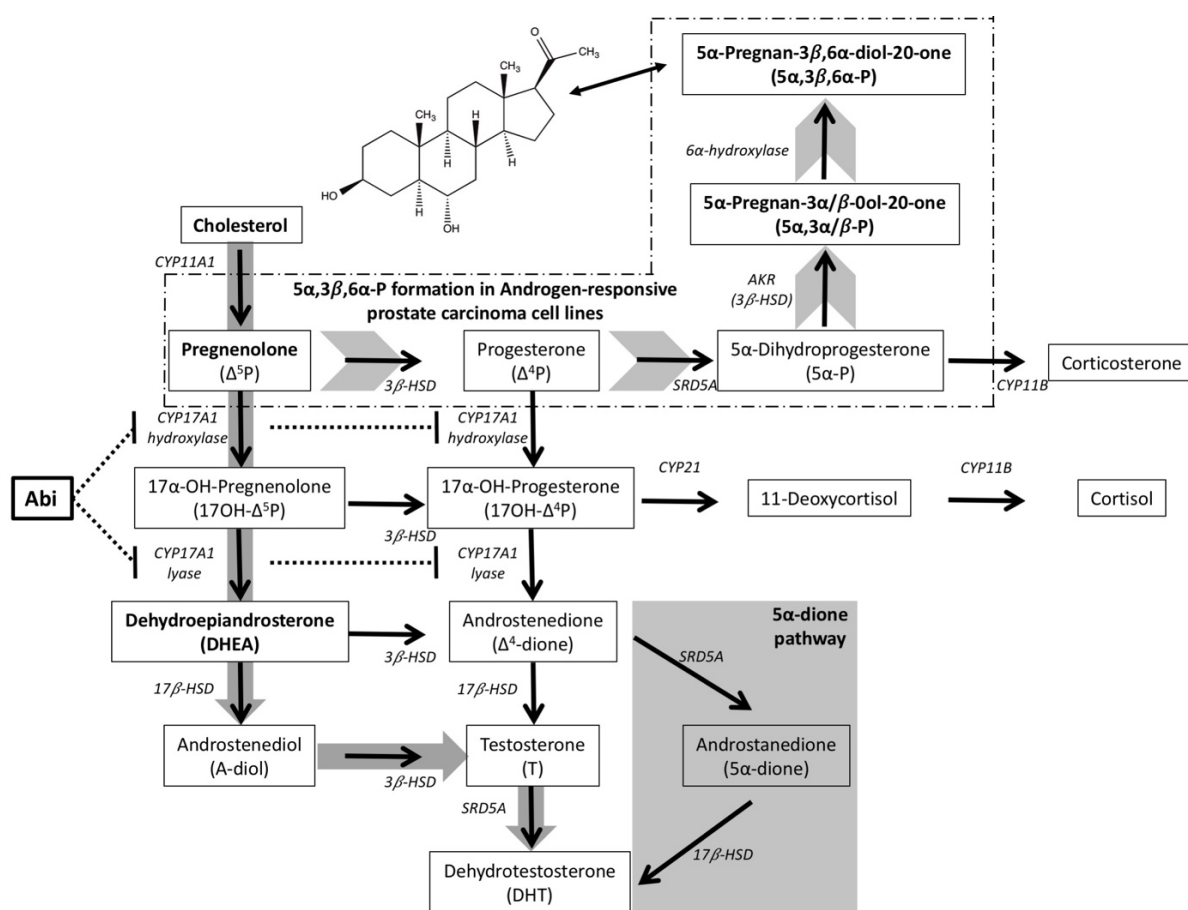


Figure 4. Schematic representation of steroidogenic biosynthesis leading to the production of corticosteroids and androgens from primordial steroid precursor cholesterol. Classical androgen axis (grey arrows) leads to the production of AR ligands testosterone and DHT by a series of sequential metabolizing enzymes with intricate tissue- and cell-type specificity. Non-classical pathways, i.e., 5 α -dione (shaded area) and proposed 5 α -3 β ,6 α -P (dashed area), are suggested actors in mis-regulated signalling mechanisms. Abi abrogates systemic androgen production by the inhibition (flat arrows) of the CYP17A1 enzyme. Abbreviations: HSD, hydroxysteroid dehydrogenase; CYP, cytochrome P450; SRD5A, 5 α -reductase; AKR, aldo-keto reductase; Abi, abiraterone.

6.3.1 Endocrine Signalling of Androgens in the Human Prostate

The biological effects of androgens are particularly required for cell differentiation, growth, and maturation of male sexual organs, including the human prostate (128). In men, androgen

biosynthesis from cholesterol takes place primarily in the testes through a series of sequential metabolic steps (Figure 4), with smaller amounts being supplemented by cortical cells of the adrenal glands from circulating dehydroepiandrosterone (DHEA) (129). Testosterone is the primary product of the androgen endocrine system and the most well-known kind of androgen. Its biological effects involve the promotion of secondary male sexual characteristics such as the increase in muscle and bone masses and the development of body hair (130). Testosterone is converted to dihydrotestosterone (DHT), the most potent human androgen, upon reaching the prostate by the activity of the 5α -reductase enzyme (131).

Circulating hormones can only be directly sensed by a subset of cognate receptor⁺ cells that exist in a precise spatial distribution for signal sensing and message transmission to neighbouring cells in a paracrine manner (132). Not surprisingly, the adult prostate is a complex structure of highly specialized members. Fibromuscular stroma cells comprised of mesenchymal lineages surround secretory ducts of basal and luminal epithelial cells, with punctuated cells of neuroendocrine (NE) origin (133), all of which are responsible for tissue organization and function. Development and maintenance of the gland rely on endocrine and paracrine signals of stromal and epithelial cells in response to androgen signalling and neuroendocrine stimuli that are androgen-independent. Paracrine communication of stromal cells regulates epithelial growth and differentiation of basal and proliferative/secretory luminal cells, ensuring the healthy physiological compliance of the prostate (37). In addition, neuroendocrine cells also provide trophic signals in a paracrine manner to epithelial populations through the secretion of neuropeptides, growth factors and parathyroid-like hormone, amongst others (134).

Testosterone and DHT exercise their communicative roles upon binding to the androgen receptor (AR) in the cellular cytoplasmic space. The AR is a member of the nuclear hormone receptor family of transcription factors encoded by a single copy gene on the X chromosome. AR activation can occur through classical or non-classical signalling mechanisms. Canonical activation and signalling involve the dissociation from chaperones upon testosterone or DHT binding, resulting in the migration of this ligand-receptor complex to the cell nucleus and formation of homodimers that tightly bind to androgen response elements (AREs). In the nucleus, AR recruits several other regulators in order to ultimately transcribe target genes (135) and establish cross-talks with many other pathways associated with cellular signalling and apoptosis (136). In this scenario, AR⁺ stromal cells sense androgens and translate their stimuli into cues as paracrine signals to neighbouring AR⁻ epithelial and neuroendocrine cells (126) (Figure 5). Non-classical activation occurs when the bound AR activates non-genomic

INTRODUCTION

cytoplasmic signalling pathways, or AREs but in the absence of ligand (137). In addition, binding of non-androgenic ligands result in allosteric changes of the receptor and ensue a differential gene expression pattern intimately related to the physiological and genetic context of the target cell and its milieu (125). Finally, the androgen communication axis ends with the activity of UDP-glucuronyltransferases (UGTs) (131), leading to their elimination and cessation of further biotransformation processes.

6.3.2 Prostate Cancer and the Role of the AR in Disease

Due to their convoluted balance and pleiotropic effects, mis-regulation of the communication pathways in steroid signalling may have catastrophic results, as observed in endocrine neoplasms of the thyroid (138), pancreas (139), ovaries and endometrium (140), as well as pituitary (141) and prostate (142) glands. Interestingly, AR-related mechanisms have been found in a number of typically AR-independent malignancies (135), such as mantle cell lymphoma and bladder, liver, and kidney cancers, stressing the complexity and importance of this receptor in diseased states. In this work, we focus on its role in prostate cancer pathology. In the United States, prostate cancer was the leading cause of cancer (220.800 newly diagnosed cases) and the second leading cause of cancer-related deaths (27.540 individuals) in 2015 (143). To date, mainstay treatment of prostate cancer relies on its initial dependency of androgen signalling through the AR observed in the seminal work of Huggins and Hodges in 1941 (144). Since then, androgen deprivation therapy (ADT) through anatomical or, more recently, chemical castration has been successful in treating 80% of prostate cancer patients (145). However, the high incidence of cancer mortality is linked to more advanced stages of the disease where ADT ultimately fails, AR signalling is sustained despite treatment, and patients eventually relapse with a more aggressive, androgen-independent form of the disease (146) termed castration-resistant prostate cancer (CRPC) (147).

In the cancer microenvironment, AR-driven phenotypical changes arise from a perturbed communication between stroma and epithelium (148). Smooth muscle is replaced by cancer-associated fibroblasts that actively react to the environment and enhance tumorigenic epithelial growth, cell invasion and metastasis (148) (Figure 5). This perturbed communication is characterised by a shift from normal paracrine signalling to abnormal autocrine/intracrine mechanisms that lead to cancer progression and resistance to treatment (37,126,133) whereby cancer cells produce hormones and oncogenic growth factors in a positive forward feedback loop. Researchers worldwide have postulated a variety of possible mechanisms underlying the development of CRPC. AR-dependent mechanisms involve the punctuated progression of genetic mutations (chromoplexy) into states of high genomic instability governed by broader

chromosomal rearrangements and hypermutational events (chromothripsis) (149), and can be broadly grouped into 1) *de novo* androgen synthesis *in situ* – prostate (independence of endocrine functions) (150); 2) increased expression of the AR and its coactivators (151); and very importantly, 3) AR mutations on the receptor's ligand binding domain (LBD) and splice variants of its intrinsically disordered N-terminal binding domain (ID-NTD), involved in conformational flexibility and high receptor promiscuity (125,134,146). AR splice variants (AR-Vs) are notoriously promiscuous and represent a significant therapeutic challenge and a hallmark of progression in patients with advanced forms of the disease (152,153). Their expression is significantly increased and drive PC progression during ADT (154) where activation occurs in the absence of (native) ligands (155) and mediate therapy resistance. Two of the most important variants include AR-V7 and AR-V567, which lack androgen binding sites and induce autonomous tumour formation and proliferation in metastatic and CRPC specimens in human patients (156). Splice variants and mutated ARs are involved in the outlaw (activation by growth factors and tyrosine kinases) and promiscuous (nonandrogenic steroid binders) pathways (134).

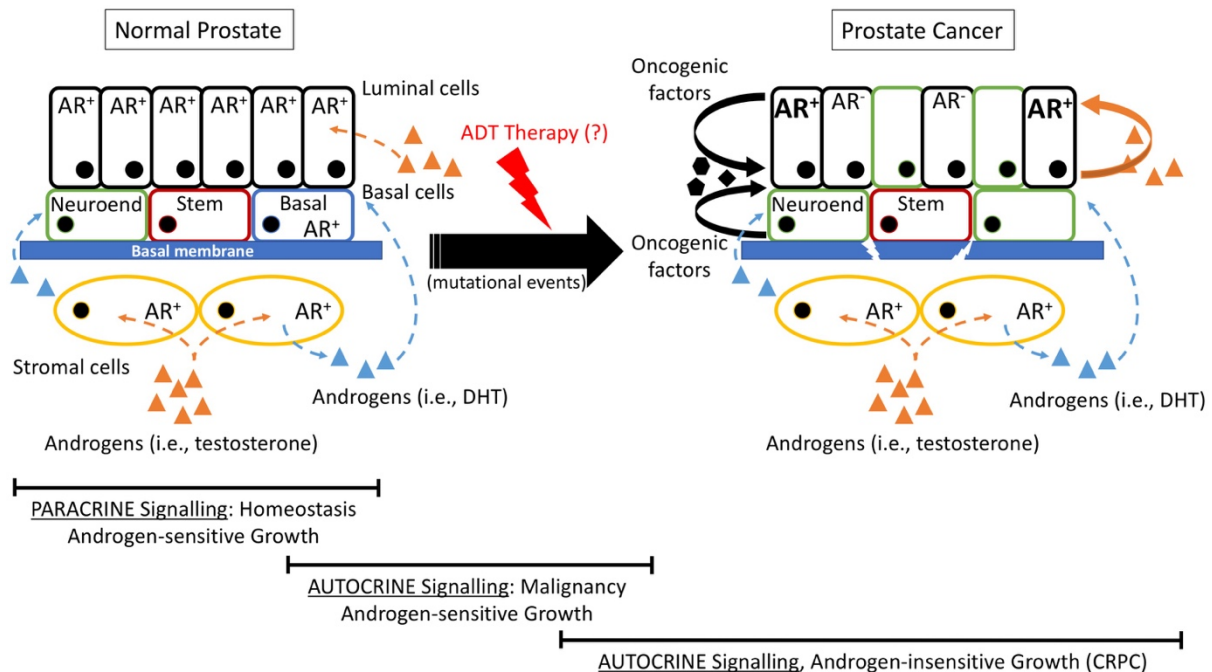


Figure 5. Mis-regulation of the communication mechanisms of the gland are observed in advanced cases of the disease and are perhaps driven by ADT therapy as a means of cancer adaptation and resistance to treatment. The paracrine mechanisms for prostate homeostasis consist of signalling between stromal and epithelial (basal & luminal) cells in response to androgens (left). A shift to autocrine AR signalling leads to tumour growth and development. Shortly thereafter, AR-independent oncogenic events by AR⁻ and neuroendocrine cells culminate in rupture of the basal membrane and metastasis (right). Abbreviations: DHT, dihydrotestosterone; AR, androgen receptor; ADT, androgen deprivation therapy; Neuroend, neuroendocrine cells.

Various endocrine-based therapies are directed toward inhibiting AR activity (157), but AR-independent mechanisms (bypass pathways) are likely to occur concomitantly, namely, microenvironment-dependent (de)differentiation of epithelial and neuroendocrine cells (149)

INTRODUCTION

and tumour suppressor degradation/anti-apoptotic protein overexpression (146), both of which are intimately linked to the cancer-related signalling pathway PI3K/Akt/mTOR (133,135,158,159). More recently, AR has been associated with the modulation and acceleration of non-coding microRNAs (miRNAs) gene expression with oncogenic and anti-apoptotic activity in hormone-dependent cancerous tissues (160,161).

6.3.3 Disrupting Cancer Intercellular Communication and Resistance to Treatment

The clinical relevance and requirement of AR-dependent signalling in prostate cancer (AR overexpression and androgen-regulated genes) have prompted the synthesis, development, and commercialization of several compounds targeting the LBD of full-length wild-type AR (146,158). First-generation antagonists included non-steroidal inhibitors flutamide, nilutamide, and bicalutamide, which block androgen binding by competitive inhibition (162). Treatment with first-generation drugs was ineffective and inferior to anatomical castration (163) insofar some of these antiandrogens had the consequential ability to function as AR agonists. However, they were successful in making evident some of the molecular mechanisms underlying treatment resistance, including LBD point mutations and ensuing promiscuity (164,165). Second-generation antagonist enzalutamide has a much higher affinity for the AR compared to its predecessors, minimal to absent agonist capabilities, and its favourable results rely on three distinct inhibition mechanisms: impaired AR nuclear translocation, AR binding to AREs, and recruitment of coactivators (166). Despite the promising activities of enzalutamide and other AR antagonists, urgent challenges remain in the successful treatment of advanced prostate cancer since AR⁻ cells cannot be targeted by AR antagonists and might play a role in resistance and recurrence of CRPC, with low response to treatment and poor prognosis. Both AR⁻ and androgen-independent AR⁺ cells present steroid intercellular communication mechanisms associated with endocrine therapy resistance (167).

The biotransformation of cholesterol into late androgens is catalysed by tissue-specific enzymes with differential regional and substrate selectivity (Figure 4) (131). Generally, Δ^5 steroid pregnenolone is obtained by the cleavage of the side chain in cholesterol molecules through the activity of mitochondrial enzyme CYP11A1 in the adrenal cortex, dwarfing the steroidogenic output of the testes and other organs such as adipose tissue and the brain (168). The oxidation of 3β -hydroxy- Δ^5 -steroids (pregnenolone, 17α -OH-pregnenolone, DHEA and androstenediol (A-diol)) into their 3-keto- Δ^4 -congeners is performed by the 3β -HSD1/2 isoenzymes by the prostate and other steroidogenic tissues where the double bond between C5 and C6 is

isomerized to that between C4 and C5 (169). Alternatively, pregnenolone can also be acted upon by the dual-function CYP17A1 microsomal enzyme, converting C21 compounds into C19 steroids in testes and adrenal glands (169). The sequential activities of CYP17A1 17 α -hydroxylase and 17,20-lyase functions result in the formation of 17-keto androgens such as DHEA and androstenedione (AD). In addition, testosterone is obtained by the promiscuous aldoketo reductase 1 (AKR1C3) enzyme that reduces AD to testosterone in the adrenals or by 3 β -HSD2 from circulating DHEA. Finally, the last reaction in the classical androgen biosynthetic pathway involves the conversion of testosterone to DHT by both isoforms of the steroid 5 α -reductase (SRD5A1/2). As previously mentioned, redundant “backdoor” pathways may develop in cancer cells able to produce their own steroids in an autocrine/intracrine manner (168,170). Therefore, blockage of androgen biosynthesis by pharmacological means (chemical castration) was another treatment avenue pursued concomitant to receptor antagonism.

Prior to the arrival of second-generation AR antagonists into the market, 14 α -demethylase antifungal inhibitor ketoconazole showed a promising reduction of circulating androgen levels through weak and non-specific CYP17A1 inhibitory properties (171). Due to the high doses necessary in order to achieve sufficient CYP17A1 inhibition, ketoconazole fell out of favour in prostate cancer treatment owing to considerable neurological, respiratory and hepatic toxicities (171,172). It did, however, argue for the therapeutic potential of more selective CYP17A1 inhibitors in hampering the biosynthesis of androgens and ensuing AR activation. One such inhibitor and the current standard treatment for metastatic prostate cancer (in combination with enzalutamide) is abiraterone (Abi) (158,171). Abi is a pregnenolone-derived steroidal antiandrogen with a 3-pyridil substituent and a double-bond between the 16 and 17 positions of the steroidal skeleton that successfully reduces extragonadal testosterone synthesis (158). These added structural features are responsible for both its potency and selectivity against CYP17A1 lyase and hydroxylase functions (171) *via* covalent binding of its pyridine nitrogen to the heme iron in the enzyme (173). Continuous efforts in the field of polypharmacology led to the development of galeterone (TOK001), a compound with a unique dual mechanism of action targeting both the androgen receptor (as an antagonist but in addition also increasing AR protein degradation), including CRPC drug resistant variant 7 (AR-V7), and preferentially the lyase function of CYP17A1 enzyme, thereby avoiding the necessity of glucocorticoid co-administration therapy.

Unfortunately, despite the important progress in prostate cancer treatment, the benefits of state-of-the-art therapies, including Abi and enzalutamide, are short-lived, and resistance invariably occurs (134,146,158). Patients presenting primary (within the first three months) or acquired

INTRODUCTION

(any time thereafter) resistance to both drugs make evident the limitations of current therapies (169). Resistance mechanisms involve upregulation of steroidogenic enzymes that compensate for CYP17A1 inhibition and bypass AR transcriptional programmes (158). This apparently inevitable refractory behaviour is due to the extreme plasticity of oncogenic pathways and enzymatic machinery found in cancer cells. In the case of prostate cancer, these might develop from steroids upstream of CYP17A1 activity, whereby the excess of progestogenic steroids appear to stimulate AR-Vs, thus resulting in the selection of AR⁺ malignant phenotypes (174), and androgen-independent, AR⁻ neuroendocrine lineages (148). Reports on the possibility of ADT enhancing disease aggressiveness and disrupting cellular genotypes (very much like the selective pressures of antibiotics in the case of microbial resistance) (Figure 5) suggest that altered molecular targets should be exploited (148) and is treated with greater detail on Chapter 3.

7 AIM OF THE THESIS

Cell-to-cell communication systems have evolved in unicellular and multicellular organisms as intricate adaptation mechanisms to ensure homeostasis, growth, and survival in response to complex environmental challenges and nutritional cues. In pathological scenarios, the ability to engage in these convoluted intercellular signalling networks often result in resistance development against targeted therapies, as individual or clustered cells strive to cooperate in order to outlast treatment and endure. In that regard, the quorum sensing phenomena of the multidrug resistant bacterium *Pseudomonas aeruginosa* and the plasticity of oncogenic prostate cellular phenotypes belong to a common communication spectrum where autocrine/paracrine signalling leads to highly deleterious outcomes and pathogenesis.

Recalcitrant *Pseudomonas* infections rely on a variety of intrinsic, acquired, and adaptive resistance mechanisms that readily render the use of current antibiotics ineffective and vastly outpace the development of new bactericidal compounds. Therefore, the emergence of antivirulence quorum sensing inhibitors in overcoming existing, and circumventing novel, resistances constitutes an attractive alternative. To that end, interference with *Pseudomonas*-specific signalling molecule synthesis and sensing hinder effective bacterial communication and abrogate acute virulence and chronic-like biofilm formation without affecting the commensal microbiota. The first goal of this thesis is to highlight the potential clinical relevance of targeting the PQS-quorum sensing network *in vitro* and *in vivo*. Not only potent and selective PqsR antagonists successfully hampered bacterial pathogenicity, but the rational design of dual-target PqsD/PqsR inhibitor further potentiated therapeutic benefits in addressing the often-present redundancy of existing QS signalling pathways.

Furthermore, the second goal of this work is to help understand some of the resistance mechanisms of prostate epithelium cancer cells to state-of-the-art androgen castration therapy with CYP17 inhibitor Abiraterone. We show the discovery and characterization of a resistance-related, neurosteroid-derived mitogenic compound, 5 α -pregnan-3 β ,6 α -diol-20-one, and the CYP17-independent formation of androgen precursor, DHEA. Our results add further evidence to the increasingly demonstrated phenomenon of oncogenic plasticity and neurotransdifferentiation of endocrine tumours. In this case, normalcy-related endocrine/paracrine mechanisms gradually shift to malignancy-related autocrine/autonomic pathways. These elusive mis-regulated, self-sufficient chemical languages evade current therapeutic strategies and argue for a shift in our clinical understanding of prostate cancer signalling.

8 RESULTS

8.1 Chapter 1 – Application of Dual Inhibition Concept within Looped Autoregulatory Systems toward Antivirulence Agents against *Pseudomonas aeruginosa* Infections

Andreas Thomann*, Antonio G. G. de Mello Martins*, Christian Brengel, Martin Empting, and Rolf W. Hartmann

* These authors contributed equally to this work.

Reprinted with permission from *ACS Chem Biol* **2016**, 11(5):1279-86.

Copyright © 2016, American Chemical Society.

Application of Dual Inhibition Concept within Looped Autoregulatory Systems toward Antivirulence Agents against *Pseudomonas aeruginosa* Infections

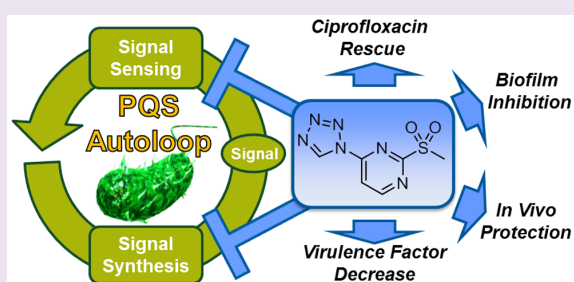
Andreas Thomann,^{§,†} Antonio G. G. de Mello Martins,^{§,†} Christian Brengel,[†] Martin Empting,^{*,†,‡} and Rolf W. Hartmann^{*,†,‡}

[†]Helmholtz Institute for Pharmaceutical Research Saarland (HIPS), Department for Drug Design and Optimization, Campus E8.1, 66123 Saarbrücken, Germany

[‡]Department of Pharmacy, Pharmaceutical and Medicinal Chemistry, Saarland University, Campus C2.3, 66123 Saarbrücken, Germany

Supporting Information

ABSTRACT: *Pseudomonas aeruginosa* quorum-sensing (QS) is a sophisticated network of genome-wide regulation triggered in response to population density. A major component is the self-inducing pseudomonas quinolone signal (PQS) QS system that regulates the production of several nonvital virulence- and biofilm-related determinants. Hence, QS circuitry is an attractive target for antivirulence agents with lowered resistance development potential and a good model to study the concept of polypharmacology in autoloop-regulated systems *per se*. Based on the finding that a combination of PqsR antagonist and PqsD inhibitor synergistically lowers pyocyanin, we have developed a dual-inhibitor compound of low molecular weight and high solubility that targets PQS transcriptional regulator (PqsR) and PqsD, a key enzyme in the biosynthesis of PQS-QS signal molecules (HHQ and PQS). *In vitro*, this compound markedly reduced virulence factor production and biofilm formation accompanied by a diminished content of extracellular DNA (eDNA). Additionally, coadministration with ciprofloxacin increased susceptibility of PA14 to antibiotic treatment under biofilm conditions. Finally, disruption of pathogenicity mechanisms was also assessed *in vivo*, with significantly increased survival of challenged larvae in a *Galleria mellonella* infection model. Favorable physicochemical properties and effects on virulence/biofilm establish a promising starting point for further optimization. In particular, the ability to address two targets of the PQS autoinduction cycle at the same time with a single compound holds great promise in achieving enhanced synergistic cellular effects while potentially lowering rates of resistance development.



Polypharmacology, or addressing two or more disease-related targets at the same time, has proven to have a significant impact on the treatment efficacy of, e.g., cancer,^{1,2} bacterial^{3,4} and viral infections,⁵ high blood pressure,⁶ asthma,⁷ and hormone-related diseases⁸ in clinical setups. These multitarget effects are in most cases achieved by a combination of selective single target agents. Drug combinations can either act synergistically, whereby the combined effect is greater than the sum of their separate responses, or additively, when the resulting activity is the outcome of their combined individual effects, both of which are shown to have favorable outcomes on lowered resistance development in cancer⁹ and microbial¹⁰ infections.¹¹ Unfortunately, such multidrug cocktails may incur several drawbacks, such as undesired drug–drug interactions and increasingly complex dosing schemes resulting in a lesser compliance of patients to follow the prescribed intake schedules.¹² To reduce those problems, development of multitarget drugs is a worthwhile endeavor. In many of the

above-mentioned intricate systems, self-inducing autoloop cycles can be found. In this study, we describe the concept of such a multitarget approach in positively regulated autoloop systems to achieve beneficial and synergistic inhibitory effects against *Pseudomonas aeruginosa* (PA) infections. Autoinducing pathways are widely spread in mammalian,¹³ plant,¹⁴ and bacterial kingdoms¹⁵ and regulate vital functions in a variety of organisms.

As a model system to provide proof of this concept, we chose the cell-density-dependent¹⁶ *Pseudomonas* quinolone signal quorum-sensing system (PQS-QS) of *Pseudomonas aeruginosa*, which was intensively studied by us in the past.^{17–19} In PA, PQS and 2-heptyl-4-quinolone (HHQ) are the natural agonists of PqsR, which is the transcriptional regulator of the *pqsABCDE*

Received: February 5, 2016

Accepted: February 16, 2016

Published: February 16, 2016

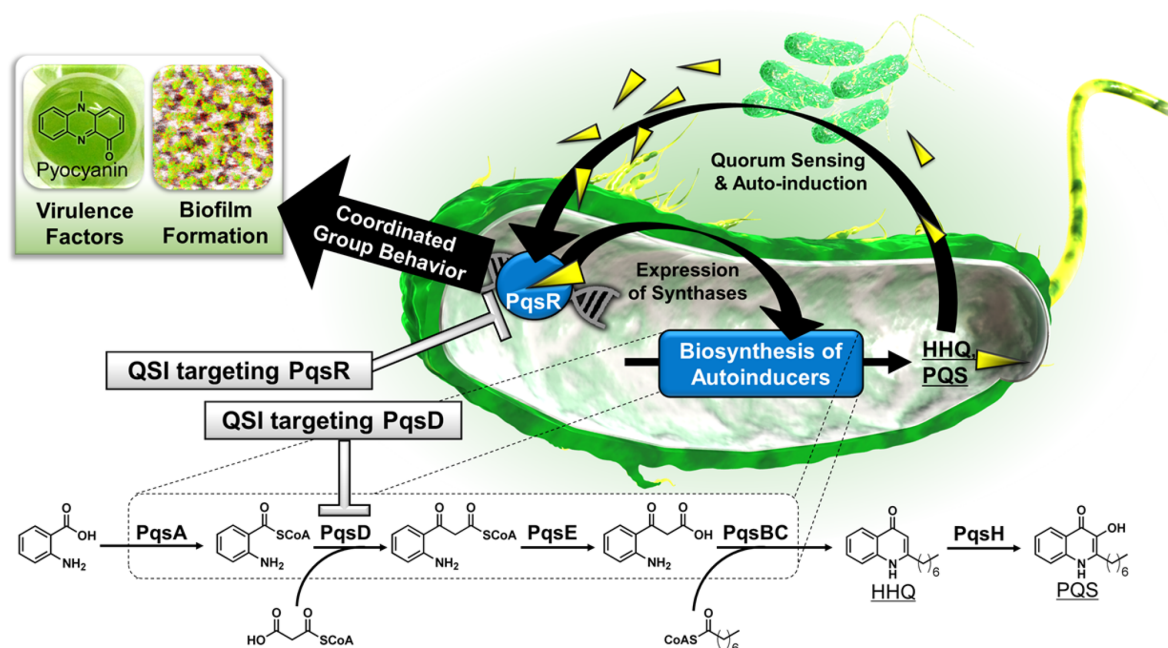


Figure 1. Schematic representation of the *Pseudomonas* quinolone signal (PQS) quorum-sensing system, involved in virulence factor production and biofilm formation. Anthranilate is converted by the *pqsABCDE* gene products into 2-heptyl-4-quinolone (HHQ), which can be converted intracellularly into PQS by the action of PqsH. HHQ and PQS are ligands of the Pqs Receptor (PqsR). Simultaneous inhibition of PQS synthesis (e.g., through PqsD) and interference with the autoloop transcriptional regulator PqsR lead to increased reduction of pathogenicity-associated biomarkers.

operon (Figure 1).²⁰ This operon harbors the genes encoding for the synthases responsible for PQS production. Thus, as soon as PQS and/or HHQ activate PqsR, they induce their own production and the concentration of signal molecules rises exponentially (Figure 1).²¹ Interference experiments, combined with mutational analysis, revealed PqsR and PqsD to be attractive drug targets for reducing pathogenicity of PA *in vivo*.^{17,22} Thus, PQS-QS displays an ideal and relevant model to study the concept of polypharmacology in such positive feedback loops with the possibility to directly transfer the results herein toward other similarly controlled biological systems. Furthermore, we directly put the lessons learned from drug combination experiments to an application for the straightforward rational design of the first drug-like dual-target PqsD/R inhibitors. Additionally, an optimized compound was achieved that shows promising reduction of two major virulence factors and biofilm inhibition *in vitro*. Finally, this optimized dual inhibitor displayed convincing activity in an *in vivo* acute PA infection model.

RESULTS AND DISCUSSION

Combination of PqsD Inhibitor and PqsR Antagonist Prominently Reduces Relevant Marker Pyocyanin through Synergistic Activity. As proof of principle to assess the amenability of the PQS-QS system to dual-target inhibition with improved outcome, we initially investigated the combinatorial effect of a PqsD inhibitor and a PqsR antagonist on a QS-dependent PA-exclusive secondary metabolite, pyocyanin.^{23,24} Pyocyanin is one of PA's most prominent virulence factors with distinct roles in acute infection establishment and biofilm formation. Pyocyanin also substantially contributes to the generation of reactive oxygen species

(ROS) by inhibiting the activity of catalase in eukaryotic cells. ROS is one of *Pseudomonas*' adaptations to environmental competition against other microbes and is the cause for its cytotoxicity toward eukaryotic cells.²⁵ As a consequence, pyocyanin production is linked to increased inflammation, modulation of iron metabolism, and tissue necrosis.²⁶ Its important physiological role in diseased states and correlation with the QS system suggest that by monitoring pyocyanin levels we may gain relevant insights into the suitability of dual inhibition that efficiently targets PA virulence.

We cultured *P. aeruginosa* (PA14) wild type in the presence of different concentrations of a PqsD inhibitor **1**¹⁹ and PqsR antagonist **2**,¹⁷ as a single treatment or combination therapy. As seen in Figure 2, 500 μM of **1** alone does not influence the production of pyocyanin, but interestingly, when added in combination with 15 μM of **2**, we observed a dose-dependent decrease in pyocyanin production. Notably, the decrease from 38% (**2** alone) to 34%, 23%, and 18% (**2** added of 100 μM , 300 μM , and 500 μM of **1**, respectively) is highly significant at higher concentrations of **1**, corroborating the synergistic activity of two PQS-QS inhibitors with different modes of action. These results further demonstrate that a biomarker negative synthase inhibitor (e.g., compound **1**) can indirectly increase the potency of a receptor antagonist (e.g., **2**) presumably by decreasing the natural ligand concentration and thus lowering competition to the receptor's binding site. However, when extending the exposure of PA14 to PqsD inhibitor **1**, we observed a slight, yet significant, reduction of pyocyanin after 48 h of incubation (see Supporting Information, section IIc). Obviously, a continuous attenuation of PQS/HHQ production through PqsD inhibition can result in an antivirulence effect.

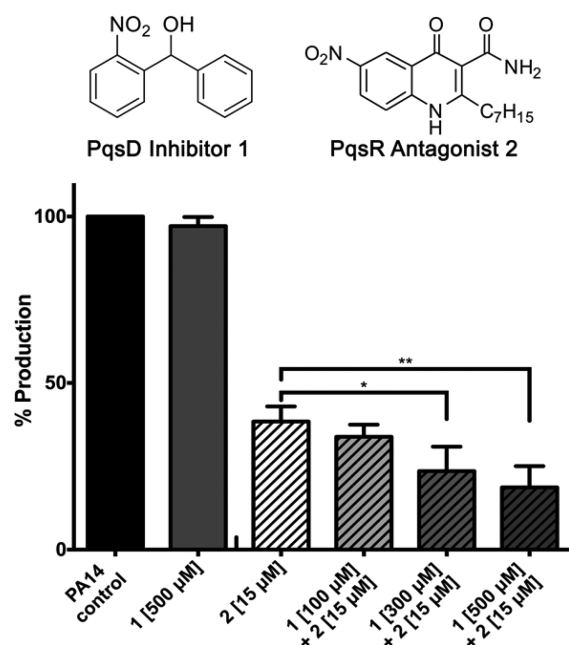


Figure 2. Synergistic activity of PqsD inhibitor 1 and PqsR antagonist 2 on pyocyanin inhibition in PA14 wild type. Treatment with 500 μM of 1 alone did not alter pyocyanin production. However, basal pyocyanin production under inhibition with 15 μM of 2 is significantly increased upon combinatorial titrated administration of 1 (100 μM , 300 μM , and 500 μM , respectively), indicative of synergistic activity. All values are relative to a control without inhibitors. Error bars represent the standard deviation of three independent experiments ($n = 3$). * = $p < 0.05$, ** = $p < 0.005$.

Application of Concept Study toward the Rational Design of Dual PqsD/R Inhibitors. Having demonstrated the potential of combining synthase inhibition and receptor antagonism, we searched through our in-house inhibitor library with regard to structural similarity of selective PqsD and PqsR

inhibitors. From this search, we found compound 3, which was designed as a PqsR antagonist ($\text{IC}_{50} = 26 \mu\text{M}$) with good activity on PA's virulence factor pyocyanin (Figure 3) and a quite similar compound, 4, which was designed to target PqsD ($\text{IC}_{50} = 1.7 \mu\text{M}$) based on SPR screening results recently reported by us (Figure 3).²⁷ As for 1, compound 4 displayed no inhibitory activity on pyocyanin even at the maximum soluble concentration.

Although, both compounds are selective for their respective targets, they share the same molecular scaffold: a pyrimidine core decorated with a triazole and a sulfone moiety (Figure 3). Thus, we decided to synthesize compound 5 and assess its biological activity, as it represents a simplified molecule consisting only of the shared structural features. Notably, the obtained compound 5 showed inhibition of both targets. Moreover, in very good accordance to our conceptual studies (*vide supra*), compound 5 showed a stronger reduction of pyocyanin compared to the equipotent PqsR selective precursor 3 (Figure 3). These results indicate that the concept of dual inhibition with combination experiments and the observed synergism can be directly combined in one compound. With regard to ligand lipophilicity efficiency (LLE), a metric used in medicinal chemistry to evaluate the activity of a compound based on its molecular weight and lipophilicity for further drug design, 5 showed a LLE = 0.56 on both targets which is above the suggested minimum score of 0.3.²⁸ To further improve the potential of 5 based on its LLE, we decided to modify it *via* a bioisosteric replacement of C4 at the triazole substituent. Introducing a nitrogen at this site yielded the tetrazole congener 6 (Figure 3). To confirm the regiochemistry of the introduced tetrazole moiety, we crystallized intermediate 6a²⁹ and verified the structure by X-ray analysis (CCDC-No.: 1432241, Supporting Information, section 1b.). As expected for the tetrazole substituent, lipophilicity of 6 dropped compared to 5, leading to an increase of the LLE score (PqsR = 0.67; PqsD = 0.66) and better solubility. Notably, activity on PqsR was slightly increased, while activity on PqsD was retained, resulting in an overall IC_{50} on pyocyanin of 86 μM (Figure 3).

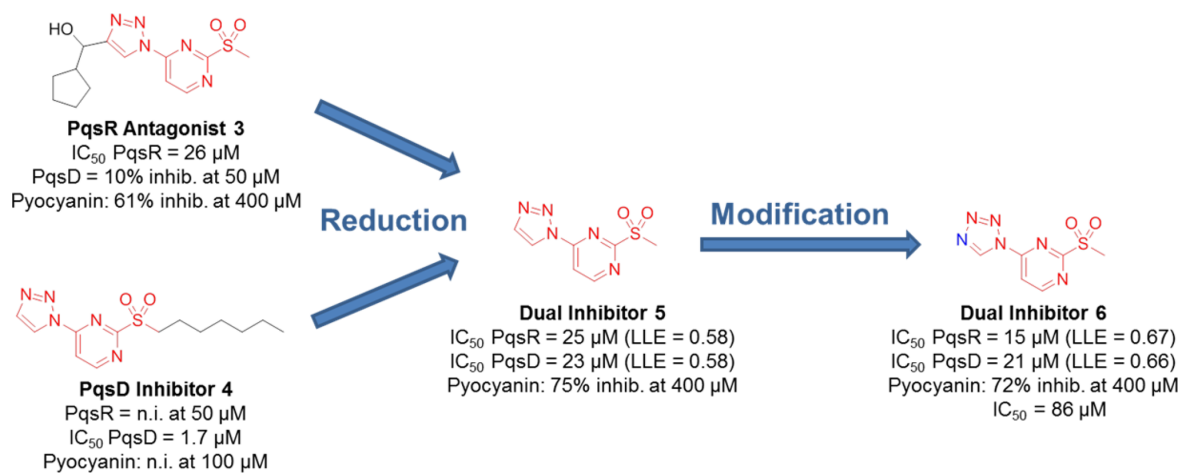


Figure 3. Reduction of structurally related PqsR antagonist 3 and PqsD inhibitor 4 to the common molecular core resulting in the first dual-active compound 5 (red). In comparison to 3, 5 shows higher activity on pyocyanin, although being similarly active on PqsR, corroborating the findings of the combination experiments (Figure 2). Bioisosteric modification (blue) led to dual inhibitor 6 with improved physicochemical properties as shown by its increased ligand lipophilicity efficiency (LLE).

Dual Inhibitor Not Only Affects Pyocyanin Production but Also Modulates the Generation of a Second Virulence Factor, Pyoverdine (PVD). Pyoverdines are *Pseudomonas*' primary siderophores. These fluorescent signaling molecules are used by the bacterium in iron scavenging and metabolism and are closely related to the production of other virulence factors in acute infections, as well as the correct architectural construction of biofilms.^{30,31} Since the absence of PVD in deficient mutants has shown to drastically reduce infection ability,³² and iron acquisition *in vitro* is linked to biofilm formation,³³ PVD metabolism provides a connection between acute pathogenicity and biofilm-related severe infections. The intrinsic relationship of PQS and PVD signaling pathways in iron metabolism and virulence has been shown to be mutual: on one hand, PQS induces the expression of genes involved in the biosynthesis of PVD,³⁴ on the other, PvdS, one of the major regulators in the biosynthesis of PVD, controls the expression of PqsR.^{35,36} Hence, we investigated whether our PQS dual inhibitor would have a beneficial effect on PVD inhibition by targeting PQS biosynthesis. We grew PA14 wild-type cultures in the presence of increasing concentrations of **6** (Figure 4). In accordance with our assumption, **6** was able to

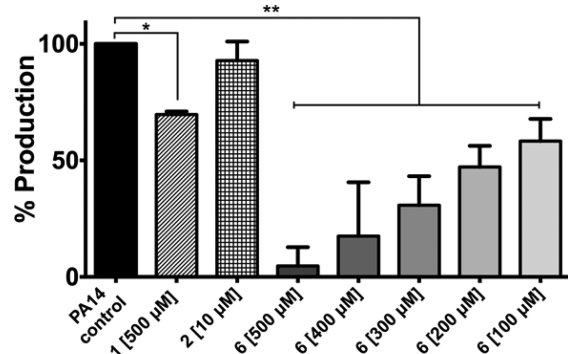


Figure 4. Effects of compounds **1**, **2**, and **6** on pyoverdine production. Compound **6** showed a prominent, significant decrease in pyoverdine levels in a concentration-dependent manner. At the highest concentration of 500 μM , pyoverdine production was almost completely arrested (5% \pm 8), and halved at the lowest inhibitor concentration of 100 μM (58% \pm 10). All values are relative to a control without inhibitors. Error bars represent standard deviation of three independent experiments ($n = 3$). * = $p < 0.05$, ** = $p < 0.005$.

decrease PVD significantly in all tested concentrations (500 μM to 100 μM). Production of the siderophore was essentially blocked at the highest tested concentration of **6**, while compounds **1** and **2** had only moderate or low effects in this assay (69.7% \pm 1.3 and 92.8% \pm 8.2, respectively). Thus, dual inhibitor **6** is not only able to target pyocyanin biosynthesis, but also addresses PVD production, disrupting iron metabolism, and virulence factor production, ultimately reducing the environmental competitive advantage of PA, as well as its pathogenicity to lower levels that better respond to treatment. These beneficial cellular effects may contribute to attenuation of biofilm formation and establishment—a scenario that we further investigated in our next experiments.

Compound 6 Reduces Biofilm Formation and Restores Antibiotic Efficacy. Biofilms are one of the major clinically relevant resistance mechanisms of PA against antibiotic treatment,³⁷ immune responses,³⁸ and antimicrobial peptides³⁹ in particular. Thus, reduction of biofilm mass holds the potential to enable immunological clearance of the pathogen and restore antibiotic activity, features of undoubtedly high interest. The development of biofilms is dependent on the PQS Quorum sensing network, as shown in previous knockout studies.⁴⁰ Recently, we showed that PqsD inhibitor **1** reduces PA biofilms at high concentrations (reduction of biofilm volume to 62% at 500 μM).¹⁹ Furthermore, antibiofilm activities have been reported for PqsR antagonists designed on the basis of the natural ligand HHQ,⁴¹ the biological precursor of PQS (Figure 1), and we observed a reduction in biofilm volume by compound **2** to 84.8% \pm 4.7 at 15 μM (see supplementary Figure 5). These target-related effects and the reduction of the biofilm-associated virulence factor PVD (*vide supra*) motivated us to test whether our dual target compound **6** was also active on preventing biofilm formation. Indeed, **6** displayed prominent effects on biofilm development with an IC_{50} of 100 μM (Figure 5A, circles). This is in good accordance with previously obtained data regarding biofilm inhibition targeting either PqsR or PqsD.^{19,41,42}

We concluded that the dual inhibition concept might not only pronouncedly reduce pyocyanin formation but also result in stronger inhibition of PA biofilm. To further validate the target of **6** under biofilm-conditions, we assessed whether the dual inhibitor is still active on a PqsR deficient mutant strain of PA. We observed a reduced activity of about 1 log unit of the ΔpqsR mutant strain compared to wild type PA. This result, on the one hand, underlines the target-related activity but also shows that the compound has an additional target involved in

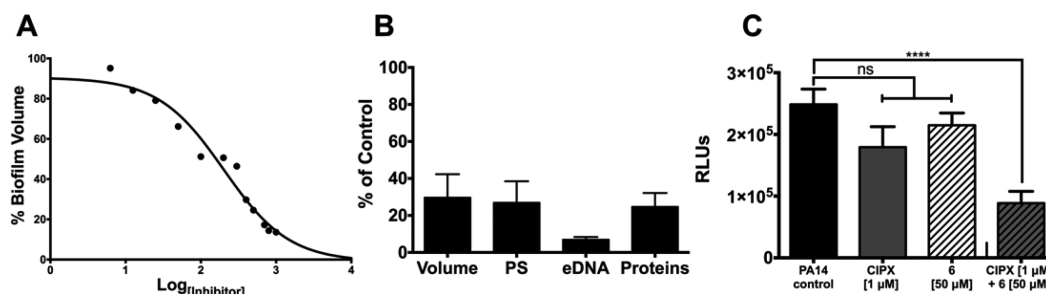


Figure 5. Dose-dependent reduction of biofilm in PA14 wild type cultures treated with compound **6** (A). Pronounced reduction of extracellular DNA (eDNA), polysaccharides (PS), and proteins of the biofilm matrix (Volume) was found at 400 μM of **6** (B). Activity of 1 μM ciprofloxacin (CIPX) was increased by a combination of the antibiotic with 50 μM of **6** under biofilm conditions (C). Error bars represent standard error of at least two independent experiments. ns = not significant, **** = $p < 0.0001$.

biofilm formation. A biofilm is a heterogeneous matrix composed of different components, e.g., polysaccharides (PS), proteins, lipopolysaccharides (LPS), and extracellular DNA (eDNA).⁴³ The latter has been described as responsible for resistance development against aminoglycoside⁴⁴ and fluoroquinolone antibiotics⁴⁵ as well as increased tolerance against host defensins.⁴⁶ Moreover, release of eDNA is directly regulated by the presence of pyocyanin⁴⁷ and PQS.⁴⁸ Hence, we were curious how **6** affects the components of the biofilm (Figure 5B). Our results demonstrate that **6** significantly inhibited eDNA release under biofilm conditions ($7\% \pm 2$ residual eDNA detected), which is in good accordance with the previous findings described above. Moreover, we observed a marked attenuation of PS and protein BF constituents down to $27\% \pm 20$ and $25\% \pm 13$, respectively. As a targeted decrease of eDNA might lead to higher efficacy of antibiotics on biofilm cultures of PA, we tested the susceptibility of PA14 against the fluoroquinolone-based antibiotic ciprofloxacin, the activity of which has been described to be hindered in the presence of eDNA.⁴⁵ Under biofilm conditions, no significant inhibition of PA viability by ciprofloxacin was observed (Figure 5C). However, in combination with **6**, which alone had no effect on the viability of PA, antibiotic activity could be restored under biofilm conditions that mimic a chronic infection *in vitro*. Furthermore, these findings complement published data regarding the application of PqsR antagonists in acute infection models.⁴² Thus, therapy of QSIs in combination with antibiotic treatment in acute and chronic PA infections holds great promise for future anti-infective drug discovery focusing on quorum sensing inhibition.

Compound **6** Reduces Pathogenicity of PA14 *In Vivo*.

Until today, a variety of *in vivo* models to assess the pathogenicity of PA were developed. We chose an animal infection model employing *Galleria mellonella* larvae which has been previously shown to have a high correlation with mouse PA infection models⁴⁹ and was also used by us to validate a PqsR antagonist *in vivo*.¹⁷ To determine efficacy of our dual-target compound **6**, *G. mellonella* larvae were inoculated with the agent in the presence and absence of PA. Interestingly, **6** was able to increase the survival rate of larvae in a dose-dependent manner with 53% survival at 1.25 nmol and 29% survival at 0.5 nmol applied dose (Figure 6). The susceptibility of larvae was described to be 50% if infected by one cell of PA.⁴⁹ Notably, in our experiments one larva was challenged with 10–13 PA cells, resulting in a very high bacterial load and hurdle to be taken by an anti-infective treatment. Regarding the average hemolymph and body weight ($450 \mu\text{L}$ and 450 mg)¹⁷ of each larvae, the most beneficial protective effect was observed at a dosage of 1.25 nmol, correspondent to a final *in vivo* concentration of $2.7 \mu\text{M}$ or 0.63 mg kg^{-1} .

Most interestingly, when assessing toxicity of **6** in *G. mellonella* we could show that even a 4 times higher concentration (5 nmol) than the effective dose was well tolerated with no observable disparity with PBS control.

CONCLUSION

In this study, we demonstrated the applicability of dual synergistic inhibition within the frame of positive feedback autoloop systems as a novel concept for the development of quorum sensing inhibitors. We chose the model PQS-QS system of *Pseudomonas aeruginosa* to demonstrate that an enzyme inhibitor **1** can increase the potency of the associated receptor antagonist **2** regarding virulence factor production.

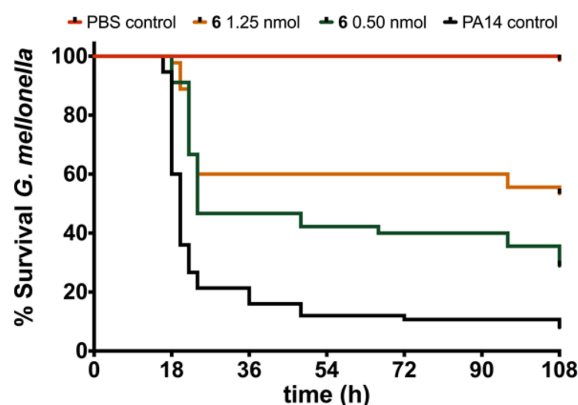


Figure 6. Dose-dependent *in vivo* protective effect of **6** on the survival of *Pseudomonas aeruginosa* PA14-challenged larvae of *Galleria mellonella*. Survival rate was significantly higher for treated larvae (0.5 nmol or 1.25 nmol) compared to the untreated control (0.5 and 1.25 nmol applied doses; $p < 0.0001$; log-rank test).

Presumably, this beneficial effect is due to lowered signal molecule levels and, therefore, less competition at the receptor's binding site. We successfully exploited this concept of dual inhibition in a rational design strategy to achieve the first dual-active inhibitor **5** targeting the PQS-QS system. This compound was further improved by bioisosteric replacement, culminating in inhibitor **6** with an enhanced efficiency/lipophilicity profile. This compound effectively reduced pyocyanin and pyoverdine, two major virulence factors of PA, in a dose-dependent manner without affecting bacterial growth. Importantly, **6** had a strong effect on PA biofilm assembly and restored the efficacy of ciprofloxacin, presumably due to hindrance of eDNA release. Finally, dual inhibitor **6** was also active *in vivo*, protecting *G. mellonella* larvae from lethal PA infections. Taken together, the presented dual inhibition strategy holds great potential to effectively interfere with intricate cellular systems. Via this promising approach, we achieved an enhanced bioactivity profile through synergistic action at two points-of-intervention (PqsD and PqsR) within a positive feedback loop (the PQS-QS system). Hence, this strategy might be a powerful tool for devising new treatment options for diseases related to complex or compensatory metabolic pathways similar to the one investigated in this study.

METHODS

Pyocyanin Assay. Pyocyanin formation was assessed as previously described^{18,23,50} with minor modifications. A single colony was removed from agar plates after 16 h of growth at $37 \text{ }^\circ\text{C}$ and transferred into 25 mL Erlenmeyer flasks with 10 mL of PPGAS medium. Following 19 h of aerobic growth with shaking at 200 rpm and $37 \text{ }^\circ\text{C}$, cultures were centrifuged at $7.450g$, washed once with 10 mL of fresh PPGAS medium, and resuspended to a final volume of 5 mL. Cultures were then diluted to a final OD_{600} of 0.02 and distributed into test tubes in 1.2 mL aliquots. Compounds **1** and **2** were added in 1:100 dilutions with a final DMSO concentration of 1% (v/v). Treated and untreated cultures were incubated for an additional 17 h under aerobic conditions as mentioned above. Pyocyanin was extracted by adding 900 μL of chloroform to 900 μL of overnight culture and subsequently re-extracted with 250 μL of 0.2 M HCl from the organic phase. OD_{520} was measured in the aqueous phase. Pyocyanin formation values were normalized to a corresponding OD_{600} of the respective sample.

Pyoverdine Assay. For the analysis of pyoverdine formation, culture workup and stock solution of compounds **1**, **2**, and **6** were performed as described above (Pyocyanin Assay). Treated and untreated cultures were incubated in 200 μL of PPGAS medium for 8 h under aerobic conditions in black 96-well plates with glass bottoms. This allowed for the simultaneous measurements of pyoverdine (fluorescent light units with excitation at 400 ± 10 and emission at 460 ± 10) and bacterial growth at OD_{600} . Inhibition of pyoverdine was normalized to OD_{600} values.

Galleria mellonella Virulence Assay. An infection model of *G. mellonella* was used to determine disruption of virulence mechanisms *in vivo* as described in the works of Lu *et al.*¹⁷ Treatment conditions of larvae included (a) sterile PBS solution, (b) PA14 suspension, (c) 0.50 nmol of compound **6** in “b,” and (d) 1.25 nmol of compound **6** in “b.” For each treatment, data from at least three independent experiments were combined.

Biofilm Assay. Commonly used crystal violet (CV) assay procedures^{51–53} were adapted for determination of biofilm mass. For the cultivation of biofilm in 96-well plates, the protocol described by Frei *et al.*⁵³ was slightly modified by replacement of the medium and the *Pseudomonas* strain used. The experiment was performed using the *P. aeruginosa* PA14 strain (including ΔpqsR mutant, kindly provided by S. Häußler) and M63 medium.⁵⁴ CV staining was used to detect compound effects on the overall biofilm biomass. The impact on eDNA was assessed by incubation of biofilm with propidium iodine solution (0.05 mg mL^{-1}) for 3 h and detection of specific fluorescence at 620 nm after a thorough washing step with 18M Ω H_2O .⁵⁵ Polysaccharide levels in biofilm were specified by congo red staining described by Ghafoor *et al.*⁵⁶ For this purpose, a 20 mg mL^{-1} congo red solution was incubated with the matured biofilm for 3 h, followed by a washing step with water and the concentration measurement at 490 nm. For the detection of protein levels, Bradford reagent was diluted 1:5 (Roti-Quant, Carl Roth) and incubated with the washed biofilm for 5 min.⁵⁷ Next, 18M Ω H_2O was used to remove unbound dye. The amount of proteins was determined by absorbance measurement at 595 nm. To investigate the killing efficacy of ciprofloxacin in combination with QS inhibitor on biofilm-encapsulated bacteria, biofilm was grown under the same conditions used for CV assay. At first, biofilm growth was initiated under QS inhibitor treatment (50 μM) or DMSO control. After washing steps, matured biofilm was incubated with 4 $\mu\text{g mL}^{-1}$ ciprofloxacin dissolved in M63 medium and grown for a further 24 h. Viability of bacteria in the biofilm was determined by BacTiter-Glo Assay using black plates.⁵⁸

Chemical Synthesis and Analytical Characterization. NMR spectra were recorded on an Avance AV 300 or a Bruker DRX 500. The residual proton, ^1H , or carbon, ^{13}C , resonances of the >99% deuterated solvents were used for internal reference of all spectra acquired (CDCl₃ ^1H 7.260 ppm, ^{13}C 77.16 ppm; DMSO-*d*₆ ^1H 2.500 ppm, ^{13}C 39.52 ppm). Electrospray ionization (ESI) mass spectrometry and LC-UV purity determination were recorded with a Surveyor LC system MSQ electrospray mass spectrometer (ThermoFisher) LC-MS couple and acetonitrile/water gradient in positive mode (+), if not indicated otherwise. Then, 1% TFA was added if necessary. Compound **6** was analyzed using a setup produced by Waters Corporation containing a 2767 Sample Manager, a 2545 binary gradient pump, a 2998 PDA detector, and a 3100 electron spray mass spectrometer. Water containing 0.1% formic acid and acetonitrile containing 0.1% formic acid were used as solvents for the analysis. A Waters X-Bridge column (C18, 150 \times 4.6 mm, 5 μM) has been used with a flow of 1 mL min^{-1} starting with 10% acid containing acetonitrile to 95% acid containing acetonitrile. All final compounds were of $\geq 95\%$ purity. Unless otherwise stated, all reagents used were purchased from commercial vendors and used without further purification.

■ ASSOCIATED CONTENT

■ Supporting Information

The Supporting Information is available free of charge on the ACS Publications website at DOI: 10.1021/acschembio.6b00117.

Spectra (^1H COSY, ^{13}C NMR, LC-MS, X-ray crystallography); synthetic procedures of described new compounds and details on PqsD and PqsR assays; growth curves, IC50 determination on Pyocyanin with **6**, LLE calculations, and antibiofilm effects of **2** (PDF)

■ AUTHOR INFORMATION

■ Corresponding Authors

*E-mail: martin.empting@helmholtz-hzi.de.

*E-mail: rolf.hartmann@helmholtz-hzi.de.

■ Author Contributions

[§]These authors contributed equally.

■ Funding

This project was funded by BMBF through grant 1616038B.

■ Notes

The authors declare no competing financial interest.

■ ACKNOWLEDGMENTS

We thank C. Maurer, S. Amann, and C. Scheidt for performing and supervising the PqsD, PqsR, and pyocyanin assays. Many thanks go to V. Huch for recording the X-ray structure of compound **6a** and B. Kirsch for helpful discussions and introduction to the *Galleria mellonella* assay. We thank C. Börger for LC-MS analysis of compound **6**.

■ ABBREVIATIONS

PQS, *Pseudomonas* Quinolone Signal; QS, Quorum Sensing; PA, *Pseudomonas aeruginosa*

■ REFERENCES

- (1) Tolaney, S. M.; Barry, W. T.; Dang, C. T.; Yardley, D. A.; Moy, B.; Marcom, P. K.; Albain, K. S.; Rugo, H. S.; Ellis, M.; Shapira, I.; Wolff, A. C.; Carey, L. A.; Overmoyer, B. A.; Partridge, A. H.; Guo, H.; Hudis, C. A.; Krop, I. E.; Burstein, H. J.; and Winer, E. P. (2015) Adjuvant paclitaxel and trastuzumab for node-negative, HER2-positive breast cancer. *N. Engl. J. Med.* 372, 134–141.
- (2) Robert, C.; Karaszewska, B.; Schachter, J.; Rutkowski, P.; Mackiewicz, A.; Stroiakovski, D.; Lichinitser, M.; Dummer, R.; Grange, F.; Mortier, L.; Chiarion-Sileni, V.; Drucis, K.; Krajsova, I.; Hauschild, A.; Lorigan, P.; Wolter, P.; Long, G. V.; Flaherty, K.; Nathan, P.; Ribas, A.; Martin, A.-M.; Sun, P.; Crist, W.; Legos, J.; Rubin, S. D.; Little, S. M.; and Schadendorf, D. (2015) Improved overall survival in melanoma with combined dabrafenib and trametinib. *N. Engl. J. Med.* 372, 30–39.
- (3) Diacon, A. H.; Pym, A.; Grobusch, M.; Patientia, R.; Rustomjee, R.; Page-Shipp, L.; Pistorius, C.; Krause, R.; Bogoshi, M.; Churchyard, G.; Venter, A.; Allen, J.; Palomino, J. C.; de Maree, T.; van Heeswijk, R. P. G.; Lounis, N.; Meyvisch, P.; Verbeeck, J.; Parys, W.; de Beule, K.; Andries, K.; and McNeeley, D. F. (2009) The diarylquinoline TMC207 for multidrug-resistant tuberculosis. *N. Engl. J. Med.* 360, 2397–2405.
- (4) Hilf, M.; Yu, V. L.; Sharp, J.; Zuravleff, J. J.; Korvick, J. A.; and Muder, R. R. (1989) Antibiotic therapy for *Pseudomonas aeruginosa* bacteremia: Outcome correlations in a prospective study of 200 patients. *Am. J. Med.* 87, 540–546.
- (5) Jarcho, J. A.; Gandhi, R. T.; and Gandhi, M. (2014) Single-pill combination regimens for treatment of HIV-1 infection. *N. Engl. J. Med.* 371, 248–259.

- (6) Sever, P. S., and Messerli, F. H. (2011) Hypertension management 2011: optimal combination therapy. *Eur. Heart J.* 32, 2499–2506.
- (7) Kerstjens, H. A. M., Engel, M., Dahl, R., Paggiaro, P., Beck, E., Vandewalker, M., Sigmund, R., Seibold, W., Moroni-Zentgraf, P., and Bateman, E. D. (2012) Tiotropium in asthma poorly controlled with standard combination therapy. *N. Engl. J. Med.* 367, 1198–1207.
- (8) Vilar, L., Naves, L. A., Machado, M. C., and Bronstein, M. D. (2015) Medical combination therapies in Cushing's disease. *Pituitary* 18, 253–262.
- (9) Samanta, D., Gilkes, D. M., Chaturvedi, P., Xiang, L., and Semenza, G. L. (2014) Hypoxia-inducible factors are required for chemotherapy resistance of breast cancer stem cells. *Proc. Natl. Acad. Sci. U. S. A.* 111, E5429–38.
- (10) Worthington, R. J., and Melander, C. (2013) Combination approaches to combat multidrug-resistant bacteria. *Trends Biotechnol.* 31, 177–184.
- (11) E. Buira, A. Jaen (2015) Impact of Fixed-Dose Combinations of Antiretrovirals on Prevalence Trends of HIV Resistance: A 7 Year Follow-Up Study. *J. AIDS Clin. Res.* 06, 10.4172/2155-6113.1000416.
- (12) Anighoro, A., Bajorath, J., and Rastelli, G. (2014) Polypharmacology: challenges and opportunities in drug discovery. *J. Med. Chem.* 57, 7874–7887.
- (13) Bombeli, T., and Spahn, D. R. (2004) Updates in perioperative coagulation: physiology and management of thromboembolism and haemorrhage. *Br. J. Anaesth.* 93, 275–287.
- (14) Petruzzelli, L., Coraggio, I., and Leubner-Metzger, G. (2000) Ethylene promotes ethylene biosynthesis during pea seed germination by positive feedback regulation of 1-aminocyclo-propane-1-carboxylic acid oxidase. *Planta* 211, 144–149.
- (15) van Hoek, M., and Hogeweg, P. (2007) The effect of stochasticity on the lac operon: an evolutionary perspective. *PLoS Comput. Biol.* 3, e111.
- (16) Swift, S., Allan Downie, J., Whitehead, N. A., Barnard, A. M., Salmond, G. P., and Williams, P. (2001) Quorum sensing as a population-density-dependent determinant of bacterial physiology. *Adv. Microb. Physiol.* 45, 199–270.
- (17) Lu, C., Maurer, C. K., Kirsch, B., Steinbach, A., and Hartmann, R. W. (2014) Overcoming the unexpected functional inversion of a PqsR antagonist in *Pseudomonas aeruginosa*: an in vivo potent antivirulence agent targeting pqs quorum sensing: An In Vivo Potent Antivirulence Agent Targeting pqs Quorum Sensing. *Angew. Chem., Int. Ed.* 53, 1109–1112.
- (18) Klein, T., Henn, C., de Jong, J. C., Zimmer, C., Kirsch, B., Maurer, C. K., Pistorius, D., Müller, R., Steinbach, A., and Hartmann, R. W. (2012) Identification of small-molecule antagonists of the *Pseudomonas aeruginosa* transcriptional regulator PqsR: biophysically guided hit discovery and optimization. *ACS Chem. Biol.* 7, 1496–1501.
- (19) Storz, M. P., Maurer, C. K., Zimmer, C., Wagner, N., Brengel, C., de Jong, J. C., Lucas, S., Müskén, M., Häussler, S., Steinbach, A., and Hartmann, R. W. (2012) Validation of PqsD as an anti-biofilm target in *Pseudomonas aeruginosa* by development of small-molecule inhibitors. *J. Am. Chem. Soc.* 134, 16143–16146.
- (20) Rutherford, S. T., and Bassler, B. L. (2012) Bacterial quorum sensing: its role in virulence and possibilities for its control. *Cold Spring Harbor Perspect. Med.* 2, a012427.
- (21) Déziel, E., Gopalan, S., Tampakaki, A. P., Lépine, F., Padfield, K. E., Saucier, M., Xiao, G., and Rahme, L. G. (2005) The contribution of MvfR to *Pseudomonas aeruginosa* pathogenesis and quorum sensing circuitry regulation: multiple quorum sensing-regulated genes are modulated without affecting lasRI, rhlRI or the production of N-acyl-L-homoserine lactones. *Mol. Microbiol.* 55, 998–1014.
- (22) Gallagher, L. A., McKnight, S. L., Kuznetsova, M. S., Pesci, E. C., and Manoil, C. (2002) Functions Required for Extracellular Quinolone Signaling by *Pseudomonas aeruginosa*. *J. Bacteriol.* 184, 6472–6480.
- (23) O'Loughlin, C. T., Miller, L. C., Siryaporn, A., Drescher, K., Semmelhack, M. F., and Bassler, B. L. (2013) A quorum-sensing inhibitor blocks *Pseudomonas aeruginosa* virulence and biofilm formation. *Proc. Natl. Acad. Sci. U. S. A.* 110, 17981–17986.
- (24) Recinos, D. A., Sekedat, M. D., Hernandez, A., Cohen, T. S., Sakhtah, H., Prince, A. S., Price-Whelan, A., and Dietrich, L. E. P. (2012) Redundant phenazine operons in *Pseudomonas aeruginosa* exhibit environment-dependent expression and differential roles in pathogenicity. *Proc. Natl. Acad. Sci. U. S. A.* 109, 19420–19425.
- (25) Mavrodi, D. V., Parejko, J. A., Mavrodi, O. V., Kwak, Y.-S., Weller, D. M., Blankenfeldt, W., and Thomashow, L. S. (2013) Recent insights into the diversity, frequency and ecological roles of phenazines in fluorescent *Pseudomonas* spp. *Environ. Microbiol.* 15, 675–686.
- (26) Priyaja, P., Jayesh, P., Philip, R., and Bright Singh, I. S. (2016) Pyocyanin induced in vitro oxidative damage and its toxicity level in human, fish and insect cell lines for its selective biological applications. *Cytotechnology* 68, 143.
- (27) Weidel, E., Negri, M., Empting, M., Hinsberger, S., and Hartmann, R. W. (2014) Composing compound libraries for hit discovery—rationality-driven preselection or random choice by structural diversity? *Future Med. Chem.* 6, 2057–2072.
- (28) Mortenson, P. N., and Murray, C. W. (2011) Assessing the lipophilicity of fragments and early hits. *J. Comput.-Aided Mol. Des.* 25, 663–667.
- (29) Thomann, A., Börger, C., Empting, M., and Hartmann, R. (2014) Microwave-Assisted Synthesis of 4-Substituted 2-Methylthio-pyrimidines. *Synlett* 25, 935–938.
- (30) Banin, E., Vasil, M. L., and Greenberg, E. P. (2005) Iron and *Pseudomonas aeruginosa* biofilm formation. *Proc. Natl. Acad. Sci. U. S. A.* 102, 11076–11081.
- (31) Cézard, C., Farvacques, N., and Sonnet, P. (2015) Chemistry and biology of pyoverdines, *Pseudomonas* primary siderophores. *Curr. Med. Chem.* 22, 165–186.
- (32) Stanners, C. P., and Goldberg, V. J. (1975) On the mechanism of neurotropism of vesicular stomatitis virus in newborn hamsters. Studies with temperature-sensitive mutants. *J. Gen. Virol.* 29, 281–296.
- (33) Visca, P., Imperi, F., and Lamont, I. L. (2007) Pyoverdine siderophores: from biogenesis to biosignificance. *Trends Microbiol.* 15, 22–30.
- (34) Diggle, S. P., Matthijs, S., Wright, V. J., Fletcher, M. P., Chhabra, S. R., Lamont, I. L., Kong, X., Hider, R. C., Cornelis, P., Cámara, M., and Williams, P. (2007) The *Pseudomonas aeruginosa* 4-quinolone signal molecules HHQ and PQS play multifunctional roles in quorum sensing and iron entrapment. *Chem. Biol.* 14, 87–96.
- (35) Bredenbruch, F., Geffers, R., Nimtz, M., Buer, J., and Häussler, S. (2006) The *Pseudomonas aeruginosa* quinolone signal (PQS) has an iron-chelating activity. *Environ. Microbiol.* 8, 1318–1329.
- (36) Jimenez, P. N., Koch, G., Thompson, J. A., Xavier, K. B., Cool, R. H., and Quax, W. J. (2012) The multiple signaling systems regulating virulence in *Pseudomonas aeruginosa*. *Microbiol. Mol. Biol. Rev.* 76, 46–65.
- (37) Drenkard, E. (2003) Antimicrobial resistance of *Pseudomonas aeruginosa* biofilms. *Microbes Infect.* 5, 1213–1219.
- (38) Alhede, M., Bjarnsholt, T., Givskov, M., and Alhede, M. (2014) *Pseudomonas aeruginosa* biofilms: mechanisms of immune evasion. *Adv. Appl. Microbiol.* 86, 1–40.
- (39) Lewenza, S. (2013) Extracellular DNA-induced antimicrobial peptide resistance mechanisms in *Pseudomonas aeruginosa*. *Front. Microbiol.* 4, 21.
- (40) Müskén, M., Di Fiore, S., Dötsch, A., Fischer, R., and Häussler, S. (2010) Genetic determinants of *Pseudomonas aeruginosa* biofilm establishment. *Microbiology* 156, 431–441.
- (41) Ilangovan, A., Fletcher, M., Rampioni, G., Pustelny, C., Rumbaugh, K., Heeb, S., Cámara, M., Truman, A., Chhabra, S. R., Emsley, J., and Williams, P. (2013) Structural basis for native agonist and synthetic inhibitor recognition by the *Pseudomonas aeruginosa* quorum sensing regulator PqsR (MvfR). *PLoS Pathog.* 9, e1003508.
- (42) Starkey, M., Lépine, F., Maura, D., Bandyopadhyaya, A., Lesic, B., He, J., Kitao, T., Righi, V., Milot, S., Tzika, A., and Rahme, L. (2014) Identification of anti-virulence compounds that disrupt quorum-

sensing regulated acute and persistent pathogenicity. *PLoS Pathog.* 10, e1004321.

(43) Wei, Q., and Ma, L. Z. (2013) Biofilm matrix and its regulation in *Pseudomonas aeruginosa*. *Int. J. Mol. Sci.* 14, 20983–21005.

(44) Chiang, W.-C., Nilsson, M., Jensen, P. Ø., Høiby, N., Nielsen, T. E., Givskov, M., and Tolker-Nielsen, T. (2013) Extracellular DNA shields against aminoglycosides in *Pseudomonas aeruginosa* biofilms. *Antimicrob. Agents Chemother.* 57, 2352–2361.

(45) Johnson, L., Horsman, S. R., Charron-Mazenod, L., Turnbull, A. L., Mulcahy, H., Surette, M. G., and Lewenza, S. (2013) Extracellular DNA-induced antimicrobial peptide resistance in *Salmonella enterica* serovar Typhimurium. *BMC Microbiol.* 13, 115.

(46) Jones, E. A., McGillivray, G., and Bakaletz, L. O. (2013) Extracellular DNA within a nontypeable *Haemophilus influenzae*-induced biofilm binds human beta defensin-3 and reduces its antimicrobial activity. *J. Innate Immun.* 5, 24–38.

(47) Das, T., and Manefield, M. (2012) Pyocyanin promotes extracellular DNA release in *Pseudomonas aeruginosa*. *PLoS One* 7, e46718.

(48) Häußler, S., and Becker, T. (2008) The pseudomonas quinolone signal (PQS) balances life and death in *Pseudomonas aeruginosa* populations. *PLoS Pathog.* 4, e1000166.

(49) Jander, G., Rahme, L. G., and Ausubel, F. M. (2000) Positive correlation between virulence of *Pseudomonas aeruginosa* mutants in mice and insects. *J. Bacteriol.* 182, 3843–3845.

(50) Essar, D. W., Eberly, L., Hadero, A., and Crawford, I. P. (1990) Identification and characterization of genes for a second anthranilate synthase in *Pseudomonas aeruginosa*: interchangeability of the two anthranilate synthases and evolutionary implications. *J. Bacteriol.* 172, 884–900.

(51) Christensen, G. D., Simpson, W. A., Younger, J. J., Baddour, L. M., Barrett, F. F., Melton, D. M., and Beachey, E. H. (1985) Adherence of coagulase-negative staphylococci to plastic tissue culture plates: a quantitative model for the adherence of staphylococci to medical devices. *J. Clin. Microbiol.* 22, 996–1006.

(52) O'Toole, G. A., Pratt, L. A., Watnick, P. I., Newman, D. K., Weaver, V. B., and Kolter, R. (1999) Genetic approaches to study of biofilms. *Methods Enzymol.* 310, 91–109.

(53) Frei, R., Breitbach, A. S., and Blackwell, H. E. (2012) 2-Aminobenzimidazole derivatives strongly inhibit and disperse *Pseudomonas aeruginosa* biofilms. *Angew. Chem., Int. Ed.* 51, 5226–5229.

(54) Elbing, K., and Brent, R. (2002) Media preparation and bacteriological tools, in *Curr. Protoc. Mol. Biol.* (Taylor, G. P., Ed.), pp 1.1.1–1.1.7, John Wiley & Sons, New York.

(55) Allesen-Holm, M., Barken, K. B., Yang, L., Klausen, M., Webb, J. S., Kjelleberg, S., Molin, S., Givskov, M., and Tolker-Nielsen, T. (2006) A characterization of DNA release in *Pseudomonas aeruginosa* cultures and biofilms. *Mol. Microbiol.* 59, 1114–1128.

(56) Ghafoor, A., Hay, I. D., and Rehm, B. H. A. (2011) Role of exopolysaccharides in *Pseudomonas aeruginosa* biofilm formation and architecture. *Appl. Environ. Microbiol.* 77, 5238–5246.

(57) Lembre, P., Lorentz, C., Di Martino, P. (2012) Exopolysaccharides of the Biofilm Matrix: A Complex Biophysical World, in *The Complex World of Polysaccharides* (Karunaratne, D. N., Ed.) 1st ed., pp 371–392, InTech, Rijeca.

(58) Sule, P., Wadhawan, T., Wolfe, A. J., Prüß, B. M. (2008) Promega Notes. *Promega Notes* 99. www.promega.de.

8.2 Chapter 2 – Effects of Next Generation PqsR-targeting Anti-infectives against Biofilm and Virulence of *Pseudomonas aeruginosa*

The following persons also contributed to the results described in this chapter:

1. Michael Zender: Synthesis and characterization of compounds; ITC measurements.
2. Christian Brengel: Helped coordinate and perform biofilm experiments.
3. Giuseppe Allegretta: HHQ and 2-AA measurements.
4. Benjamin Kirsch: Performance of *E. coli*-based PqsR assay.
5. Christine K Maurer: Performance of pyocyanin assay and solubility measurements.
6. Stefanie Wagner: Lectin experiments and expression levels.

INTRODUCTION

“It is time to close the book on infectious diseases, and declare the war against pestilence won” – even if the origin of this statement cannot be precisely tracked down¹, it reflects the conventional wisdom² over decades in the 20th century. But this popular belief was quickly abandoned due to the alarming occurrence of multi- and pan-resistant microbial pathogens.³ This situation has even been worsened by shortening the research efforts in the field of antibacterial drug discovery.^{4,5} Nowadays, we are facing a lack of novel treatment options for many human pathogens which acquired resistance against nearly all available antibiotics.⁶ The development of compounds which reduce bacterial virulence without affecting viability has attracted increasing attention during the last years. These antivirulence drugs have the potential to overcome the burden of rapid development and spreading of resistance mechanisms and may help to regenerate the antimicrobial development pipeline.⁷

Inspired by this idea, we and others targeted the virulence of *Pseudomonas aeruginosa*, a Gram-negative opportunistic human pathogen, by interference with bacterial cell-to-cell communication.⁸ The release of virulence determinants is regulated mainly by a process called quorum sensing (QS).⁹ QS enables *P. aeruginosa* to coordinate gene expression collectively dependent on bacterial cell-density *via* the release and sensing of small diffusible molecules.⁹ *P. aeruginosa* employs the *las*^{10,11} and *rhl*^{12,13} QS systems which use acetyl homoserine lactones (AHLs) as signaling molecules, prevalent among Gram-negative bacteria. Furthermore, this bacterium uses a rather unique system called *pqs*¹⁴ (*Pseudomonas* quinolone signal) applying alkylquinolones (AQs). The autoinducers 2-heptyl-3-hydroxy-4(1H)-quinolone (PQS) and its precursor 2-heptyl-4-quinolone (HHQ) activate the transcriptional regulator PqsR¹⁵ (*Pseudomonas* quinolone signaling receptor also referred to as MvfR).^{16,17,18} The activated receptor regulates the expression of various genes involved in the production of virulence factors e.g. pyocyanin¹⁶, elastase, lectines etc.¹⁹ Additionally PqsR up-regulates the expression of the HHQ biosynthesis operon *pqsA-E* to form an autoinductive loop.^{20,21} Moreover, the *pqs* system is involved in the establishment of *P. aeruginosa* biofilms *via* multiple ways. Mutants lacking of a functional *pqs* system showed a reduced release of eDNA²² and expression of lectins A/B¹⁹. Both are integral parts for the *P. aeruginosa* biofilm architecture.^{22,23} *P. aeruginosa* strains which switched to a sessile biofilm lifestyle are the main cause of chronic persistent pneumonia found in cystic fibrosis patients.^{24,25} Bacteria growing in the biofilm mode adapt to intense antibiotic treatment and to the host immune response.²⁵ Taken together, the *pqs* system and its central regulator PqsR play a critical role during the acute and chronic infections.

Following a ligand-based approach, we were able to transform the native agonist HHQ into the potent antagonists showing a lack of activity due to metabolic conversion in *P. aeruginosa*.^{26,27} Further optimization led to the analog **1** which was able to fully protect *Galleria mellonella* larvae from a lethal *P. aeruginosa* infection providing the first *in vivo* proof of concept.²⁷ In a similar approach quinazolinone-based antagonists were developed and the first crystal structure of the ligand-binding domain (LBD) of PqsR was solved.²⁸ The potential of PqsR as drug target was further corroborated by the benzamido-benzimidazole antagonists **2** and **3**. These antagonists originated from a high throughput screening (HTS) campaign. **3** was demonstrated to be efficacious in mouse acute infection models as standalone treatment and as a pathoblocker-antibiotic combination therapy.²⁹ All discovered antagonist suffer from poor physicochemical properties. To address this issue we initiated two fragment screening campaigns^{30,31} which led to chemically diverse ligands. The optimization of 2-amino-pyridine derivatives (**4**) resulted in nanomolar active antagonists.³²

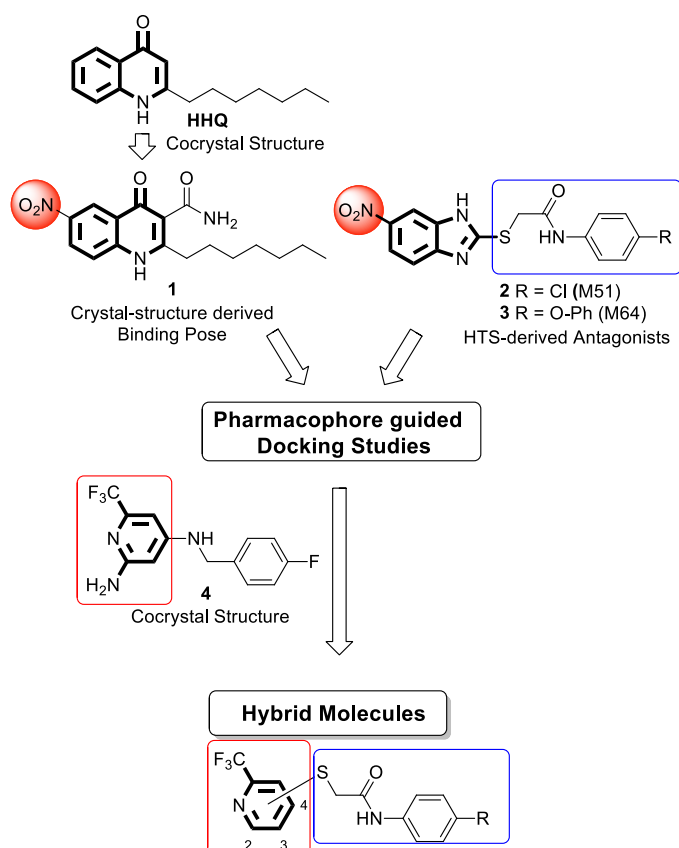


Figure 1. Published PqsR antagonists (**1-4**) and schematic representation of the applied medicinal chemistry strategy.

In this manuscript, we report on the nifty development of hybrid compounds by merging of the reported HTS hit **2** and the fragment-screening-derived antagonist **4**. We were able to generate a plausible binding-pose of **2** based on a pharmacophore-guided docking approach. An overlay

CHAPTER 2

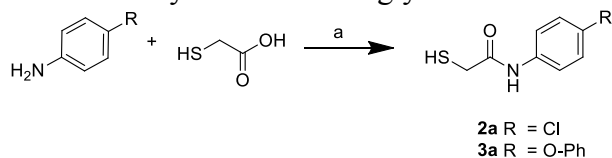
with the crystal structure of **4** led to the synthesis of hybrid compounds consisting of a trifluoromethyl-pyridine headgroup derived from a fragment screening³² and the thioglycolamide-aryl moieties of **2** and **3**, respectively. These hybrid compounds showed an improved physico-chemical profile while keeping high on-target and antivirulence activities. Furthermore, these compounds displayed specific effects on *P. aeruginosa* biofilms by abolishing the release of eDNA.

RESULTS AND DISCUSSION

Chemistry

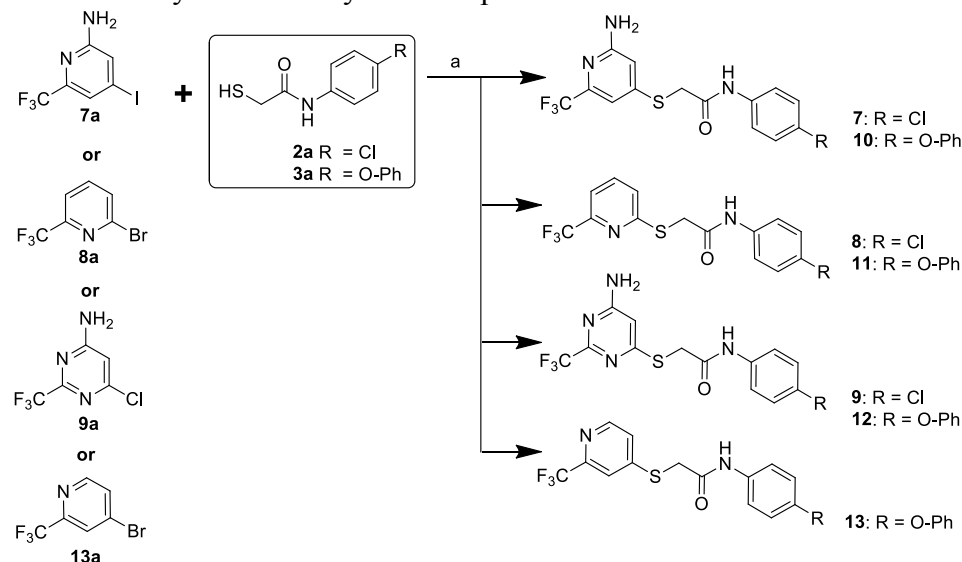
Fragment hits **5** and **6** were obtained from commercial suppliers. The synthesis of the key precursors **2a** and **3a** is shown in Scheme 1. The particular anilines were condensed with thioglycolic acid in neat reaction at 130°C under an argon atmosphere.³³ After cooling to RT the product was isolated in good yields by simple trituration with isopropanol and filtration.

Scheme 1. Synthesis of Thioglycolamide Precursors^a,



^aReagents and Conditions: a) pressure vial, neat, 130°C, Ar.

The heteroaryl halide **7a** was synthesized as described in our previous publication.³² Precursors **8a**, **9a** and **13a** were obtained from commercial suppliers. Hybrid compounds **7-12** were synthesized as outlined in Scheme 2. Heteroaryl halides **7a-9a**, **13a** were reacted with **2a** and **3a** in a classical S_NAr reaction using potassium carbonate as base to give the final products **7-13**.

Scheme 2. Synthesis of Hybrid Compounds.

^aReagents and Conditions: a) K_2CO_3 , DMF, $-20^\circ C$ to RT, Ar.

In-silico studies

Fragment-based lead discovery and HTS are often described as “mutually exclusive” strategies although there are complementary aspects of both approaches as well.³⁴ The discovery of benzamido-benzimidazole PqsR antagonists²⁹ (**2** and **3**) by a HTS screening inspired us to investigate on their binding mode (Figure 1) in order to combine these insights with structural information of the identified fragment hits. The nitro moiety was identified as obvious common feature in the quinolone class (**1**)²⁶ and in the benzamido-benzimidazole class (**2** and **3**)²⁹. Hence, we hypothesized that both antagonist classes overlap at this position in the LBD. The structure of the LBD in complex with the quinolone derivatives NHQ²⁸ (2-nonyl-4-quinolone) and HHQ³² were resolved. Based on these crystallographic results we derived a binding pose of the highly similar antagonist **1** (Figure 2A). Following our hypothesis, the nitro moiety and the adjacent aryl ring were defined as essential pharmacophore points. Subsequently, a pharmacophore-guided docking study with compound **2** was conducted. **2** was used due to lower number of rotatable bonds compared to **3** what facilitated a more accurate docking due to lower degrees of conformational freedom in the ligand.

The thioglycol amide linker adopted an angled position in all generated docking poses which positioned the 4-chloro-phenyl ring in the alkyl sidechain pocket of HHQ. We superimposed these docking poses with the crystal structure of **4** (Figure 2B and 2C). The trifluoromethyl moiety of **4** is similarly oriented as the nitro group of **1** and **2**. This finding was in line with the SAR observed by Lu *et al.* where the nitro group was exchanged by trifluoromethyl without any change of the antagonistic activity.²⁶ To further validate our binding hypothesis, we used

fragment competition studies. The amino-pyridine headgroup of **4** binds into the quinolone pocket (Figure 2B) and fragment **5** was used as a mimic thereof. According to our hypothesis the 5-nitro-benzimidazole heterocycle of **2** also occupies the same part of the pocket. In this case, fragment **6** was used.

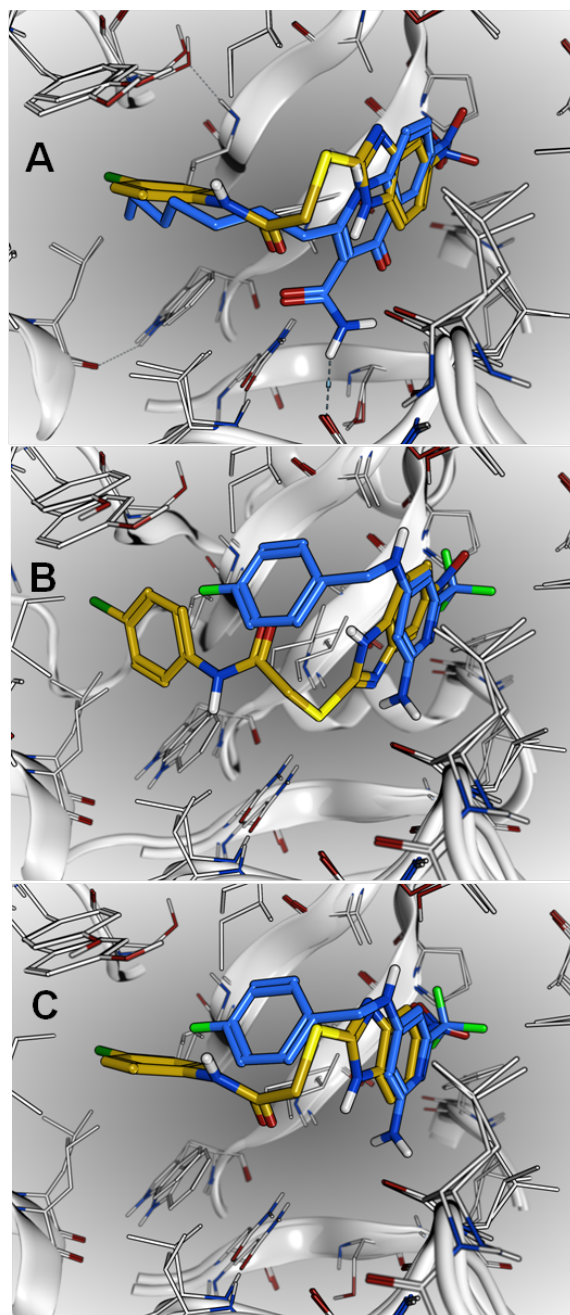


Figure 2. PqsR docking studies: (A) overlay of modeled binding mode of **1** (blue) and highest scored docking pose for **2** (yellow). (B) overlay of the crystal structure of **4** and highest ranked docking pose of **2** (yellow). (C) alternative binding pose of **2** (yellow) superimposed with crystal structure of **4**.

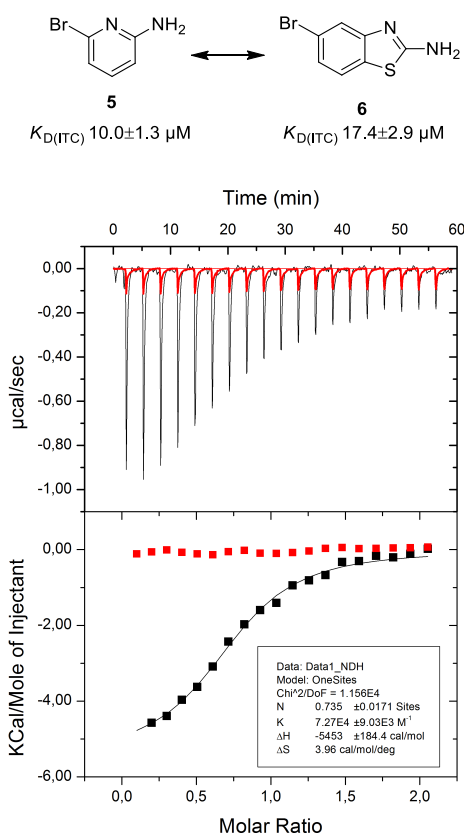


Figure 3. ITC competition experiments. Raw ITC data are shown on top and integrated normalized data on bottom. Titration of 150 μM PqsR with 1500 μM **6** (■, black curve); Titration of 150 μM PqsR with 1500 μM **6** in the presence of 1500 μM compound **5** (Δ, red curve).

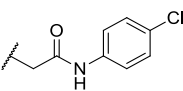
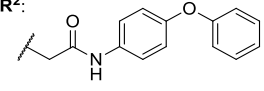
According to isothermal titration calorimetry (ITC) competition experiments both fragments compete for binding to PqsR (Figure 3) what is indicated by the loss of heat release when **6** is titrated to PqsR in the presence of **5**. This finding clearly corroborates our binding model. Overall, the most striking difference between the particular docking poses of **2** was observed for the most flexible linker part. Comparing the poses depicted in Figure 2B and 2C, the position of the benzimidazole is shifted leading to altered linker geometry. These results promoted the positions 2-4 at the pyridine as possible attachment points for the thioglycolamide aryl moiety (Figure 1). In a parallel approach, the 4-position was discovered as vector for growing the trifluoromethyl pyridine headgroup.³² Thus, this position was included and the fact that similar heteroaryl compounds were also reported as hits from the HTS campaign³⁵ encouraged us to pursue also the 2-position as possible attachment point. The 3-position, however, was lower

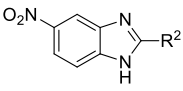
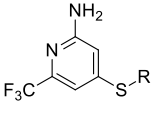
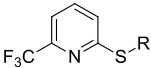
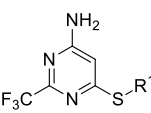
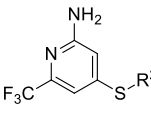
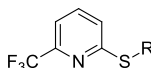
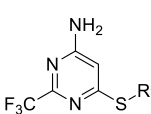
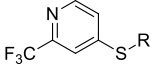
ranked in priority due to the more difficult synthetic feasibility caused by the higher electron density in meta-position of the pyridine ring.

Hybrid antagonists

Compounds **7** and **8** were rapidly accessible via a nucleophilic substitution reaction in 2- and 4-position of the pyridine ring, respectively. At first, potential PqsR antagonists were evaluated in a heterologous *E. coli* reporter gene system. This system allows an undistorted analysis of agonistic or antagonistic properties without the penetration problems observed in *P. aeruginosa* and possible bacteria-mediated deactivation of test compounds.²⁷ Compounds displaying sufficient antagonistic properties were further analyzed for their effect on the virulence factor pyocyanin and the signaling molecule HHQ in *P. aeruginosa*. Moreover, the solubility of the compounds under assay conditions was determined. Subsequently, the ligand lipophilicity efficiency (LLE) was calculated which evaluates the potency normalized for the heavy atom count of a compound taking also lipophilicity into account.³⁶ Hybrid molecules **7** and **8** showed antagonistic activities in the nanomolar range and were able to translate these activities into inhibition of pyocyanin in the low micromolar range (Table 1). Additionally, both compounds were able to affect the levels of the signaling molecule HHQ and their superimposition suggested synthesizing compound **9**. The latter showed a comparable profile to **8** regarding antagonistic activity and pyocyanin inhibition but a significantly lowered clogD, which was also reflected in a slightly improved LLE. Encouraged by these results and inspired by the SAR reported by Starkey *et al.*²⁹ we decided to exchange the chloro substituent for a phenoxy moiety (**10-12**). For all three headgroups an enhanced antagonistic activity was observed. There was a 22 fold (**7** vs. **10**) and 33 fold (**9** vs. **12**) boost in activity for the 4-position linked headgroups with amino function, whereas we measured a 2-fold increase (**8** vs. **11**) for the at the 2-position linked pyridine. These findings raised the question whether the presence of the NH₂ moiety or the positioning of thioglycolamide linker in 2- or 4-position of the pyridine nitrogen is pivotal for antagonistic activity. As an answer, the missing link **13** was synthesized. The latter showed a 2-fold improved antagonistic activity (**10** IC₅₀ = 0.019±0.001 μM vs. **13** IC₅₀ = 0.008±0.003 μM) leading to the conclusion that the amino group is an accessory feature to enhance the physicochemical properties but not fundamental for activity when combined with the R² tail. In contrary, the positioning of the pyridine nitrogen is more determining. The attachment of the linker in 4-position of the pyridine is clearly favored (**11** IC₅₀ = 0.086±0.05 μM vs. **13** IC₅₀ = 0.008±0.003 μM).

Table 1. Biological and physico-chemical properties of PqsR antagonists.

R¹:  R²: 

#	Structure	Antagonistic Activity IC ₅₀ [μM] ^a	Pyocyanin Inhibition IC ₅₀ [μM] ^b	HHQ Inhibition [μM] ^c	Solubility [μM] ^d	clogD pH 7.4 ^e	LLE (Astex) ^f
3 (M64)		0.005±0.001	0.12±0.01	0.22	25	4.7	0.29
7		0.426±0.10	12 ± 0.7	42±1 @ 50 μM	100	3.7	0.27
8		0.176±0.10	4.8 ± 0.3	30±8 @ 50 μM	50	3.7	0.30
9		0.233±0.02	8.3± 4.6	40±2 @ 50 μM	100	3.0	0.33
10		0.019 ± 0.001	0.276 ± 0.016	0.52 ±0.05	25	4.4	0.28
11		0.086 ± 0.05	0.822 ± 0.30	44±3 @ 5 μM	12.5	4.5	0.24
12		0.007 ± 0.004	0.384 ± 0.134	2.29±0.1	50	3.0	0.36
13		0.008 ± 0.003	0.339±0.02	0.54±0.05	12.5	4.3	0.30

^aevaluated in an *E. coli* reporter gene assay in the presence of 50 nM PQS; IC₅₀ represents the concentration of the half maximal antagonistic activity. ^bmeasured photometrically after extraction from PA14 cultures; IC₅₀ represents the concentration of 50% inhibition. ^cmeasured by UPLC-MS from PA14 cultures and referenced against DMSO control. ^ddetermined in PPGAS medium at 1% DMSO by visual inspection ^ecalculated using ACD/Percepta 2015. ^fligand lipophilicity efficiency³⁶ determined from antagonistic activity, heavy atom count and clogD.

It was of major interest to quantify the effect of the top candidates **10** and **12** on the 2-aminoacetophenone (2-AA) in PA14 wt. 2-AA is a shunt product of the AHQ biosynthesis process³⁷ and promotes chronic infection phenotypes³⁸ as well as accumulation of persister cells³⁹ in *P. aeruginosa*. Compound **10** showed potent inhibition of 2-AA production ($IC_{50} = 1.2 \pm 0.2 \mu M$) whereas the effect of compound **12** leveled out at around 50% (Figure 4). Remarkably, both compounds showed comparable effects regarding pyocyanin inhibition (Figure 4) and antagonistic activity in the reporter gene assay (Table 1). A similar scenario was observed for the inhibition of HHQ production (**10** $IC_{50} = 0.54 \pm 0.05$ vs. **12** $IC_{50} = 2.29 \pm 0.1$). These data emphasizes that small changes (pyridine to pyrimidine) within a molecule can drastically influence the efficacy of the antagonists to inhibit the AHQ biosynthesis and virulence expression (pyocyanin).

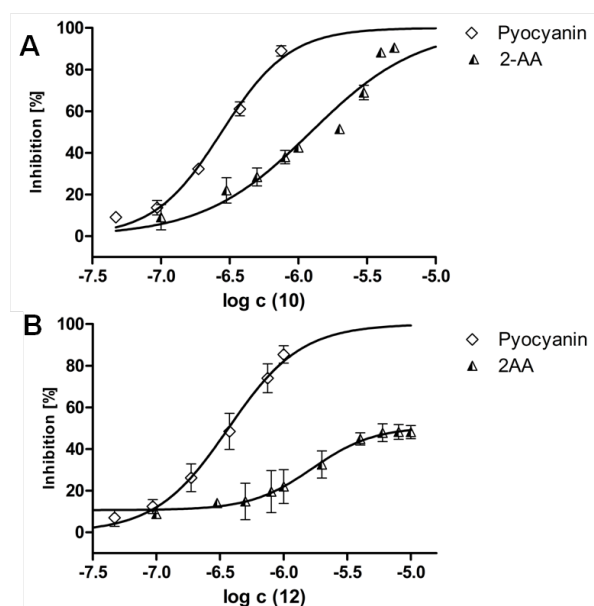


Figure 4. Dose-response curves for the inhibition of pyocyanin and 2-AA in PA14 wt for compound **10** (A, upper row) and **12** (B, lower row). Given data represent the mean of at least two independent experiments with $n=3$. Non linear regression analysis (continuous black line) was applied to determine IC_{50} values using a four variables model with constrains (bottom = 0 and top = 100 % except for the effect of **12** on 2-AA) included in Graph Pad Prism (5.04).

Compounds containing an amino-pyridine and -pyrimidine scaffold are frequently reported as inhibitors of different kinases.^{40,41} Therefore, we analyzed selected compounds for potential cytotoxic effects on eukaryotic HEK293 cells (SI Table S1). None of the tested compounds affected cell viability except for compound **7** but only at a significantly higher concentration than the measured effect on pyocyanin. Additionally, the scaffolds were subjected to an *in silico* toxicology prediction⁴² using the Derek Nexus database. This screening displayed no alerts concerning the amino-pyridine and -pyrimidine headgroups.

Overall, compound **12** showed the best combination of nanomolar antagonistic activity, potent pyocyanin inhibition and remarkable physicochemical properties, which is reflected by a strikingly better LLE value compared to the benchmark compound **3**.

Effects on static biofilms and lecB expression in *P. aeruginosa*

Compound **12** was selected for further evaluation in a static biofilm assay. The bacteria growing in sessile biofilm phenotype are prevalently found in most chronic infections caused by *P. aeruginosa*.²⁵ Biofilms are bacterial communities embedded in a self-produced polymeric matrix attached to a surface.⁴³ The structural components of this matrix are mainly polysaccharides, proteins and DNA.⁴⁴ The establishment of a biofilm is a complex regulatory process, which necessitates close coordination by the involved regulatory systems. The *pqs* QS system clearly affects *P. aeruginosa* biofilm formation¹⁹ regulatory mechanisms by triggering the release of eDNA²² and lectinA/B expression.²³ Besides its function as cell-connecting component during biofilm development,⁴⁵ eDNA protects sessile bacteria from host immune response and antibacterial treatment by the complexation of cationic peptides and xenobiotics.⁴⁶ LectinA/B are carbohydrate-binding proteins which plays an important role for surface attachment and stability of *P. aeruginosa* biofilms.^{23,47} The effect of PqsR antagonists on *P. aeruginosa* biofilms was first reported by Ilangovan *et al.*²⁸ However, the doses employed for these experiments have not been reported. Hence, we sought to investigate the biofilm effects of our antagonist in more detail. PA14 static biofilms were grown in the presence of 5 μ M of the antagonist **12** for 24 h. We evaluated total biofilm volume (biomass) as well as the *pqs*-dependent biofilm component eDNA (Figure 4A). While the PqsR antagonist **12** displayed only minor effects on the whole biovolume, it completely inhibited the accumulation of eDNA. This observation is in line with our results for the *pqsR* negative mutant. Moreover, compounds **10** and **12** showed potent inhibition of lectinB in *P. aeruginosa* (Figure 4B). Notably, these experiments were performed in planktonic PAO1 cultures due to experimental feasibility and the specificity of the used antibody.

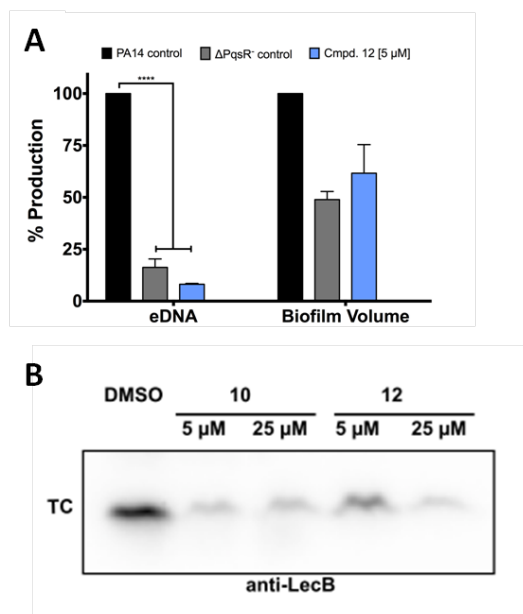


Figure 4. (A) Effects of compound **12** on PA14 static biofilms. While only a low effect was observed on total biofilm volume, compound **12** was able to drastically reduce eDNA accumulation to levels comparable with the *pqsR*⁻ mutant strain. Error bars represent standard error of at least two independent experiments. **** = $p < 0.0001$. (B) Western blot analysis of LecB expression in *P. aeruginosa* PAO1. Total cell (TC) fractions were analyzed by immunoblotting using anti-LecB serum. Cultures were grown for 24 h in absence or presence of compound **10** or **12** (5 μM or 25 μM).

CONCLUSION

Growing in a biofilm mode is the native form of bacterial lifestyle.⁴⁸ This lifestyle allows bacteria to colonize different niches and protects the single organism against severe external conditions.^{43,48} These insights altered the perspective on our bacterial opponent - from planktonic unicellular organisms to highly organized sessile communities. Nevertheless, learning, how these communities are organized, enables the development of alternative treatment strategies for the post antibiotic era.⁴⁹ In this study, we describe the development of improved lead compounds interfering with *P. aeruginosa* cell-to-cell communication with the aim to contribute to the development pipeline towards novel, innovative antimicrobials. Based on cocrystal structures and *in silico* methods, we developed a plausible binding-pose for the HTS hit **2**.²⁹ An overlay with the cocrystal-structure of in-house fragment derived antagonist **4**³² showed that both scaffolds partially overlap in the quinolone binding pocket of PqsR. This finding raised the idea to merge the trifluoro-pyridine headgroup with the benzamido-benzimidazole scaffold (**2** and **3**). This strategy resulted in the straightforward development of hybrid PqsR antagonists resulting in potent pyocyanin and HHQ inhibition in *P. aeruginosa* while keeping superior physicochemical properties. In doing so, the potentially problematic nitro moiety at the benzimidazole core was exchanged by a more drug-like trifluoromethyl

group. Subsequently, these compounds were profiled for their effects on PA14 static biofilms. For some of the described biofilm inhibiting compounds the exact mode of action is poorly understood or their effect might be mediated through a direct physicochemical interaction with the biofilm matrix.⁵⁰ In contrast, the effects of our PqsR antagonist were in accordance with the biofilm profile generated by a *pqsR* mutant strain: the overall biovolume was only slightly affected but the *pqs*-mediated release of eDNA was completely abolished. To what extent the reduction of eDNA affects the biofilm structure and permeability will be addressed in future experiments.

Taken together, in this approach we successfully combined the best features of two apparently mutual worlds – phenotypic HTS and fragment screening – in order to push the development of antivirulence agents against severe *P. aeruginosa* infections.

EXPERIMENTAL SECTION

***In silico* studies (ME).** The structure of the PqsR:1 complex was modelled based on a solved X-ray structure of HHQ bound to its receptor (unpublished results). The original coordinates were loaded into Molecular Operating Environment (MOE 2014, Chemical Computing Group) and the additional carboxamide and nitro substituents were attached to the ligand using the “Builder” function. Then the resulting complex structure was energy minimized using the standard LigX parameters together with the AMBER10:EHT forcefield to yield the model of compound **1** in complex with PqsR.

The structure of the PqsR:2 complex was generated through a pharmacophore-guided docking. To this end, a two-feature pharmacophore model comprising an aromatic cycle and an electron-withdrawing group, which were placed inside the quinolone pocket of PqsR. A solved X-ray structure of bound antagonist **4** was used as template (unpublished results). Then, the built-in “induced-fit” docking protocol was applied using the described pharmacophore as placement constraint, AMBER10:EHT force field, and standard parameters. The two highest scoring docking poses of compound **2** were additionally energy minimized to yield the complex structures depicted in Figure 2.

Reporter Gene Assay in *E. coli*. The ability of the compounds to either stimulate or antagonize the PqsR-dependent transcription was analysed as previously described²⁶ using a β -galactosidase reporter gene assay in *E. coli*⁵¹ expressing PqsR.

Pyocyanin Assay. Pyocyanin produced by *P. aeruginosa* PA14 was determined as reported previously²⁶ according to the method of Essar *et al.*⁵²

Isothermal titration calorimetry ITC titrations were carried out as previously reported.^{30,31}

Determination of Extracellular HHQ and 2-AA. Extracellular levels of HHQ from PA14 *pqsH* cultures were determined as previously reported^{27,53} according to the methods of Lépine *et al.*⁵⁴ For the quantification of 2-AA PA14 wt was used following the same protocol as for HHQ quantification whether a slightly modified sample work-up was performed. Briefly, 750 μ L of culture was diluted with the same volume of 1 μ M *d*₄HHQ in acetonitrile, shaken for 5 min at 1,500 rpm, and centrifuged at 14,000 rpm for 10 min. Afterwards 1 mL of supernatant of each sample was transferred in a vial for analysis by HPLC-MS/MS. Calibration curve of 2-AA was prepared according to the same procedure using PA14 *pqsA* mutant as biomatrix.

Biofilm assay in PA14 For the determination of biofilm components in PA14 static biofilms, we followed reported procedures with a few modifications.^{22,55} Briefly, cultures of PA14 (or PA14*pqsR*) were grown in M63 medium in 96 well plates (Greiner, clear flat bottom) for 24 h at 37°C in the presence of test compound added as DMSO stock solution or DMSO as control to give 1% (v/v) final DMSO concentration. After washing the matured biofilm with PBS and water, biofilm components were stained either with crystal violet (0.1 mg/ml dissolved in water/ethanol 95/5 (v/v)) for the whole biomass or with propidium iodine solution (0.05 mg/ml dissolved in water). For quantification of the whole biomass absorbance was measured at 590 nm and for eDNA fluorescence at 620 nm using FLUOstar Omega (BMG Labtech). Given values represent the mean of at least two independent experiments with n=5. Differences in between treated and untreated samples were evaluated using a one way ANOVA followed by a two-sided Holm-Sidak's multiple comparison test using GraphPad Prism version 6.0f for Mac OS X, GraphPad Software. Differences were considered significant at a *p*-value < 0.05.

LectinB expression *P. aeruginosa* PAO1 cultures were grown in LB medium at 37 °C. Compounds were dissolved in DMSO. Compound **10** or **12** was added to 2.5 mL LB and the DMSO concentrations were adjusted to keep the same concentrations in all samples. Overnight cultures were used to inoculate fresh LB medium to an OD₆₀₀ of 0.02 and 2.5 mL of this bacterial culture was added to the 2.5 mL LB samples containing compound **10** or **12** or only DMSO. The final cultures had an starting OD₆₀₀ of 0.01 and final compound concentration of 5 μ M or 25 μ M. Bacterial cultures were incubated at 37 °C (200 rpm) for 24 h. Bacteria were harvested by centrifugation at 21380 rcf for 10 minutes. The supernatant was discarded and pellets were resuspended in SDS loading buffer (50 mM Tris-HCl pH 6.8, 10% (v/v) glycerol, 2% (v/v) SDS, 100 mM DTT, bromphenolblue) and denatured by heating (98 °C, 5 min). Total cell extracts were analyzed by 15% SDS-PAGE and Coomassie staining (SI Figure S3) or

immune blotting. In each case, total cell extracts of approximately 2×10^8 bacteria were loaded per lane. For detection of LecB in total cells, proteins were transferred onto a nitrocellulose membrane (Amersham; GE Healthcare). After blocking the membrane (5% milk in PBST (137 mM NaCl, 2.7 mM KCl, 10 mM Na_2HPO_4 , 1.8 mM KH_2PO_4 and 0.2% Tween)) immunodetection was carried out using rabbit antiserum against LecB (1:500 in 5% milk in PBST). Detection was performed using the goat anti-rabbit secondary antibody conjugated to horseradish peroxidase (1:5000 in 5% milk in PBST; Dianova), before development with chemiluminescent substrate (100 mM Tris-HCl pH 8.5, 0.009% H_2O_2 , 1.25 mM luminol, 225 μM coumaric acid) and detection with a Fusion imager (Vilber Lourmat).

Chemical and Analytical Methods. ^1H and ^{13}C NMR spectra were recorded as indicated on a Bruker DRX-500 instrument or a Bruker Fourier 300 instrument. Chemical shifts are given in parts per million (ppm), and referenced against the residual solvent peak. Coupling constants (J) are given in hertz. Mass spectrometry and purity determination (LC/MS) was performed either on a SpectraSystems-MSQ LCMS system (Thermo Fisher Scientific) consisting of a pump, an autosampler, VWD detector or on Waters LCMS-System consisting of a 767 sample Manager, a 2545 binary gradient pump, a 2998 PDA detector and a 3100 electron spray mass spectrometer. All solvents were HPLC grade. The purity of tested final products was $> 95\%$. Procedures were not optimized regarding yield. Microwave assisted synthesis was carried out in a Discover microwave synthesis system (CEM). Column chromatography was performed using the automated flash chromatography system Combiflash Rf+ (Teledyne Isco) equipped with RediSepRf silica columns. Final products were dried in high vacuum.

General Procedure A: *N*-phenyl-2-mercaptoacetamide precursors

Aniline (1 eq) was filled into a crimp vial (Biotage[®]). The vial was evacuated and backfilled with argon (3 times). 2-mercaptoacetic acid (1 eq) was added (neat reaction) and the vial flushed with argon (5 min). The reaction mixture was heated to 130°C in a metal block for 1.5 h. The mixture was allowed to cool to RT. The resulting solid was suspended in isopropanol and filtered. The resulting white cake was washed with IPA to give the titled product.

General Procedure B: Hybrid compounds

Heteroaryl halide (0.35 mmol) and K_2CO_3 (1.05 mmol) was suspended in DMF (1 ml) using a crimp vial (Biotage[®]). The vial was purged with argon. A solution of *N*-phenyl-2-mercaptoacetamide (0.38 mmol) in 1 ml DMF was added while cooling in an ice-bath. The mixture was again purged with argon. The reaction was aged at RT for 6 h. The mixture was poured into water and extracted with ethylacetate (3 times). The combined organics were

washed with Na₂CO₃ saturated solution and brine. The organic extract was dried over Na₂SO₄, filtered and dried. Purification was done by automated flash chromatography or preparative HPLC.

2-((2-amino-6-(trifluoromethyl)pyridin-4-yl)thio)-N-(4-chlorophenyl)acetamide (7) was synthesized according to general procedure B from 4-iodo-6-(trifluoromethyl)pyridin-2-amine (100 mg, 0.347 mmol and *N*-(4-chlorophenyl)-2-mercaptoacetamide (77 mg, 0.382 mmol). The crude product was purified by automated flash chromatography using a gradient of petroleum ether to pure ether. Further purification by prep HPLC afforded the titled product as white solid (24 mg, 0.066 mmol, 19 % yield). ¹H NMR (300 MHz, DMSO-*d*₆) ♥ ppm 3.99 (s, 2 H), 6.56 (s, 3 H), 6.89 (d, *J*=1.3 Hz, 1 H), 7.23 - 7.45 (m, 1 H), 7.52 - 7.68 (m, 2 H), 10.44 (s, 1 H); ¹³C NMR (75 MHz, DMSO-*d*₆) ♥ ppm 35.12, 105.53 (q, ³*J*(C,F)=2.2 Hz, 1 C), 106.79, 125.21 (q, ¹*J*(C,F)=275.0 Hz, 1 C), 120.77 (2 C), 127.19, 128.71 (2 C), 137.62, 145.00 (q, ²*J*(C,F)=32.8 Hz, 1 C), 149.43, 159.75, 166.06; MS (ESI +) *m/z* 362 (M+H)⁺, 403 (M+ACN+H)⁺.

N-(4-chlorophenyl)-2-((6-(trifluoromethyl)pyridin-2-yl)thio)acetamide (8) was synthesized according to general procedure B from 2-bromo-6-(trifluoromethyl)pyridine (226 mg, 1,000 μmol) and *N*-(4-chlorophenyl)-2-mercaptoacetamide (212 mg, 1.050 mmol). The mixture was stirred for 1 h at -78 °C and then at 0 °C for 1 h. Purification was done by automated flash chromatography using a gradient of petroleum ether and ethylacetate. The crude product was titrated with DCM/pentane and filtered to give the titled product as a white solid (65 mg, 0.19 mmol, 18 % yield). ¹H NMR (500 MHz, DMSO-*d*₆) ♥ ppm 4.11 (s, 2 H), 7.30 - 7.39 (m, 2 H), 7.53 - 7.64 (m, 3 H), 7.70 (d, *J*=7.9 Hz, 1 H), 7.92 (t, *J*=6.9 Hz, 1 H), 10.40 (s, 1 H); ¹³C NMR (126 MHz, DMSO-*d*₆) ♥ ppm 34.73, 116.59, 121.23 (q ¹*J*(C,F)=272.0 Hz, 1 C), 120.66 (s, 2 C), 125.17, 126.86, 128.58 (s, 2 C), 137.92, 138.38, 146.10 (q, ²*J*(C,F)=32.0 Hz, 1 C), 159.57, 166.10; MS (ESI +) *m/z* not found.

2-((6-amino-2-(trifluoromethyl)pyrimidin-4-yl)thio)-N-(4-chlorophenyl)acetamide (9) was synthesized according to general procedure B from 6-chloro-2-(trifluoromethyl)pyrimidin-4-amine (100 mg, 0.51 mmol) and *N*-(4-chlorophenyl)-2-mercaptoacetamide (102 mg, 0.51 mmol). Purification was done by automated flash chromatography using a gradient petroleum ether and ethylacetate (9/1 to 1/1) to give the titled compound as light yellow solid (45 mg, 0.124 mmol, 24% yield). ¹H NMR (500 MHz, DMSO-*d*₆) ♥ ppm 4.03 (s, 2 H), 6.50 (s, 1 H), 7.27 - 7.42 (m, 2 H), 7.49 (br. s., 2 H), 7.53 - 7.67 (m, 2 H), 10.40 (s, 1 H); ¹³C NMR (126 MHz, DMSO-*d*₆) ♥ ppm 34.22, 100.99, 119.42 (q, ¹*J*(C,F)=275.8 Hz, 1 C), 120.73 (2 C),

127.00, 128.70 (2 C), 137.89, 154.52 (q, $^2J(\text{C},\text{F})=33.0$ Hz, 1 C), 163.27, 166.06, 166.62; MS(ESI+) m/z 363 (M+H)⁺.

2-((2-amino-6-(trifluoromethyl)pyridin-4-yl)thio)-N-(4-phenoxyphenyl)acetamide (10)

was synthesized according to general procedure B from 4-iodo-6-(trifluoromethyl)pyridin-2-amine (100 mg, 0.35 mmol) and 2-mercapto-*N*-(4-phenoxyphenyl)acetamide (99 mg, 0.38 mmol). Purification was done by automated flash chromatography using a gradient of petroleum ether and diethyl ether (1/1 to 2/8). Further purification by prep HPLC to give 2-((2-amino-6-(trifluoromethyl)pyridin-4-yl)thio)-*N*-(4-phenoxyphenyl)acetamide (20 mg, 0.05 mmol, 14 % yield) as white solid. ^1H NMR (300 MHz, CHLOROFORM-*d*) \blacklozenge ppm 3.83 (s, 2 H), 4.76 (s, 2 H), 6.44 (d, $J=0.8$ Hz, 1 H), 6.91 (d, $J=1.4$ Hz, 1 H), 6.95 - 7.05 (m, 4 H), 7.07 - 7.14 (m, 1 H), 7.29 - 7.37 (m, 2 H), 7.39 - 7.47 (m, 2 H), 8.22 (s, 1 H); ^{13}C NMR (75 MHz, DMSO-*d*₆) \blacklozenge ppm 35.08, 105.56 (q, $^1J(\text{C},\text{F})=3.0$ Hz, 1 C), 106.80, 117.93 (2 C), 119.43 (2 C), 121.61 (d, $^1J(\text{C},\text{F})=274.0$ Hz, 1 C), 120.95 (2 C), 123.03, 129.95 (2 C), 134.55, 145.03 (q, $^2J(\text{C},\text{F})=32.0$ Hz, 1 C), 149.55, 152.08, 157.22, 159.77, 165.71; MS(ESI+) m/z 420 (M+H)⁺, 461 (M+ACN+H)⁺.

***N*-(4-phenoxyphenyl)-2-((6-(trifluoromethyl)pyridin-2-yl)thio)acetamide (11)**

was synthesized according to general procedure B from 2-bromo-6-(trifluoromethyl)pyridine (100 mg, 0.44 mmol) and 2-mercapto-*N*-(4-phenoxyphenyl)acetamide (115 mg, 0.44 mmol) e mixture was poured into water solution and extracted using EA. Combined organics were washed with brine, dried (Na₂SO₄), filtered and concentrated. Purification was done by automated flash chromatography using a gradient of petroleum ether and ethylacetate (9/1 to pure ethylacetate) to give the titled product as off white solid (135 mg, 0.334 mmol, 75 % yield). ^1H NMR (500 MHz, DMSO-*d*₆) \blacklozenge ppm 4.12 (s, 2 H), 6.88 - 7.03 (m, 4 H), 7.09 (t, $J=7.4$ Hz, 1 H), 7.31 - 7.41 (m, 2 H), 7.57 (d, $J=8.8$ Hz, 2 H), 7.60 (d, $J=7.6$ Hz, 1 H), 7.71 (d, $J=8.2$ Hz, 1 H), 7.92 (t, $J=7.9$ Hz, 1 H), 10.32 (s, 1 H); ^{13}C NMR (126 MHz, DMSO-*d*₆) \blacklozenge ppm 34.66, 116.58 (q, $^1J(\text{C},\text{F})=2.8$ Hz, 1 C), 117.85 (2 C), 121.27 (q, $^1J(\text{C},\text{F})=274.9$ Hz, 1 C), 119.37 (2 C), 120.85 (2 C), 122.95, 125.16, 129.92 (2 C), 134.83, 138.39, 146.10 (q, $^2J(\text{C},\text{F})=33.9$ Hz, 1 C), 151.79, 157.27, 159.70, 165.72; MS(ESI+) m/z 427 (M+Na)⁺.

2-((6-amino-2-(trifluoromethyl)pyrimidin-4-yl)thio)-*N*-(4-phenoxyphenyl)acetamide (12)

was synthesized according to general procedure B from 6-chloro-2-(trifluoromethyl)pyrimidin-4-amine (200 mg, 1.012 mmol) and 2-mercapto-*N*-(4-phenoxyphenyl)acetamide (263 mg, 1.012 mmol). Purification was done by automated flash chromatography using a gradient of petroleum ether and ethylacetate (9/1 to pure ethylacetate) to give the titled product as white

CHAPTER 2

solid (45 mg, 0.107 mmol, 11 % yield). ^1H NMR (500 MHz, $\text{DMSO-}d_6$) \blacklozenge ppm 4.03 (s, 2 H), 6.51 (s, 1 H), 6.89 - 7.04 (m, 4 H), 7.10 (t, $J=7.4$ Hz, 1 H), 7.30 - 7.40 (m, 2 H), 7.50 (br. s., 2 H), 7.55 - 7.62 (m, 2 H), 10.30 (s, 1 H); ^{13}C NMR (126 MHz, $\text{DMSO-}d_6$) \blacklozenge ppm 34.09, 100.91, 119.35 (q, $^1J(\text{C,F})=275.8$ Hz, 1 C), 117.86 (2 C), 119.40 (2 C), 120.87 (2 C), 122.97, 129.93 (2 C), 134.73, 151.87, 154.46 (q, $^2J(\text{C,F})=34.8$ Hz, 1 C), 157.24, 163.24, 165.61, 166.71. MS(ESI+) m/z 421 (M+H) $^+$.

***N*-(4-phenoxyphenyl)-2-((2-(trifluoromethyl)pyridin-4-yl)thio)acetamide (13)** was synthesized according to general procedure B from 4-bromo-2-(trifluoromethyl)pyridine (200 mg, 0.885 mmol) and 2-mercapto-*N*-(4-phenoxyphenyl)acetamide (229 mg, 0.885 mmol). Purification was done by automated flash chromatography using a gradient of petroleum ether and ethylacetate (petroleum ether pure to 8/2) to give the titled product as white solid (210 mg, 0.519 mmol, 59% yield). ^1H NMR (500 MHz, $\text{DMSO-}d_6$) \blacklozenge ppm 4.14 (s, 2 H), 6.90 - 7.04 (m, 4 H), 7.05 - 7.19 (m, 1 H), 7.30 - 7.42 (m, 2 H), 7.50 - 7.61 (m, 2 H), 7.66 (dd, $J=5.4, 1.6$ Hz, 1 H), 7.88 (d, $J=1.6$ Hz, 1 H), 8.56 (d, $J=5.4$ Hz, 1 H), 10.40 (s, 1 H); ^{13}C NMR (126 MHz, $\text{DMSO-}d_6$) \blacklozenge ppm 34.85, 117.26 (d, $^3J(\text{C,F})=2.7$ Hz, 1 C), 117.96 (2 C), 121.49 (q, $^1J(\text{C,F})=274.0$ Hz, 1 C), 119.45 (2 C), 120.95 (2 C), 123.06, 123.49, 129.95 (2 C), 134.44, 146.37 (q, $^2J(\text{C,F})=33.0$ Hz, 1 C), 149.47, 151.35, 152.14, 157.18, 165.59; MS(ESI+) m/z 405 (M+H) $^+$.

REFERENCES

1. Spellberg, B.; Taylor-Blake, B. On the exoneration of Dr. William H. Stewart: debunking an urban legend. *Infect. Dis. Poverty*. 2013, 2, 3.
2. Pier, G. B. On the greatly exaggerated reports of the death of infectious diseases. *Clin. Infect. Dis.* 2008, 47, 1113–1114.
3. Alanis, A. J. Resistance to antibiotics: are we in the post-antibiotic era? *Arch. Med. Res.* 2005, 36, 697–705.
4. Boucher, H. W.; Talbot, G. H.; Bradley, J. S.; Edwards, J. E.; Gilbert, D.; Rice, L. B.; Scheld, M.; Spellberg, B.; Bartlett, J. Bad bugs, no drugs: no ESKAPE! An update from the Infectious Diseases Society of America. *Clin. Infect. Dis.* 2009, 48, 1–12.
5. Projan, S. J. Why is big Pharma getting out of antibacterial drug discovery? *Curr. Opin. Microbiol.* 2003, 6, 427–430.
6. Falagas, M. E.; Bliziotis, I. A. Pandrug-resistant Gram-negative bacteria: the dawn of the post-antibiotic era? *Int. J. Antimicrob. Agents*. 2007, 29, 630–636.
7. Clatworthy, A. E.; Pierson, E.; Hung, D. T. Targeting virulence: a new paradigm for antimicrobial therapy. *Nat. Chem. Biol.* 2007, 3, 541–548.
8. Rampioni, G.; Leoni, L.; Williams, P. The art of antibacterial warfare: Deception through interference with quorum sensing-mediated communication. *Bioorg. Chem.* 2014, 55, 60–68.
9. Schuster, M.; Peter Greenberg, E. A network of networks. *Int. J. Med. Microbiol.* 2006, 296, 73–81.
10. Gambello, M. J.; Iglewski, B. H. Cloning and characterization of the *Pseudomonas aeruginosa* lasR gene, a transcriptional activator of elastase expression. *J. Bacteriol.* 1991, 173, 3000–3009.
11. Passador, L.; Cook, J. M.; Gambello, M. J.; Rust, L.; Iglewski, B. H. Expression of *Pseudomonas aeruginosa* virulence genes requires cell-to-cell communication. *Science*. 1993, 260, 1127–1130.
12. Ochsner, U. A.; Koch, A. K.; Fiechter, A.; Reiser, J. Isolation and characterization of a regulatory gene affecting rhamnolipid biosurfactant synthesis in *Pseudomonas aeruginosa*. *J. Bacteriol.* 1994, 176, 2044–2054.
13. Ochsner, U. A.; Reiser, J. Autoinducer-mediated regulation of rhamnolipid biosurfactant synthesis in *Pseudomonas aeruginosa*. *Proc. Natl. Acad. Sci. U. S. A.* 1995, 92, 6424–6428.
14. Pesci, E. C.; Milbank, J. B. J.; Pearson, J. P.; McKnight, S.; Kende, A. S.; Greenberg, E. P.; Iglewski, B. H. Quinolone signaling in the cell-to-cell communication system of *Pseudomonas aeruginosa*. *Proc. Natl. Acad. Sci. U. S. A.* 1999, 96, 11229–11234.
15. Cao, H.; Krishnan, G.; Goumnerov, B.; Tsongalis, J.; Tompkins, R.; Rahme, L. G. A quorum sensing-associated virulence gene of *Pseudomonas aeruginosa* encodes a LysR-like transcription regulator with a unique self-regulatory mechanism. *Proc. Natl. Acad. Sci. U. S. A.* 2001, 98, 14613–14618.
16. Gallagher, L. A.; McKnight, S. L.; Kuznetsova, M. S.; Pesci, E. C.; Manoil, C. Functions Required for Extracellular Quinolone Signaling by *Pseudomonas aeruginosa*. *J. Bacteriol.* 2002, 184, 6472–6480.
17. Déziel, E.; Lépine, F.; Milot, S.; He, J.; Mindrinos, M. N.; Tompkins, R. G.; Rahme, L. G. Analysis of *Pseudomonas aeruginosa* 4-hydroxy-2-alkylquinolines (HAQs) reveals a role for 4-hydroxy-2-heptylquinoline in cell-to-cell communication. *Proc. Natl. Acad. Sci. U. S. A.* 2004, 101, 1339–1344.
18. Xiao, G.; Deziel, E.; He, J.; Lépine, F.; Lesic, B.; Castonguay, M.-H.; Milot, S.; Tampakaki, A. P.; Stachel, S. E.; Rahme, L. G. MvfR, a key *Pseudomonas aeruginosa*

- pathogenicity LTTR-class regulatory protein, has dual ligands. *Mol. Microbiol.* 2006, 62, 1689–1699.
19. Diggle, S. P.; Winzer, K.; Chhabra, S. R.; Worrall, K. E.; Cámara, M.; Williams, P. The *Pseudomonas aeruginosa* quinolone signal molecule overcomes the cell density-dependency of the quorum sensing hierarchy, regulates *rhl*-dependent genes at the onset of stationary phase and can be produced in the absence of LasR. *Mol. Microbiol.* 2003, 50, 29–43.
 20. Wade, D. S.; Calfee, M. W.; Rocha, E. R.; Ling, E. A.; Engstrom, E.; Coleman, J. P.; Pesci, E. C. Regulation of *Pseudomonas* Quinolone Signal Synthesis in *Pseudomonas aeruginosa*. *J. Bacteriol.* 2005, 187, 4372–4380.
 21. Xiao, G.; He, J.; Rahme, L. G. Mutation analysis of the *Pseudomonas aeruginosa* *mvfR* and *pqsABCDE* gene promoters demonstrates complex quorum-sensing circuitry. *Microbiology.* 2006, 152, 1679–1686.
 22. Allesen-Holm, M.; Barken, K. B.; Yang, L.; Klausen, M.; Webb, J. S.; Kjelleberg, S.; Molin, S.; Givskov, M.; Tolker-Nielsen, T. A characterization of DNA release in *Pseudomonas aeruginosa* cultures and biofilms. *Mol. Microbiol.* 2006, 59, 1114–1128.
 23. Diggle, S. P.; Stacey, R. E.; Dodd, C.; Camara, M.; Williams, P.; Winzer, K. The galactophilic lectin, LecA, contributes to biofilm development in *Pseudomonas aeruginosa*. *Environ. Microbiol.* 2006, 8, 1095–1104.
 24. Singh, P. K.; Schaefer, A. L.; Parsek, M. R.; Moninger, T. O.; Welsh, M. J.; Greenberg, E. P. Quorum-sensing signals indicate that cystic fibrosis lungs are infected with bacterial biofilms. *Nature.* 2000, 407, 762–764.
 25. Høiby, N.; Ciofu, O.; Bjarnsholt, T. *Pseudomonas aeruginosa* biofilms in cystic fibrosis. *Future Microbiol.* 2010, 5, 1663–1674.
 26. Lu, C.; Kirsch, B.; Zimmer, C.; Jong, J. C. de; Henn, C.; Maurer, C. K.; Musken, M.; Haussler, S.; Steinbach, A.; Hartmann, R. W. Discovery of antagonists of PqsR, a key player in 2-alkyl-4-quinolone-dependent quorum sensing in *Pseudomonas aeruginosa*. *Chem. Biol. (Oxford, U. K.).* 2012, 19, 381–390.
 27. Lu, C.; Maurer, C. K.; Kirsch, B.; Steinbach, A.; Hartmann, R. W. Overcoming the unexpected functional inversion of a PqsR antagonist in *Pseudomonas aeruginosa*: an in vivo potent antivirulence agent targeting *pqs* quorum sensing. *Angew. Chem., Int. Ed.* 2014, 53, 1109–1112.
 28. Ilangovan, A.; Fletcher, M.; Rampioni, G.; Pustelny, C.; Rumbaugh, K.; Heeb, S.; Camara, M.; Truman, A.; Chhabra, S. R.; Emsley, J.; Williams, P. Structural basis for native agonist and synthetic inhibitor recognition by the *Pseudomonas aeruginosa* quorum sensing regulator PqsR (MvfR). *PLoS Pathog.* 2013, 9, e1003508.
 29. Starkey, M.; Lepine, F.; Maura, D.; Bandyopadhyaya, A.; Lesic, B.; He, J.; Kitao, T.; Righi, V.; Milot, S.; Tzika, A.; Rahme, L. Identification of anti-virulence compounds that disrupt quorum-sensing regulated acute and persistent pathogenicity. *PLoS Pathog.* 2014, 10, e1004321.
 30. Klein, T.; Henn, C.; Jong, J. C. de; Zimmer, C.; Kirsch, B.; Maurer, C. K.; Pistorius, D.; Müller, R.; Steinbach, A.; Hartmann, R. W. Identification of small-molecule antagonists of the *Pseudomonas aeruginosa* transcriptional regulator PqsR: biophysically guided hit discovery and optimization. *ACS Chem. Biol.* 2012, 7, 1496–1501.
 31. Zender, M.; Klein, T.; Henn, C.; Kirsch, B.; Maurer, C. K.; Kail, D.; Ritter, C.; Dolezal, O.; Steinbach, A.; Hartmann, R. W. Discovery and biophysical characterization of 2-amino-oxadiazoles as novel antagonists of PqsR, an important regulator of *Pseudomonas aeruginosa* virulence. *J. Med. Chem.* 2013, 56, 6761–6774.
 32. Zender, M.; Witzgall, F.; Kiefer, A.; Kirsch, B.; Maurer, C. K.; Kany, A.; Börger, C.; Blankenfeldt, W.; Empting, M.; Hartmann Rolf W. Flexible-Fragment-Growing Boosts

- Potency of Quorum Sensing Inhibitors against *Pseudomonas aeruginosa* virulence Structure-guided fragment-growing of 2-Amino-pyridines to target PqsR, a main regulator of *Pseudomonas aeruginosa* virulence. (not published).
33. Shaitanov, P. V.; Lukashov S.S.; Turov O.V.; Yarmoluk S.M. Synthesis and structural study of N-substituted-1,7-dithia-4-azaspiro[4.4]nonan-3-one 7,7-dioxides. *Ukr. Bioorg. Acta.* 2007, 2, 56–61.
 34. Barker, J.; Hesterkamp, T.; Whittaker, M. Integrating HTS and fragment-based drug discovery. *Drug Discovery World.* 2008, 69–75.
 35. Rahme, L.; Lepine, F.; Starkey, M.; Lesic-Arsic, B. Antibiotic tolerance inhibitors. WO2012116010 A2.
 36. Mortenson, P.; Murray, C. Assessing the lipophilicity of fragments and early hits. *J. Comput.-Aided Mol. Des.* 2011, 25, 663–667.
 37. Drees, S. L.; Fetzner, S. PqsE of *Pseudomonas aeruginosa* Acts as Pathway-Specific Thioesterase in the Biosynthesis of Alkylquinolone Signaling Molecules. *Chem. Biol. (Oxford, U. K.).* 2015, 22, 611–618.
 38. Kesarwani, M.; Hazan, R.; He, J.; Que, Y.-A.; Que, Y.; Apidianakis, Y.; Lesic, B.; Xiao, G.; Dekimpe, V.; Milot, S.; Deziel, E.; Lépine, F.; Rahme, L. G. A quorum sensing regulated small volatile molecule reduces acute virulence and promotes chronic infection phenotypes. *PLoS Pathog.* 2011, 7, e1002192.
 39. Que, Y.-A.; Hazan, R.; Strobel, B.; Maura, D.; He, J.; Kesarwani, M.; Panopoulos, P.; Tsurumi, A.; Giddey, M.; Wilhelmy, J.; Mindrinos, M. N.; Rahme, L. G. A quorum sensing small volatile molecule promotes antibiotic tolerance in bacteria. *PloS one.* 2013, 8, e80140.
 40. Hilton, S.; Naud, S.; Caldwell, J. J.; Boxall, K.; Burns, S.; Anderson, V. E.; Antoni, L.; Allen, C. E.; Pearl, L. H.; Oliver, A. W.; Wynne Aherne, G.; Garrett, M. D.; Collins, I. Identification and characterisation of 2-aminopyridine inhibitors of checkpoint kinase 2. *Bioorg. Med. Chem.* 2010, 18, 707–718.
 41. Jain, R.; Mathur, M.; Lan, J.; Costales, A.; Atallah, G.; Ramurthy, S.; Subramanian, S.; Setti, L.; Feucht, P.; Warne, B.; Doyle, L.; Basham, S.; Jefferson, A. B.; Lindvall, M.; Appleton, B. A.; Shafer, C. M. Discovery of Potent and Selective RSK Inhibitors as Biological Probes. *J. Med. Chem.* 2015, 58, 6766–6783.
 42. Muster, W.; Breidenbach, A.; Fischer, H.; Kirchner, S.; Müller, L.; Pähler, A. Computational toxicology in drug development. *Drug discovery today.* 2008, 13, 303–310.
 43. Costerton, J. W. Bacterial Biofilms. *Science.* 1999, 284, 1318–1322.
 44. Sutherland, I. The biofilm matrix – an immobilized but dynamic microbial environment. *Trends Microbiol.* 2001, 9, 222–227.
 45. Whitchurch, C. B.; Tolker-Nielsen, T.; Ragas, P. C.; Mattick, J. S. Extracellular DNA required for bacterial biofilm formation. *Science.* 2002, 295, 1487.
 46. Mulcahy, H.; Charron-Mazenod, L.; Lewenza, S. Extracellular DNA chelates cations and induces antibiotic resistance in *Pseudomonas aeruginosa* biofilms. *PLoS Pathog.* 2008, 4, e1000213.
 47. Tielker, D. *Pseudomonas aeruginosa* lectin LecB is located in the outer membrane and is involved in biofilm formation. *Microbiology.* 2005, 151, 1313–1323.
 48. Costerton, J. W.; Cheng, K. J.; Geesey, G. G.; Ladd, T. I.; Nickel, J. C.; Dasgupta, M.; Marrie, T. J. Bacterial biofilms in nature and disease. *Annu. Rev. Microbiol.* 1987, 41, 435–464.
 49. Kostakioti, M.; Hadjifrangiskou, M.; Hultgren, S. J. Bacterial biofilms: development, dispersal, and therapeutic strategies in the dawn of the postantibiotic era. *Cold Spring Harbor Perspect. Med.* 2013, 3, a010306.

CHAPTER 2

50. Worthington, R. J.; Richards, J. J.; Melander, C. Small molecule control of bacterial biofilms. *Org. Biomol. Chem.* 2012, 10, 7457–7474.
51. Cugini, C.; Calfee, M. W.; Farrow, J. M. 3.; Morales, D. K.; Pesci, E. C.; Hogan, D. A. Farnesol, a common sesquiterpene, inhibits PQS production in *Pseudomonas aeruginosa*. *Mol. Microbiol.* 2007, 65, 896–906.
52. Essar, D. W.; Eberly, L.; Hadero, A.; Crawford, I. P. Identification and characterization of genes for a second anthranilate synthase in *Pseudomonas aeruginosa*: interchangeability of the two anthranilate synthases and evolutionary implications. *J. Bacteriol.* 1990, 172, 884–900.
53. Storz, M. P.; Maurer, C. K.; Zimmer, C.; Wagner, N.; Brengel, C.; Jong, J. C. de; Lucas, S.; Müsken, M.; Häussler, S.; Steinbach, A.; Hartmann, R. W. Validation of PqsD as an anti-biofilm target in *Pseudomonas aeruginosa* by development of small-molecule inhibitors. *J. Am. Chem. Soc.* 2012, 134, 16143–16146.
54. Lepine, F.; Milot, S.; Deziel, E.; He, J.; Rahme, L. G. Electrospray/mass spectrometric identification and analysis of 4-hydroxy-2-alkylquinolines (HAQs) produced by *Pseudomonas aeruginosa*. *J. Am. Soc. Mass Spectrom.* 2004, 15, 862–869.
55. (55) Frei, R.; Breitbach, A. S.; Blackwell, H. E. 2-Aminobenzimidazole derivatives strongly inhibit and disperse *Pseudomonas aeruginosa* biofilms. *Angew. Chem., Int. Ed.* 2012, 51, 5226–5229.

8.3 Chapter 3 – CYP17A1-independent Production of the Neurosteroid-derived 5 α -pregnan-3 β ,6 α -diol-20-one in Androgen-responsive Prostate Cancer Cell Lines under Serum Starvation and Inhibition by Abiraterone

The following persons also contributed to the results described in this chapter:

1. Giuseppe Allegretta: Synthesis and characterization of Δ^4 -Abiraterone, HPLC-MS/MS analyses, and structure elucidation.
2. Michael Hoffmann: HPLC-ESI-ToF-MS analyses.
3. Antoine Abou Fayad: NMR measurements and structure elucidation.

INTRODUCTION

With an estimated 220,800 newly diagnosed cases and 27,540 deaths in 2015, prostate cancer (PC) is the leading cause of cancer and the second leading cause of cancer-related deaths in the United States (1). Currently, numbers of patients with metastatic prostate cancer are increasing (2), leading to even higher death rates in the upcoming years.

A central player in the development and progression of prostate cancer is the androgen receptor (AR), a ligand-responsive transcription factor responsible for the expression of a plethora of cancer-related genes (3,4). Patients initially benefit from androgen deprivation therapy (ADT), however, ultimately develop castration-resistant prostate cancer (CRPC) accounting for persistently high mortality rates (5). Potential mechanisms underlying CRPC have been postulated and include clonal selection (6), adaptive up-regulation of antiapoptotic and survival gene networks (7–9), cytoprotective chaperones (10,11), and alternative mitogenic pathways (12–15), ultimately reactivating androgen-regulated processes and sustaining AR signaling (5,16,17).

The potent androgen dihydrotestosterone (DHT) is the primary ligand-activator of the AR and can still be detected in CRPC at sufficient levels for receptor activation (18–20). Classical pathways for the formation of late androgens (testosterone and DHT), irrespective of the production site, depend on the stepwise modification of steroid precursor pregnenolone by a complex enzymatic machinery (21) (Figure 1, grey arrows). The dual-function CYP17A1 enzyme is pivotal in the biosynthesis of active steroids and, most importantly, androgens (22). This fact explains the successful application of abiraterone (Abi), administered as the pro-drug Abi Acetate (AA), which is a potent irreversible inhibitor of CYP17A1 that binds to its catalytic site (23–26).

Despite initial response, substantial evidence has emerged in which persistent androgen signaling occurs despite AA treatment (27,28), and most tumors become refractory to treatment within 6-12 months (29). A more thorough understanding of the mechanisms involved in and the elucidation of the pathways leading to CRPC and resistance to Abi is paramount to improve outcomes for patients. Increase in intratumoral androgen concentrations, AR overexpression, and mutations leading to ligand promiscuity and/or independence, as well as modifications in co-factors that modulate AR function are possible explanations for this phenomenon (30). However, AR-related events are not the sole resistance mechanisms found in advanced PC. Increasingly evident are the roles played by prostate cancer cells' epithelial plasticity in developing a neuroendocrine phenotype (31–34), particularly under androgen-deprived conditions including patients resistant to Abi (35).

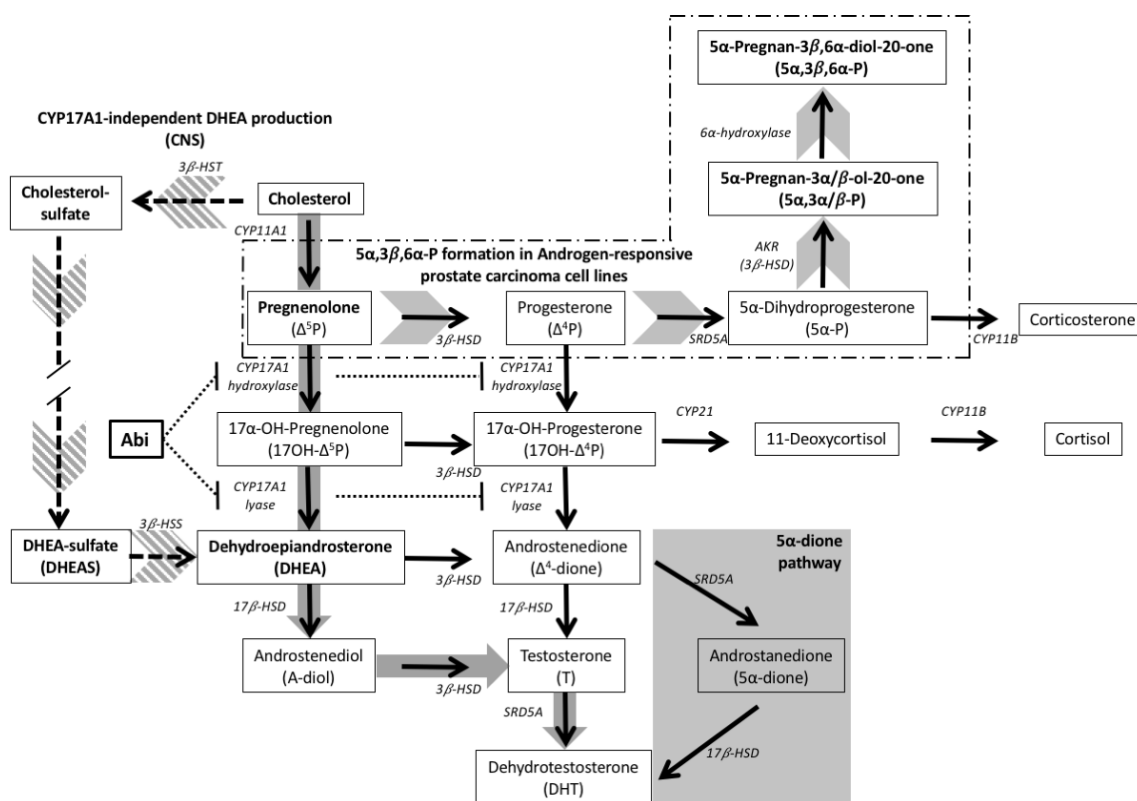


Figure 1. Schematic representation of steroidogenic biosynthesis leading to the production of corticosteroids and androgens. In the classical androgen production pathway (**grey arrows**), cholesterol is converted to C21 precursors pregnenolone and progesterone by CYP11A1. Progestagens are then converted to C19 adrenal androgens by the activity of CYP17A1-hydroxylase and -lyase functions. DHEA is acted on by 3 β -HSD or 17 β -HSD, eventually leading to testosterone and DHT production. DHT formation can also occur in an alternative (5 α -dione) pathway from androstenedione (**shaded area**). Under starvation conditions in androgen-responsive prostate carcinoma cell lines, pregnenolone metabolism leads preferentially to the production of 5 α -pregnan-3 β ,6 α -diol-20-one through the sequential activities of 3 β -HSD, SRD5A, 3-keto reductase and 6 α -hydroxylase enzymes (**grey arrowheads, dashed area**). The addition of the CYP17A1 inhibitor Abi (**dotted lines**), halts pregnenolone metabolism and leads to DHEA surge and accumulation in a CYP17A1-independent pathway, likely due to the multiple enzymatic inhibition activities of Abi-derived metabolite, D4A. A mechanism for DHEA formation in these conditions resembles the proposed, hypothetical mechanism in nervous tissue without CYP17A1 activity (**hatched arrowheads**). HSD: hydroxysteroid dehydrogenase; CYP: Cytochrome P450; HST: hydroxysteroid sulfotransferase; HSS: hydroxysteroid sulfate sulfatase; SRD5A: 5 α -reductase; AKR: aldo-keto reductase; CNS: central nervous system.

The aim of our study was to evaluate the steroid metabolism of prostate carcinoma cell lines under serum starvation. Furthermore, we aimed at assessing the effects of inhibitors like Abi on the steroid metabolic pathways in these cells.

MATERIALS AND METHODS***Chemicals***

Radiometric standards used include [1,2-³H]-11-deoxycortisol 40.0 Ci mmol⁻¹, [1,2-³H]-deoxycorticosterone (DOC) 60.0 Ci mmol⁻¹, [1,2,6,7-³H]-testosterone (T) 110.0 Ci mmol⁻¹ (American Radiolabeled Chemicals, Inc., St. Louis, MO); [11,2,6,7-³H(N)]-progesterone 99.1 Ci mmol⁻¹, [2,4,6,7-³H(N)]-estradiol 81.0 Ci mmol⁻¹, [2,4,6,7-³H(N)]-estrone 73.1 Ci mmol⁻¹, [1β-³H(N)]-androst-4-ene-3,17-dione 24.0 Ci mmol⁻¹, [1,2,6,7-³H(N)]-corticosterone 76.5 Ci mmol⁻¹, [4-¹⁴C]-dihydrotestosterone (DHT) 0.05 Ci mmol⁻¹, [1,2-³H(N)]-cholesterol 40-60 Ci mmol⁻¹, and [7-³H(N)]-pregnenolone 25.0 Ci mmol⁻¹ (PerkinElmer Life Sciences, Inc., Wellesley, MA). Enzyme inhibitors included CYP inhibitor Abi (3β-17-(3-pyridinyl)-androsta-5,16-dien-3-ol) (Chem-Impex International, Inc., Wood Dale, IL), tetradeuterated Abi (*d*₄-Abi; 3β-17-(2,4,5,6-tetradeuteriopyridin-3-yl)-androsta-5,16-dien-3-ol) (AlsaChim, Illkirch-Graffenstaden, France), and steroid sulfatase inhibitor STX64 (6-oxo-6,7,8,9,10,11-hexahydrocyclohepta(*c*)chromen-3-yl sulfamate) (Sigma-Aldrich, St. Louis, MO). Non-radioactive steroids pregnenolone, pregnenolone-20,21-¹³C₂-16,16-d₂, and allopregnanolone were purchased from Sigma-Aldrich. Stock solutions of these standards were prepared with analytical grade reagents as follows, 45:55 acetonitrile (ACN):H₂O solution for chromatographic experiments, methanol for mass spectrometry, and ethanol for *in vitro* incubation.

Cell lines and culture conditions

Prostate carcinoma cell lines: A subset of PC cell lines was used to encompass different cancer phenotypes: LNCaP, C4.2, VCaP and PC3. The cell lines VCaP, and C4.2 were kindly provided by Paul Thelen (Department of Urology, Georg-August-University Göttingen, Germany) and Amino Zoubeidi (The Vancouver Prostate Centre, University of British Columbia, Vancouver, BC, Canada). LNCaP and PC3 cells were purchased from DSMZ (Braunschweig, Germany). The cell lines LNCaP and C4.2 were authenticated in January 2015 by IGD Saar GmbH using STR-analysis (PowerPlex™16) on the ABI PRISM™ 310 Genetic Analyzer (Applied Biosystems). Mycoplasma contamination was assessed regularly by standard PCR.

LNCaP and C4.2 cell lines were cultured in Roswell Park Memorial Institute (RPMI) 1640 standard medium (Sigma-Aldrich) supplemented with 10% fetal calf serum (FCS) (Sigma-Aldrich). PC3 cells were maintained in Dulbecco's modified Eagle's medium (DMEM) (Sigma-Aldrich) supplemented with 10% FCS and 1% non-essential amino acids (Sigma-Aldrich). VCaP cells were cultured in DMEM medium without phenol red (Gibco | Thermo

Fisher Scientific, Waltham, MA), added of 10% FCS, 2% pyruvate Na and 1% L-Glutamine (Sigma-Aldrich). Cells were routinely grown at 37 °C under 5% CO₂ atmosphere in 150 mm tissue culture dishes (Sarstedt, Nümbrecht, Germany) containing 20 mL of media. For sub-culturing, attached cells were washed twice with PBS, detached with a trypsin-EDTA solution (0.05%/0.02%, v/v in PBS), and re-seeded at ratios of 1:4 for LNCaP and C4.2, 1:6 for PC3 cells, and 1:2 for VCaP.

Metabolic conversion and steroid identification

In our initial radiometric- and immunoassay-based analyses, we did not observe any significant differences in steroid levels between cell-free supernatant and cell lysate samples. Therefore, our total steroid measurements are representative of culture's supernatant. For standard radioactivity detector-coupled high-pressure liquid chromatography (radio-HPLC) and enzyme immunoassay (EIA) experiments, PC cells were seeded in Cell⁺ 24-well plates (Sarstedt) with 0.5 mL cell suspension containing 1.5×10^6 , 1.0×10^6 and 2.5×10^6 cells per well (LNCaP/C4.2, PC3, and VCaP, respectively). After 24 h, the full medium was exchanged for serum-free steroid deprived media and cells were kept under these starvation conditions for an additional 96 h. Finally, cells were exposed to biologically relevant levels of pregnenolone (10 nM) and progesterone (3 nM) (36), or supraphysiological levels of allopregnanolone (500 nM) (37), with or without Abi and STX64 inhibitors for 48 h. Radioactive steroid precursors [7-³H(N)]-pregnenolone or [11,2,6,7-³H(N)]-progesterone were added for metabolic pathway analysis with radio-HPLC. Non-radioactive precursor pregnenolone was used in immunoassays for total supernatant concentrations of late androgens.

When scaling up cell cultures for metabolite identification, treated and untreated samples were cultivated in 500 cm² Cell Culture Treated TripleFlasks™ (Thermo Fisher Scientific) with 200 mL media per flask. Steroid extraction and sample concentration were performed in serial extraction steps with analytical grade ethyl acetate (EtOAc) (Sigma-Aldrich) and subjected to identical HPLC separation and fraction collection routines before HPLC-ESI-ToF-MS analysis.

Steroid extraction

Supernatants were extracted twice with EtOAc (1:1, v/v) and the organic layers were evaporated using a Centrivap™ centrifugal evaporation system (Thermo Fisher Scientific) at 35 °C. Samples were then reconstituted in 60 µL of 45:55 ACN:H₂O for radioactively-labelled HPLC experiments, 50 µL methanol for HPLC-ESI-ToF-MS, 250 µL deuterated chloroform (CDCl₃) for NMR analysis, and 200 µL of assay buffer for EIAs.

HPLC separation and detection of steroids

CHAPTER 3

Radiometric detection of radiolabeled compounds: HPLC radiometric detection was performed with an Agilent Technologies 1200 Series separation module coupled with a Ramona Star Detector (Raytest, Straubenhardt, Germany) equipped with a 0.5 mL flow cell. A Macherey-Nagel (Düren, Germany) Nucleodur 100-5 C18ec column (125×3 mm, 5 µm), equilibrated with 37.5:62.5 ACN:H₂O and ramped linearly to 61:39 ACN:H₂O within 50 min, was used to separate radiolabeled standards, before re-equilibration under the initial conditions was triggered. All solvents were HPLC grade with 0.1% of trifluoroacetic acid (TFA). Flow rate during liquid chromatography was fixed at 0.5 mL min⁻¹, while Quickszint Flow 302 scintillation fluid (Zinsser Analytic, Frankfurt, Germany) was added before the scintillation cell with a flow rate of 0.9 mL min⁻¹.

Separation and fractionation of non-labeled metabolite: HPLC was performed with the same devices, flow rate, and solvent system as described above. However, an improved separation method was achieved when equilibrating the column to 75:25 H₂O:ACN and applying a linear gradient to 65:35 H₂O:ACN within 60 min before a 5 min wash step with 100% ACN and returning to the initial conditions. Chromatograms obtained from radiolabeled standards were used as means of comparison of their retention times with that of the [7-³H(N)]-pregnenolone-derived metabolites on the same chromatographic method. The improved protocol was used to collect the fractions of untreated samples and those treated with pregnenolone, pregnenolone-20,21-¹³C₂-16,16-d₂, and allopregnanolone in the chromatographic interval between 31 and 36 minutes.

HPLC-ESI-ToF-MS measurements and data analysis

All measurements were performed on a Dionex Ultimate3000 RSLC system (Thermo Fisher Scientific) using a Waters BEH C18 dp column (50×2.1 mm, 1.7 µm) thermostated at 45 °C. Separation of 1 µl sample was achieved by a linear gradient with H₂O to ACN at a flow rate of 600 µL min⁻¹. The gradient was initiated by a 1 min isocratic step at 95:5 H₂O:ACN, followed by an increase to 95% ACN in 6 or 13.5 min to end up with a 1.5 min plateau step at 95% ACN before re-equilibration under the initial conditions. All solvents used were HPLC-grade with 0.1% of formic acid (MS grade). UV-spectra were recorded by a DAD in the range from λ = 200 - 600 nm. The LC flow was split to 75 µL min⁻¹ before entering the maXis 4G hr-ToF mass spectrometer (Bruker, Bremen, Germany) using a standard ESI source. Mass spectra were acquired in centroid mode ranging from 150 - 2000 *m/z* at a 2 Hz scan speed.

NMR analysis of 5α-pregnan-3β,6α-diol-20-one

Extracted, isolated, and purified metabolite from C4.2 cell culture supernatant was dissolved in deuterated chloroform (CDCl_3) and ^1H , HSQC, HMBC and COSY spectra were recorded using an Ascend 700 MHz NMR spectrometer (Bruker). Based on the data obtained and published results (1S–3S), assignments were assessed accordingly.

Synthesis and analysis of Δ^4 -abiraterone

Compound synthesis: Δ^4 -Abi was synthesized through Oppenauer oxidation from Abi. Abi (50 mg, 0.125 mmol) and aluminum isopropoxide (128 mg, 0.625 mmol, Sigma-Aldrich) were dissolved in a mixture of toluene (15 mL) and acetone (5 mL) under nitrogen atmosphere and refluxed for 8 h. Reaction progress was monitored by TLC analysis on silica gel 60 F₂₅₄ (Merck, Kenilworth, NJ) under UV-C light. After complete conversion, the volatiles were removed under reduced pressure, and the crude mixture was resuspended in brine and extracted with EtOAc (3 × 15 mL). The organic phases were separated, combined, and dried over sodium sulfate. After filtration, the volatiles of the filtrate were removed under reduced pressure. Purification of the residue by column chromatography on silica gel 60 (63–200 μm) with a mixture of chloroform:MeOH (98.5:1.5, v/v) as eluent gave 32 mg (0.092 mmol, 74% yield) of a yellowish crystalline solid. The purity of Δ^4 -Abi was checked by analytical HPLC using a Dionex Ultimate3000 (Thermo Fisher Scientific) system with a DAD detector monitoring UV absorbance at $\lambda = 254$ nm and a Macherey-Nagel Nucleoshell RP18plus column (100×2 mm, 2.7 μm) coupled to a Bruker amaZon SL mass spectrometer equipped with a standard ESI source. MS (ESI+) m/z : $[\text{M}+\text{H}]^+ = 348.24$. Purity (UV) = >99%. ^1H and ^{13}C -NMR spectra were recorded on a Bruker DRX-500 instrument at 300K. Chemical shifts are reported in δ values (ppm) and referenced on the signal of ^1H -isotopologic solvent residues (CDCl_3 : $^1\text{H} = 7.26$, $^{13}\text{C} = 77.16$). Splitting patterns are designated as follows: s, singlet; d, doublet; dd, doublet of doublet. The coupling constants (J) are given in hertz (Hz).

^1H -NMR (500 MHz, CDCl_3): 1.03 (s, 3H), 1.25 (s, 3H), 1.35–2.50 (complex), 5.76 (s, 1H), 6.01 (s, 1H), 7.25 (dd, $J = 8.0$, $J = 5.0$, 1H), 7.66 (d, $J = 7.5$, 1H), 8.48 (d, $J = 4.0$, 1H), 8.63 (s, 1H). Spectroscopic data matches previously described findings (25,38). ^{13}C -NMR (125 MHz, CDCl_3): 16.6, 17.2, 20.9, 31.6, 31.7, 32.8, 33.9, 34.1, 35.0, 35.6, 38.7, 47.3, 53.9, 56.8, 123.1, 124.0, 129.2, 132.8, 133.8, 147.7, 147.8, 151.4, 170.9, 199.5. Spectroscopic data matches previously described findings (38). High-resolution mass spectrum was recorded using HPLC-ESI-ToF-MS as described above. Experimental $[\text{M}+\text{H}]^+ = 348.2313$; calculated $[\text{M}+\text{H}]^+ = 348.2322$.

HPLC-MS/MS analysis of Δ^4 -Abi

CHAPTER 3

The compounds Abi and D4A, as well as internal standard d_4 -Abi, were analyzed through an Accela HPLC system (Thermo Fisher Scientific) coupled with a triple quadrupole mass spectrometer TSQ Quantum Access Max (Thermo Fisher Scientific) equipped with an HESI-II source. Separation was achieved by a Macherey-Nagel Nucleodur C₁₈ Isis column (125×2 mm, 3 μm) thermostated at 30 °C. The mobile phase consisted of 70:30 MeOH:H₂O for 1 min, followed by 85:5:10 MeOH:H₂O:ACN for 2 min before returning to initial conditions at a flow rate of 400 μL min⁻¹. All solvents used were HPLC grade added of 0.1% formic acid (MS grade). Compounds were ionized using electrospray ionization (ESI) in positive ion mode with the following parameters: spray voltage: 4000 V; vaporizer temperature: 350 °C; sheath gas pressure (nitrogen): 30 units; auxiliary gas pressure (nitrogen): 35 units; skimmer offset voltage: 0 V; capillary temperature: 270 °C. Selected reaction monitoring was used for detecting Abi (350.115→155.973 [quantitative], collision energy: 54 V, tube lens: 110 V; 350.115→332.013 [qualitative], collision energy: 41 V, tube lens: 120 V), Δ⁴-Abi (348.100→155.953 [quantitative], collision energy: 52 V, tube lens: 120 V; 348.100→334.062 [qualitative], collision energy: 41 V, tube lens: 110 V) and d_4 -Abi (354.135→159.975; collision energy: 51 V; tube lens: 120 V) employing: scan width: 0.010 m/z ; scan time: 0.300 s; peak width: 0.70. Calibration curves were prepared following the same protocol and conditioned media without the addition of exogenous compounds, spiked with known concentrations of analytes and 500 nM of d_4 -Abi.

Total steroid quantification with EIAs

Extraction of free steroids was performed as described above. Aliquots of 500 μL of cell culture supernatant were extracted with EtOAc. Vials were vortexed for 10 min at 1,500 rpm and subsequently centrifuged for another 10 min at 10,000 g . Steroid-containing supernatants were transferred to fresh reaction tubes and evaporated. Dehydroepiandrosterone (DHEA), dihydrotestosterone (DHT), and testosterone (T) levels were determined by competitive enzymatic immunoassay (EIA) according to the manufacturer's protocols (DRG Instruments GmbH, Marburg, Germany). Changes in steroid concentrations were assessed against untreated controls (no addition of exogenous precursor substrates or enzyme inhibitors).

Statistical analyses

Differences between treated and untreated samples were evaluated using a one-way ANOVA followed by a two-sided Holm-Sidak's multiple comparison test using GraphPad Prism version 6.0f for Mac OS X (GraphPad Software, La Jolla California USA). Differences were considered significant at a p -value <0.05.

RESULTS

Steroid Precursors Are Metabolized to a Single Product in Androgen-Responsive Cell Lines Under Serum Starvation

Mimicking the environmental conditions of cancer cells in CRPC patients after androgen deprivation therapy (ADT), we assessed the steroid metabolism of human PC cell lines under serum starvation conditions. Radioactive steroid detection following administration of relevant levels of pregnenolone (10 nM) (36) identified a single, unknown product that did not correspond to any common standards (Table 1, Supplementary Figure 1).

Table 1. Radiometric standards were analyzed for retention time (RT) correspondence when compared to pregnenolone-derived metabolite produced by androgen-sensitive cell lines. All experiments were performed in triplicates.

³ H-steroid	Radiometric RT (min)
Pregnenolone	30.67
Progesterone	28.82
DHT	19.50
Androstenedione	12.83
Estrone	12.62
DOC	11.08
Testosterone	10.19
Estradiol	8.93
Corticosterone	5.23
11-deoxycortisol	4.38
<i>Pregnenolone-derived metabolite</i>	<i>4.96</i>

This product was exclusively present in the androgen responsive cell lines LNCaP (mutated androgen receptor), C4.2 (androgen-independent AR), and VCaP (overexpressed wild-type AR), while PC3 (absent AR) cells did not metabolize pregnenolone (Figure 2-A).

We advanced our investigation using a deuterated isotopologue of pregnenolone for an untargeted analysis of pregnenolone-treated and -untreated samples using HPLC-ESI-ToF-MS. Treated samples generated a peak at 4.45 ± 0.01 min (Figure 2-B, *left*) that is absent in control samples, prompting for the analysis of its mass spectra fragmentation. The peak corresponding to this unknown metabolite was found to be 335.2590 Da. As expected –with a 4 Da shift– HPLC-ESI-ToF-MS analysis of deuterated pregnenolone showed a metabolite with an exact

mass of 339.2774 Da (Figure 2-B, *right*), confirming that the obtained compound is indeed derived from this primordial precursor.

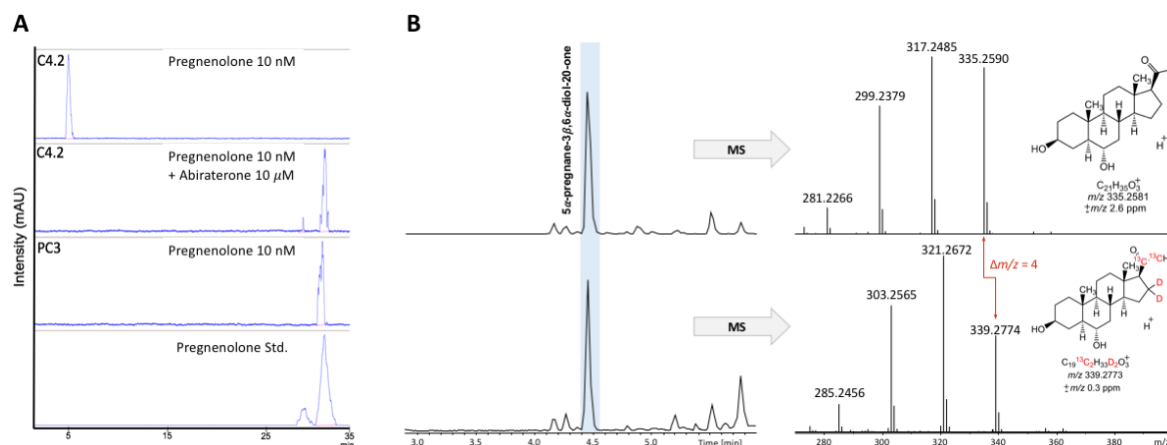


Figure 2. (A) Representative chromatographic profiles of androgen-responsive cell lines indicate the formation of a single product from pregnenolone precursor (10 nM) after 48 h of metabolism. The addition of Abi (10 μ M) renders androgen-responsive cells incapable of metabolizing pregnenolone, similarly to AR-absent PC3 cells. (B) Chromatograms (total ion current, TIC) and mass spectra obtained by HPLC-ESI-ToF-MS analysis of the metabolic product from C4.2 cell cultures treated with 10 nM native (*top*) and isotope-labeled (*bottom*) pregnenolone confirming the pregnenolone-derived nature of the newly identified metabolite. LC graphs (*left*) show the production of 5 α -pregnan-3 β ,6 α -diol-20-one from pregnenolone substrates, confirmed by NMR spectra analysis. Inserts show expected m/z -values of the putative metabolites and corresponding mass shift.

Precursor Metabolism Is Independent of CYP17A1 Activity and Leads to 5 α -pregnane Steroid Formation

Treatment of androgen-responsive cells with the CYP17A1 inhibitor Abi completely abolished steroid metabolism, identical to what was observed in PC3 cells (Figure 2-A, *center panels*). This observation initially suggested the involvement of CYP17A1 activity on product formation. However, in contrast to pregnenolone-treated samples, progesterone metabolism led to the same downstream metabolite and was maintained even under CYP17A1 inhibition (Figure 3-A). A kinetic analysis showed that androgen-responsive cells metabolize these precursors almost exclusively to a single product (Figure 3-B), in a pathway independent from CYP17A1 and likely dependent on the activity of 3 β -HSD.

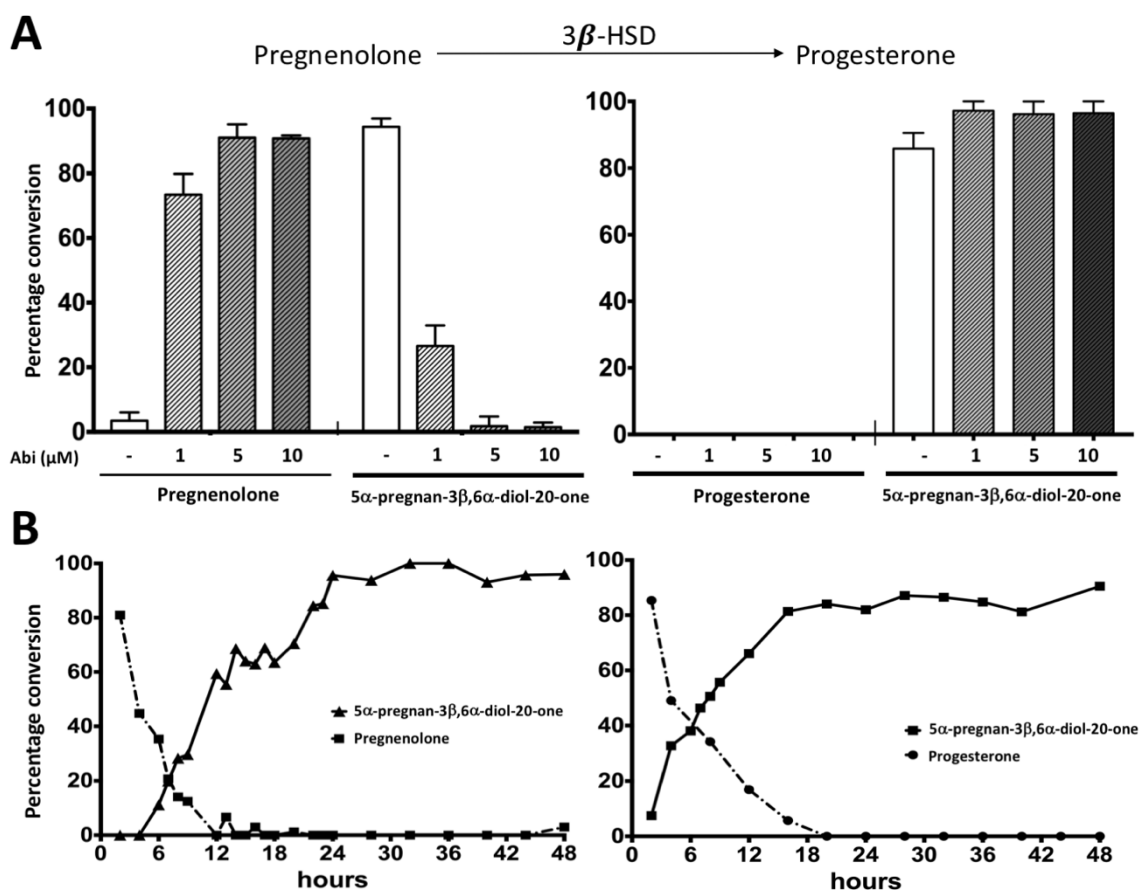


Figure 3. (A) Abi administration strongly inhibits the formation of 5 α -pregnan-3 β ,6 α -diol-20-one metabolite from pregnenolone precursor. However, it shows no effects on the metabolism of downstream precursor progesterone to the same end-product, suggesting that metabolic hindrance is likely associated with the inhibition of the 3 β -HSD enzyme and in a CYP17A1 independent manner. Results are shown as mean \pm SEM of at least two biological replicates. (B) Kinetics of pregnenolone and progesterone metabolism in androgen-responsive C4.2 cells. Pregnenolone and progesterone are avidly metabolized to 5 α -pregnan-3 β ,6 α -diol-20-one, with nearly complete conversions at 24 h and 18 h, respectively.

Analysis of the metabolic potential of our cell lines on the neuroactive steroid allopregnanolone (Allo), one of the major metabolites of progesterone in extrahepatic tissues (39,40), determined that Allo is indeed an intermediate on the pathway under investigation (Supplementary Figure 2). As evidence built indicating this compound to be a 5 α -pregnane, we proceeded to NMR analysis of purified metabolite samples (Supplementary Figure 3). Of notice, NMR data showed that the hydrogen in position 6 displayed a characteristic triplet of doublets having two couplings related to axial-axial hydrogens ($J = 10.6$ Hz), and one coupling related to axial-equatorial hydrogens ($J = 4.5$ Hz). Consequently, the hydrogen in position 6 must be axial compared to the steroid plane (β configuration), while the hydroxy group equatorial (α configuration). Furthermore, as in position 7 there is a methylene group with equatorial and axial hydrogen. The hydrogen in position 5 must be axial compared to the molecule plane (α

configuration) (Supplementary Table 1 and Supplementary Figure 4). Finally, NMR data confirmed the compound identity to be 5 α -pregnan-3 β ,6 α -diol-20-one (5 α ,3 β ,6 α -P) (Supplementary Table 1 and Supplementary Figure 4).

Formation of 5 α -pregnan-3 β ,6 α -diol-20-one is Hampered by Abiraterone Metabolism

Li and colleagues (41) showed the multi-enzyme inhibition potential of Abi-derived metabolite, D4A, which blocks 3 β -HSD (IC_{50} = 19 nM) and SRD5A (IC_{50} = 1.2 μ M) enzymes in addition to parental CYP17A1 inhibition. Since the canonical pathway for 5 α ,3 β ,6 α -P production from pregnenolone initially depends on the activity of 3 β -HSD and SRD5A (Figure 1, solid arrowheads), we further analyzed our samples for the presence of D4A. HPLC-MS/MS analysis confirmed the conversion of Abi to D4A after 48h of treatment to varying degrees (Figure 4). D4A levels in PC supernatants accounted for 12.50 \pm 2.43 nM, 101.86 \pm 4.31 nM, 61.48 \pm 7.48 nM, and 4.86 \pm 0.64 nM in LNCaP, C4.2, VCaP, and PC3 cell lines, respectively.

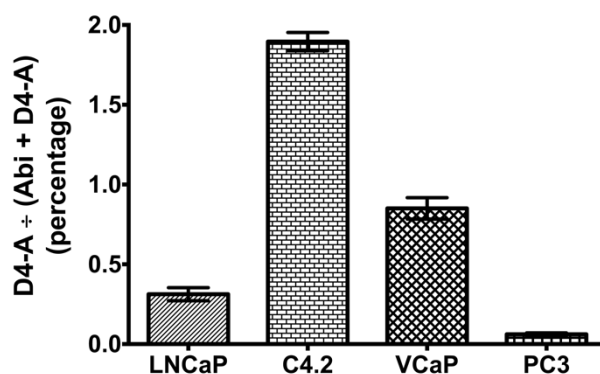


Figure 4. Metastatic prostate carcinoma cell lines are able to convert Abi to D4A. Cells were treated with 10 μ M Abi for 48 h. Abi and D4A (as a percentage of Abi + D4A) were quantified by HPLC-MS/MS compared to a standard curve. Results are shown as mean \pm SEM. All experiments were conducted in triplicates.

Blockage of initial metabolic steps likely arrests precursor metabolism and potentiates Δ^5 -steroid accumulation as discussed below.

Abiraterone Leads to DHEA and DHT Increase in a Neuroendocrine-like Testosterone-Independent Pathway

As seen in our EIA results, the addition of pregnenolone alone did not significantly increase the production of late androgens testosterone and DHT (Figure 5-A) or androgen precursor DHEA (Figure 5-B) in any of the tested cell lines under serum-starved conditions. This fact again suggests that pregnenolone does not play a role in androgen *de novo* synthesis and is consistent with the results of our radio-HPLC experiments.

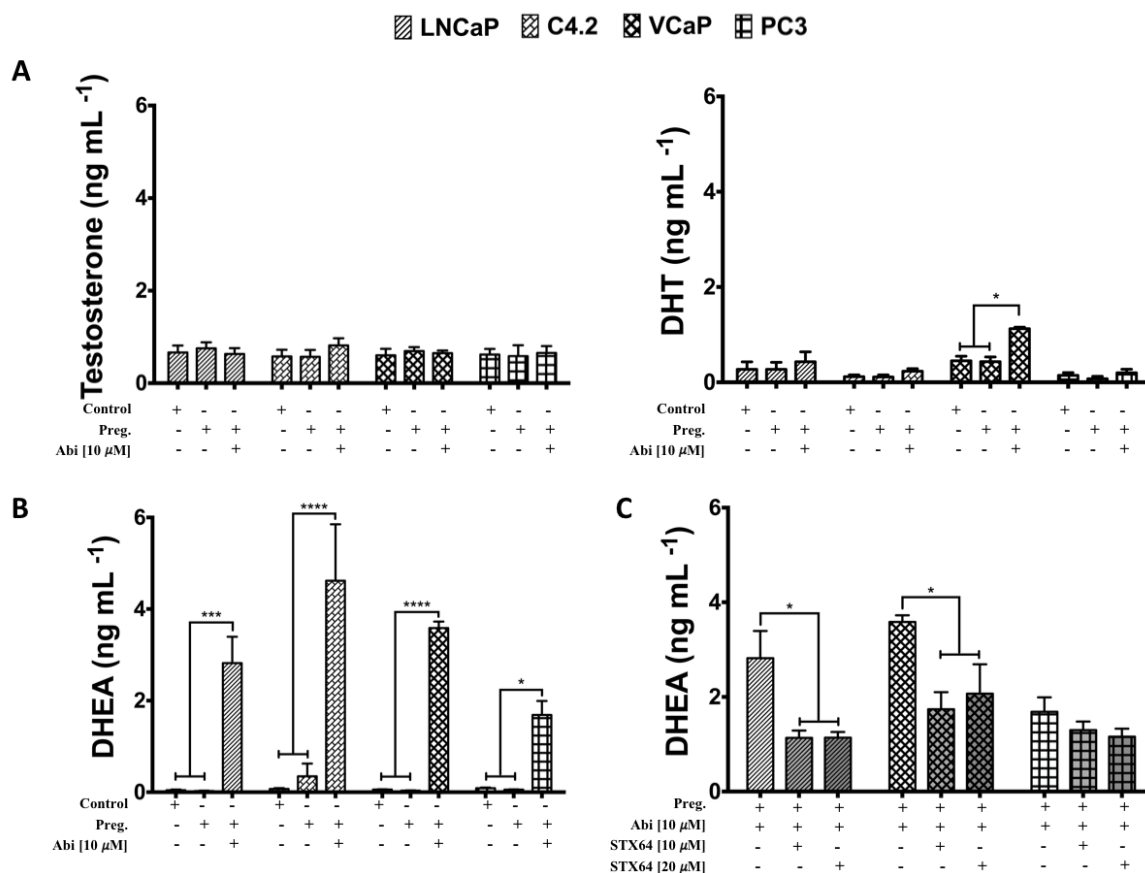


Figure 5. Mean \pm SEM concentration of indicated androgens measured by enzyme immunoassays (EIAs) of the supernatant fraction derived from different prostate carcinoma cell lines when starved for 96 h and cultured in the presence of steroid precursor pregnenolone (10 nM) for 48 h, added or not of inhibitor Abi and STX64. (A) Pregnenolone did not change the levels of late androgens T and DHT, arguing against *de novo* steroidogenesis from this precursor. (B) Concomitant treatment with abiraterone leads to significantly higher levels of DHEA in cultured cells. Abiraterone cross-reactivity is negligible at: 0.0039%. (C) Formation of DHEA can be partially inhibited upon administration of steroid sulfatase inhibitor STX64, suggesting that DHEA-S might be the immediate source of measured DHEA in a metabolic pathway resembling that of nervous tissues. Experiments were conducted in triplicates unless otherwise stated. Experiments with STX64 were conducted in at least duplicates. *: $p < 0.05$, ***: $p < 0.001$, ****: $p < 0.0001$.

However, when treated with Abi, a clear and significant increase in the production of DHEA was observed in all androgen-responsive cell lines. We observed increases in DHEA levels of >100 -fold in LNCaP and VCaP, 13-fold in C4.2, and 31-fold in PC3 cells when compared to pregnenolone only-treated samples. Cross-reactivity of Abi with anti-DHEA antibodies was negligible at 0.0039% (0.33 ng mL^{-1}) and ruled out. Given the lack of *de novo* synthesis from pregnenolone, we tested the possible involvement of its upstream precursor, cholesterol. The addition of steroid sulfatase inhibitor STX64 significantly decreased DHEA production in androgen-responsive LNCaP and VCaP cells ($60 \pm 12\%$ and $51 \pm 20\%$ at $10 \mu\text{M}$, respectively) (Figure 5-C). By blocking the putative last metabolic step on this proposed pathway with

CHAPTER 3

STX64, we demonstrated that steroid sulfatase is responsible, at least partially, for the increase in DHEA levels likely from immediate precursor DHEA-S. Altogether, our data suggests that the *de novo* synthesis of androgens takes place from cholesterol, and not pregnenolone, in cancer cells that adopted a neuroendocrine phenotype under serum-starved conditions.

DISCUSSION

The sources for androgen formation and AR signaling in prostate cancer patients undergoing ADT have long been a matter of debate. Given the convoluted scenario of the steroidogenesis potential of different cancer cell types, we included phenotypically distinct cell lines in our research to simulate the different mechanisms involved in the gain of resistance and CRPC observed in patients and its link to treatment with the CYP17A1 inhibitor Abi.

In this study, we have shown that androgen-responsive cell lines did not produce any of the expected late androgens (i.e., androstenedione, T and DHT), which are directly or indirectly responsible for the canonical activation of the AR *in vivo*, from early steroid precursors pregnenolone or progesterone. We also observed that androgen-independent PC3 cells did not metabolize pregnenolone, similarly to androgen-responsive cells lines when under Abi treatment. However, CYP17A1 inhibition by Abi did not stop the metabolism of progesterone or its 5 α -pregnane metabolite, allopregnanolone. These observations suggest that the preferred pathway for early precursor metabolism does not lead to CYP17A1-dependent androgen formation and that if these cell lines are indeed capable of *de novo* synthesis, pregnenolone is presumably not the starting precursor.

Rather, precursor metabolism likely takes place in a pathway independent from CYP17A1 and dependent on the activity of the 3 β -HSD, a crucial enzyme responsible for the conversion of Δ^5 steroid precursors into cognate Δ^4 metabolites. In contrast to wild-type PC3 cells, androgen-responsive cell lines express mutant 3 β -HSD with increased metabolic activity (19,42). Up-regulation and increased activity of enzymes linked to androgen synthesis in steroid-depleted environments is a well-known phenomenon in CRPC and alterations in the steroidogenic potential of prostate carcinoma cells under different metabolic inhibitors, such as Abi (i.e., increase in DHT levels in the absence of progesterone), have been reported (43). Another commonly upregulated and abnormally active enzyme in prostate cancer is the SRD5A (44–47), which catalyzes the conversion of progesterone to its 5 α -pregnane metabolites (i.e., 5 α -dihydroprogesterone (5 α -P) and Allo), as well as of testosterone to the potent AR ligand, DHT. In line with these facts, our work describes for the first time the formation of 5 α -pregnan-3 β ,6 α -diol-20-one in prostate cancer cell lines, a metabolite that depends on the sequential steps

of the steroidogenic enzymes 3 β -HSD, SRD5A, 3-keto reductase (AKR), and 6 α -hydroxylase (Figure 1, *solid arrowheads*). Interestingly, it has been shown by others that 5 α ,3 β ,6 α -P formation from progesterone is linked to proliferative activities in a variety of other malignant cell types, namely human testicular and ovarian carcinomas (48), human breast cancer (49), and human leukemic monoblast (50) cells. A more direct association with advanced PC lacked until now. These groups investigated the putative biological activities of intermediates in the pathway to 5 α ,3 β ,6 α -P and suggested a strong positive correlation between the formation of 5 α -pregnane metabolites and cancer mitogenesis and metastasis in signaling pathways also found in the prostate cancer environment (50–54). Proposed clinical implications on progesterone metabolism suggest that an imbalance in the ratios of progesterone metabolites in cancerous tissues affects cells to change from normalcy (i.e., 3 α -reduced metabolites) to increased proliferation and detachment behaviors (i.e., 5 α -reduced metabolites) (51).

The molecular mechanisms by which 5 α ,3 β ,6 α -P aggravates cancer phenotypes are not yet fully elucidated. However, mounting evidence indicates that progesterone and its metabolites are capable of eliciting rapid responses through membrane progesterone receptors (mPR) (55–57). Such interactions with non-genomic receptors (i.e., PGRMC1) (57) are not suppressed by drugs targeting steroid nuclear receptors and by initiating different and highly detrimental G-protein-associated signaling pathways (i.e., PI3K/Akt) that may prevent cell cycle arrest, evade apoptosis and stimulate cancer stem cell maintenance and de-differentiation (53).

In addition to the increased expression/activity of 3 β -HSD (19,42) and SRD5A (44–47), noteworthy is the presence of AKR1C in this pathway. The AKR1C family of enzymes are key players in steroid hormone metabolism with some degree of promiscuous binding abilities to structurally related steroidal compounds (58). AKR1C expression and activity appear to be responsive to changes in steroid levels. Four AKR1C isoforms exist that could catalyze the reduction of 5 α -P into downstream tetrahydrosteroids. More specifically AKR1C3, which is also upregulated in prostate cancer (47) and has been implicated in cancer cell survival and proliferation, as well as in the modulation of sensitivity to treatment (59), and AKR1C1 that has been shown to exhibit 3 β -HSD activity. Due to their metabolic versatility and apparent promiscuity, the determination of which AKR1C isoform would be responsible for the conversion of the precursors shown in our experiments remains to be confirmed.

In addition, our data is in line with the multiple-enzyme inhibitory potential of D4A (41), a compound found in our Abi-treated samples. D4A is the product of the 3 β -HSD-mediated metabolism of Abi (a limiting factor on metabolite formation due to a negative feedback loop)

CHAPTER 3

as a result of structure similarity of this inhibitor with native ligands such as DHEA and Δ^5 -androstenediol (A-diol). In contrast to its parent compound, D4A inhibits additional enzymes involved in steroid biosynthesis including 3β -HSD and SRD5A. These enzymes, together with CYP17A1, constitute the essential machinery in the cell for the steroidogenesis of androgens from progestagen precursors in classical steroidogenesis pathways. In our experimental setup, 3β -HSD is likely the main target responsible for the observed arrest in precursor metabolism in androgen-responsive cells by at least two possible mechanisms. Firstly, by direct D4A-driven inhibition of enzymatic activity and secondly, by Abi acting as a competitive ligand for the enzyme binding site against native 3β -HSD ligands such as pregnenolone, especially given the fact that Abi levels at 10 μ M are 1000-fold higher than those of the native ligand at biologically relevant levels. Furthermore, the lack of pregnenolone metabolism in PC3 cells also hints at the pivotal role of 3β -HSD under serum starved conditions. These cells have been shown to have a native lowered activity of the 3β -HSD enzyme (42) that may be further decreased by a preferred reductive function of the enzyme compared to its androgen-responsive counterparts (60).

The fact that DHEA levels increased so dramatically without corresponding elevation in downstream metabolites' levels suggests the presence of a limiting factor on the conversion rate of DHEA. This fact constitutes another strong indication of the D4A-mediated blockage of 3β -HSD and SRD5A activities upon administration of Abi to our *in vitro* system, at which point these enzymes would not be able to metabolize DHEA further into its androgenic metabolites (similarly to the arrest seen in pregnenolone \rightarrow $5\alpha,3\beta,6\alpha$ -P metabolism).

As previously mentioned, Pham and colleagues demonstrated the quantitative and qualitative alterations in steroidogenic potentials of prostate cancer cells *in vitro* by different steroid precursors and inhibitors (43). It is likely that not only steroid depletion during starvation conditions but also Abi and pregnenolone, mimicking an *in vivo* ADT treatment environment, are collectively responsible for the observed phenomena in our setups and the emergence of previously unknown bypass mechanisms for androgen biosynthesis, which are discussed below. The work of Maayan and colleagues (61) on the increased DHEA production by neuro-like cells in a CYP17A1-independent manner under castration conditions in mice recapitulates the phenotypic changes that we observed in our experiments. The transdifferentiation of adenocarcinoma cells into a neuroendocrine prostatic carcinoma-like phenotype (NE-like PC cells) has been increasingly demonstrated and appears to be strongly induced in an androgen-depleted environment (31–34), posing as a mechanism in the development of resistance to androgen deprivation therapy. NE-like PC cells originate from the transdifferentiation of cancer

epithelial cells and lead to androgen independence and tumor progression. Baulieu and colleagues (62) showed the CYP17A1-independent formation of DHEA occurs in rat brains incubated with cholesterol. While the metabolizing enzymes are yet to be elucidated, it suggests that *de novo* metabolism may take place from an upstream compound to pregnenolone in nervous tissue. Precursors of cholesterol and cholesterol-sulfate (the latter implicated as a differentiating compound in cancerous tissues (63)), include homocysteine and oxidized LDL (both of which could be a source for precursor formation) (64). Cholesterol and its sulfate form would eventually be converted to DHEA-sulfate (DHEA-S), the most abundant circulating steroid hormone in humans, and sequentially to DHEA (Figure 1, hatched arrow) (65,66). The blockage of steroid sulfatase by STX64 in our experiments shows the cholesterol-driven synthesis of androgen precursors under serum starved conditions and Abi treatment, highlighting the versatility of cancer cells in development of resistance to therapy.

CONCLUSION

Altogether, our study adds further evidence to the complex networks in the steroid metabolism of prostate carcinoma cells. We identified the mitogenic metabolite 5α -pregnan- 3β , 6α -diol-20-one as a product from pregnenolone under starvation conditions in androgen-responsive cells for the first time. This process could only be abolished by Abi at its initial metabolic step. Together with the increase in DHEA production in Abi-treated samples via a cholesterol-dependent pathway, our results hint at a neuroendocrine transdifferentiation of epithelial prostate cancer cells. NE-like PC cells are associated with poor treatment prognosis and increased androgen independence. Our work calls for further characterization of prostate carcinoma cells in androgen-depleted environments and elucidates the fate of early steroid precursors in androgen-responsive cells, paving the way for a new understanding of the biological relevance of progesterone metabolites in prostate cancer, efficacy of Abi treatment, and the development of resistance.

REFERENCES

1. Siegel RL, Miller KD, Jemal A. Cancer Statistics, 2015. *CA Cancer J Clin.* 2015;65:5–29.
2. Weiner AB, Matulewicz RS, Eggner SE, Schaeffer EM. Increasing Incidence of Metastatic Prostate Cancer in the United States (2004–2013). *Prostate Cancer Prostatic Dis.* 2016;19:395–7.
3. Wang Q, Li W, Zhang Y, Yuan X, Xu K, Yu J, et al. Androgen Receptor Regulates a Distinct Transcription Program in Androgen-Independent Prostate Cancer. *Cell.* 2009;138:245–56.
4. Hendriksen PJM. Evolution of the Androgen Receptor Pathway during Progression of Prostate Cancer. *Cancer Res.* 2006;66:5012–20.
5. Scher HI. Biology of Progressive, Castration-Resistant Prostate Cancer: Directed Therapies Targeting the Androgen-Receptor Signaling Axis. *J Clin Oncol.* 2005;23:8253–61.
6. Isaacs JT. The Biology of Hormone Refractory Prostate Cancer. *Urol Clin North Am.* 1999;26:263–73.
7. Giménez-Bonafé P, Fedoruk MN, Whitmore TG, Akbari M, Ralph JL, Ettinger S, et al. YB-1 is Upregulated during Prostate Cancer Tumor Progression and Increases P-glycoprotein Activity. *Prostate.* 2004;59:337–49.
8. Fedoruk MN, Giménez-Bonafé P, Guns ES, Mayer LD, Nelson CC. P-glycoprotein Increases the Efflux of the Androgen Dihydrotestosterone and Reduces Androgen Responsive Gene Activity in Prostate Tumor Cells. *Prostate.* 2004;59:77–90.
9. Gleave M, Tolcher A, Miyake H, Nelson C, Brown B, Beraldi E, et al. Progression to Androgen Independence is Delayed by Adjuvant Treatment with Antisense Bcl-2 Oligodeoxynucleotides after Castration in the LNCaP Prostate Tumor Model. *Clin Cancer Res.* 1999;5:2891–8.
10. Rocchi P. Heat Shock Protein 27 Increases after Androgen Ablation and Plays a Cytoprotective Role in Hormone-Refractory Prostate Cancer. *Cancer Res.* 2004;64:6595–602.
11. Rocchi P. Increased Hsp27 after Androgen Ablation Facilitates Androgen-Independent Progression in Prostate Cancer via Signal Transducers and Activators of Transcription 3-Mediated Suppression of Apoptosis. *Cancer Res.* 2005;65:11083–93.
12. Culig Z. Androgen Receptor Cross-talk with Cell Signalling Pathways. *Growth Factors.* 2004;22:179–84.
13. Craft N, Shostak Y, Carey M, Sawyers CL. A Mechanism for Hormone-Independent Prostate Cancer through Modulation of Androgen Receptor Signaling by the HER-2/neu Tyrosine Kinase. *Nat Med.* 1999;5:280–5.
14. Miyake H. Overexpression of Insulin-Like Growth Factor Binding Protein-5 Helps Accelerate Progression to Androgen-Independence in the Human Prostate LNCaP Tumor Model through Activation of Phosphatidylinositol 3'-Kinase Pathway. *Endocrinology.* 2000;141:2257–65.
15. So A, Gleave M, Hurtado-Col A, Nelson C. Mechanisms of the Development of Androgen Independence in Prostate Cancer. *World J Urol.* 2005;23:1–9.
16. Smaletz O, Scher HI. Outcome Predictions for Patients with Metastatic Prostate Cancer. *Semin Urol Oncol.* 2002;20:155–63.
17. Walsh P. Docetaxel and Estramustine Compared With Mitoxantrone and Prednisone for Advanced Refractory Prostate Cancer. *J Urol.* 2005;173:457–457.
18. Titus MA. Testosterone and Dihydrotestosterone Tissue Levels in Recurrent Prostate Cancer. *Clin Cancer Res.* 2005;11:4653–7.
19. Montgomery RB, Mostaghel EA, Vessella R, Hess DL, Kalhorn TF, Higano CS, et al.

- Maintenance of Intratumoral Androgens in Metastatic Prostate Cancer: A Mechanism for Castration-Resistant Tumor Growth. *Cancer Res.* 2008;68:4447–54.
20. Sharifi N. Minireview: Androgen Metabolism in Castration-Resistant Prostate Cancer. *Mol Endocrinol.* 2013;27:708–14.
 21. Attard G, Beldegrun AS, de Bono JS. Selective Blockade of Androgenic Steroid Synthesis by Novel Lyase Inhibitors as a Therapeutic Strategy for Treating Metastatic Prostate Cancer. *BJU Int.* 2005;96:1241–6.
 22. Pinto-Bazurco Mendieta M a E, Hu Q, Engel M, Hartmann RW. Highly Potent and Selective Nonsteroidal Dual Inhibitors of CYP17/CYP11B2 for the Treatment of Prostate Cancer To Reduce Risks of Cardiovascular Diseases. *J Med Chem.* 2013;56:6101–7.
 23. de Bono JS, Logothetis CJ, Molina A, Fizazi K, North S, Chu L, et al. Abiraterone and Increased Survival in Metastatic Prostate Cancer. *N Engl J Med.* 2011;364:1995–2005.
 24. Ryan CJ, Smith MR, de Bono JS, Molina A, Logothetis CJ, de Souza P, et al. Abiraterone in Metastatic Prostate Cancer without Previous Chemotherapy. *N Engl J Med.* 2013;368:138–48.
 25. Potter GA, Barrie SE, Jarman M, Rowlands MG. Novel Steroidal Inhibitors of Human Cytochrome P45017.alpha (17.alpha-Hydroxylase-C17,20-lyase): Potential Agents for the Treatment of Prostatic Cancer. *J Med Chem.* 1995;38:2463–71.
 26. Chan FCY, Potter GA, Barrie SE, Haynes BP, Rowlands MG, Houghton J, et al. 3- and 4-Pyridylalkyl Adamantanecarboxylates: Inhibitors of Human Cytochrome P450 17 α (17 α -Hydroxylase/C 17,20 -Lyase). Potential Nonsteroidal Agents for the Treatment of Prostatic Cancer. *J Med Chem.* 1996;39:3319–23.
 27. Nelson PS. Molecular States Underlying Androgen Receptor Activation: A Framework for Therapeutics Targeting Androgen Signaling in Prostate Cancer. *J Clin Oncol.* 2012;30:644–6.
 28. Yuan X, Cai C, Chen S, Chen S, Yu Z, Balk SP. Androgen Receptor Functions in Castration-Resistant Prostate Cancer and Mechanisms of Resistance to New Agents Targeting the Androgen Axis. *Oncogene.* 2014;33:2815–25.
 29. Arora VK, Schenkein E, Murali R, Subudhi SK, Wongvipat J, Balbas MD, et al. Glucocorticoid Receptor Confers Resistance to Antiandrogens by Bypassing Androgen Receptor Blockade. *Cell.* 2013;155:1309–22.
 30. Tilki D, Evans CP. The Changing Landscape of Advanced and Castration Resistant Prostate Cancer: Latest Science and Revised Definitions. *Can J Urol.* 2014;21:7–13.
 31. Hirano D, Okada Y, Minei S, Takimoto Y, Nemoto N. Neuroendocrine Differentiation in Hormone Refractory Prostate Cancer Following Androgen Deprivation Therapy. *Eur Urol.* 2004;45:586–92.
 32. Yuan T-C, Veeramani S, Lin M-F. Neuroendocrine-Like Prostate Cancer Cells: Neuroendocrine Transdifferentiation of Prostate Adenocarcinoma cells. *Endocr Relat Cancer.* 2007;14:531–47.
 33. Parimi V, Goyal R, Poropatich K, Yang XJ. Neuroendocrine Differentiation of Prostate Cancer: A Review. *Am J Clin Exp Urol.* 2014;2:273–85.
 34. Beltran H, Prandi D, Mosquera JM, Benelli M, Puca L, Cyrta J, et al. Divergent Clonal Evolution of Castration-Resistant Neuroendocrine Prostate Cancer. *Nat Med.* 2016;22:298–305.
 35. Small EJ, Youngren J, Alumkal J, Evans C, Ryan C J, Lara P, Beer T, Witte O, Baertsch R SJ. Characterization of Neuroendocrine Prostate Cancer (NEPC) in Patients with Metastatic Castration Resistant Prostate Cancer (mCRPC) Resistant to Abiraterone (Abi) or Enzalutamide (Enz): Preliminary Results from the SU2C/PCF/AACR West Coast Prostate Cancer. *J Clin Oncol.* 2015;33:(suppl; abstr 5003).

36. Kumagai J, Hofland J, Erkens-Schulze S, Dits NFJ, Steenbergen J, Jenster G, et al. Intratumoral conversion of adrenal androgen precursors drives androgen receptor-activated cell growth in prostate cancer more potently than de novo steroidogenesis. *Prostate*. 2013;73:1636–50.
37. Genazzani AR, Petraglia F, Bernardi F, Casarosa E, Salvestroni C, Tonetti A, et al. Circulating Levels of Allopregnanolone in Humans: Gender, Age, and Endocrine Influences. *J Clin Endocrinol Metab*. 1998;83:2099.
38. Garrido M, Peng H-M, Yoshimoto FK, Upadhyay SK, Bratoeff E, Auchus RJ. A-Ring Modified Steroidal Azoles Retaining Similar Potent and Slowly Reversible CYP17A1 Inhibition as Abiraterone. *J Steroid Biochem Mol Biol*. 2014;143:1–10.
39. Dombroski R, Casey ML, MacDonald PC. Human Saturated Steroid 6 α -Hydroxylase 1. *J Clin Endocrinol Metab*. 1997;82:1338–44.
40. Brunton PJ. Neuroactive Steroids and Stress Axis Regulation: Pregnancy and Beyond. *J Steroid Biochem Mol Biol*. 2016;160:160–8.
41. Li Z, Bishop AC, Alyamani M, Garcia JA, Dreicer R, Bunch D, et al. Conversion of Abiraterone to D4A Drives Anti-Tumour Activity in Prostate Cancer. *Nature*. 2015;523:347–51.
42. Chang KH, Li R, Kuri B, Lotan Y, Roehrborn CG, Liu J, et al. A Gain-of-Function Mutation in DHT Synthesis in Castration-Resistant Prostate Cancer. *Cell*. 2013;154:1074–84.
43. Pham S, Deb S, Ming DS, Adomat H, Hosseini-Beheshti E, Zoubeidi A, et al. Next-generation steroidogenesis inhibitors, dutasteride and abiraterone, attenuate but still do not eliminate androgen biosynthesis in 22RV1 cells in vitro. *J Steroid Biochem Mol Biol*. 2014;144:436–44.
44. Mostaghel EA. Steroid Hormone Synthetic Pathways in Prostate Cancer. *Transl Androl Urol*. 2013;2:212–27.
45. Locke JA, Guns ES, Lubik AA, Adomat HH, Hendy SC, Wood CA, et al. Androgen Levels Increase by Intratumoral De novo Steroidogenesis during Progression of Castration-Resistant Prostate Cancer. *Cancer Res*. 2008;68:6407–15.
46. Hofland J, van Weerden WM, Dits NFJ, Steenbergen J, van Leenders GJLH, Jenster G, et al. Evidence of Limited Contributions for Intratumoral Steroidogenesis in Prostate Cancer. *Cancer Res*. 2010;70:1256–64.
47. Stanbrough M, Bubley GJ, Ross K, Golub TR, Rubin MA, Penning TM, et al. Increased Expression of Genes Converting Adrenal Androgens to Testosterone in Androgen-Independent Prostate Cancer. *Cancer Res*. 2006;66:2815–25.
48. O'Hare MJ, Nice EC, McIlhinney RAJ, Capp M. Progesterone Synthesis, Secretion and Metabolism by Human Teratoma-Derived Cell-Lines. *Steroids*. 1981;38:719–37.
49. Fennessey P V., Pike AW, Gonzalez-Aller C, Horwitz KB. Progesterone Metabolism in T47Dco Human Breast Cancer Cells—I. 5 α -Pregnan-3 β ,6 α -diol-20-one is the Secreted Product. *J Steroid Biochem*. 1986;25:641–8.
50. Suzuki T, Murry BA, Darnel AD, Sasano H. Progesterone Metabolism in Human Leukemic Monoblast U937 Cells. *Endocr J*. 2002;49:539–46.
51. Wiebe JP. Progesterone Metabolites in Breast Cancer. *Endocr Relat Cancer*. 2006;13:717–38.
52. Sinreih M, Anko M, Zukunft S, Adamski J, Rižner TL. Important Roles of the AKR1C2 and SRD5A1 Enzymes in Progesterone Metabolism in Endometrial Cancer Model Cell Lines. *Chem Biol Interact*. 2015;234:297–308.
53. Vares G, Sai S, Wang B, Fujimori A, Nenoj M, Nakajima T. Progesterone Generates Cancer Stem Cells through Membrane Progesterone Receptor-Triggered Signaling in Basal-Like Human Mammary Cells. *Cancer Lett*. 2015;362:167–73.

54. Dubrovskaja A, Kim S, Salamone RJ, Walker JR, Maira S-M, Garcia-Echeverria C, et al. The Role of PTEN/Akt/PI3K Signaling in the Maintenance and Viability of Prostate Cancer Stem-Like Cell Populations. *Proc Natl Acad Sci*. 2009;106:268–73.
55. Thomas P, Pang Y. Membrane Progesterone Receptors: Evidence for Neuroprotective, Neurosteroid Signaling and Neuroendocrine Functions in Neuronal Cells. *Neuroendocrinology*. 2012;96:162–71.
56. Zhang C. Progesterone Protects Ovarian Cancer Cells from Cisplatin-Induced Inhibitory Effects through Progesterone Receptor Membrane Component 1/2 as well as AKT Signaling. *Oncol Rep*. 2013;30:2488–94.
57. Taraborrelli S. Physiology, Production and Action of Progesterone. *Acta Obstet Gynecol Scand*. 2015;94:8–16.
58. Penning TM, Chen M, Jin Y. Promiscuity and Diversity in 3-Ketosteroid Reductases. *J Steroid Biochem Mol Biol*. 2015;151:93–101.
59. Doig CL, Battaglia S, Khanim FL, Bunce CM, Campbell MJ. Knockdown of AKR1C3 Exposes a Potential Epigenetic Susceptibility in Prostate Cancer Cells. *J Steroid Biochem Mol Biol*. 2016;155:47–55.
60. Rižner TL, Lin HK, Peehl DM, Steckelbroeck S, Bauman DR, Penning TM. Human Type 3 3α -Hydroxysteroid Dehydrogenase (Aldo-Keto Reductase 1C2) and Androgen Metabolism in Prostate Cells. *Endocrinology*. 2003;144:2922–32.
61. Maayan R, Touati-Werner D, Ram E, Galdor M, Weizman A. Is brain dehydroepiandrosterone synthesis modulated by free radicals in mice? *Neurosci Lett*. 2005;377:130–5.
62. Baulieu E-E, Robel P. Dehydroepiandrosterone (DHEA) and Dehydroepiandrosterone Sulfate (DHEAS) as Neuroactive Neurosteroids. *Proc Natl Acad Sci*. 1998;95:4089–91.
63. Eberlin LS, Dill AL, Costa AB, Ifa DR, Cheng L, Masterson T, et al. Cholesterol Sulfate Imaging in Human Prostate Cancer Tissue by Desorption Electrospray Ionization Mass Spectrometry. *Anal Chem*. 2010;82:3430–4.
64. Seneff S, Davidson RM, Lauritzen A, Samsel A, Wainwright G. A novel hypothesis for atherosclerosis as a cholesterol sulfate deficiency syndrome. *Theor Biol Med Model*. 2015;12:9.
65. Sánchez-Guijo A, Neunzig J, Gerber A, Oji V, Hartmann MF, Schuppe H-C, et al. Role of steroid sulfatase in steroid homeostasis and characterization of the sulfated steroid pathway: Evidence from steroid sulfatase deficiency. *Mol Cell Endocrinol*. 2016;437:142–53.
66. McKay TB, Hjortdal J, Sejersen H, Karamichos D. Differential Effects of Hormones on Cellular Metabolism in Keratoconus In Vitro. *Sci Rep*. 2017;7:42896.

9 FINAL DISCUSSION

This thesis aimed at highlighting the potential clinical relevance of interfering with resistance-associated cell-to-cell communication mechanisms in *Pseudomonas aeruginosa* infections and deepening our understanding of such mechanisms in human prostate cancer cell lines *in vitro*. In the first, the biological evaluation of *pqs* QS signalling blockage outcomes is assessed in the comparison of PqsD inhibitors and PqsR antagonists' synergistic activities versus a dual-inhibitor on silencing PQS-related auto-/paracrine signalling. The amenability of pathoblockers as alternatives and adjuvants to current antibiotic therapies was tested on *in cellulo* and *in vivo* assays and is discussed below.

In the latter, the structural elucidation of a neurosteroid-derived molecule was shown in prostate cancer cells for the first time based on *in vitro* data. In addition to the discovery of this previously described mitogenic compound, we investigated ADT-associated resistance against abiraterone *in vitro*. These studies may be highly relevant to PC pathogenesis with prospective implications on current treatment strategies of castration-resistant neoplasms in patients undergoing ADT.

9.1 Biological Evaluation of PqsD and PqsR Dual-Inhibitor in *Pseudomonas aeruginosa*

9.1.1 Synergistic Effects of PqsD Inhibition and PqsR Antagonism in Virulence Factor Pyocyanin Production

The extensive work of our group in targeting the PqsD synthase and the PQS receptor, PqsR, is prolific in generating compounds of small molecular weight that successfully inhibit and antagonise these targets of the *pqs* QS system separately (64,113,120,175–177). We hypothesised that a combination of the beneficial biological effects observed independently for PqsD inhibitors (biofilm inhibition) (175) and PqsR antagonists (reduction of virulence factor production –pyocyanin (PCN) – and overall pathogenicity) (120) would result in an improved outcome with lower resistance development potential.

A proof-of-concept approach involved the straightforward assessment of compounds **1** and **2** (Chapter 1) used separately and in combination in our in-house whole-cell pyocyanin assay (120). This virulence factor belongs to the class of phenazines, a broad class of bacterial secondary metabolites involved in redox activities (178). In PA, PCN is the exponent of these

pyrazine ring-based compounds produced at late growth stages under high cell density conditions (179) and vital for survival and competition in their natural environment. Under tight control of the *pqs* QS system (180,181), PCN is pivotal in driving acute PA infections by supplying reactive oxygen species (ROS) such as toxic superoxide (O_2^-) and hydrogen peroxide (H_2O_2) *via* reduction of molecular oxygen *in vivo*. In addition, it is argued that in chronic infections, PCN facilitates the binding of eDNA to PA cells, promoting attachment, aggregation, and stability in biofilms (182,183). Acute cytotoxic damage to eukaryotic host tissues, also observed in cystic fibrosis patients (184), is due to the oxidative stress resultant from ROS production, NADPH consumption, host glutathione/catalase depletion, and neutrophil killing (118). The highly detrimental effects in host homeostasis caused by the activity of PCN is abrogated in *PqsR* mutants *in vivo* (118). This fact provides compelling arguments for the assessment of PCN levels as an evaluation step in the successful design and development of *pqs* QS antivirulence compounds.

The addition of PqsD inhibitor **1** and PqsR antagonist **2** generated a significant synergistic benefit, where their combined effect on PCN reduction was greater than the sum of each individual outcome. Notably, PCN production under single treatment with 15 μ M of compound **2** was improved by 20% when administered in combination with 500 μ M of compound **1**, which in itself is not able to reduce PCN levels at this concentration under standard assay conditions. The apparent inefficiency of single PqsD inhibitors in decreasing PqsR-driven gene expression and phenotypic adaptation in acute and chronic settings might be explained by two non-mutually exclusive hypotheses: firstly, the emergence of alternative pathways that bypass canonical biosynthesis of signalling molecules is a well-researched mechanism to compensate for their (exogenously) impaired production (185–187); secondly, as in the case for steroid signalling *via* nuclear receptors, minute amounts of ligands that persist even under strong, but not absolute inhibition of the synthases may still lead to receptor activation and ensuing gene expression and virulence factor production. In the latter case, if PqsD inhibition is below complete synthesis arrest (94), traces of HAQ signalling molecules might be sufficient to sustain the expression of virulent communication. However, the application of dual inhibition within the same feedback autoloop of *pqs* QS shows the promising potentiation effects of the antivirulence strategy in virulence factor production. In this case, the decrease in signalling molecule production by inhibition of PqsD synthase may translate its benefits in lowering competition of native ligands against PqsR antagonists to the receptor's binding site, indirectly increasing antagonistic potency.

9.1.2 The Favourable Pleiotropic Effects of a Dual-Inhibitor Compound in Targeting *pqs* QS Communication

In an effort to combine the encouraging effects observed upon dual inhibition of the *pqs* QS system, we screened our in-house libraries for compounds sharing a structural similarity in PqsD and PqsR inhibitors. A pyrimidine backbone decorated with a triazole and a sulfone moiety were found in PqsR antagonist compound **3** and PqsD inhibitor compound **4** and became the starting point for the rational design of our dual-inhibitors (Chapter 1). The first dual inhibitor synthesised, compound **5**, (by my colleague, Dr. Andreas Thomann) consisted only of this simplified pyrimidine backbone displaying exclusively the shared structural features from compounds **3** and **4**. *In vitro* assessment of dual-target inhibition was performed following the protocols established in-house (through the extensive work of Dr. Christine Maurer) and showed that compound **5** is an inhibitor of both PqsD and PqsR. In addition, compound **5** was able to successfully reduce pyocyanin levels with a slight improvement compared to its PqsR antagonist precursor, compound **3** (added reduction of 14%, making up a total of 75% inhibition of this virulence factor at 400 μ M). These results suggest that dual inhibition is not only a promising strategy in QS sensing interference but can also be achieved in a single drug. Finally, dual-target compound **6** was obtained by the bioisosteric replacement of C4 at the triazole substituent with a nitrogen, yielding the tetrazole congener **6**. This improved dual-inhibitor showed significant inhibition on both synthase and receptor targets with a slight improvement on PqsR antagonism (IC_{50} values from 26 μ M down to 15 μ M) compared to compound **5** while retaining activity against PqsD compared to the selective inhibitor, compound **4**.

In addition, low molecular weight (226,21 Da) compound **6** also demonstrated high solubility and negligible cytotoxicity against bacterial cells, keeping faithful to the antivirulence concept. This lack of effect on bacterial growth was assessed in thorough growth kinetics of the pathogens, making sure that observed outcomes were in fact related to the absence of bacteriostatic/bactericidal mechanisms and not due to delayed growth observed with some classes of antibiotics.

9.1.2.1 Effects on Virulence Factor (PCN) and Siderophore Production

Dual-inhibition with compound **6** significantly reduced PCN formation with an IC_{50} level of 86 μ M. Compared to target affinity and potency of selective PqsR antagonists already synthesised (unpublished data – Chapter 2) and published elsewhere (91,120,188) on PCN inhibition, compound **6** displays only a moderate activity. However, it stands its ground as a proof-of-

concept approach and highlights the added benefits of dual-inhibition, especially given its pleiotropic benefits described below.

As previously mentioned, PA reacts to environmental cues as part of its complex adaptive resistance mechanisms (44,55) resulting in the reprogramming of gene expression patterns. While many of these changes evolved as adaptation mechanisms to natural variations in the pathogen's biological niches, they also play a role in modulating versatile phenotypic fluctuations as part of a larger competition and pathogenic armamentarium. In these circumstances, PA actively influences its surrounding microenvironments *via* the production of, for example, nutrient scavengers that sustain growth and signal virulent pathways (189). One such nutrient is iron, essential for PA's survival insofar its involvement in a variety of biochemical pathways and physiological homeostasis. During infection, iron is sequestered by eukaryotic cells in an attempt to "starve" pathogens by limiting its bioavailability (190). In PA, iron uptake is regulated by the Fur protein, which also acts as a transcriptional repressor of multiple virulence genes upon binding of Fur to iron (191). *In vivo*, PA sequesters iron from the surrounding environment through pyoverdine (PVD) and pyochelin in order to activate pathogenic pathways involved in acute infections and biofilm formation (192,193). The relationship between *pqs* QS and PVD production is not yet fully elucidated, but reports show that PVD biosynthesis depends on *pqs* QS gene expression modulation, with PQS actively chelating iron in PA's microenvironment, and PVD indirectly controlling the activation of the *pqs* pathway through PqsR activity on iron metabolism (110,194,195). The roles played by PVD in PA's acute pathogenicity and the connection to adaptive responses in chronic settings through biofilm formation and homeostasis, while interacting with the *pqs* QS system (196), prompted the evaluation of our dual-inhibitor on PVD production. We showed that successfully targeting HHQ and PQS biosynthesis, QSI's may also reduce the conserved environmental competitive advantage of iron scavenging mechanisms, rendering pathogen less virulent and likely more susceptible to adjuvant treatment and/or the hosts' immune response. In our *in vitro* setup, dual-inhibitor **6** successfully decreased PVD at all tested concentrations (95% reduction at 500 μ M through to 42% reduction at 100 μ M) in a dose-dependent manner, outperforming single PqsR (7% reduction) and PqsD inhibitors (30% reduction) significantly.

It is important to note that the affinity and selectivity of compound **6** to the PVD synthase (PvdS) was not directly assessed in our experiments. Rather, the observed effects are argued to originate indirectly, from the specific interference with the pathogen's *pqs* QS mechanism through a decrease in HHQ and PQS levels, as also shown by the selective PqsD inhibitor, compound **1**. Moreover, iron is intimately related to microbial fitness in a variety of

DISCUSSION

microorganisms. It is, therefore, categorized as a “public good” of bacterial communities, where cooperating individuals altruistically invest in their production or availability and might be related to mechanisms that go beyond our current understanding of QS and other communication systems. Comprehensible research has shown that interference with quorum sensing might inadvertently affect microbial fitness (197–199) if, for example, nutrient scarcity evolves into Darwinian selective pressure, with microorganisms adapting to the new environmental conditions through the expression of conserved resistomes to ensure growth. Therefore, QSIs or quorum quenching compounds that may affect nutrient availability (such as those reported for the Las system (197)) need to be studied very carefully in order to ensure promising outcomes without concealing possible resistance development potential. Within the timeframe studied, however, compound **6** did not show signs of growth deficiency and the beneficial inhibitory effects of PCN and PVD virulence factors that are linked to biofilm formation were promptly investigated.

9.1.2.2 Effects of QSIs on Biofilm Formation and Extracellular Polymeric Substance Constitution

The formation of heterogeneous microbial communities of specialized bacterial subpopulations is one of the hallmarks of PA’s chronic infections and surface colonization in clinical and industrial settings (49,106,107). Biofilms are complex structures composed of extracellular substances that provide structural stability as well as air, nutrients, and the paracrine diffusion of quorum sensing molecules and virulence factors throughout these communities and amongst its members (49). The mostly self-produced EPS matrix is composed of exopolysaccharides – attachment facilitation (Pel and Psl) and suppression of host immune response (alginate), extracellular proteins – amyloid fibres that provide structural stabilization and tolerance to physical stress, and eDNA – cell cohesive adhesion, formation of shuttling channels and antibiotic deterrence (particularly aminoglycosides, fluoroquinolones and host defensins) that is different than intrinsic or acquired resistances (49,106). Overall biofilm formation and specially eDNA production have been shown to be under the influence of the *pqs* QS system, particularly PQS-driven virulence factors such as PCN (180,185) and HQNO (102) production. Together with Dr. Christian Brengel, we have assessed the effects of dual-inhibitor **6** in hampering biofilm formation by analysing biovolume levels in 24 h grown biofilms with crystal violet (CV). With an IC_{50} of 100 μ M in hampering biofilm development, compound **6** reiterates the role of the *pqs* QS system in biofilm formation (175,200). Though indiscriminative, CV staining gives an overview of biofilm integrity and formation capabilities under treatment in a

straightforward, inexpensive manner. However, by staining components of the EPS as well as live and dead organisms (both of which are important in the making up of biofilm communities) CV provides very little information on the actual number of living cells, which would be paramount in evaluating anti-biofilm efficacy of antimicrobial substances, and does not layer the relative constituency of different EPS components. To that end, various staining approaches were employed in order to circumvent CV limitations and more precisely evaluate QSIs anti-biofilm efficacies, namely congo red diazo dye (exopolysaccharides), propidium iodine fluorescent dye (eDNA), and Bradford protein assay (extracellular proteins). Dual-inhibition proved particularly efficient in decreasing eDNA levels (93% inhibition) at 400 μ M, which led to the assessment of ciprofloxacin activity rescue in a BacTiter-Glo™ metabolic assay to directly evaluate living bacteria populations within the biofilm. In accordance with our assumptions and the promising silencing of *pqs* QS bacterial communication for clinical treatment, dual inhibitor **6** restored antibiotic efficacy in biofilms previously treated with our compound. It has been argued that the lack of activity of ciprofloxacin against biofilm is partially due to the presence of eDNA (201), which sequesters the antibiotic in its polymeric network. Our results corroborated these assumptions and highlighted the prospective benefits of employing QSIs also as adjuvant and prophylactic therapies in addition to current clinical treatments.

It is vital, however, to highlight the current drawbacks and limitations concerning *in vitro* biofilm studies. Given the highly convoluted mechanisms and heterogeneity of structures and organisms involved in its formation, a thorough understanding of biofilm-related processes has not been achieved to date. To this end, reliable and reproducible detection and quantification techniques are urgently needed but still remain a challenge to researchers worldwide. As highlighted above, the exact objectives of investigation on biofilm structures must be taken into account when devising which techniques to use for a more detailed understanding. Different targets (EPS constituents, live/dead bacterial cells, or structural/morphological changes) demand different experimental approaches, as well as the determination of “what constitutes success” for efficacious treatments. In addition, the variety of protocols employed in different laboratories also needs to be considered insofar the sensitive biofilm-related responses to diverse assay parameters such as static growth *vs* flow chambers, and (fluorescence) microscopy *vs* colorimetric staining techniques (107,202,203). These circumstantial variations hinder direct comparisons and objective evaluation of anti-biofilm approaches and compounds currently under study by different research groups. Moreover, the phenotypic plasticity of PA cultures *in vitro* stresses the necessity of developing consistent and reliable chronic infection

DISCUSSION

models with factual relevance to conditions observed *in vivo* without the occurrence of *in vitro* artefacts (64,204), such as the formation of mushroom-shaped structures not seen in the *in vivo* environment.

Despite the current limitations of modelling the biofilm life cycle *in vitro*, the results discussed above do argue for the potential clinical relevance of dual-target inhibition within the autoinduction loop of the *pqs* QS system. The rescue of antibiotic efficacy in the treatment of inherently drug-resistant sessile phenotypes and the synergistic activities in hampering virulence factor formation in planktonic cultures encouraged us to deepen our studies in an early *in vivo* infection model.

9.1.2.3 Dual-Inhibition Efficacy in the *Galleria mellonella* Acute Infection Model

In our work, the greater wax moth (*Galleria mellonella*) acute infection model (120) was used as a pre-screen to mammalian infection models in order to investigate host-pathogen interactions and reduce potential failure rates in late animal testing steps. The use of this early *in vivo* model has a number of advantages at this stage of pre-clinical testing. Its placement represents a strategic “bridge” in assessing the applicability of promising *in vitro* compounds within the antivirulence concept to more clinically-relevant infection scenarios. Overall, the greater wax moths have innate and humoral immune responses that contain elements remarkably similar to those found in vertebrate systems (205), including a complement-like system, phagocytic cells (206), and the production of host antimicrobial peptides to fight infections (207). From a practicality standpoint, these larvae can be given precise dosages of bacterial inocula and compounds (87) in inexpensive, easy to perform studies with no ethical implications to their use. Finally, the satisfactory predictive power of this model for PA pathogenicity was shown in the significant positive correlation of wild-type and *PqsR* mutant virulence of PA14 strains in mice and *G. mellonella* (208).

Our results show that dual-inhibitor **6** significantly improved larvae survival with all tested doses. Ultimately, a 6,6-fold increase was achieved with the administration of 0,63 mg kg⁻¹ (2,7 μM) of the compound, bringing the number of challenged larvae at the end of the assay from 8% through to 53%. Furthermore, a four times higher dose was well tolerated by *G. mellonella* with no observable detrimental effects (98% survival) in our toxicity assessment. Notably, at 10–13 CFUs/injection, the average bacterial load was particularly challenging during treatment with 10-fold increased inocula compared to the assay’s protocol. It is logical to expect that an even higher protective effect would have been displayed at lower CFU injections, further validating the use of QSIs in hampering PA virulence in acute *in vivo* infections. Finally, when

comparing the actual compound concentration administered to the challenged larvae with the compound's IC_{50} towards PCN inhibition (86 μ M), we observe a roughly 30-fold disparity between the two, highlighting the importance of employing more complex host systems for compound testing. A number of reasons can be enumerated to account for this differences, namely: 1) redundancies of QS and virulence-related biological systems, whereby PqsR may also play a role in addition to PCN production (such as cytotoxic HQNO, exotoxins, and siderophores); 2) the actual load of bacterial populations used in different assays; 3) synergism with host's immune responses to PA infections; and 4) the environmental growth conditions (defined minimal media *vs* the much more complex invertebrate physiological microenvironment) that modulate PA phenotypic responses. Taken together, we have shown that dual inhibition synergistically protected greater wax moth larvae from fatal PA infections by interfering with the bacteria's ability to communicate effectively and become virulent. Our strategy paves the way for future compound potency optimization with lower resistance development potential and decreased interference with the host's physiologic homeostasis (toxicity) and natural microbiome (selectivity).

9.1.3 Conclusion and Outlook – Synergistic Interference of *pqs* QS Communication System

With the dire challenge that multiple and extreme drug resistant pathogenic organisms currently pose to human health, QS inhibition has proven to be a suitable and promising target within emerging alternative treatment strategies. The feasibility and relevance of disrupting QS mechanisms is not entirely new and can be seen in the highly complex microbial interactions in nature where bacteria and fungi interfere with the molecular languages of a competitor/predator (209–211). As innovative therapies, the sole generation of novel chemical entities may not be enough to outsmart the redundancy and plasticity of biological systems shown by the consistent failures of conventional antibiotic development. Alternatively, these new entities should hybridize novel targeting (QSIs) and smart delivery systems (nanoparticles/liposomes) that increase targeted bioavailability, enhance outer membrane penetration, and reduce efflux in order to curb treatment resistance. To accomplish that, attention to and development of reliable and relevant *in vitro* and *in vivo* testing platforms are paramount, such as murine and higher order vertebrate models. The QS dual-inhibition approach with a single compound display numerous advantages in treating microbial infections. Inherently, it enhances patient compliance and excludes unwanted drug-drug interactions that might be responsible for adverse effects that render treatment inefficient. It also holds greater

DISCUSSION

potential in intrinsically avoiding resistance development since larger combinatorial mechanisms (i.e., non-deleterious mutational events) would be necessary to circumvent dual-target treatment efficacy. However, challenges remain aplenty: abrogation of a single QS system may lead to promiscuous/overlapping mechanisms filling in the pathogen's complex communication pathways, and dual-target potency should ideally be equipotent in order to allow for reasonable dosing schemes. Furthermore, if QSIs inadvertently hamper social behaviours that are linked to bacterial survival, resistance selective pressures may again take place. Finally, the timely application of QS inhibition should consider the acute and sessile life cycles of the pathogen with proper prophylactic or adjuvant strategies being applied accordingly in synergistic drug combinations. All in all, design and development of novel dual-target compounds need to weigh-in the benefits and challenges of single system *vs* multisystem inhibition carefully to ensure redundancy avoidance and unhinge resistance development simultaneously against PA's autocrine and paracrine communication systems.

9.2 Layering the Intercellular Communication of Prostate Cancer Cell Lines – Androgens and Beyond

In order to investigate some of the diverse mechanisms driving growth and survival of tumour cells in advanced prostate cancer, we selected a number of phenotypically different epithelial cell lines. The distinctions were based on AR and androgen requirements that may lead to endocrine independence and migration to ADT resistance. More specifically, three AR⁺ and androgen-responsive (LNCaP – hypersensitive, androgen-dependent mutated AR, C4.2 – promiscuous, androgen-independent mutated AR, and VCaP – overexpressed wild-type AR) and one AR⁻ (PC3) carcinoma cell lines were chosen to mimic the variety of resistant individuals found in the CRPC microenvironment. Notably, C4.2 cells, albeit androgen-independent, respond to androgen signalling similarly to its androgen-dependent counterparts and is, therefore, classified as an androgen-responsive cell type. Recent reports provide contradicting evidence with respect to the source of androgens found in intraprostatic tissues in the clinics. One the one hand, some state that androgens can be synthesised *de novo* from steroid precursors by epithelial cells *in situ* (212,213), on the other, late adrenal precursors appear to be the more likely players in androgen synthesis by stromal and epithelial cells (214). In both cases, regardless of the initial source, androgens are assumed to sustain AR signalling and ensuing cancer progression *via* testosterone and DHT binding despite ADT in an autocrine/paracrine manner. Therefore, we employed radioactive detector-couple HPLC (radio-

HPLC) and steroid enzyme-linked immunosorbent assay (ELISA) techniques to investigate the steroidogenic potential of these cells in androgen biosynthesis with primordial precursor ^3H -pregnenolone. Surprisingly, none of the initially expected androgens were generated in androgen-responsive cells, rather a previously described, neurosteroid-derived mitogenic compound (215–217), 5α -pregnan- $3\beta,6\alpha$ -diol-20-one ($5\alpha,3\beta,6\alpha$ -P), was found for the first time in prostate-related malignancies. This neurosteroid compound hints at a neuroendocrine transdifferentiation of androgen-responsive prostate carcinoma cells and highlights the plasticity of signalling pathways exhibited in neoplastic cells depending on its cellular context (i.e., migration from a paracrine to an autocrine communication fashion) (218–221). The discovery and characterization of $5\alpha,3\beta,6\alpha$ -P is further discussed below.

9.2.1 Assessing Primordial Precursor Metabolism

9.2.1.1 *The Pregnenolone Precursor-Specific Metabolism in Prostate Carcinoma Cell Lines*

The use of radioactively-labelled compounds allows for the assessment of its specific metabolism since radioactivity will only be found in downstream metabolites as long as metabolisation does not occur at the labelled sites. This is the case for the [$7\text{-}^3\text{H(N)}$]-pregnenolone isotopologue used in our experiments, where tritium labelling at C7 would remain intact throughout compound metabolism in case of late androgens testosterone and DHT – sequential modifications at positions 17 (*via* CYP17A1 and 17β -HSD), 3 (*via* 3β -HSD), yielding testosterone, and 5 (*via* 5α -reductase), resulting in the final metabolite of the androgen axis, DHT. The optimized HPLC chromatogram was based on an in-house protocol for metabolite extraction, and subsequent analyses (222) with radioactivity only found in the extracted organic fraction, with no traces left in the aqueous phase. Our radiometric results show that only androgen-responsive cell lines metabolised pregnenolone and the sole product of metabolism after 48 h of incubation in starved cultures (*vis a vis* the castrated conditions found in patients undergoing ADT) was a compound with retention time similar to that of corticosteroids (4.96 min *vs* 4.38 min – 11-deoxycortisol – and 5.23 min – corticosterone) but not testosterone (10.19 min) or DHT (19.50 min). Following the site-specific premises described above, we proceeded with an untargeted HPLC-ESI-ToF-MS analysis of conditioned media with native and deuterated pregnenolone (pregnenolone-20,21- $^{13}\text{C}_2$ -16,16- d_2). As expected, we obtained again a single compound with a 4 Da shift in its exact mass depending exclusively on the isotopology of its precursors (native: 335.2590, deuterated: 339.2774), which confirmed the assumptions that this so far unidentified non-androgen was indeed derived

DISCUSSION

from this primordial precursor and not from intracellular-derived intermediates. A thorough NMR analysis of purified and concentrated cell culture samples incubated with native precursors finally confirmed the identity of this metabolite to be $5\alpha,3\beta,6\alpha$ -P.

The fact that only AR⁺ cells were capable of generating $5\alpha,3\beta,6\alpha$ -P from pregnenolone precursor indicates the occurrence of AR-driven steroidogenic mechanisms that might be independent of androgen binding *per se*. While further studies are in order to detail these observations, it becomes evident that the otherwise precisely symbiotic balance between androgenic ligands and AR through paracrine mechanisms is subjected to a communication imbalance. Rather than an outright *bypass* pathway, where AR requirement is circumvented in stimulating prostate cancer cells to proliferate (made clear by the lack of pregnenolone metabolism in AR⁻ PC3 cells), the detrimental plasticity of epithelial cells that we witnessed in our experiments is likely due to the emergence of AR-driven activation of *promiscuous* (nonandrogenic steroids) or *outlaw* (non-steroid signalling molecules) pathways. As a response to AR binding to mis-regulated AREs, the transcription of otherwise AR-unrelated genes may lead to the expression of other steroidogenic enzymes and receptors involved in new signalling pathways for disease progression and resistance to treatment, further discussed below.

9.2.1.2 Immunoassay-Based Quantification of Total Steroids

Despite its relevance in making evident the specific pathways through which given precursors are further metabolised into, the exclusive assessment of steroidogenic potentials with this technique is not without caveats. While on the one hand, we could show that in our setups these four prostate carcinoma cell lines are not capable of *de novo* androgen biosynthesis from early steroid precursors such as pregnenolone, on the other, it restricts steroidogenesis evaluation by excluding the presence of non-labelled precursors and intermediates in the same or distinct pathways. This is due to the possibility of steroid depots being formed during culture conditions with media containing cholesterol and other steroids. In this convoluted scenario, the high affinity of these molecules to cytosolic globulins (i.e., sex hormone-binding globulin (SHBG) and transcortins (binding of progesterone and corticosteroids)) may conceal the formation of sex hormones or corticosteroids under analyses during and after starvation conditions (223).

Therefore, we complemented our evaluations with the quantification of total steroids in culture with highly sensitive immunological detection methods. The principles of these steroid-specific ELISA tests rely on the high specificity of antibody epitopes against antigenic sites of unique side groups and substituents within the four-membered steroid nucleus. Appropriate calibration curves were performed by spiking unconditioned media with known amounts of corresponding

steroids to ensure assay validity and exclude unspecific or cross-reactive binding to non-target molecules. The combination of our results shows that indeed the addition of pregnenolone to these cells does not lead to the formation of androgens, other sex hormone steroids or corticosteroids. On the contrary, AR⁺ cells exclusively metabolised early precursor into AR-driven 5 α ,3 β ,6 α -P, while AR⁻ cells appeared not to depend on steroid hormones to sustain growth, likely in a phenomenon where non-steroid “outlaw” compounds such as growth factors and receptor tyrosine kinases play a more significant role in driving disease progression and metastases.

9.2.2 Alternative Steroidogenic Pathways in AR-Driven Autocrine Signalling

The biological relevance of 5 α ,3 β ,6 α -P in prostate cancer cells remains to be fully elucidated. However, a number of hypotheses can be derived from the results obtained herewith. While being described for the first time in the prostate cancer context, the formation of 5 α ,3 β ,6 α -P from progesterone precursor has been linked a number of proliferative activities in other malignant endocrine cell types such as testicular and ovarian carcinomas cell types (215) and breast cancer (216). This was shown by a strong positive correlation between the formation of 5 α -pregnane intermediates in alternative progesterone-related pathways and cancer mitogenesis/metastasis. A proposed pathway for the formation of 5 α ,3 β ,6 α -P involves the sequential activities of 3 β -HSD, 5 α -reductase, AKR1C1 (all of which have been shown to be overexpressed or overactive in metastatic, castration-resistant samples (224–226)), and 6 α -hydroxylase (216). Even though the definite molecular mechanisms by which 5 α ,3 β ,6 α -P aggravates malignancy are currently unclear, an imbalance in the auto- and paracrine communication mechanisms of pregnenolone and progesterone 3 α - vs 5 α -reduced metabolites results in the migration from normalcy (3 α -induced homeostasis) to detrimental proliferation and detachment behaviours (5 α -induced malignancy) (227). Mounting evidence suggests that the harmful activities of 5 α -reduced metabolites are independent of nuclear steroid receptors (androgen or otherwise) and instead elicit rapid intracellular signalling cascades through non-genomic membrane progesterone receptors (i.e., PGRMC1) (228). Clearly, membrane signalling is not suppressed by drugs targeting steroid nuclear receptors, and thus, the activation of deleterious cancer-related pathways such as G-protein, PI3K, and ERK1/2 signalling can occur undisturbed. The ensuing signalling cascade of these non-genomic receptors was shown to prevent cell cycle arrest and apoptosis, stimulate cancer cell generation and maintenance,

DISCUSSION

and dedifferentiation of epithelial and stromal cells (229). It is reasonable to hypothesise that the observed correlation with AR dependency for this likely AR-independent phenomenon in AR⁺ cell lines lies in the gonadal steroid (i.e., testosterone) control of such membrane receptors expression (230). AR⁺ sensor cells that translate endocrine cues into paracrine signals switch functions towards autocrine mediation and subsequent tumorigenesis. In this case, non-classical AR activity possibly drives tumour progression *via* two related mechanisms: 1) overexpression or increased activity of steroidogenic enzymes leading to the formation of non-androgenic but signalling-capable steroids (as in 5 α ,3 β ,6 α -P), and 2) (increased) expression of cognate non-genomic membrane receptors for intracellular signalling of cancer-related pathways. This pleiotropic activity of the non-classical AR activation in pathological states creates an ideal microenvironment for cancer progression and development.

While a deeper understanding of the molecular relevance and biosynthesis of 5 α ,3 β ,6 α -P is warranted, our work highlights alternative steroidogenic pathways that may be linked to the autocrine mis-regulation observed in epithelial cancer cells. These are, in turn, outside of the scope of current treatment strategies and may account for the observed resistance to treatment in clinical settings. To test this assumption, we made use of the selective CYP17A1 inhibitor abiraterone, currently, the state-of-the-art treatment (administered as pro-drug abiraterone-acetate: Zytiga®) co-administered with potent AR competitive antagonist enzalutamide for advanced prostate cancer patients.

9.2.3 The CYP17A1-Independent Hindrance of Steroidogenesis with Abiraterone

9.2.3.1 Formation of Δ^4 -Abi and 3 β -HSD Inhibition on 5 α ,3 β ,6 α -P Formation

As previously mentioned, Abi is a potent and selective CYP17A1 inhibitor. *In vitro* experiments and clinical data support its efficacy by the abrogation of late androgen synthesis from early precursors, with undetectable levels of circulating extragonadal steroids (149). Therapeutic strategies rely on the pivotal catalytic roles that both CYP17A1 enzymatic functions have in the biotransformation of progestagens through to sex hormones. However, intratumoral analyses revealed the persistence of low androgens concentrations still capable of eliciting AR-signalling in prostate cancer cells despite successful CYP17A1 blockage, a hallmark of CRPC relapse. Resistance to treatment has been postulated as a multi-factorial phenomenon possibly including increased expression of intraprostatic CYP17A1 and emergence of AR splice variants through which cross-activation by alternative and hypersensitivity to canonical ligands happen.

Due to the fact that Abi is a selective CYP17A1 inhibitor and this enzyme is not present in the biosynthetic pathway of $5\alpha,3\beta,6\alpha$ -P, it was surprising at first to witness the complete blockage of metabolite formation from biologically relevant levels of pregnenolone (10 nM) after treatment with Abi (10 μ M). Coincidentally, during our studies, Li and colleagues (231) reported the conversion of Abi to its Δ^4 cognate after 3β -HSD-mediated metabolism into Δ^4 -Abi (D4A) in human patients with multi-enzyme inhibition capabilities. The amenability of Abi conversion to the 3-keto congener D4A by 3β -HSD metabolism is rooted in the structural similarity of the parental Δ^5 3β -hydroxyl steroid-like structure with the enzyme's Δ^5 native ligands, such as DHEA and Δ^5 -androstenediol. This Δ^4 compound, therefore, has additional binding (and inhibitory) abilities to 3β -HSD and 5α -reductase, probably due to its steroid A and B rings being identical to testosterone in addition to parental CYP17A1 blockage. The first two being essential in the synthesis of $5\alpha,3\beta,6\alpha$ -P.

Further investigations in our group showed the presence of D4A in cell culture supernatants in the nM range, namely 12.50 nM, 101.85 nM, and 61.50 nM in LNCaP, C4.2, and VCaP cell lines, respectively. Furthermore, Abi administration was only able to arrest metabolism of pregnenolone, not of progesterone. Since the only known enzymatic reaction between these two progestagens is dependent upon 3β -HSD activity, we assumed that D4A is the responsible compound for the metabolic halt in metabolism displayed in our radio-HPLC experiments, not Abi. To corroborate our *in vitro* findings and our current hypothesis, further experiments with D4A as the treatment compound are necessary. Nonetheless, this fact alone would not account for the observed patient resistance to Abi treatment since, by means of its D4A metabolite, Abi would supposedly also successfully inhibit the formation of mitogenic $5\alpha,3\beta,6\alpha$ -P *in vivo*. Our total steroid assessment of Abi-treated samples, however, paints a different, more complete picture, discussed below.

9.2.3.2 Immunological Assays Hint at a Neuroendocrine Phenotype Transition of Prostate Epithelial Cells in a CYP17A1-Independent Microenvironment

The *de novo* synthesis of late androgens (testosterone and DHT) or androgen precursor (DHEA) from pregnenolone has been consistently argued against in our radio-HPLC and immunoassays discussed above. However, Abi co-administration led to increases in DHEA levels in orders of 20- to 100-fold. DHEA, the most abundant circulating steroid in humans and the major source of extragonadal steroids in its sulfate form (DHEA-S), does constitute a major player in the possible mechanisms of Abi resistance. Adding further evidence in solving another piece of

DISCUSSION

this steroidogenic puzzle, we observed that DHEA levels found in the supernatant were partially, but significantly, hampered with co-administration of commercially available steroid sulfatase (STS) inhibitor, STX64. This STS inhibitor readily reduced DHEA production in androgen-responsive cells by 60% and 51% in LNCaP and VCaP cell lines, respectively. Taken together, our observations of androgen-responsive, Abi-treated cells suggest that while on the one hand prostate epithelial carcinoma cells are not capable of *de novo* steroidogenesis from primordial steroid precursor pregnenolone, on the other, treatment with Abi and to a lesser extent D4A leads to the emergence of alternative pathways responsible for DHEA production in a CYP17A1-independent manner. The central and early activity of CYP17A1 in steroid metabolism and canonical DHEA formation in all peripheral tissues (including the prostate and adrenal glands, and gonadal tissues) raises questions as to which mechanisms are set in place to support DHEA synthesis and, most importantly, what are the precursors involved in this case. Since DHEA is the immediate precursor for testosterone and DHT synthesis sustaining AR activation and cancer progression, the phenomenon observed herewith could constitute one of the explanations for Abi treatment resistance seen in advanced and metastatic prostate tumours in patients.

Although the steroidogenic pathways involved in this resistance-associated process are beyond the scope of this thesis, based on the works of Maayan *et al* (232) and Baulieu *et al* (233) in the CYP17A1-independent synthesis of DHEA in the central nervous system (CNS), we probed the possible role played by the immediate precursor upstream of pregnenolone: cholesterol. In summary, a hypothetical scenario would suggest that adenocarcinoma cells transdifferentiate into neuroendocrine (NE) prostatic carcinoma-like cells (a phenomenon being increasingly demonstrated in androgen-depleted environments) with phenotypes that are CYP17A1-independent insofar their production of DHEA from cholesterol by metabolizing enzymes yet to be elucidated. NE-like PC cells originate either *de novo* or through the acquisition of genomic and epigenetic alterations in the transdifferentiation process of cancer epithelial cells during disease progression, both of which appear to act as adaptive responses to systemic therapies (234). Radio-HPLC experiments were conducted with ³H-cholesterol and initially, no conversion to DHEA was observed in this set-up. This could be reasoned by two different arguments: 1) the possibility of cholesterol depots in the cells, which may be consumed during starvation conditions and 2) the alternative use of cholesterol and cholesterol sulphate (the latter implicated as a differentiating compound in cancerous tissues (235)) precursors such as homocysteine and oxidized low-density lipoprotein (LDL) present in culture media, also contributing to depot formation. It is clear that additional experiments would be necessary to

provide further evidence of cholesterol involvement or lack thereof, in this hypothetical pathway, including protein/mRNA data for the steroidogenic enzymes under investigation. Furthermore, the assessment of NE cellular populations would be highly beneficial in stratifying the subpopulations and clonal evolution that may be responsible for this autocrine signalling migration. This, in turn, can be achieved by employing a number of different techniques: genome-wide analysis or qPCR of NE-related transcripts such as Trp53, Rb1 and MYCN which are typical of poorly differentiated NE tumours, as well as immunocytochemistry of characteristic markers in neurosecretory cells (i.e., chromogranin A, synaptophysin, CD56 and neuro-specific enolase).

Finally, it must be considered the possibility that the overall quantitative and qualitative alterations found in steroidogenic potentials of prostate cancer cells during our *in vitro* studies are caused by the artificial use of different steroid precursors and inhibitors. It is likely that not only steroid depletion during starvation conditions but also the employment of Abi and pregnenolone, mimicking an *in vivo* ADT treatment environment, are collectively responsible for the observed phenomena in our setups and the emergence of previously unknown bypass mechanisms for androgen biosynthesis. Since genomic and phenotypic alterations depend on specific drivers of organ site and disease context, the biomarker potential of $5\alpha,3\beta,6\alpha$ -P and the rise of DHEA in Abi-treated patients as possible causes for treatment resistance must be assessed in actual clinical settings (i.e., prostate tissue, human plasma). However, the extremely restricted availability of patient samples from human biopsies and the logistics and ethical hurdles that need to be overcome in such studies, highlight the practicality and importance of *in vitro* data and models. These are a powerful tool to understand the plasticity of cancer cells' molecular mechanisms in tightly regulated environments, being able to single out unique variables in the complex and redundant mechanisms taking place, which would otherwise be impossible to determine.

9.2.4 Conclusion and Outlook – Mis-Regulation of Steroid Signalling in Prostate Cancer

Despite renewed efforts in the design and development of efficacious drugs for the treatment of advanced prostate cancer, disease relapse and death are highly detrimental outcomes that persist in almost all treated patients. The clinical relevance and occurrence of intraprostatic androgen signalling even under a castrated environment make evident the continuous need to better understand the drivers of lineage plasticity that lead to ADT treatment resistance.

DISCUSSION

Our work sheds light on at least one cell-autonomous mechanism for uncontrolled proliferation *via* the persistent mis-regulated cross-talk between the AR and oncogenic signalling pathways. In this scenario, the typical response of prostate cells in translating endocrine cues to paracrine signalling that sustains normalcy shifts to autocrine mechanisms that regulate the intracrine synthesis of androgens and mitogenic players in malignant tumours. Thus, available therapies are rendered ineffective and might instead stimulate these unfavourable events. The lack of mechanistic understanding of pathway initiation and maintenance of these new chemical languages in diseased states hamper the discovery of new, suitable targets in order to increase therapy efficacy without cancer recurrence. The results discussed above call for further characterization of prostate carcinoma cells in androgen-depleted environments and elucidate the fate of early steroid precursors in androgen-responsive cells, paving the way for a new comprehension of the biological relevance of progesterone metabolites in prostate cancer, the efficacy of Abi treatment, and the development of resistance.

The polypharmacological approach used today to treat patients with Abi and enzalutamide has provided significant improvements compared to single therapies. However, the pleiotropic activities of the AR and the variety of novel AR-driven pathways appear to demand a more diversified drug combination approach. These should prevent the appearance of pathway redundancy that predisposes the strategy to resistance. Thus, the discovery of new targets in these pathways should capitalize therapeutic strategies and increase therapy efficacy. Finally, successful treatment for drug-resistant or metastatic tumours should not be based solely on the discovery of novel druggable chemical entities. The timing of treatment is another invaluable asset at the disposal of clinicians. Curiously, a parallel with the principles of bacterial QS inhibition can be seen in the remarkable performance of abiraterone in the recent STAMPEDE trial (236). When administered to treatment-naïve patients (as opposed to those exposed to hormonal therapy or presenting advanced disease), Abi silences the endocrine androgen communication axis at an early stage, efficiently avoiding phenotypic migration and activation of oncogenic reciprocal signalling feedback pathways. If resistance to treatment will also appear in this novel treatment set up remains to be seen.

10 REFERENCES

1. Anbar AD, Knoll AH. Proterozoic ocean chemistry and evolution: a bioinorganic bridge? *Science*. 2002;297:1137–42.
2. Donoghue PCJ, Antcliffe JB. Early life: Origins of multicellularity. *Nature*. 2010;466:41–2.
3. Bull L. On the evolution of multicellularity and eusociality. *Artif Life*. 1999;5:1–15.
4. Abedin M, King N. The premetazoan ancestry of cadherins. *Science*. 2008;319:946–8.
5. Rokas A. The molecular origins of multicellular transitions. *Curr Opin Genet Dev*. 2008;18:472–8.
6. Rokas A. The Origins of Multicellularity and the Early History of the Genetic Toolkit For Animal Development. *Annu Rev Genet*. 2008;42:235–51.
7. Sebe-Pedros A, Roger AJ, Lang FB, King N, Ruiz-Trillo I. Ancient origin of the integrin-mediated adhesion and signaling machinery. *Proc Natl Acad Sci*. 2010;107:10142–7.
8. Bosco D, Haefliger J-A, Meda P. Connexins: Key Mediators of Endocrine Function. *Physiol Rev*. 2011;91:1393–445.
9. Biernaskie JM, West SA. Cooperation, clumping and the evolution of multicellularity. *Proc R Soc B Biol Sci*. 2015;282:20151075.
10. Szathmáry E, Smith JM. The major evolutionary transitions. *Nature*. 1995;374:227–32.
11. West SA, Gardner A. Adaptation and Inclusive Fitness. *Curr Biol*. 2013;23:R577–84.
12. Allen B, Nowak MA. There is no inclusive fitness at the level of the individual. *Curr Opin Behav Sci*. 2016;12:122–8.
13. Bassler BL. How bacteria talk to each other: regulation of gene expression by quorum sensing. *Curr Opin Microbiol*. 1999;2:582–7.
14. Carruba G, Webber MM, Quader STA, Amoroso M, Cocciadiferro L, Saladino F, et al. Regulation of cell-to-cell communication in non-tumorigenic and malignant human prostate epithelial cells. *Prostate*. 2002;50:73–82.
15. Ryan RP, Dow JM. Diffusible signals and interspecies communication in bacteria. *Microbiology*. 2008;154:1845–58.
16. Eberl L. N-Acyl Homoserinelactone-mediated Gene Regulation in Gram-negative Bacteria. *Syst Appl Microbiol*. 1999;22:493–506.
17. Schauder S. The languages of bacteria. *Genes Dev*. 2001;15:1468–80.
18. Sperandio V, Mellies JL, Delahay RM, Frankel G, Adam Crawford J, Nguyen W, et al. Activation of enteropathogenic *Escherichia coli* (EPEC) LEE2 and LEE3 operons by *Ler*. *Mol Microbiol*. 2000;38:781–93.
19. Jarraud S, Lyon GJ, Figueiredo AMS, Gerard L, Vandenesch F, Etienne J, et al. Exfoliatin-producing strains define a fourth *agr* specificity group in *Staphylococcus aureus*. *J Bacteriol*. 2000;182:6517–22.
20. Barber CE, Tang JL, Feng JX, Pan MQ, Wilson TJG, Slater H, et al. A novel regulatory system required for pathogenicity of *Xanthomonas campestris* is mediated by a small diffusible signal molecule. *Mol Microbiol*. 1997;24:555–66.
21. Chun W, Cui J, Poplawsky A. Purification, characterization and biological role of a pheromone produced by *Xanthomonas campestris* pv. *campestris*. *Physiol Mol Plant*

REFERENCES

- Pathol.* 1997;51:1–14.
22. Hirakawa H, Inazumi Y, Masaki T, Hirata T, Yamaguchi A. Indole induces the expression of multidrug exporter genes in *Escherichia coli*. *Mol Microbiol.* 2004;55:1113–26.
 23. Lee J, Jayaraman A, Wood TK. Indole is an inter-species biofilm signal mediated by SdiA. *BMC Microbiol.* 2007;7:42.
 24. Dworkin J. The Medium Is the Message: Interspecies and Interkingdom Signaling by Peptidoglycan and Related Bacterial Glycans. *Annu Rev Microbiol.* 2014;68:137–54.
 25. Baltz RH. Antimicrobials from Actinomycetes: Back to the future. *Microbiol.* 2007;2:125–31.
 26. Davies J, Spiegelman GB, Yim G. The world of subinhibitory antibiotic concentrations. *Curr Opin Microbiol.* 2006;9:445–53.
 27. Bosco D, Haefliger J-A, Meda P. Connexins: Key Mediators of Endocrine Function. *Physiol Rev.* 2011;91:1393–445.
 28. Bonner J. The Origins of Multicellularity. *Integr Biol Issues News Rev.* 1998;1:27–36.
 29. Roth J, LeRoith D, Shiloach J, Rosenzweig JL, Lesniak MA, Havrankova J. The evolutionary origins of hormones, neurotransmitters, and other extracellular chemical messengers: implications for mammalian biology. *N Engl J Med.* 1982;306:523–7.
 30. Brooke MA, Nitoiu D, Kelsell DP. Cell-cell connectivity: desmosomes and disease. *J Pathol.* 2012;226:158–71.
 31. Hervé JC, Derangeon M. Gap-junction-mediated cell-to-cell communication. *Cell Tissue Res.* 2013;352:21–31.
 32. Jose AM. Movement of regulatory RNA between animal cells. *Genesis.* 2015;53:395–416.
 33. Minciocchi VR, Freeman MR, Di Vizio D. Extracellular Vesicles in Cancer: Exosomes, Microvesicles and the Emerging Role of Large Oncosomes. *Semin Cell Dev Biol.* 2015;40:41–51.
 34. Toni R, Mirandola P, Gobbi G, Vitale M. Neuroendocrine regulation and tumor immunity. *Eur J Histochem.* 2007;51:133–8.
 35. Hawver LA, Jung SA, Ng W. Specificity and complexity in bacterial quorum-sensing systems. *FEMS Microbiol Rev.* 2016;40:738–52.
 36. Rasamiravaka T, El Jaziri M. Quorum-Sensing Mechanisms and Bacterial Response to Antibiotics in *P. aeruginosa*. *Curr Microbiol.* 2016;73:747–53.
 37. Lee C. Cellular interactions in prostate cancer. *Br J Urol.* 1997;79 Suppl 1:21–7.
 38. Bornstein S., Rutkowski H, Vrezas I. Cytokines and steroidogenesis. *Mol Cell Endocrinol.* 2004;215:135–41.
 39. Feraco D, Blaha M, Khan S, Green JM, Plotkin BJ. Host environmental signals and effects on biofilm formation. *Microb Pathog.* 2016;99:253–63.
 40. Lyczak JB, Cannon CL, Pier GB. Establishment of *Pseudomonas aeruginosa* infection: lessons from a versatile opportunist. *Microbes Infect.* 2000;2:1051–60.
 41. Gastmeier P, Geffers C, Brandt C, Zuschneid I, Sohr D, Schwab F, et al. Effectiveness of a nationwide nosocomial infection surveillance system for reducing nosocomial infections. *J Hosp Infect.* 2006;64:16–22.
 42. Paterson DL. The epidemiological profile of infections with multidrug-resistant *Pseudomonas aeruginosa* and *Acinetobacter* species. *Clin Infect Dis.* 2006;43 Suppl 2:S43–8.

43. Taylor PK, Yeung ATY, Hancock REW. Antibiotic resistance in *Pseudomonas aeruginosa* biofilms: Towards the development of novel anti-biofilm therapies. *J Biotechnol*. 2014;191:121–30.
44. Chatterjee M, Anju CP, Biswas L, Anil Kumar V, Gopi Mohan C, Biswas R. Antibiotic resistance in *Pseudomonas aeruginosa* and alternative therapeutic options. *Int J Med Microbiol*. 2016;306:48–58.
45. Jeukens J, Boyle B, Kukavica-Ibrulj I, Ouellet MM, Aaron SD, Charette SJ, et al. Comparative genomics of isolates of a *Pseudomonas aeruginosa* epidemic strain associated with chronic lung infections of cystic fibrosis patients. *PLoS One*. 2014;9:e87611.
46. Obritsch MD, Fish DN, MacLaren R, Jung R. National surveillance of antimicrobial resistance in *Pseudomonas aeruginosa* isolates obtained from intensive care unit patients from 1993 to 2002. *Antimicrob Agents Chemother*. 2004;48:4606–10.
47. Sabuda DM, Laupland K, Pitout J, Dalton B, Rabin H, Louie T, et al. Utilization of Colistin for Treatment of Multidrug-Resistant *Pseudomonas aeruginosa*. *Can J Infect Dis Med Microbiol*. 2008;19:413–8.
48. Johansen HK, Moskowitz SM, Ciofu O, Pressler T, Høiby N. Spread of colistin resistant non-mucoid *Pseudomonas aeruginosa* among chronically infected Danish cystic fibrosis patients. *J Cyst Fibros*. 2008;7:391–7.
49. Rabin N, Zheng Y, Opoku-Temeng C, Du Y, Bonsu E, Sintim HO. Biofilm formation mechanisms and targets for developing antibiofilm agents. *Future Med Chem*. 2015;7:493–512.
50. Zambelloni R, Marquez R, Roe AJ. Development of Antivirulence Compounds: A Biochemical Review. *Chem Biol Drug Des*. 2015;85:43–55.
51. Adegoke A, Faleye A, Singh G, Stenström T. Antibiotic Resistant Superbugs: Assessment of the Interrelationship of Occurrence in Clinical Settings and Environmental Niches. *Molecules*. 2016;22:29.
52. Vranakis I, Goniotakis I, Psaroulaki A, Sandalakis V, Tselentis Y, Gevaert K, et al. Proteome studies of bacterial antibiotic resistance mechanisms. *J Proteomics*. 2014;97:88–99.
53. Kester JC, Fortune SM. Persisters and beyond: Mechanisms of phenotypic drug resistance and drug tolerance in bacteria. *Crit Rev Biochem Mol Biol*. 2014;49:91–101.
54. Kohanski MA, DePristo MA, Collins JJ. Sublethal Antibiotic Treatment Leads to Multidrug Resistance via Radical-Induced Mutagenesis. *Mol Cell*. 2010;37:311–20.
55. Sanchez-Romero MA, Casades J. Contribution of phenotypic heterogeneity to adaptive antibiotic resistance. *Proc Natl Acad Sci*. 2014;111:355–60.
56. Fernández L, Hancock REW. Adaptive and mutational resistance: Role of porins and efflux pumps in drug resistance. *Clin Microbiol Rev*. 2012;25:661–81.
57. Hancock REW, Bell A. Antibiotic uptake into gram-negative bacteria. *Eur J Clin Microbiol Infect Dis*. 1988;7:713–20.
58. Morita Y, Tomida J, Kawamura Y. MexXY multidrug efflux system of *Pseudomonas aeruginosa*. *Front Microbiol*. 2012;3:408.
59. Alvarez-Ortega C, Wiegand I, Olivares J, Hancock REW, Martinez JL. Genetic Determinants Involved in the Susceptibility of *Pseudomonas aeruginosa* to -Lactam Antibiotics. *Antimicrob Agents Chemother*. 2010;54:4159–67.
60. Umadevi S, Joseph NM, Kumari K, Easow JM, Kumar S, Stephen S, et al. Detection of extended spectrum beta lactamases, AmpC beta lactamases and metallobeta lactamases

REFERENCES

- in clinical isolates of ceftazidime resistant *Pseudomonas aeruginosa*. *Brazilian J Microbiol.* 2011;42:1284–8.
61. Poole K, Srikumar R. Multidrug Efflux in *Pseudomonas aeruginosa* Components, Mechanisms and Clinical Significance. *Curr Top Med Chem.* 2001;1:59–71.
 62. Langae TY, Gagnon L, Huletsky A. Inactivation of the ampD gene in *Pseudomonas aeruginosa* leads to moderate-basal-level and hyperinducible AmpC β -lactamase expression. *Antimicrob Agents Chemother.* 2000;44:583–9.
 63. Brooks BD, Brooks AE. Therapeutic strategies to combat antibiotic resistance. *Adv Drug Deliv Rev.* 2014;78:14–27.
 64. Wagner S, Sommer R, Hinsberger S, Lu C, Hartmann RW, Empting M, et al. Novel Strategies for the Treatment of *Pseudomonas aeruginosa* Infections. *J Med Chem.* 2016;59:5929–69.
 65. Boucher HW, Talbot GH, Bradley JS, Edwards JE, Gilbert D, Rice LB, et al. Bad Bugs, No Drugs: No ESCAPE! An Update from the Infectious Diseases Society of America. *Clin Infect Dis.* 2009;48:1–12.
 66. Davis EM, Li D, Shahrooei M, Yu B, Muruve D, Irvin RT. Evidence of extensive diversity in bacterial adherence mechanisms that exploit unanticipated stainless steel surface structural complexity for biofilm formation. *Acta Biomater.* 2013;9:6236–44.
 67. Kolomiets E, Swiderska MA, Kadam RU, Johansson EM V., Jaeger K-E, Darbre T, et al. Glycopeptide Dendrimers with High Affinity for the Fucose-Binding Lectin LecB from *Pseudomonas aeruginosa*. *ChemMedChem.* 2009;4:562–9.
 68. Ahiwale S, Tamboli N, Thorat K, Kulkarni R, Ackermann H, Kapadnis B. In Vitro Management of Hospital *Pseudomonas aeruginosa* Biofilm Using Indigenous T7-Like Lytic Phage. *Curr Microbiol.* 2011;62:335–40.
 69. Gill EE, Franco OL, Hancock REW. Antibiotic adjuvants: Diverse strategies for controlling drug-resistant pathogens. *Chem Biol Drug Des.* 2015;85:56–78.
 70. Ormala AM, Jalasvuori M. Phage therapy: Should bacterial resistance to phages be a concern, even in the long run? *Bacteriophage.* 2013;3:e24219.
 71. Adabi M, Talebi-Taher M, Arbabi L, Afshar M, Fathizadeh S, Minaeian S, et al. Spread of efflux pump overexpressing-mediated fluoroquinolone resistance and multidrug resistance in *Pseudomonas aeruginosa* by using an efflux pump inhibitor. *Infect Chemother.* 2015;47:98–104.
 72. Davies J, Davies D. Origins and Evolution of Antibiotic Resistance. *Microbiol Mol Biol Rev.* 2010;74:417–33.
 73. Deep A, Chaudhary U, Gupta V. Quorum sensing and bacterial pathogenicity: From molecules to disease. *J Lab Physicians.* 2011;3:4.
 74. Clatworthy AE, Pierson E, Hung DT. Targeting virulence: a new paradigm for antimicrobial therapy. *Nat Chem Biol.* 2007;3:541–8.
 75. Werner G, Strommenger B, Witte W. Acquired vancomycin resistance in clinically relevant pathogens. *Future Microbiol.* 2008;3:547–62.
 76. Rampioni G, Leoni L, Williams P. The art of antibacterial warfare: Deception through interference with quorum sensing–mediated communication. *Bioorg Chem.* 2014;55:60–8.
 77. Atkinson S, Williams P. Quorum sensing and social networking in the microbial world. *J R Soc Interface.* 2009;6:959–78.
 78. Cheung GYC, Wang R, Khan BA, Sturdevant DE, Otto M. Role of the accessory gene

- regulator agr in community-associated methicillin-resistant *Staphylococcus aureus* pathogenesis. *Infect Immun*. 2011;79:1927–35.
79. Zhu L, Lau GW. Inhibition of competence development, horizontal gene transfer and virulence in streptococcus pneumoniae by a modified competence stimulating peptide. *PLoS Pathog*. 2011;7.
 80. Bassler BL, Miller MB. Quorum Sensing. *The Prokaryotes*. Berlin: Springer; 2013. page 495–509.
 81. Lee J, Zhang L. The hierarchy quorum sensing network in *Pseudomonas aeruginosa*. *Protein Cell*. 2015;6:26–41.
 82. Nealson KH, Platt T, Hastings JW. Cellular control of the synthesis and activity of the bacterial luminescent system. *J Bacteriol*. 1970;104:313–22.
 83. Galloway WRJD, Hodgkinson JT, Bowden SD, Welch M, Spring DR. Quorum sensing in Gram-negative bacteria: Small-molecule modulation of AHL and AI-2 quorum sensing pathways. *Chem Rev*. 2011;111:28–67.
 84. Kim K, Kim YU, Koh BH, Hwang SS, Kim S-H, Lépine F, et al. HHQ and PQS, two *Pseudomonas aeruginosa* quorum-sensing molecules, down-regulate the innate immune responses through the nuclear factor- κ B pathway. *Immunology*. 2010;129:578–88.
 85. Pesci EC, Milbank JBL, Pearson JP, McKnight S, Kende AS, Greenberg EP, et al. Quinolone signalling in the cell-to-cell communication system of *Pseudomonas aeruginosa*. *PNAS*. 1999;96:11229–34.
 86. Tay S, Yew W. Development of Quorum-Based Anti-Virulence Therapeutics Targeting Gram-Negative Bacterial Pathogens. *Int J Mol Sci*. 2013;14:16570–99.
 87. Papaioannou E, Utari P, Quax W. Choosing an Appropriate Infection Model to Study Quorum Sensing Inhibition in *Pseudomonas* Infections. *Int J Mol Sci*. 2013;14:19309–40.
 88. Lee J, Wu J, Deng Y, Wang J, Wang C, Wang J, et al. A cell-cell communication signal integrates quorum sensing and stress response. *Nat Chem Biol*. 2013;9:339–43.
 89. Maura D, Hazan R, Kitao T, Ballok AE, Rahme LG. Evidence for Direct Control of Virulence and Defense Gene Circuits by the *Pseudomonas aeruginosa* Quorum Sensing Regulator, MvfR. *Sci Rep*. 2016;6:34083.
 90. Déziel E, Gopalan S, Tampakaki AP, Lépine F, Padfield KE, Saucier M, et al. The contribution of MvfR to *Pseudomonas aeruginosa* pathogenesis and quorum sensing circuitry regulation: multiple quorum sensing-regulated genes are modulated without affecting lasRI, rhlRI or the production of N-acyl- l-homoserine lactones. *Mol Microbiol*. 2004;55:998–1014.
 91. Starkey M, Lepine F, Maura D, Bandyopadhyaya A, Lesic B, He J, et al. Identification of Anti-virulence Compounds That Disrupt Quorum-Sensing Regulated Acute and Persistent Pathogenicity. *PLoS Pathog*. 2014;10:e1004321.
 92. Pérez-Rueda E, Collado-Vides J. The repertoire of DNA-binding transcriptional regulators in *Escherichia coli* K-12. *Nucleic Acids Res*. 2000;28:1838–47.
 93. Dubern J-F, Diggle SP. Quorum sensing by 2-alkyl-4-quinolones in *Pseudomonas aeruginosa* and other bacterial species. *Mol Biosyst*. 2008;4:882–8.
 94. Gallagher LA, McKnight SL, Kuznetsova MS, Pesci EC, Manoil C. Functions required for extracellular quinolone signaling by *Pseudomonas aeruginosa*. *J Bacteriol*. 2002;184:6472–80.
 95. McGrath S, Wade DS, Pesci EC. Dueling quorum sensing systems in *Pseudomonas aeruginosa* control the production of the *Pseudomonas* quinolone signal (PQS). *FEMS*

REFERENCES

- Microbiol Lett.* 2004;230:27–34.
96. Coleman JP, Hudson LL, McKnight SL, Farrow JM, Calfee MW, Lindsey CA, et al. *Pseudomonas aeruginosa* PqsA is an anthranilate-coenzyme A ligase. *J Bacteriol.* 2008;190:1247–55.
 97. Dulcey CE, Dekimpe V, Fauvelle DA, Milot S, Groleau MC, Doucet N, et al. The end of an old hypothesis: The *pseudomonas* signaling molecules 4-hydroxy-2-alkylquinolines derive from fatty acids, not 3-ketofatty acids. *Chem Biol.* 2013;20:1481–91.
 98. Drees SL, Fetzner S. PqsE of *Pseudomonas aeruginosa* Acts as Pathway-Specific Thioesterase in the Biosynthesis of Alkylquinolone Signaling Molecules. *Chem Biol.* 2015;22:611–8.
 99. Schertzer JW, Brown SA, Whiteley M. Oxygen levels rapidly modulate *Pseudomonas aeruginosa* social behaviours via substrate limitation of PqsH. *Mol Microbiol.* 2010;77:1527–38.
 100. Welch M, Hodgkinson JT, Gross J, Spring DR, Sams T. Ligand binding kinetics of the quorum sensing regulator PqsR. *Biochemistry.* 2013;52:4433–8.
 101. Gruber JD, Chen W, Parnham S, Beauchesne K, Moeller P, Flume PA, et al. The role of 2,4-dihydroxyquinoline (DHQ) in *Pseudomonas aeruginosa* pathogenicity. *PeerJ.* 2016;4:e1495.
 102. Hazan R, Que YA, Maura D, Strobel B, Majcherczyk PA, Hopper LR, et al. Auto Poisoning of the Respiratory Chain by a Quorum-Sensing-Regulated Molecule Favors Biofilm Formation and Antibiotic Tolerance. *Curr Biol.* 2016;26:195–206.
 103. Que Y-A, Hazan R, Strobel B, Maura D, He J, Kesarwani M, et al. A Quorum Sensing Small Volatile Molecule Promotes Antibiotic Tolerance in Bacteria. Kaufmann GF, editor. *PLoS One.* 2013;8:e80140.
 104. Thomann A, de Mello Martins AGG, Brengel C, Empting M, Hartmann RW. Application of Dual Inhibition Concept within Looped Autoregulatory Systems toward Antivirulence Agents against *Pseudomonas aeruginosa* Infections. *ACS Chem Biol.* 2016;11:1279–86.
 105. Doğaner BA, Yan LKQ, Youk H. Autocrine Signaling and Quorum Sensing: Extreme Ends of a Common Spectrum. *Trends Cell Biol.* 2016;26:262–71.
 106. Ciofu O, Tolker-Nielsen T, Jensen PØ, Wang H, Høiby N. Antimicrobial resistance, respiratory tract infections and role of biofilms in lung infections in cystic fibrosis patients. *Adv Drug Deliv Rev.* 2015;85:7–23.
 107. Srivastava S, Bhargava A. Biofilms and human health. *Biotechnol Lett.* 2016;38:1–22.
 108. Gloag ES, Turnbull L, Huang A, Vallotton P, Wang H, Nolan LM, et al. Self-organization of bacterial biofilms is facilitated by extracellular DNA. *Proc Natl Acad Sci.* 2013;110:11541–6.
 109. Xiao G, Déziel E, He J, Lépine F, Lesic B, Castonguay MH, et al. MvfR, a key *Pseudomonas aeruginosa* pathogenicity LTTR-class regulatory protein, has dual ligands. *Mol Microbiol.* 2006;62:1689–99.
 110. Diggle SP, Matthijs S, Wright VJ, Fletcher MP, Chhabra SR, Lamont IL, et al. The *Pseudomonas aeruginosa* 4-Quinolone Signal Molecules HHQ and PQS Play Multifunctional Roles in Quorum Sensing and Iron Entrapment. *Chem Biol.* 2007;14:87–96.
 111. Pistorius D, Ullrich A, Lucas S, Hartmann RW, Kazmaier U, Müller R. Biosynthesis of 2-Alkyl-4(1H)-Quinolones in *Pseudomonas aeruginosa*: Potential for Therapeutic

- Interference with Pathogenicity. *ChemBioChem*. 2011;12:850–3.
112. Weidel E, Negri M, Empting M, Hinsberger S, Hartmann RW. Composing compound libraries for hit discovery – rationality-driven preselection or random choice by structural diversity? *Future Med Chem*. 2014;6:2057–72.
 113. Storz MP, Allegretta G, Kirsch B, Empting M, Hartmann RW. From in vitro to in cellulose: structure–activity relationship of (2-nitrophenyl)methanol derivatives as inhibitors of PqsD in *Pseudomonas aeruginosa*. *Org Biomol Chem*. 2014;12:6094.
 114. Allegretta G, Weidel E, Empting M, Hartmann RW. Catechol-based substrates of chalcone synthase as a scaffold for novel inhibitors of PqsD. *Eur J Med Chem*. 2015;90:351–9.
 115. Sahner JH, Empting M, Kamal A, Weidel E, Groh M, Börger C, et al. Exploring the chemical space of ureidothiophene-2-carboxylic acids as inhibitors of the quorum sensing enzyme PqsD from *Pseudomonas aeruginosa*. *Eur J Med Chem*. 2015;96:14–21.
 116. Allesen-Holm M, Barken KB, Yang L, Klausen M, Webb JS, Kjelleberg S, et al. A characterization of DNA release in *Pseudomonas aeruginosa* cultures and biofilms. *Mol Microbiol*. 2006;59:1114–28.
 117. Cao H, Krishnan G, Goumnerov B, Tsongalis J, Tompkins R, Rahme LG. A quorum sensing-associated virulence gene of *Pseudomonas aeruginosa* encodes a LysR-like transcription regulator with a unique self-regulatory mechanism. *Proc Natl Acad Sci*. 2001;98:14613–8.
 118. Lau GW, Ran H, Kong F, Hassett DJ, Mavrodi D. *Pseudomonas aeruginosa* Pyocyanin Is Critical for Lung Infection in Mice. *Infect Immun*. 2004;72:4275–8.
 119. Lu C, Kirsch B, Zimmer C, de Jong JC, Henn C, Maurer CK, et al. Discovery of Antagonists of PqsR, a Key Player in 2-Alkyl-4-quinolone-Dependent Quorum Sensing in *Pseudomonas aeruginosa*. *Chem Biol*. 2012;19:381–90.
 120. Lu C, Maurer CK, Kirsch B, Steinbach A, Hartmann RW. Overcoming the Unexpected Functional Inversion of a PqsR Antagonist in *Pseudomonas aeruginosa* : An In Vivo Potent Antivirulence Agent Targeting pqs Quorum Sensing. *Angew Chemie Int Ed*. 2014;53:1109–12.
 121. Klein T, Henn C, de Jong JC, Zimmer C, Kirsch B, Maurer CK, et al. Identification of Small-Molecule Antagonists of the *Pseudomonas aeruginosa* Transcriptional Regulator PqsR: Biophysically Guided Hit Discovery and Optimization. *ACS Chem Biol*. 2012;7:1496–501.
 122. Zender M, Klein T, Henn C, Kirsch B, Maurer CK, Kail D, et al. Discovery and biophysical characterization of 2-amino-oxadiazoles as novel antagonists of PqsR, an important regulator of *Pseudomonas aeruginosa* virulence. *J Med Chem*. 2013;56:6761–74.
 123. Rajaram RD, Brisken C. Paracrine signaling by progesterone. *Mol Cell Endocrinol*. 2012;357:80–90.
 124. Hanukoglu I. Steroidogenic enzymes: Structure, function, and role in regulation of steroid hormone biosynthesis. *J Steroid Biochem Mol Biol*. 1992;43:779–804.
 125. Kumar R. Steroid hormone receptors and prostate cancer: role of structural dynamics in therapeutic targeting. *Asian J Androl*. 2016;18:682.
 126. Hilton HN, Graham JD, Clarke CL. Minireview: Progesterone Regulation of Proliferation in the Normal Human Breast and in Breast Cancer: A Tale of Two Scenarios? *Mol Endocrinol*. 2015;29:1230–42.

REFERENCES

127. D’Uva G, Lauriola M. Towards the emerging crosstalk: ERBB family and steroid hormones. *Semin Cell Dev Biol*. 2016;50:143–52.
128. Le B, Chen H, Zirkin B, Burnett A. New targets for increasing endogenous testosterone production: clinical implications and review of the literature. *Andrology*. 2014;2:484–90.
129. Kempná P, Marti N, Udhane S, Flück CE. Regulation of androgen biosynthesis – A short review and preliminary results from the hyperandrogenic starvation NCI-H295R cell model. *Mol Cell Endocrinol*. 2015;408:124–32.
130. Hiort O. The differential role of androgens in early human sex development. *BMC Med*. 2013;11:152.
131. Qin X, Liu M, Wang X. New insights into the androgen biotransformation in prostate cancer: A regulatory network among androgen, androgen receptors and UGTs. *Pharmacol Res*. 2016;106:114–22.
132. Tornillo G, Smalley MJ. ERrrr... Where are the Progenitors? Hormone Receptors and Mammary Cell Heterogeneity. *J Mammary Gland Biol Neoplasia*. 2015;20:63–73.
133. Zhou Y, Bolton EC, Jones JO. Androgens and androgen receptor signaling in prostate tumorigenesis. *J Mol Endocrinol*. 2014;54:R15–29.
134. Wadhwa B, Dumbre R. Achieving resistance specificity in prostate cancer. *Chem Biol Interact*. 2016;260:243–7.
135. Schweizer MT, Yu EY. AR-Signaling in Human Malignancies: Prostate Cancer and Beyond. *Cancers (Basel)*. 2017;9:7.
136. Heemers H V., Tindall DJ. Androgen Receptor (AR) Coregulators: A Diversity of Functions Converging on and Regulating the AR Transcriptional Complex. *Endocr Rev*. 2007;28:778–808.
137. O’Hara L, Smith LB. Androgen receptor roles in spermatogenesis and infertility. *Best Pract Res Clin Endocrinol Metab*. 2015;29:595–605.
138. Asa SL. The evolution of differentiated thyroid cancer. *Pathology*. 2017;49:229–37.
139. Ryan DP, Hong TS, Bardeesy N. Pancreatic Adenocarcinoma. *N Engl J Med*. 2014;371:1039–49.
140. de Melo AC, Paulino E, Garces ÁHI. A Review of mTOR Pathway Inhibitors in Gynecologic Cancer. *Oxid Med Cell Longev*. 2017;2017:1–8.
141. Pekic S, Popovic V. DIAGNOSIS OF ENDOCRINE DISEASE: Expanding the cause of hypopituitarism. *Eur J Endocrinol*. 2017;176:R269–82.
142. Vlachostergios PJ, Puca L, Beltran H. Emerging Variants of Castration-Resistant Prostate Cancer. *Curr Oncol Rep*. 2017;19:32.
143. Siegel RL, Miller KD, Jemal A. Cancer Statistics, 2015. *CA Cancer J Clin*. 2015;65:5–29.
144. Huggins C, Hodges C V. Studies on Prostatic Cancer. I. The Effect of Castration, of Estrogen and of Androgen Injection on Serum Phosphatases in Metastatic Carcinoma of the Prostate. *Cancer Res*. 1941;1:293 LP-297.
145. Lu-Yao GL, Albertsen PC, Moore DF, Shih W, Lin Y, DiPaola RS, et al. Fifteen-year survival outcomes following primary androgen-deprivation therapy for localized prostate cancer. *JAMA Intern Med*. 2014;174:1460–7.
146. Fujimoto N. Role of the Androgen-Androgen Receptor Axis in the Treatment Resistance of Advanced Prostate Cancer: From Androgen-Dependent to Castration Resistant and Further. *J UOEH*. 2016;38:129–38.

147. Scher HI. Biology of Progressive, Castration-Resistant Prostate Cancer: Directed Therapies Targeting the Androgen-Receptor Signaling Axis. *J Clin Oncol*. 2005;23:8253–61.
148. Packer JR, Maitland NJ. The molecular and cellular origin of human prostate cancer. *Biochim Biophys Acta - Mol Cell Res*. 2016;1863:1238–60.
149. Seisen T, Rouprêt M, Gomez F, Malouf GG, Shariat SF, Peyronnet B, et al. A comprehensive review of genomic landscape, biomarkers and treatment sequencing in castration-resistant prostate cancer. *Cancer Treat Rev*. 2016;48:25–33.
150. Montgomery RB, Mostaghel EA, Vessella R, Hess DL, Kalthorn TF, Higano CS, et al. Maintenance of Intratumoral Androgens in Metastatic Prostate Cancer: A Mechanism for Castration-Resistant Tumor Growth. *Cancer Res*. 2008;68:4447–54.
151. Fujimoto N, Miyamoto H, Mizokami A, Harada S, Nomura M, Ueta Y, et al. Prostate Cancer Cells Increase Androgen Sensitivity by Increase in Nuclear Androgen Receptor and Androgen Receptor Coactivators; A Possible Mechanism of Hormone-Resistance of Prostate Cancer Cells. *Cancer Invest*. 2007;25:32–7.
152. Mostaghel EA, Marck BT, Plymate SR, Vessella RL, Balk S, Matsumoto AM, et al. Resistance to CYP17A1 Inhibition with Abiraterone in Castration-Resistant Prostate Cancer: Induction of Steroidogenesis and Androgen Receptor Splice Variants. *Clin Cancer Res*. 2011;17:5913–25.
153. Yamamoto Y, Lorient Y, Beraldi E, Zhang F, Wyatt AW, Nakouzi N Al, et al. Generation 2.5 Antisense Oligonucleotides Targeting the Androgen Receptor and Its Splice Variants Suppress Enzalutamide-Resistant Prostate Cancer Cell Growth. *Clin Cancer Res*. 2015;21:1675–87.
154. Yu Z, Chen S, Sowalsky AG, Voznesensky OS, Mostaghel EA, Nelson PS, et al. Rapid Induction of Androgen Receptor Splice Variants by Androgen Deprivation in Prostate Cancer. *Clin Cancer Res*. 2014;20:1590–600.
155. Dehm SM, Tindall DJ. Alternatively spliced androgen receptor variants. *Endocr Relat Cancer*. 2011;18:R183–96.
156. Nakazawa M, Antonarakis ES, Luo J. Androgen Receptor Splice Variants in the Era of Enzalutamide and Abiraterone. *Horm Cancer*. 2014;5:265–73.
157. Kung H-J, Evans CP. Oncogenic activation of androgen receptor. *Urol Oncol Semin Orig Investig*. 2009;27:48–52.
158. Graham L, Schweizer MT. Targeting persistent androgen receptor signaling in castration-resistant prostate cancer. *Med Oncol*. 2016;33:44.
159. Ciccicarese C, Massari F, Iacovelli R, Fiorentino M, Montironi R, Di Nunno V, et al. Prostate cancer heterogeneity: Discovering novel molecular targets for therapy. *Cancer Treat Rev*. 2017;54:68–73.
160. Berindan-Neagoe I, Calin GA. Molecular Pathways: microRNAs, Cancer Cells, and Microenvironment. *Clin Cancer Res*. 2014;20:6247–53.
161. Fletcher CE, Dart DA, Bevan CL. Interplay between steroid signalling and microRNAs: implications for hormone-dependent cancers. *Endocr Relat Cancer*. 2014;21:R409–29.
162. Knudsen KE, Scher HI. Starving the Addiction: New Opportunities for Durable Suppression of AR Signaling in Prostate Cancer. *Clin Cancer Res*. 2009;15:4792–8.
163. Bales GT, Chodak GW. A controlled trial of bicalutamide versus castration in patients with advanced prostate cancer. *Urology*. 1996;47:38–43.
164. Taplin ME, Bubley GJ, Ko YJ, Small EJ, Upton M, Rajeshkumar B, et al. Selection for

REFERENCES

- androgen receptor mutations in prostate cancers treated with androgen antagonist. *Cancer Res.* 1999;59:2511–5.
165. Chen CD, Welsbie DS, Tran C, Baek SH, Chen R, Vessella R, et al. Molecular determinants of resistance to antiandrogen therapy. *Nat Med.* 2004;10:33–9.
 166. Tran C, Ouk S, Clegg NJ, Chen Y, Watson PA, Arora V, et al. Development of a second-generation antiandrogen for treatment of advanced prostate cancer. *Science (80-)*. 2009;324:787–90.
 167. Simões BM, Alferez DG, Howell SJ, Clarke RB. The role of steroid hormones in breast cancer stem cells. *Endocr Relat Cancer.* 2015;22:T177–86.
 168. Bird IM, Abbott DH. The hunt for a selective 17,20 lyase inhibitor; learning lessons from nature. *J Steroid Biochem Mol Biol.* 2016;163:136–46.
 169. Buttiglieri C, Tucci M, Bertaglia V, Vignani F, Bironzo P, Di Maio M, et al. Understanding and overcoming the mechanisms of primary and acquired resistance to abiraterone and enzalutamide in castration resistant prostate cancer. *Cancer Treat Rev.* 2015;41:884–92.
 170. Grist E, De Bono JS, Attard G. Targeting extra-gonadal androgens in castration-resistant prostate cancer. *J. Steroid Biochem. Mol. Biol.* 2015. page 157–63.
 171. Ang JE, Olmos D, de Bono JS. CYP17 blockade by abiraterone: further evidence for frequent continued hormone-dependence in castration-resistant prostate cancer. *Br J Cancer.* 2009;100:671–5.
 172. Gupta AK, Foley KA, Versteeg SG. New Antifungal Agents and New Formulations Against Dermatophytes. *Mycopathologia.* 2017;182:127–41.
 173. DeVore NM, Scott EE. Structures of cytochrome P450 17A1 with prostate cancer drugs abiraterone and TOK-001. *Nature.* 2012;482:116–9.
 174. Stein M, Singer E, Patel N, Bershadskiy A, Sokoloff A. Androgen synthesis inhibitors in the treatment of castration-resistant prostate cancer. *Asian J Androl.* 2014;16:387.
 175. Storz MP, Maurer CK, Zimmer C, Wagner N, Brengel C, De Jong JC, et al. Validation of PqsD as an anti-biofilm target in *Pseudomonas aeruginosa* by development of small-molecule inhibitors. *J Am Chem Soc.* 2012;134:16143–6.
 176. Sahner JH, Brengel C, Storz MP, Groh M, Plaza A, Müller R, et al. Combining in silico and biophysical methods for the development of *Pseudomonas aeruginosa* quorum sensing inhibitors: an alternative approach for structure-based drug design. *J Med Chem.* 2013;56:8656–64.
 177. Lu C. Discovery and Optimization of the First PqsR Antagonists as Anti-virulence Agents Combating *Pseudomonas aeruginosa* Infections. Helmholtz Institute for Pharmaceutical Research Saarland; 2014.
 178. Guttenberger N, Blankenfeldt W, Breinbauer R. Recent developments in the isolation, biological function, biosynthesis, and synthesis of phenazine natural products. *Bioorg Med Chem.* 2017;36:26–36.
 179. Laursen JB, Nielsen J. Phenazine Natural Products: Biosynthesis, Synthetic Analogues, and Biological Activity. *Chem Rev.* 2004;104:1663–86.
 180. Rampioni G, Pustelny C, Fletcher MP, Wright VJ, Bruce M, Rumbaugh KP, et al. Transcriptomic analysis reveals a global alkyl-quinolone-independent regulatory role for PqsE in facilitating the environmental adaptation of *Pseudomonas aeruginosa* to plant and animal hosts. *Environ Microbiol.* 2010;12:1659–73.
 181. Hazan R, He J, Xiao G, Dekimpe V, Apidianakis Y, Lesic B, et al. Homeostatic Interplay between Bacterial Cell-Cell Signaling and Iron in Virulence. Whiteley M,

- editor. *PLoS Pathog.* 2010;6:e1000810.
182. Das T, Kutty SK, Kumar N, Manefield M. Pyocyanin facilitates extracellular DNA binding to *Pseudomonas aeruginosa* influencing cell surface properties and aggregation. *PLoS One.* 2013;8:e58299.
 183. Das T, Kutty SK, Tavallaie R, Ibugo AI, Panchompoo J, Sehar S, et al. Phenazine virulence factor binding to extracellular DNA is important for *Pseudomonas aeruginosa* biofilm formation. *Sci Rep.* 2015;5:8398.
 184. Rada B, Jendrysik MA, Pang L, Hayes CP, Yoo D, Park JJ, et al. Pyocyanin-Enhanced Neutrophil Extracellular Trap Formation Requires the NADPH Oxidase. *PLoS One.* 2013;8:e54205.
 185. Diggle SP, Winzer K, Chhabra SR, Worrall KE, Cámara M, Williams P. The *Pseudomonas aeruginosa* quinolone signal molecule overcomes the cell density-dependency of the quorum sensing hierarchy, regulates rhl-dependent genes at the onset of stationary phase and can be produced in the absence of LasR. *Mol Microbiol.* 2003;50:29–43.
 186. Dandekar AA, Greenberg EP. Microbiology: Plan B for quorum sensing. *Nat Chem Biol.* 2013;9:292–3.
 187. Knoten CA, Wells G, Coleman JP, Pesci EC. A Conserved Suppressor Mutation in a Tryptophan Auxotroph Results in Dysregulation of *Pseudomonas* Quinolone Signal Synthesis. *J Bacteriol.* 2014;196:2413–22.
 188. Kamal AAM, Petretera L, Eberhard J, Hartmann RW. Structure–functionality relationship and pharmacological profiles of *Pseudomonas aeruginosa* alkylquinolone quorum sensing modulators. *Org Biomol Chem.* 2017;15:4620–30.
 189. Porcheron G, Dozois CM. Interplay between iron homeostasis and virulence: Fur and RyhB as major regulators of bacterial pathogenicity. *Vet Microbiol.* 2015;179:2–14.
 190. Reinhart A, Oglesby-Sherrouse A. Regulation of *Pseudomonas aeruginosa* Virulence by Distinct Iron Sources. *Genes (Basel).* 2016;7:126.
 191. Hassett DJ, Sokol PA, Howell ML, Ma JF, Schweizer HT, Ochsner U, et al. Ferric uptake regulator (Fur) mutants of *Pseudomonas aeruginosa* demonstrate defective siderophore-mediated iron uptake, altered aerobic growth, and decreased superoxide dismutase and catalase activities. *J Bacteriol.* 1996;178:3996–4003.
 192. Banin E, Vasil ML, Greenberg EP. From The Cover: Iron and *Pseudomonas aeruginosa* biofilm formation. *Proc Natl Acad Sci.* 2005;102:11076–81.
 193. Cezard C, Farvacques N, Sonnet P. Chemistry and Biology of Pyoverdines, *Pseudomonas* Primary Siderophores. *Curr Med Chem.* 2014;22:165–86.
 194. Bredenbruch F, Geffers R, Nimtz M, Buer J, Häussler S. The *Pseudomonas aeruginosa* quinolone signal (PQS) has an iron-chelating activity. *Environ Microbiol.* 2006;8:1318–29.
 195. Nadal Jimenez P, Koch G, Thompson J a, Xavier KB, Cool RH, Quax WJ. The Multiple Signaling Systems Regulating Virulence in *Pseudomonas aeruginosa*. *Microbiol Mol Biol Rev.* 2012;76:46–65.
 196. Yang L, Nilsson M, Gjermansen M, Givskov M, Tolker-Nielsen T. Pyoverdine and PQS mediated subpopulation interactions involved in *Pseudomonas aeruginosa* biofilm formation. *Mol Microbiol.* 2009;74:1380–92.
 197. Maeda T, García-Contreras R, Pu M, Sheng L, Garcia LR, Tomás M, et al. Quorum quenching quandary: resistance to antivirulence compounds. *ISME J.* 2012;6:493–501.
 198. Garcia-Contreras R, Maeda T, Wood TK. Resistance to Quorum-Quenching

REFERENCES

- Compounds. *Appl Environ Microbiol.* 2013;79:6840–6.
199. García-Contreras R, Maeda T, Wood TK. Can resistance against quorum-sensing interference be selected? *ISME J.* 2016;10:4–10.
 200. Ilangovan A, Fletcher M, Rampioni G, Pustelny C, Rumbaugh K, Heeb S, et al. Structural Basis for Native Agonist and Synthetic Inhibitor Recognition by the *Pseudomonas aeruginosa* Quorum Sensing Regulator PqsR (MvfR). *PLoS Pathog.* 2013;9:e1003508.
 201. Johnson L, Horsman SR, Charron-Mazenod L, Turnbull AL, Mulcahy H, Surette MG, et al. Extracellular DNA-induced antimicrobial peptide resistance in *Salmonella enterica* serovar Typhimurium. *BMC Microbiol.* 2013;13:115.
 202. Kirisits MJ, Parsek MR. Does *Pseudomonas aeruginosa* use intercellular signalling to build biofilm communities? *Cell Microbiol.* 2006;8:1841–9.
 203. Pantanella F, Valenti P, Natalizi T, Passeri D, Berlutti F. Analytical techniques to study microbial biofilm on abiotic surfaces: pros and cons of the main techniques currently in use. *Ann Ig.* 2013;25:31–42.
 204. Wu H, Moser C, Wang H-Z, Høiby N, Song Z-J. Strategies for combating bacterial biofilm infections. *Int J Oral Sci.* 2014;7:1–7.
 205. Kavanagh K, Reeves EP. Exploiting the potential of insects for in vivo pathogenicity testing of microbial pathogens. *FEMS Microbiol Rev.* 2004;28:101–12.
 206. Salzet M. Vertebrate innate immunity resembles a mosaic of invertebrate immune responses. *Trends Immunol.* 2001;22:285–8.
 207. Brown SE, Howard A, Kasprzak AB, Gordon KH, East PD. A peptidomics study reveals the impressive antimicrobial peptide arsenal of the wax moth *Galleria mellonella*. *Insect Biochem Mol Biol.* 2009;39:792–800.
 208. Jander G, Rahme LG, Ausubel FM. Positive Correlation between Virulence of *Pseudomonas aeruginosa* Mutants in Mice and Insects. *J Bacteriol.* 2000;182:3843–5.
 209. Li Y-H, Tian X-L. Quorum Sensing and Bacterial Social Interactions in Biofilms: Bacterial Cooperation and Competition. *Stress Environ Regul Gene Expr Adapt Bact.* Hoboken, NJ, USA: John Wiley & Sons, Inc.; 2016. page 1195–205.
 210. Rasmussen TB, Skindersoe ME, Bjarnsholt T, Phipps RK, Christensen KB, Jensen PO, et al. Identity and effects of quorum-sensing inhibitors produced by *Penicillium* species. *Microbiology.* 2005;151:1325–40.
 211. Park J, Kaufmann GF, Bowen JP, Arbiser JL, Janda KD. Solenopsin A, a venom alkaloid from the fire ant *Solenopsis invicta*, inhibits quorum-sensing signaling in *Pseudomonas aeruginosa*. *J Infect Dis.* 2008;198:1198–201.
 212. Dillard PR, Lin M-F, Khan SA. Androgen-Independent Prostate Cancer Cells Acquire the Complete Steroidogenic Potential of Synthesizing Testosterone from Cholesterol. *Mol Cell Endocrinol.* 2008;295:115–20.
 213. Bennett NC, Hooper JD, Lambie D, Lee CS, Yang T, Vesey D a, et al. Evidence for steroidogenic potential in human prostate cell lines and tissues. *Am J Pathol.* 2012;181:1078–87.
 214. Kumagai J, Hofland J, Erkens-Schulze S, Dits NFJ, Steenbergen J, Jenster G, et al. Intratumoral conversion of adrenal androgen precursors drives androgen receptor-activated cell growth in prostate cancer more potently than de novo steroidogenesis. *Prostate.* 2013;73:n/a.
 215. O'Hare MJ, Nice EC, McIlhinney RAJ, Capp M. Progesterone Synthesis, Secretion and Metabolism by Human Teratoma-Derived Cell-Lines. *Steroids.* 1981;38:719–37.

216. Horwitz KB, Pike AW, Gonzalez-Aller C, Fennessey P V. Progesterone metabolism in T47Dco human breast cancer cells—II. Intracellular metabolic path of progesterone and synthetic progestins. *J Steroid Biochem.* 1986;25:911–6.
217. Suzuki T, Murry BA, Darnel AD, Sasano H. Progesterone Metabolism in Human Leukemic Monoblast U937 Cells. *Endocr J.* 2002;49:539–46.
218. Hirano D, Okada Y, Minei S, Takimoto Y, Nemoto N. Neuroendocrine Differentiation in Hormone Refractory Prostate Cancer Following Androgen Deprivation Therapy. *Eur Urol.* 2004;45:586–92.
219. Yuan T-C, Veeramani S, Lin M-F. Neuroendocrine-Like Prostate Cancer Cells: Neuroendocrine Transdifferentiation of Prostate Adenocarcinoma cells. *Endocr Relat Cancer.* 2007;14:531–47.
220. Parimi V, Goyal R, Poropatich K, Yang XJ. Neuroendocrine Differentiation of Prostate Cancer: A Review. *Am J Clin Exp Urol.* 2014;2:273–85.
221. Beltran H, Prandi D, Mosquera JM, Benelli M, Puca L, Cyrta J, et al. Divergent Clonal Evolution of Castration-Resistant Neuroendocrine Prostate Cancer. *Nat Med.* 2016;22:298–305.
222. Zhu W, Hu Q, Hanke N, van Koppen CJ, Hartmann RW. Potent 11 β -Hydroxylase Inhibitors with Inverse Metabolic Stability in Human Plasma and Hepatic S9 Fractions To Promote Wound Healing. *J Med Chem.* 2014;57:7811–7.
223. Caldwell JD, Jirikowski GF. Sex hormone binding globulin and corticosteroid binding globulin as major effectors of steroid action. *Steroids.* 2014;81:13–6.
224. Chang KH, Li R, Kuri B, Lotan Y, Roehrborn CG, Liu J, et al. A Gain-of-Function Mutation in DHT Synthesis in Castration-Resistant Prostate Cancer. *Cell.* 2013;154:1074–84.
225. Hofland J, van Weerden WM, Dits NFJ, Steenbergen J, van Leenders GJLH, Jenster G, et al. Evidence of Limited Contributions for Intratumoral Steroidogenesis in Prostate Cancer. *Cancer Res.* 2010;70:1256–64.
226. Stanbrough M. Increased Expression of Genes Converting Adrenal Androgens to Testosterone in Androgen-Independent Prostate Cancer. *Cancer Res.* 2006;66:2815–25.
227. Wiebe JP. Progesterone Metabolites in Breast Cancer. *Endocr Relat Cancer.* 2006;13:717–38.
228. Taraborrelli S. Physiology, Production and Action of Progesterone. *Acta Obstet Gynecol Scand.* 2015;94:8–16.
229. Vares G, Sai S, Wang B, Fujimori A, Nenoï M, Nakajima T. Progesterone Generates Cancer Stem Cells through Membrane Progesterone Receptor-Triggered Signaling in Basal-Like Human Mammary Cells. *Cancer Lett.* 2015;362:167–73.
230. Koensgen D, Mustea A, Klamann I, Sun P, Zafrakas M, Lichtenegger W, et al. Expression analysis and RNA localization of PAI-RBP1 (SERBP1) in epithelial ovarian cancer: Association with tumor progression. *Gynecol Oncol.* 2007;107:266–73.
231. Li Z, Bishop AC, Alyamani M, Garcia JA, Dreicer R, Bunch D, et al. Conversion of Abiraterone to D4A Drives Anti-Tumour Activity in Prostate Cancer. *Nature.* 2015;523:347–51.
232. Maayan R, Touati-Werner D, Ram E, Galdor M, Weizman A. Is brain dehydroepiandrosterone synthesis modulated by free radicals in mice? *Neurosci Lett.* 2005;377:130–5.
233. Baulieu E-E, Robel P. Dehydroepiandrosterone (DHEA) and Dehydroepiandrosterone

REFERENCES

- Sulfate (DHEAS) as Neuroactive Neurosteroids. *Proc Natl Acad Sci.* 1998;95:4089–91.
234. Rickman DS, Beltran H, Demichelis F, Rubin MA. Biology and evolution of poorly differentiated neuroendocrine tumors. *Nat Med.* 2017;23:1–10.
235. Eberlin LS, Dill AL, Costa AB, Ifa DR, Cheng L, Masterson T, et al. Cholesterol Sulfate Imaging in Human Prostate Cancer Tissue by Desorption Electrospray Ionization Mass Spectrometry. *Anal Chem.* 2010;82:3430–4.
236. James ND, de Bono JS, Spears MR, Clarke NW, Mason MD, Dearnaley DP, et al. Abiraterone for Prostate Cancer Not Previously Treated with Hormone Therapy. *N Engl J Med.* 2017;doi: 10.1056/NEJMoa1702900.

11 APPENDIX

11.1 Supporting Information

11.1.1 Chapter 1

Supporting Information

Application of dual inhibition concept within looped autoregulatory systems towards anti-virulence agents against *Pseudomonas aeruginosa* infections

Andreas Thomann^{†,‡}, Antonio G. G. de Mello Martins^{†,‡}, Christian Brengel[†], Martin Empting^{†,‡}, Rolf W. Hartmann^{†,§,*}

† Helmholtz Institute for Pharmaceutical Research Saarland (HIPS), Department for Drug Design and Optimization, Campus E 8.1, 66123 Saarbrücken, Germany;

§ Department of Pharmacy, Pharmaceutical and Medicinal Chemistry, Saarland University, Campus C 2.3, 66123 Saarbrücken, Germany;

‡ These authors contributed equally to this work.

E-mail: rolf.hartmann@helmholtz-hzi.de and martin.empting@helmholtz-hzi.de

Content

I. General experimental information - Chemistry

- a. Chemical synthesis of compounds 3–6
- b. Crystallization of **6a** and X-ray crystallography
- c. ¹³C-NMR and HSQC spectra of compounds 3–6
- d. LC purity of compounds 3–6

II. General experimental information - Biology

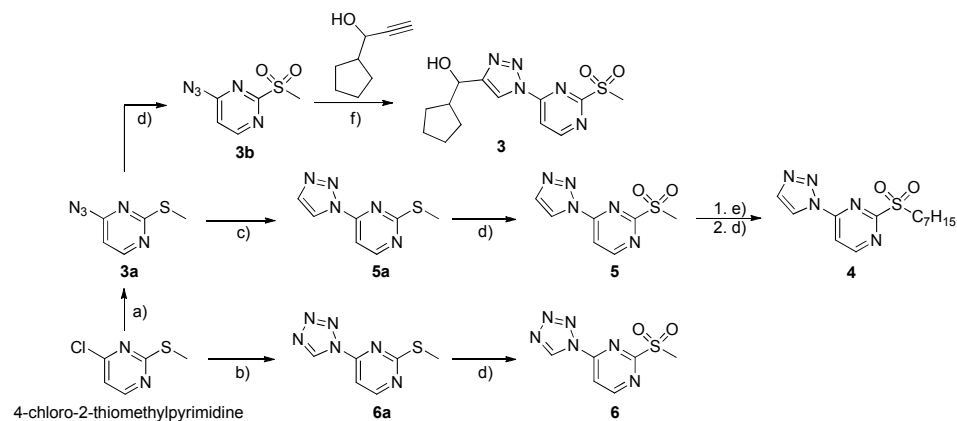
- a. Chemicals, bacterial strains, and media
- b. Pyocyanin assay
- c. Prolonged pyocyanin assay
- d. Growth curves of *P. aeruginosa* PA14
- e. Biofilm inhibition by compound 2
- f. PqsD *in vitro* assay
- g. PqsR *in vitro* assay

III. References

I. General experimental information - Chemistry

I. General experimental information - Chemistry

a. Chemical Synthesis of compounds 3–6



Scheme S1. a) see reference 1b; b) See reference 1a; c) TMS-Acetylene, CuSO₄, sodium ascorbate, *tert*BuOH:H₂O, r.t.; d) Oxone, EtOAc:H₂O, r.t.; e) heptane-1-thiol, DMF, K₂CO₃, 0°C; f) 1-cyclopentylprop-2-yn-1-ol, CuSO₄, sodium ascorbate, *tert*BuOH:H₂O, r.t.

Compounds **3a**, **3b** and **6a** were synthesized as reported before.^{1,2}

2-(methylthio)-4-(1H-1,2,3-triazol-1-yl)pyrimidine (5a): To a solution of **3a** (1.0 eq) and TMS-acetylene (2.0 eq) in *tert*BuOH:water (1:1) was added CuSO₄·5H₂O (0.02 eq) and sodium ascorbate (0.1 eq). The mixture was stirred at room temperature for 16 h. Brine was added and the aqueous layer was extracted three times with ethyl acetate. The combined organic layers were concentrated in vacuum and purified by flash chromatography (petroleum ether/ethyl acetate 8:2) to yield **5a** as a white solid (58% yield). ¹H NMR (300 MHz, CDCl₃) δ 2.64 (s, 3H), 7.84 (d, J = 5.5, 1H), 7.87 (s, 1H), 8.62 (s, 1H), 8.71 (d, J = 5.4 Hz, 1H). ¹³C NMR (75 MHz, CDCl₃) δ 14.3, 104.9, 121.1, 134.6, 154.9, 159.8, 173.7. MS (ESI) m/z: 194.1 [M+H]⁺.

cyclopentyl(1-(2-(methylsulfonyl)pyrimidin-4-yl)-1H-1,2,3-triazol-4-yl)methanol (3): To a solution of **3b** (1.0 eq) and 1-cyclopentylprop-2-yn-1-ol (1.0 eq) in *tert*BuOH:water (1:1) was added CuSO₄·5H₂O (0.02 eq) and sodium ascorbate (0.1 eq). The mixture was stirred at room temperature for 16 h. Brine was added and the aqueous layer was extracted three times with ethyl acetate. The combined organic layers were concentrated in vacuum and purified by flash chromatography (hexane/ethyl acetate 7:3) to yield **3** as a white solid (49% yield). ¹H NMR (300 MHz, DMSO-d₆) δ 1.63 - 2.19 (m, 9 H), 3.51 (s, 3H), 5.29 (s, 1H), 8.42 (d, J = 5.6 Hz, 1H), 8.80 (s, 1H), 9.26 (d, J = 5.6 Hz, 1H). ¹³C NMR (75 MHz, DMSO-d₆) δ

I. General experimental information - Chemistry

23.9 (2C), 24.1, 39.7, 41.1, 41.4, 77.2, 112.7, 118.8, 155.4, 156.5, 162.0, 165.4. MS (ESI) m/z: not found [M+H]⁺. Purity 96%.

2-(heptylsulfonyl)-4-(1H-1,2,3-triazol-1-yl)pyrimidine (4): To a solution of **5** (1.0 eq) in anhydrous DMF was added K₂CO₃ (3.0 eq) at 0°C. To the vigorously stirred suspension was added heptane-1-thiol (0.9 eq). The reaction was allowed to proceed for 20 min at 0°C and then quenched with an excess of water. Brine was added and the mixture was extracted three times with ethyl acetate. The combined organic layers were concentrated in vacuum and residual DMF was removed by azeotropic distillation using heptane. The crude product was purified by flash chromatography (petroleum ether/ethyl acetate 9:1) to yield 2-(heptylthio)-4-(1H-1,2,3-triazol-1-yl)pyrimidine as white solid (45% yield). ¹H NMR (300 MHz, CDCl₃) δ 0.89 (t, J = 6.5 Hz, 3H), 1.19 - 1.41 (m, 6H), 1.41 - 1.58 (m, 2H), 1.78 (quin, J = 7.4 Hz, 2H), 3.20 (t, J = 7.4 Hz, 2H), 7.80 (d, J = 5.4 Hz, 1H), 7.85 (d, J = 1.1 Hz, 1H), 8.57 (d, J = 1.0 Hz, 1H), 8.68 (d, J = 5.4 Hz, 1H). ¹³C NMR (75 MHz, CDCl₃) δ 14.0, 22.5, 28.8, 28.9, 29.0, 31.2, 31.7, 104.8, 121.0, 134.5, 154.9, 159.8, 173.5. MS (ESI) m/z: 278.1 [M+H]⁺. 2-(heptylthio)-4-(1H-1,2,3-triazol-1-yl)pyrimidine (1.0 eq) was dissolved in ethyl acetate and Oxone^R (3.0 eq) dissolved in water was added. The biphasic system was vigorously stirred until TLC showed full conversion. Water was added and the aqueous layer was extracted three times with ethyl acetate. The combined organic layers were concentrated and the crude material was purified by flash chromatography (hexane/ethyl acetate 1:1) to yield **4** as a white solid (72% yield). ¹H NMR (300 MHz, CDCl₃) δ 0.88 (t, J = 6.9 Hz, 3H), 1.21 - 1.40 (m, 6H), 1.41 - 1.56 (m, 2H), 1.91 (quin, J = 7.8 Hz, 2H), 3.58 (t, J = 7.7 Hz, 2H), 7.92 (d, J = 1.3 Hz, 1H), 8.41 (d, J = 5.5 Hz, 1H), 8.75 (d, J = 1.4 Hz, 1H), 9.09 (d, J = 5.5 Hz, 1H). ¹³C NMR (75 MHz, CDCl₃) δ 14.0, 22.0, 22.5, 28.4, 28.6, 31.4, 51.3, 112.6, 121.9, 135.2, 156.4, 160.9, 166.0. MS (ESI) m/z: 351.1 [M+ACN+H]⁺. Purity 97%.

2-(methylsulfonyl)-4-(1H-1,2,3-triazol-1-yl)pyrimidine (5): **5a** (1.0 eq) was dissolved in ethyl acetate and Oxone^R (3.0 eq) dissolved in water was added. The biphasic system was vigorously stirred for 1 h. Water was added and the aqueous layer was extracted three times with ethyl acetate. The combined organic layers were concentrated and the crude material was purified by flash chromatography (hexane/ethyl acetate 8:2) to yield **5** as a white solid (19% yield). ¹H NMR (300 MHz, CDCl₃) δ 3.43 (d, J = 0.9 Hz, 3H), 7.92 (s, 1H), 8.42 (dd, J = 5.5, 0.9 Hz, 1H), 8.74 (s, 1H), 9.08 (dd, J = 5.5, 0.9 Hz, 1H). ¹³C NMR (75 MHz, CDCl₃) δ 39.2, 112.7, 121.9, 135.2, 156.4, 160.8, 166.2. MS (ESI) m/z: 226.1 [M+H]⁺. Purity >99%.

2-(methylsulfonyl)-4-(1H-tetrazol-1-yl)pyrimidine (6): **6a** (1.0 eq) was dissolved in ethyl acetate and Oxone^R (3.0 eq) dissolved in water was added. The biphasic system was vigorously stirred until TLC showed full conversion. Water was added and the aqueous layer was extracted three times with ethyl acetate. The combined organic layers were concentrated and filtered over a pad of silica to yield **6** as a white solid (99% yield). ¹H NMR (300 MHz, CDCl₃) δ 3.46 (s, 3H), 8.33 (d, J=5.4 Hz, 1H), 9.20 (d, J=5.4 Hz, 1H), 9.74 (s, 1H). ¹³C NMR (126 MHz, CDCl₃) δ 39.2, 113.3, 140.6, 154.4, 161.9, 166.5. MS (ESI) m/z: 227.0 [M+H]⁺, 199.1 [M-N₂+H]⁺. Purity 98%.

I. General experimental information - Chemistry

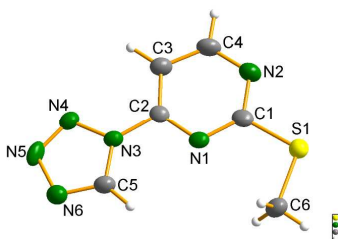
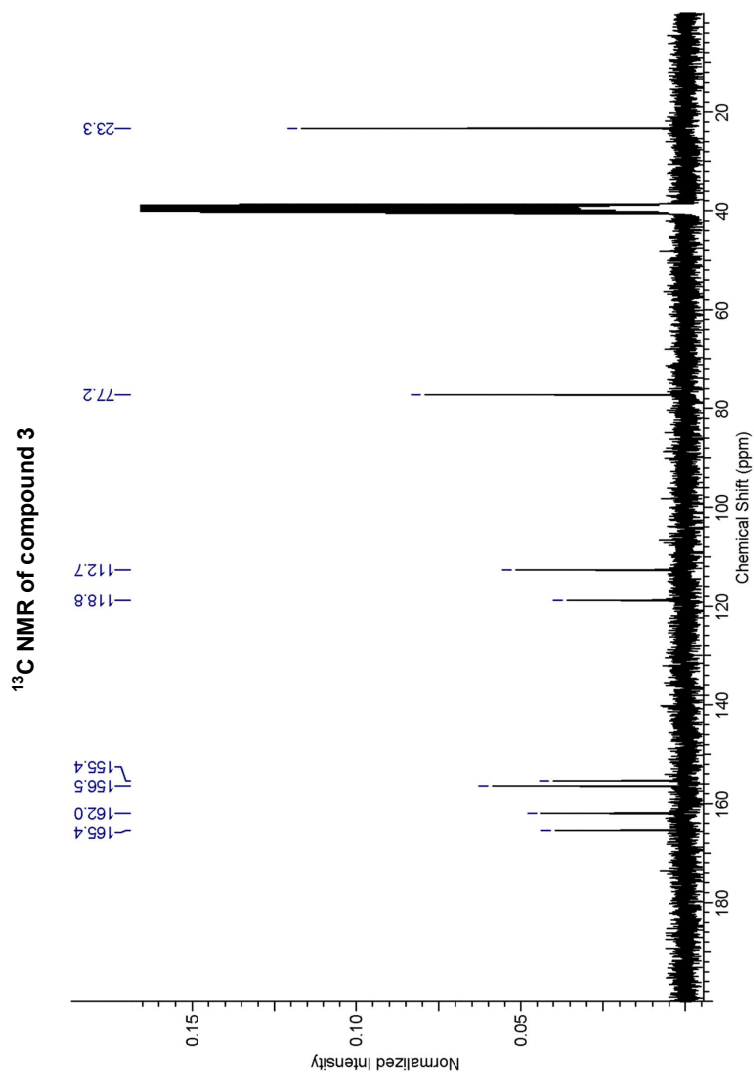
b. Crystallization of **6a** for X-ray crystallography

Figure S1. X-ray crystal structure of compound **6a** (green = nitrogen, grey = carbon, yellow = sulfur, white = hydrogen).

6a was dissolved in hot chloroform and left standing open to atmosphere to allow evaporation. Colorless needles formed after 3 weeks. CCDC 1432241 contains the supplementary crystallographic data for this paper. These data can be obtained free of charge from The Cambridge Crystallographic Data Centre via www.ccdc.cam.ac.uk/getstructures.

I. General experimental information - Chemistry

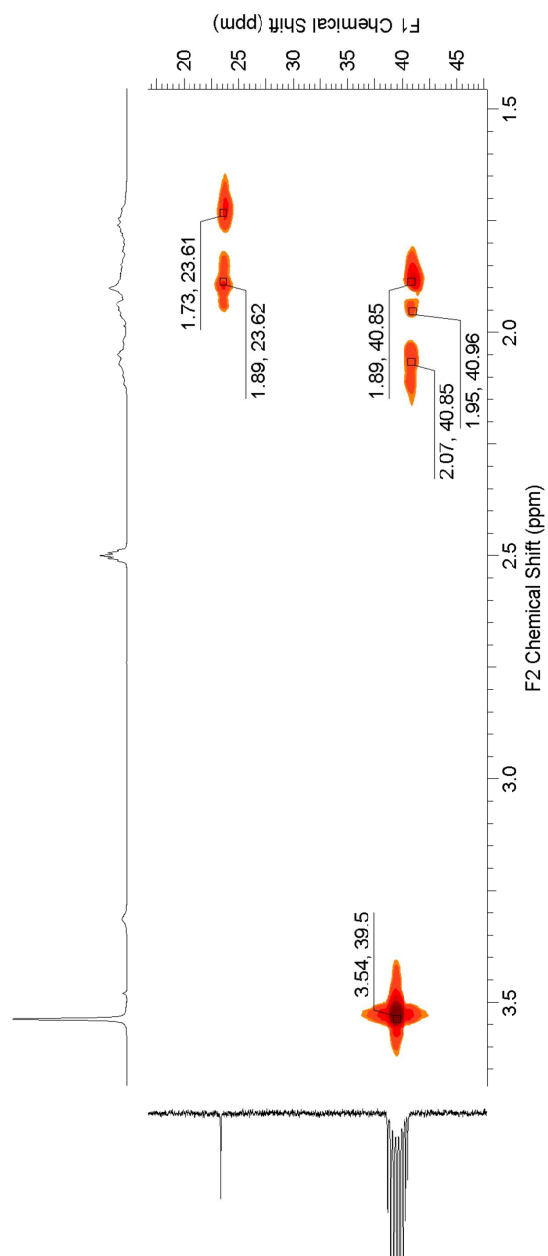
c. ^{13}C -NMR spectra



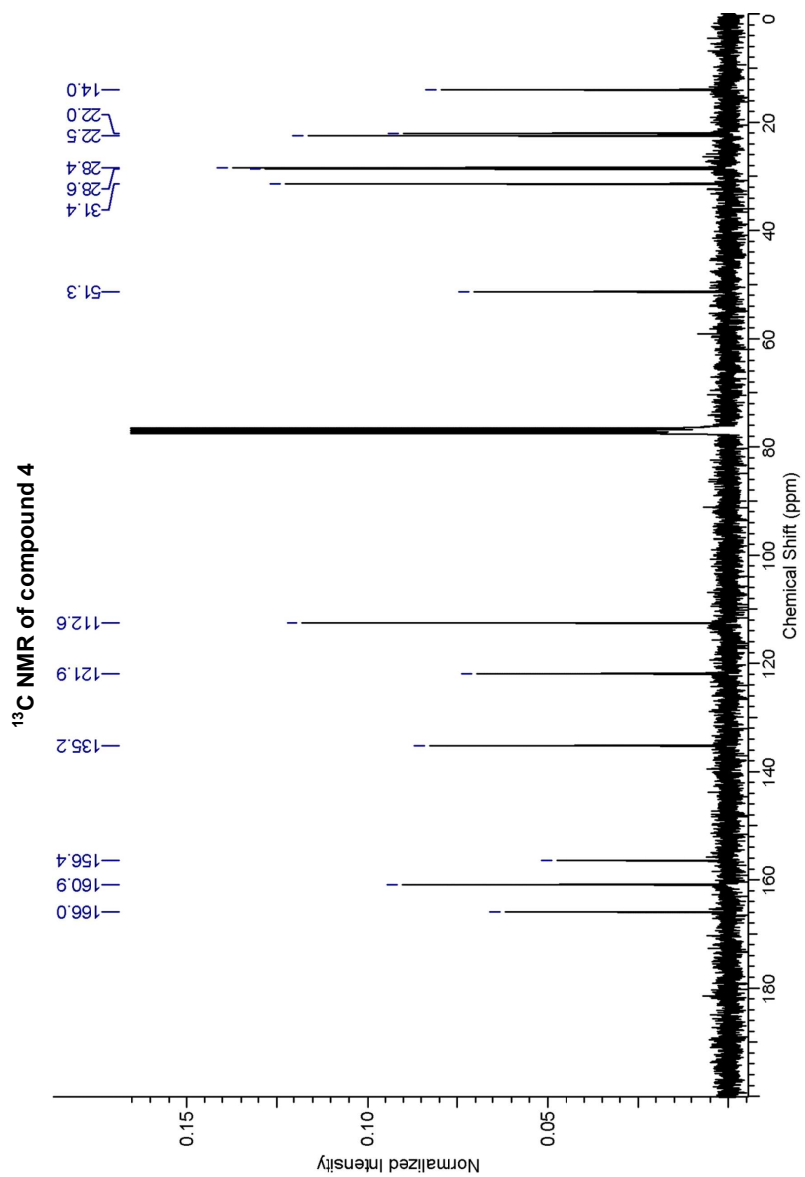
S6

I. General experimental information - Chemistry

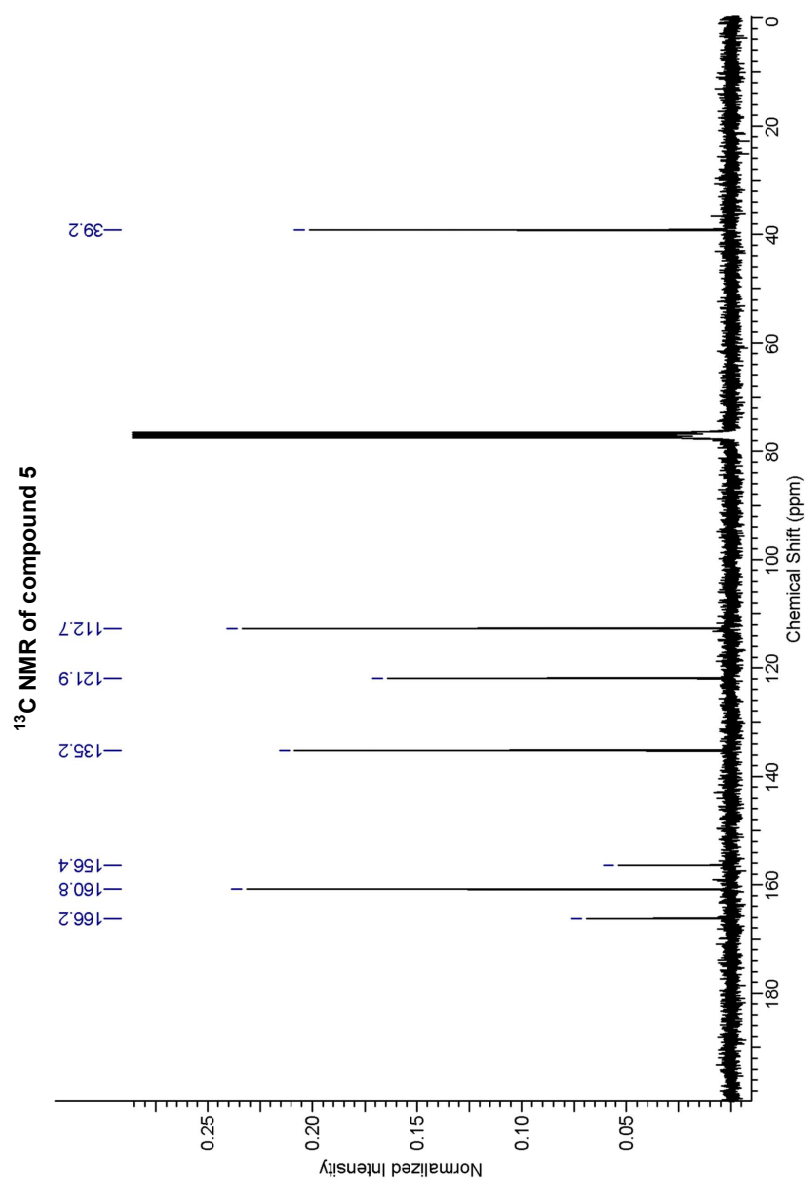
HSQC NMR of compound 3



I. General experimental information - Chemistry

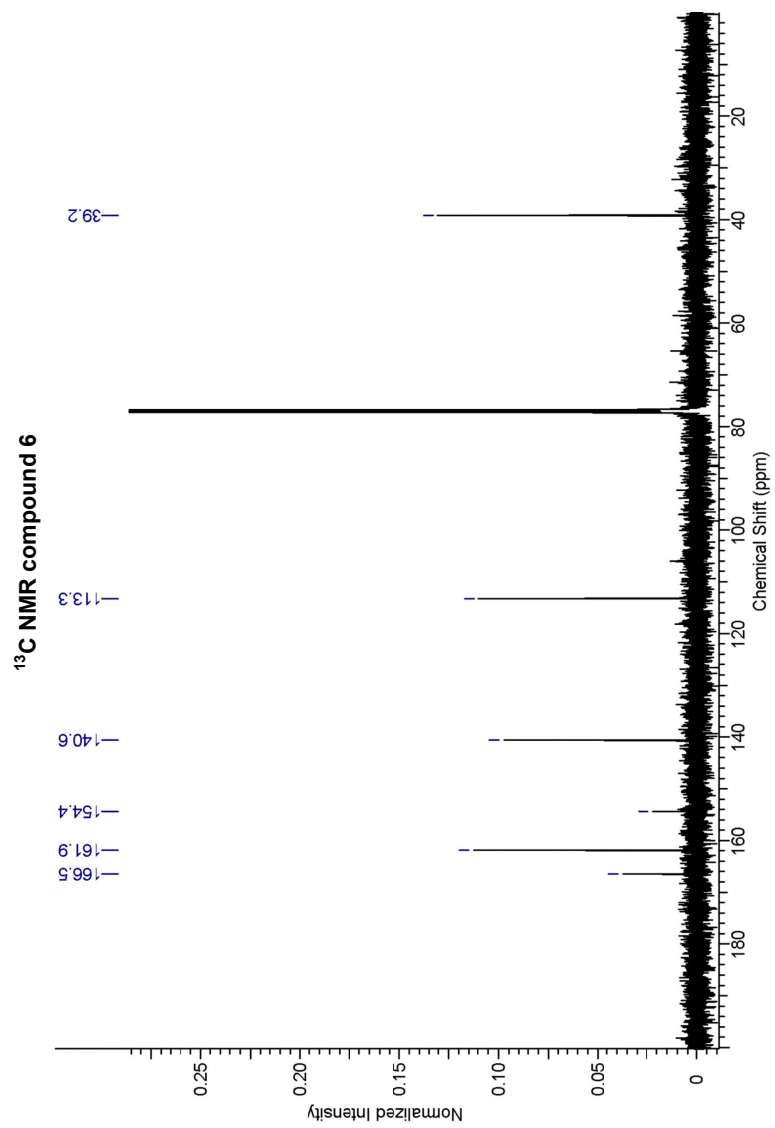


I. General experimental information - Chemistry



S9

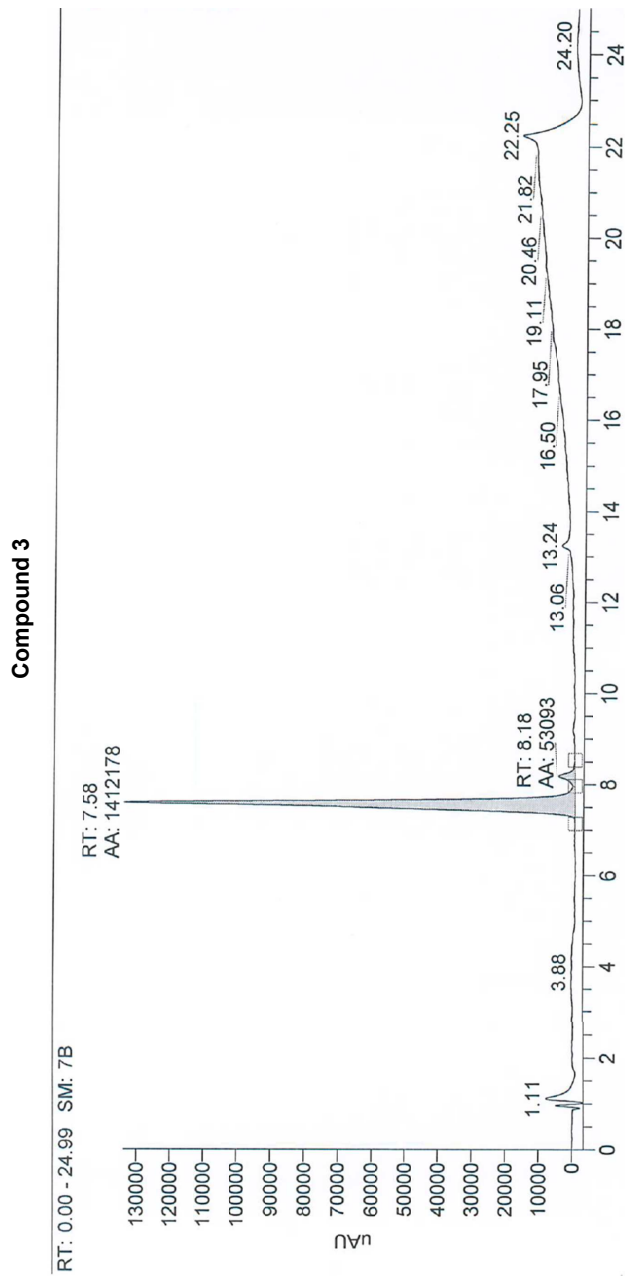
I. General experimental information - Chemistry



S10

I. General experimental information - Chemistry

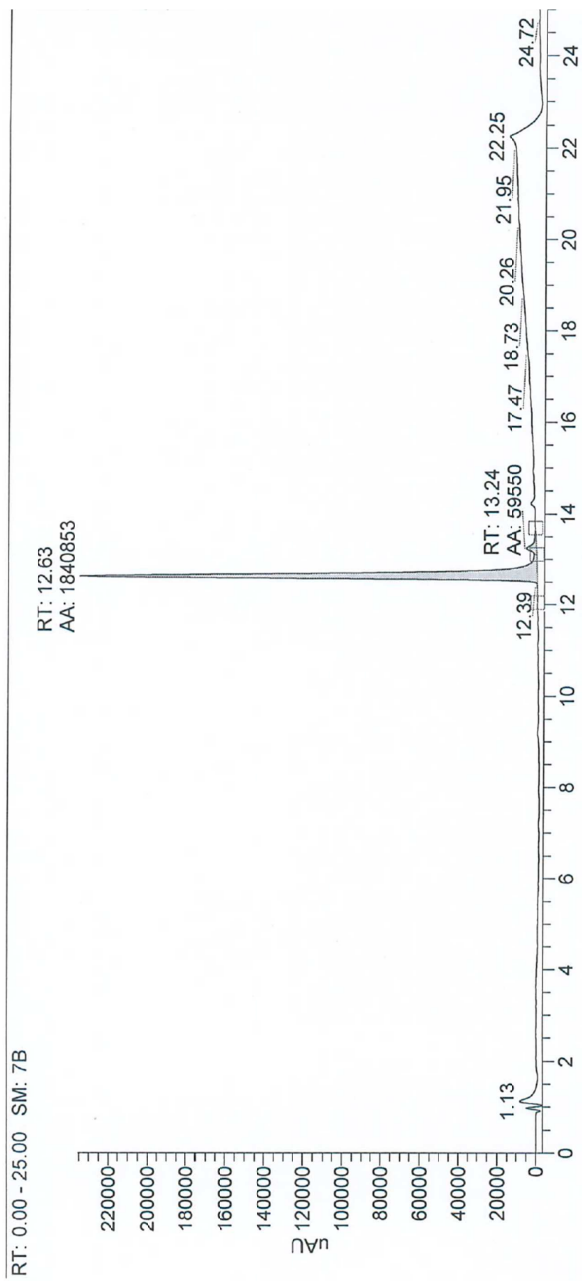
d. LC purity of compounds 3–6



S11

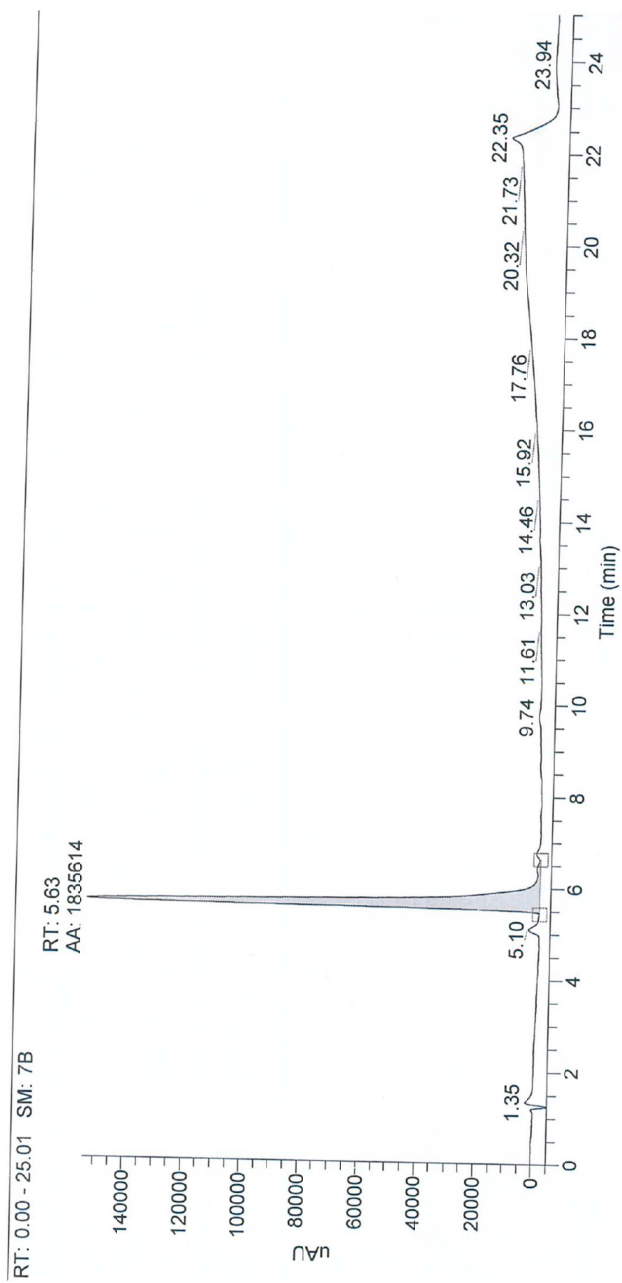
I. General experimental information - Chemistry

Compound 4



S12

I. General experimental information - Chemistry

Compound 5

S13

I. General experimental information - Chemistry

Compound 6



III. References

II. General experimental information – Biology

a. Chemicals, bacterial strains, and media

Yeast extract was obtained from Fluka, peptone and casein from Merck, Bacto™ Tryptone from BD Biosciences, and Gibco® PBS from Life Technologies. Salts and organic solvents of analytical grade were obtained from VWR.

P. aeruginosa PA14 strain, and isogenic *pqsR* knockout mutant were stored in glycerol stocks at $-80\text{ }^{\circ}\text{C}$.

Minimal medium PPGAS³ and Luria Bertani (LB) were used.

b. Pyocyanin assay

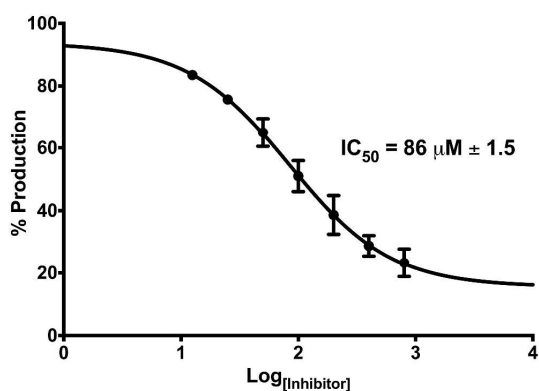


Figure S2. IC₅₀ curve of the improved inhibitory effect of **6** on pyocyanin production, an indicative of PqsR antagonism. Error bars represent standard error of three independent experiments ($n = 3$).

II. General experimental information - Biology

c. Prolonged Pyocyanin Assay.

Effect of long-term PqsD inhibition on pyocyanin formation was assessed as previously described (pyocyanin assay) with slight modifications. Initially, treated (compound **1**) and untreated cultures were incubated for 24 h under aerobic conditions. pyocyanin levels and bacterial density were determined from extracted culture aliquots. Obtained OD₆₀₀ values were used to re-calculate the necessary dilution factors of each replicate for a final density of 0.02, transferred into a new plate with fresh PPGAS medium and dimethyl sulfoxide (DMSO) or compound **1** for additional 24 h, accordingly. Pyocyanin formation and cell growth were again assessed as previously described, making up for a total of 48 h of incubation with treated samples under constant, long-term PqsD inhibition.

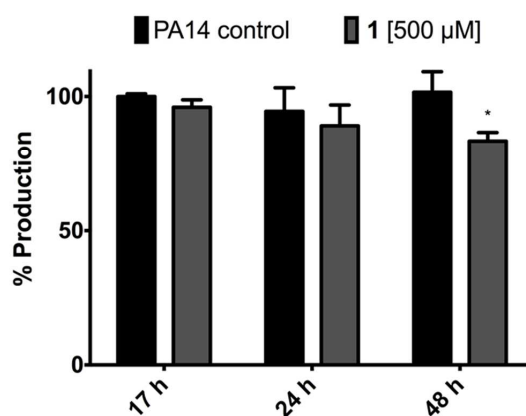


Figure S3. Long-term effect of PqsD inhibitor **1** on pyocyanin production in PA14 wild type. Treatment with 500 μM of **1** led to a reduction of pyocyanin levels to 83.5% ± 3.2 after 48 h of incubation. The differences in values (compared to control) determined for 17 h and 24 h were not significant. All values are relative to a DMSO control without addition of inhibitors. Error bars represent the standard deviation of three independent experiments (n = 3). * = p < 0.05.

II. General experimental information - Biology

d. Growth curves of *P. aeruginosa* PA14

Cultures of PA14 were diluted in PPGAS medium, adjusted to an initial OD₆₀₀ of 0.02, and 1.5 mL added in triplicates into 24-well plates (Greiner Bio-One). Cultivation conditions as described above (SI, section IIa). Stock solutions of compound **6** in DMSO were diluted 1:100 to a final DMSO concentration of 1% (v/v), DMSO alone was used as control. Bacterial growth was measured over 48 h as a function of OD₆₀₀ using FLUOstar Omega (BMG LabTech).

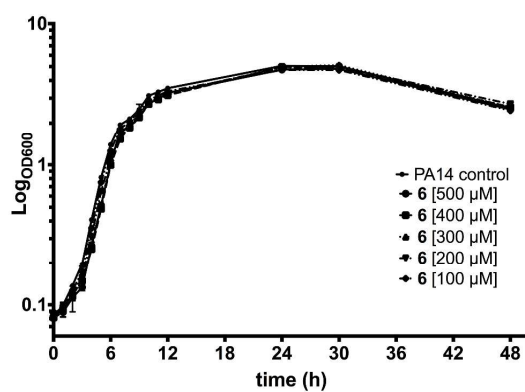


Figure S4. Growth curves of PA14 in PPGAS minimal medium in the absence (control) and presence of varying concentrations (100 μM to 500 μM) of compound **6**.

II. General experimental information - Biology

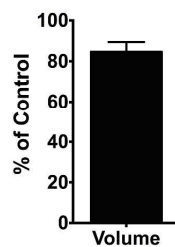
e. Antibiofilm effects of compound **2**Effects of compound **2** on Biofilm

Figure S5. Effects of compound **2** (15 μ M; solubility maximum) on volume of *P. aeruginosa* strain PA14 biofilm. Experiment was performed as described in the experimental section of the main text. Error bars represent standard error of at least two independent experiments.

f. PqsD *in vitro* assay

The assay was performed as reported before.⁴

g. PqsR *in vitro* assay

The assay was performed in *E. coli* DH5 α as reported before.⁵

II. General experimental information - Biology

III. References

- (1) Thomann, A., Börger, C., Empting, M., and Hartmann, R. (2014) Microwave-Assisted Synthesis of 4-Substituted 2-Methylthiopyrimidines. *Synlett* 25, 935–938.
- (2) Thomann, A., Zapp, J., Hutter, M., Empting, M., and Hartmann, R. W. (2015) Steering the azido-tetrazole equilibrium of 4-azidopyrimidines via substituent variation - implications for drug design and azide-alkyne cycloadditions. *Org. Biomol. Chem.* 13, 10620–10630.
- (3) Zhang, Y., and Miller, R. M. (1992) Enhanced octadecane dispersion and biodegradation by a *Pseudomonas rhamnolipid* surfactant (biosurfactant). *Appl. Environ. Microbiol.* 58, 3276–3282.
- (4) Storz, M. P., Maurer, C. K., Zimmer, C., Wagner, N., Brengel, C., de Jong, Johannes C, Lucas, S., Müsken, M., Häussler, S., Steinbach, A., and Hartmann, R. W. (2012) Validation of PqsD as an anti-biofilm target in *Pseudomonas aeruginosa* by development of small-molecule inhibitors. *J. Am. Chem. Soc.* 134, 16143–16146.
- (5) Lu, C., Maurer, C. K., Kirsch, B., Steinbach, A., and Hartmann, R. W. (2014) Overcoming the unexpected functional inversion of a PqsR antagonist in *Pseudomonas aeruginosa*: an in vivo potent antivirulence agent targeting pqs quorum sensing: An In Vivo Potent Antivirulence Agent Targeting pqs Quorum Sensing. *Angew. Chem. Int. Ed. Engl.* 53, 1109–1112.

11.1.2 Chapter 2

Content

- I. General experimental information – Biology**
 - a. *E. coli* reporter-gene assay: dose-response curves
 - b. Effects on pyocyanin in *P. aeruginosa*
 - c. UPLC-MS/MS quantification of extracellular 2-AA
 - d. Cytotoxicity assay
 - e. Lectin B expression in *P. aeruginosa*
 - f. Ligand Lipophilicity Efficiency (LLE) calculation

- II. General experimental information – Chemistry**
 - a. Synthesis of intermediates
 - b. Purity of final compounds (LC/MS determination)
 - c. UV traces HPLC
 - d. ¹H-NMR spectra

- III. Supplementary References**

I. GENERAL EXPERIMENTAL INFORMATION – BIOLOGY

a. *E. coli* reporter-gene assay: dose-response curves

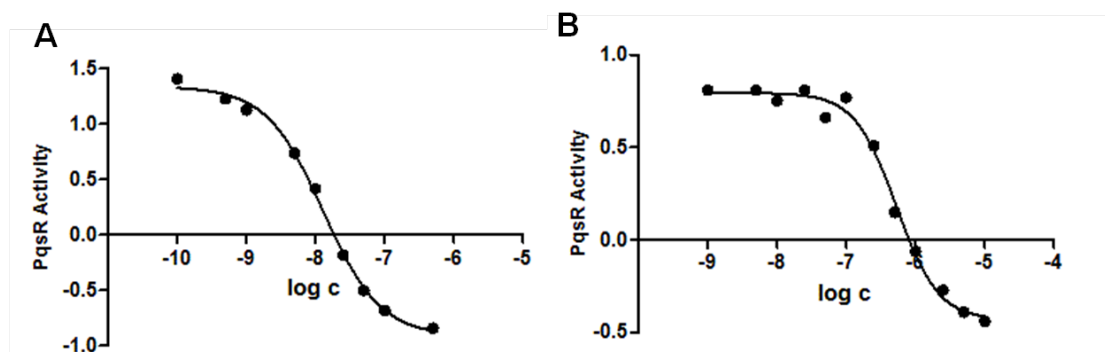


Figure S1. Antagonistic activity of different compounds measured in the *E. coli* reporter gene assay. Representative dose-response curves of **a)** compound **7** **b)** compound **12**. PqsR activity refers to the stimulation of PqsR induced by 50 nM PQS (= 1). Black dots (•) represent the PqsR activity measured in the presence of a single compound concentration. The continuous black line is the non-linear regression analysis to determine IC_{50} values using a log (inhibitor) vs. response model (Graph Pad Prism 5.04).

b. Effects on pyocyanin in *P. aeruginosa*

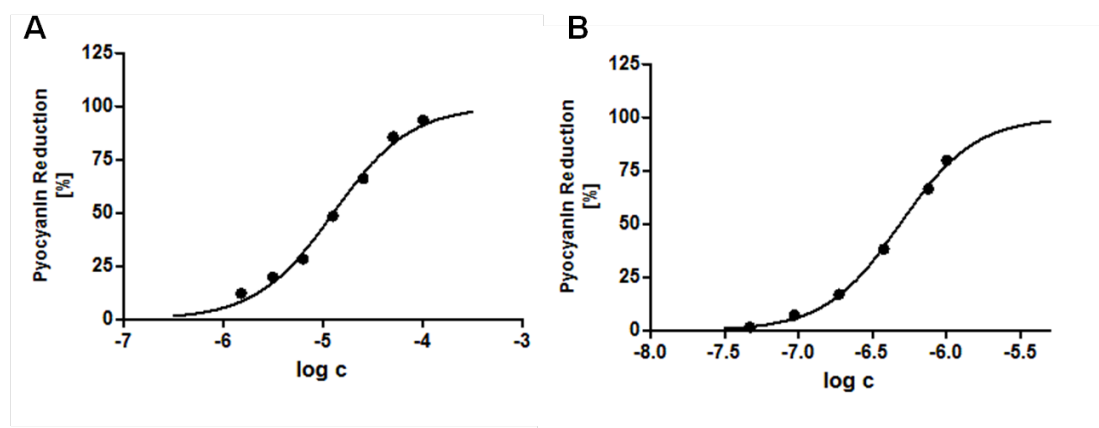


Figure S2. Inhibition of virulence factor pyocyanin was evaluated in the clinical isolate PA14. Representative dose-response curves **a)** compound **7** **b)** compound **12**. Black dots (•) represent the reduction of pyocyanin in presents of a given compound concentration relative to DMSO control (= 0 %). The continuous black line is the non-linear regression analysis to determine IC_{50} values using a log (inhibitor) vs. response model with constrains (bottom = 0; top =100) (Graph Pad Prism 5.04). UPLC-MS/MS quantification of extracellular 2-AA.

APPENDIX

c. UPLC-MS/MS quantification of extracellular 2-AA

The quantification of 2-AA was performed following a modified protocol of Kesarwani *et. al.*¹ The analysis was performed on an Accela-HPLC system (Thermo Scientific) coupled with a triple quadrupole mass spectrometer TQS Quantum Access Max (Thermo Scientific) using 5,6,7,8-tetradeutero-2-heptyl-4(1*H*)-quinolone (*d*₄-HHQ) as internal standard. An NUCLEODUR C₁₈ Pyramid column (2x125 mm, 3 μm; Macherey-Nagel) was used as stationary phase along with a mobile phase consisting of water + 0.1% formic acid (A) and methanol + 0.1% formic acid (B) at a flow rate of 0.7 ml/min. The following chromatographic conditions were applied: 0.0-0.5 isocratic 10% B, 0.5-2.0 linear gradient up to 100 % B, 2.0-3.0 isocratic 100% B, ending 3.0-4.5 initial conditions. The compounds were ionized using electrospray ionization in positive ion mode with the following parameters: spray voltage: 3500 V; vaporizer temperature: 370 °C; sheath gas pressure (nitrogen): 35 units; auxiliary gas pressure (nitrogen): 30 units; skimmer offset voltage: 0 V; capillary temperature: 270 °C. Selected reaction monitoring was used for detecting 2-AA (136.016→91.048 [quantitative], collision energy: 24 V, tube lens: 68 V; 136.016→117,998 [qualitative], collision energy: 13 V, tube lens: 68 V) and *d*₄-HHQ (248.081→162.965 [quantitative], collision energy: 32 V, tube lens: 100 V; 248.081→175.982 [qualitative], collision energy: 34 V, tube lens: 100 V) employing: scan width: 0.002 m/z; scan time: 0.100 s; peak width: 0.70.

d. Cytotoxicity assay

HEK 293 cells (2x10⁵ cells per well) were seeded in 24-well, flat-bottomed plates. Culturing of cells, incubations and OD measurements were performed as described previously with small modifications.² 24 h after seeding the cells the incubation was started by the addition of compounds in a final DMSO concentration of 1 % (v/v). The living cell mass was determined after 24, 48 and 72 h followed by the calculation of LD50 values.

Table S1. Cytotoxicity of selected compounds^a

Number	Cytotoxicity HEK293 ^a LD ₅₀ [μM]
7	30
8	>50 ^b
10	> 25 ^b
12	> 50 ^b

^aviability of HEK293 cells was quantified in the presence of test compound after 72h using MTT. ^bno effect on cell viability at solubility maximum.

e. Lectin B expression in *P. aeruginosa*

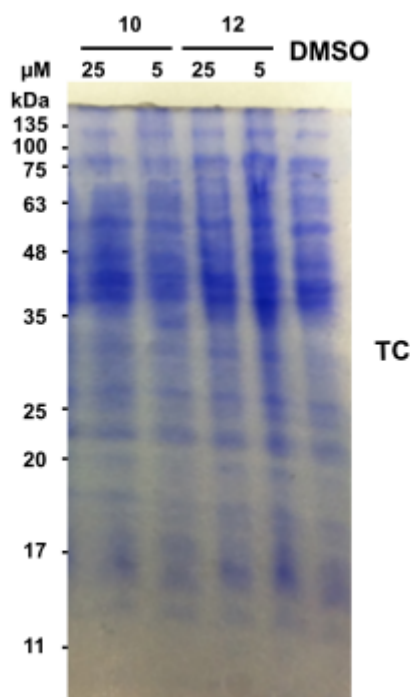


Figure S3. Expression of LecB in *P. aeruginosa* PAO1. Coomassie-stained 15% SDS-PAGE of total cell (TC) fractions of *P. aeruginosa* cultures grown for 24 h in absence or presence of compound **10** or **12** (5 μM or 25 μM).

APPENDIX

f. Ligand Lipophilicity Efficiency (LLE) calculation

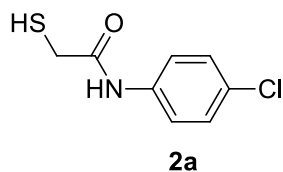
The ligand lipophilicity efficiency was calculated according to equation 1³

$$LLE = 0.11 + 1.4 * \frac{pIC_{50} - clogD}{NHA} \quad (1)$$

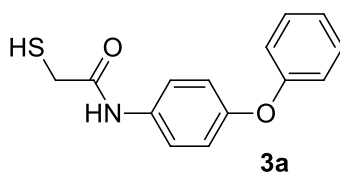
with pIC₅₀ antagonistic activity measured in *E.coli*, calculated logD (ACD/Percepta 2015) and NHA (number of heavy atoms). This equation based on the ones suggested by Mortenson and Murray⁴ and Shultz⁵.

II. GENERAL EXPERIMENTAL INFORMATION – CHEMISTRY

a. Synthesis of intermediates



N-(4-chlorophenyl)-2-mercaptoacetamide (2a) was synthesized according to general procedure A⁶ from 4-chloroaniline (2.77 g, 21.71 mmol) and 2-mercaptoacetic acid (2.00 g, 21.7 mmol) and afford the expected product as pale yellow solid (2.99 g, 14.8 mmol, 68 % yield). ¹H NMR (300 MHz, CHLOROFORM-*d*) δ ppm 2.04 (t, $J=9.2$ Hz, 1 H), 3.41 (d, $J=9.3$ Hz, 2 H), 7.28 - 7.37 (m, 2 H), 7.40 - 7.60 (m, 2 H), 8.53 (br. s., 1 H); MS (ESI+) m/z 202 (M+H)⁺.



2-mercapto-N-(4-phenoxyphenyl)acetamide (3a) was synthesized from 4-phenoxyaniline (1.00 g, 5.40 mmol) and 2-mercaptoacetic acid (0.547 g, 5.94 mmol) to give the expected product as grey solid (1.1 g, 4.24 mmol, 79 % yield). ¹H NMR (300 MHz, CHLOROFORM-*d*) δ ppm 1.96 - 2.13 (m, 1 H), 3.42 (d, $J=9.1$ Hz, 2 H), 6.97 - 7.05 (m, 4 H), 7.06 - 7.15 (m, 1 H), 7.29 - 7.40 (m, 2 H), 7.44 - 7.59 (m, 2 H), 8.51 (br. s., 1 H); MS (ESI+) m/z 260 (M+H)⁺, 282 (M+Na)⁺.

APPENDIX

b. Purity of final compounds (LC/MS determination)

Purity control was carried out on two different systems:

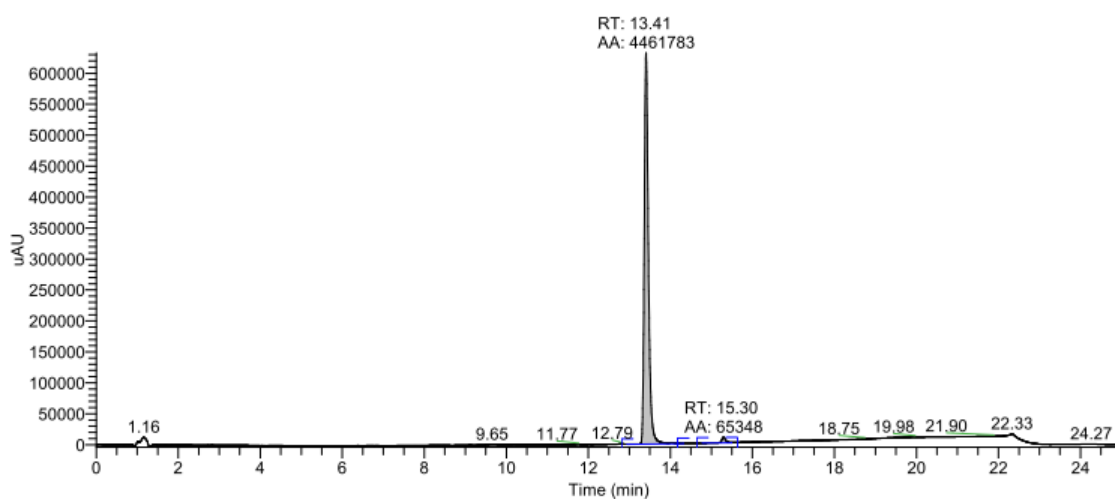
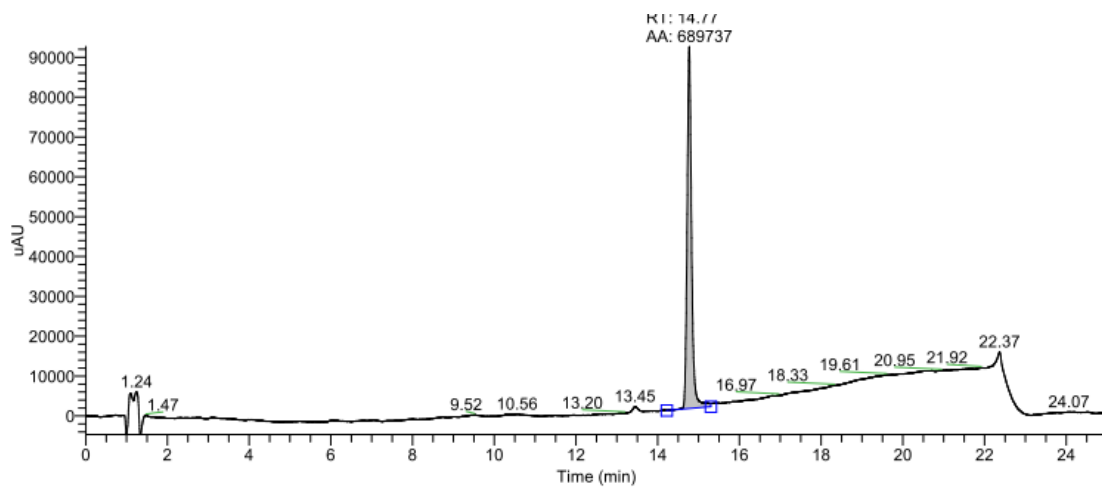
SpectraSystems LC system (Thermo Fisher Scientific) consisting of a pump, an autosampler, and a VWD detector. Mass spectrometry was performed on an MSQ electro spray mass spectrometer (Thermo Fisher Scientific). The system was operated by the standard software Xcalibur. An RP-C18 NUCLEODUR 100-5 (125x3 mm) column (Macherey-Nagel GmbH) was used as stationary phase. All solvents were HPLC grade. For purity determination, the following methods was used:

Mobil phase, A = water + 0.1% trifluoroacetic acid, B = acetonitrile + 0.1% trifluoroacetic acid; gradient, 0.0-15.0 min, 0-100% B, 15.0-20.0 min, 100% B; flow rate 0.8 mL/min.

LCMS-System (Waters) consisting of a 767 sample Manager, a 2545 binary gradient pump, a 2998 PDA detector and a 3100 electron spray mass spectrometer equipped with a C-18 column (Nucleodur 100-5 C18 ec 150 x 4.6 mm). For purity determination, the following methods was used:

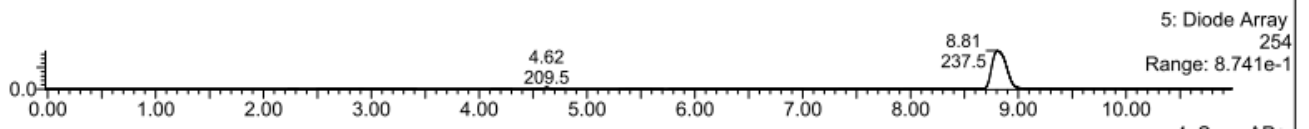
Mobil phase, A = water + 0.1% formic acid, B = acetonitrile + 0.1% formic acid; gradient, 0.0-13.0 min, 0-100% B; flow rate 1 mL/min

c. UV traces HPLC

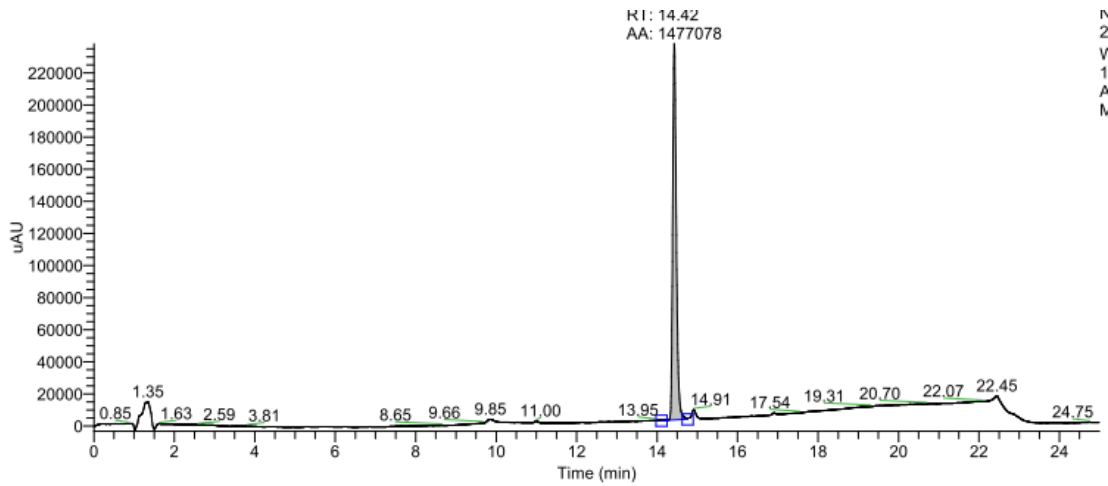
Compound 7**Compound 8**

APPENDIX

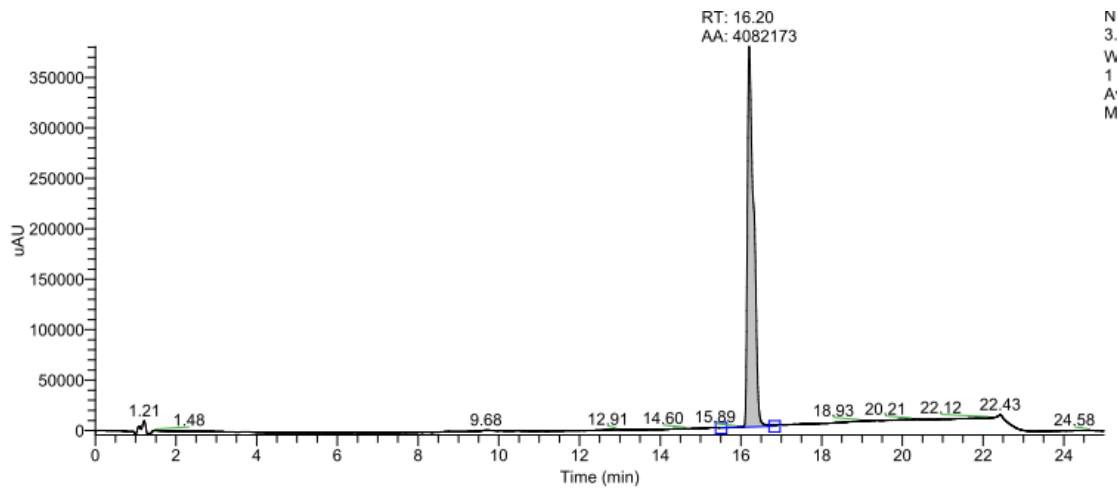
Compound 9



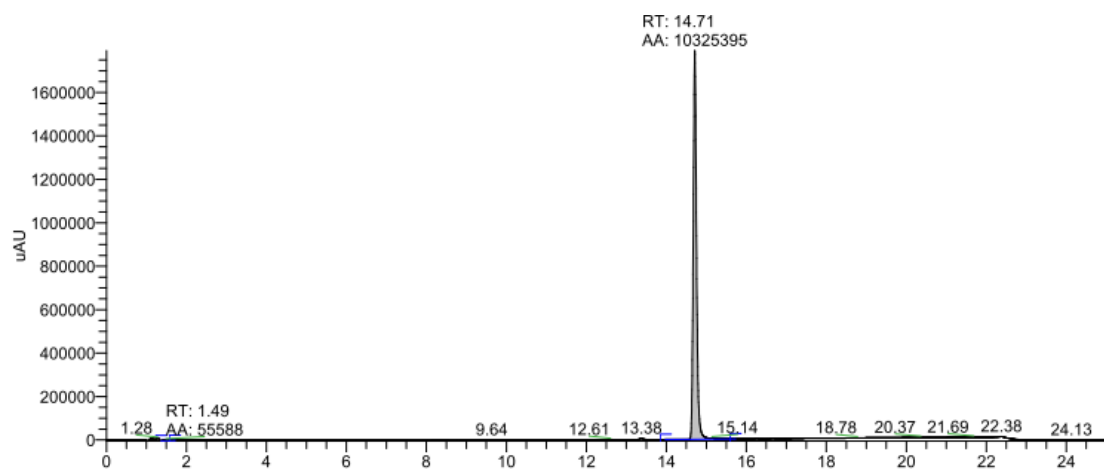
Compound 10



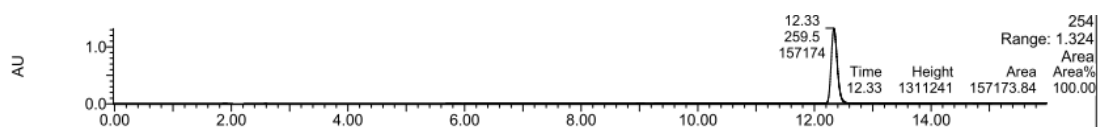
Compound 11



Compound 12



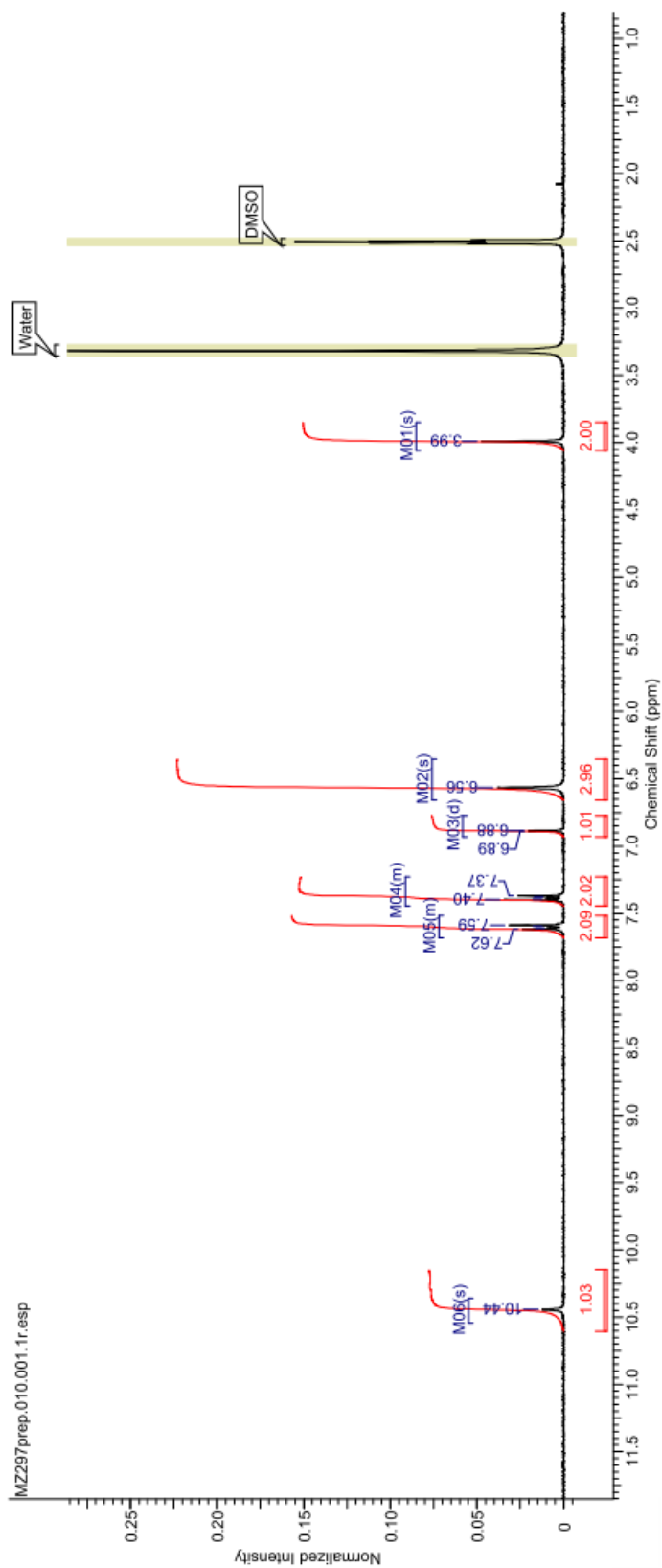
Compound 13



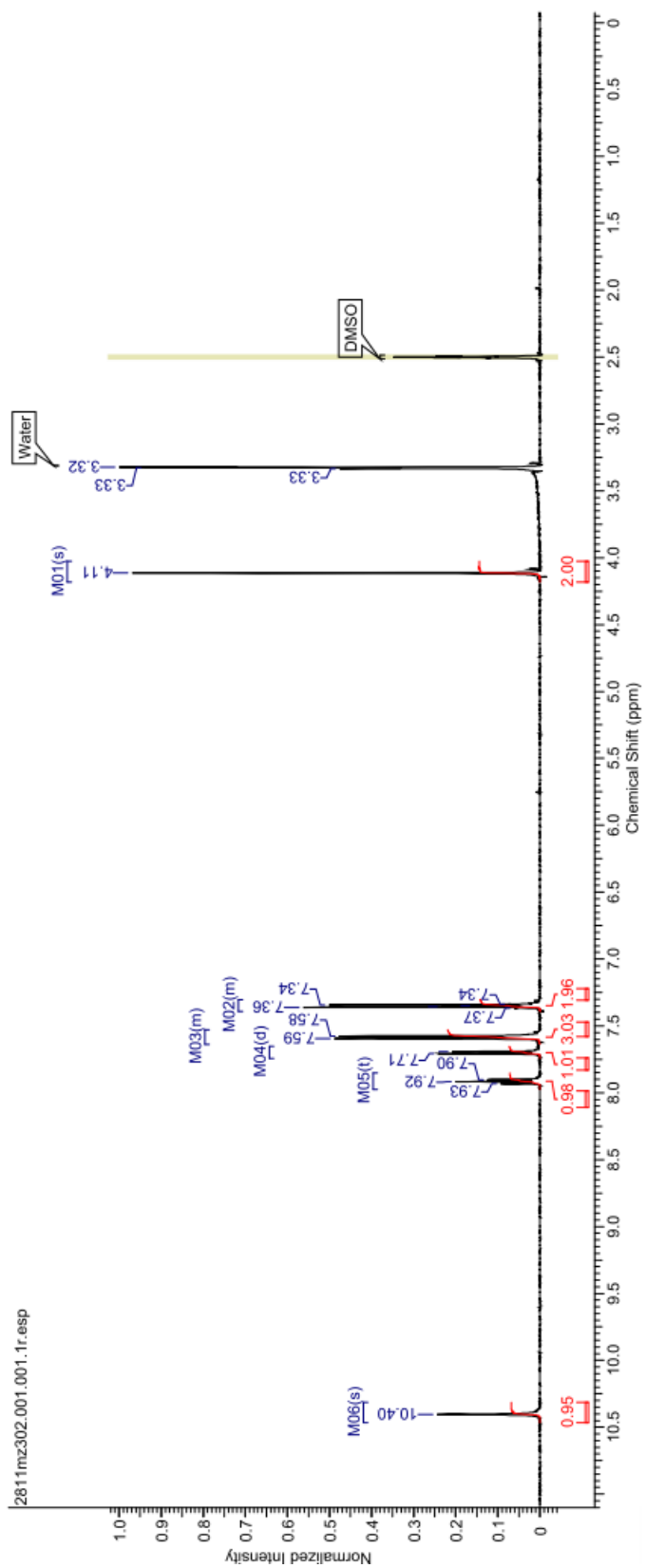
APPENDIX

d. ^1H NMR spectra

Compound 7

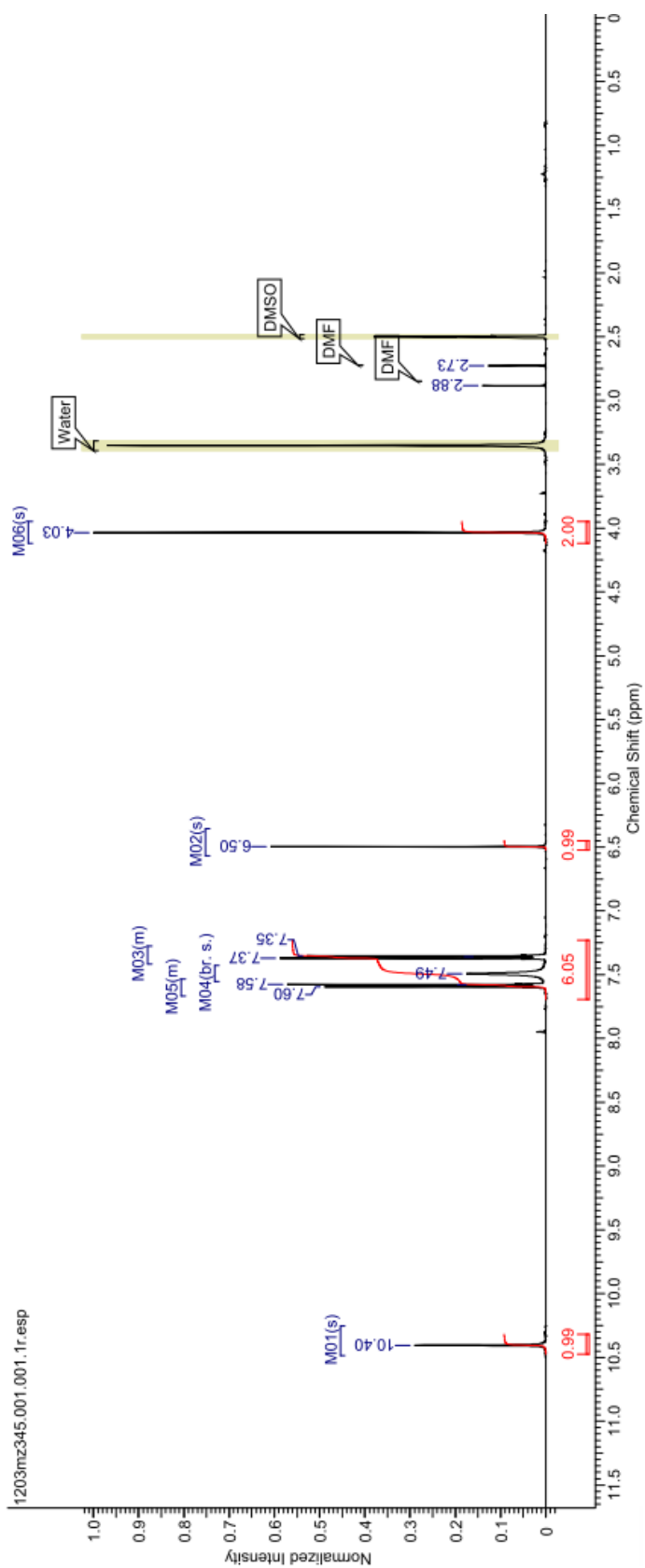


Compound 8

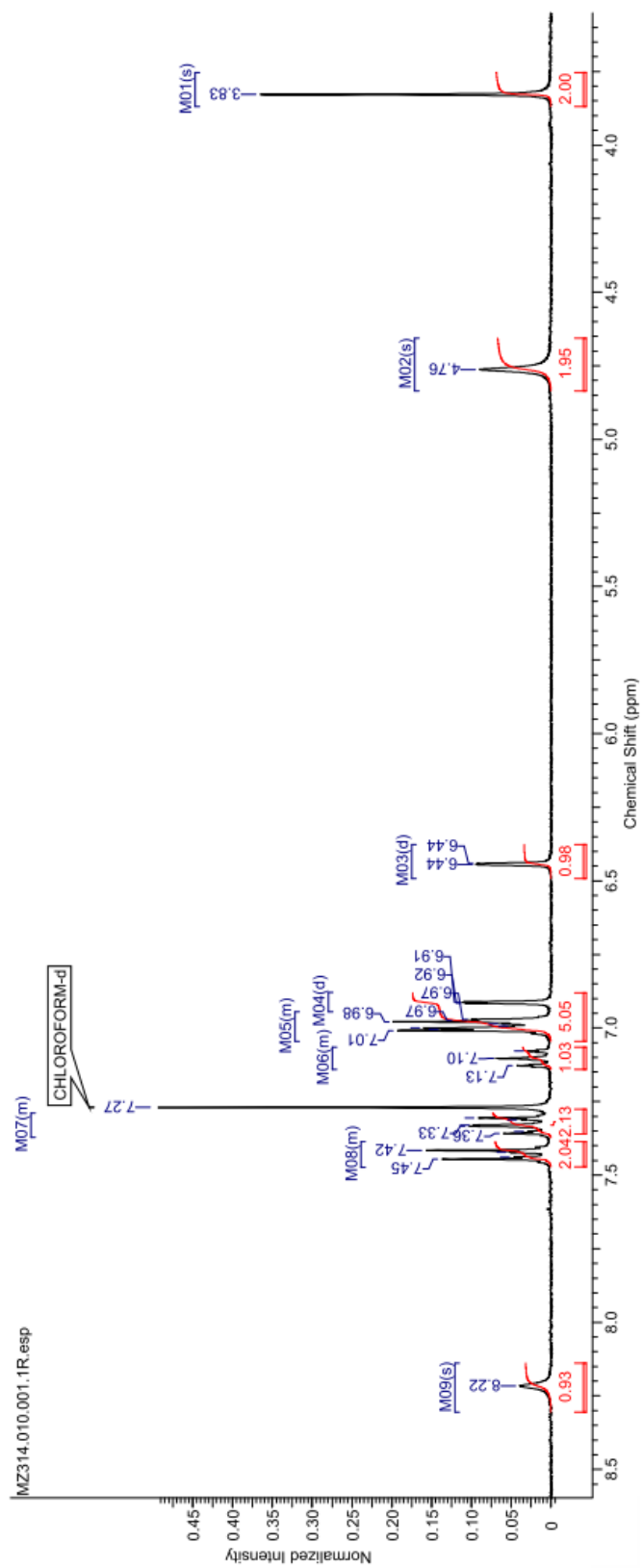


APPENDIX

Compound 9

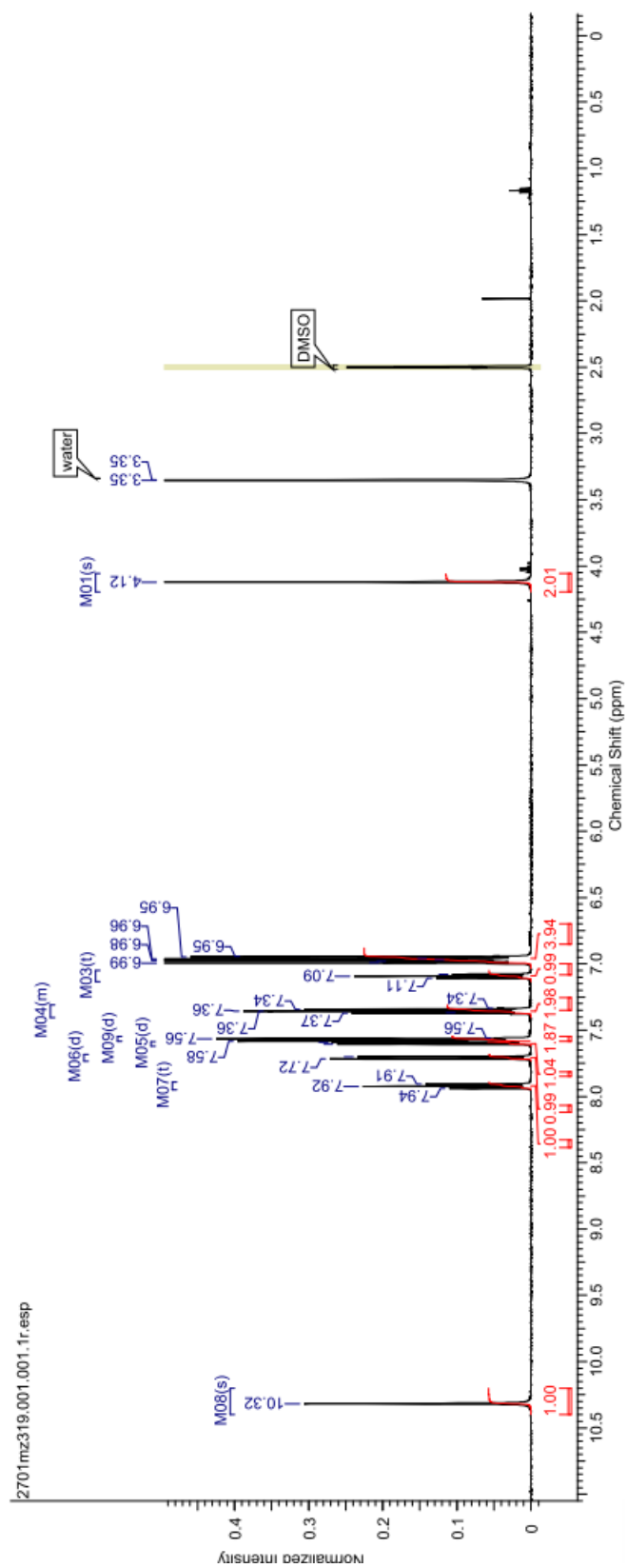


Compound 10

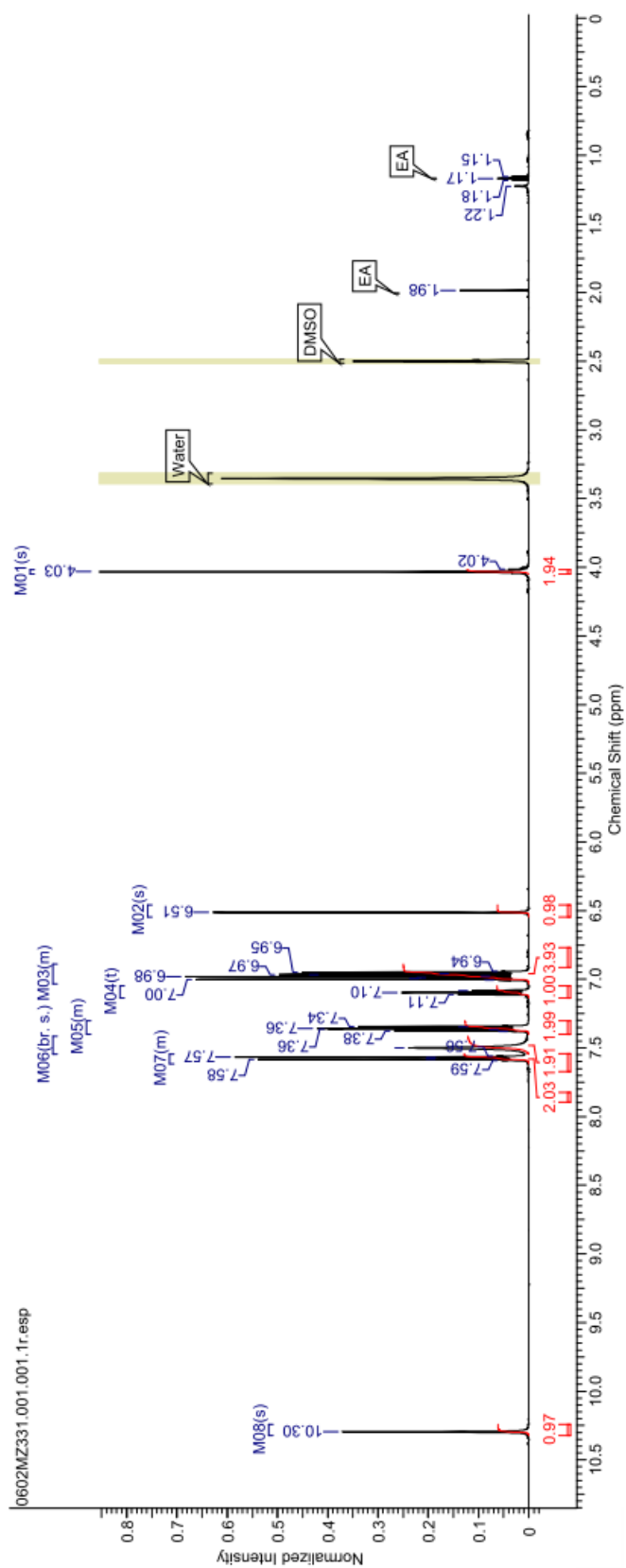


APPENDIX

Compound 11

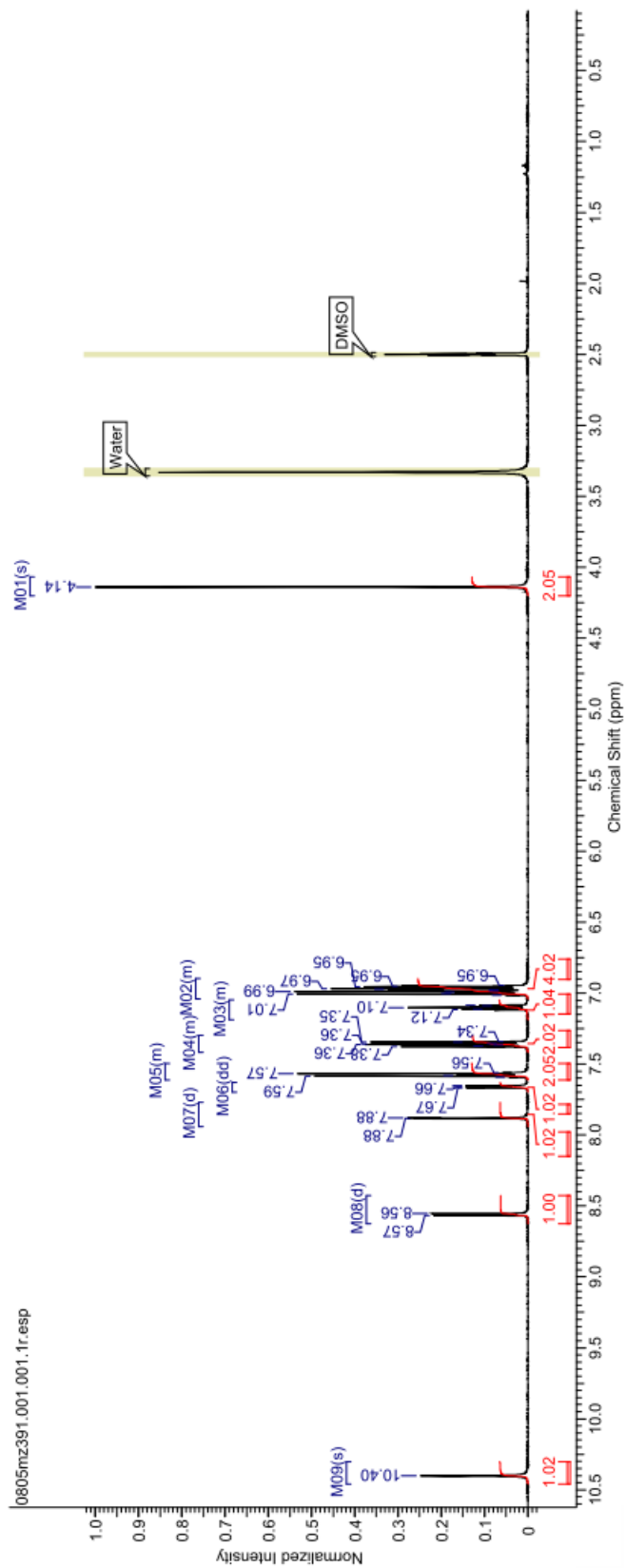


Compound 12



APPENDIX

Compound 13



III. SUPPLEMENTARY REFERENCES

- 1S. Kesarwani, M.; Hazan, R.; He, J.; Que, Y.-A.; Que, Y.; Apidianakis, Y.; Lesic, B.; Xiao, G.; Dekimpe, V.; Milot, S.; Deziel, E.; Lépine, F.; Rahme, L. G. A quorum sensing regulated small volatile molecule reduces acute virulence and promotes chronic infection phenotypes. *PLoS pathogens*. 2011, 7, e1002192.
- 2S. Hauptenthal, J.; Baehr, C.; Zeuzem, S.; Piiper, A. RNase A-like enzymes in serum inhibit the anti-neoplastic activity of siRNA targeting polo-like kinase 1. *Int. J. Cancer*. 2007, 121, 206–210.
- 3S. Thomann, A.; Zapp, J.; Hutter, M.; Empting, M.; Hartmann, R. W. Steering the azido-tetrazole equilibrium of 4-azidopyrimidines via substituent variation - implications for drug design and azide-alkyne cycloadditions. *Org. Biomol. Chem*. 2015, 13, 10620–10630.
- 4S. Mortenson, P.; Murray, C. Assessing the lipophilicity of fragments and early hits. *J. Comput.-Aided Mol. Des*. 2011, 25, 663–667.
- 5S. Shultz, M. D. Setting expectations in molecular optimizations: Strengths and limitations of commonly used composite parameters. *Bioorganic & medicinal chemistry letters*. 2013, 23, 5980–5991.
- 6S. Shaitanov, P. V.; Lukashov S.S.; Turov O.V.; Yarmoluk S.M. Synthesis and structural study of N-substituted-1,7-dithia-4-azaspiro[4.4]nonan-3-one 7,7-dioxides. *Ukr. Bioorg. Acta*. 2007, 2, 56–61.

11.1.3 Chapter 3

Content

I. General experimental information

- a. Tabular NMR data of 5α -pregnan- $3\beta,6\alpha$ -diol-20-one
- b. HPLC chromatograms of radioactively-labeled steroids
- c. HPLC isolation and purification of steroidal compound
- d. HPLC-ESI-ToF-MS – Neurosteroid allopregnanolone metabolism into 5α -pregnan- $3\beta,6\alpha$ -diol-20-one
- e. Structural representation of 5α -pregnan- $3\beta,6\alpha$ -diol-20-one

II. Supplementary References

I. GENERAL EXPERIMENTAL INFORMATION

a. Tabular NMR data of 5 α -pregnan-3 β ,6 α -diol-20-one**Table S1.** NMR data for the steroid (CDCl₃).

#	δ [ppm] ^a		Multiplet structure		Connectivity correlations	
	¹³ C	¹ H	Type ^b	<i>J</i> [Hz]	HMBC	COSY [ppm]
1	37.1	1.05 (H)	m	-	-	1.45; 1.74; 1.85
		1.74 (H ⁺)	m	-	2; 5; 6; 10; 19	1.05; 1.45; 1.85
2	30.9	1.85 (H)	m	-	-	1.05; 1.45; 1.74; 3.59
		1.45 (H ⁺)	m	-	1; 3	1.05; 1.74; 1.85; 3.59
3	71.1	3.59	tt	4.8; 11.1	2; 4	1.25; 1.45; 1.85; 2.22
4	32.1	2.22 (H)	m	-	-	1.04; 1.25; 3.59
		1.25 (H ⁺)	m	-	-	1.04; 2.22; 3.59
5	51.5	1.04	m	-	-	1.25; 2.22; 3.42
6	69.2	3.42	td	4.5; 10.6	4; 5	0.91; 1.04; 2.01
7	41.4	0.91 (H)	m	-	5; 6; 8; 9; 14; 19	1.48; 2.01; 3.42
		2.01 (H ⁺)	m	-	5; 6; 8; 9; 14; 19	0.91; 1.48; 3.42
8	34.1	1.48	m	-	7; 9; 14	0.73; 0.91; 1.22; 2.01
9	53.5	0.73	m	-	5; 7; 8; 10; 11; 14	1:32, 1:48, 1:64
10	36.0 ^c	-	-	-	-	-
11	20.9	1.64 (H)	m	-	9; 12	0.73; 1.32
		1.32 (H ⁺)	m	-	9; 12	0.73; 1.64
12	38.8	1.42 (H)	m	-	11; 13; 17; 18	1.32; 1.64; 2.04
		2.04 (H ⁺)	m	-	8; 9; 11;	1.32; 1.42; 1.64
13	44.0 ^c	-	-	-	-	-
14	56.3	1.22	m	-	8; 15	1.24; 1.48; 1.71
15	24.2	1.71 (H)	m	-	13; 14; 16; 17	1.22; 1.24; 1.68; 2.18
		1.24 (H ⁺)	m	-	14	1.22; 1.68; 1.71; 2.18
16	22.7	1.68 (H)	m	-	13; 14; 15; 17	1.24; 1.71; 2.18; 2.54
		2.18 (H ⁺)	m	-	14; 15	1.24; 1.68; 1.71; 2.54
17	63.6	2.54	t	9.2	12; 13; 16; 18; 20	1.68; 2.18
18	13.4	0.62	s	-	12; 13; 14; 17	-
19	13.4	0.84	s	-	1; 5; 9; 10	-
20	209.4 ^c	-	-	-	-	-
21	31.5	2.14	s	-	17; 20	-

^a Chemical shifts obtained from HSQC. ^b Types of multiplets from ¹H-NMR: “s” = singlet; “t” = triplet; “td” = triplet of doublets; “tt” = triplet of triplet; “m” = multiplet. ^c Chemical shifts of quaternary carbons obtained from HMBC.

APPENDIX

b. HPLC chromatograms of radioactively-labeled steroids

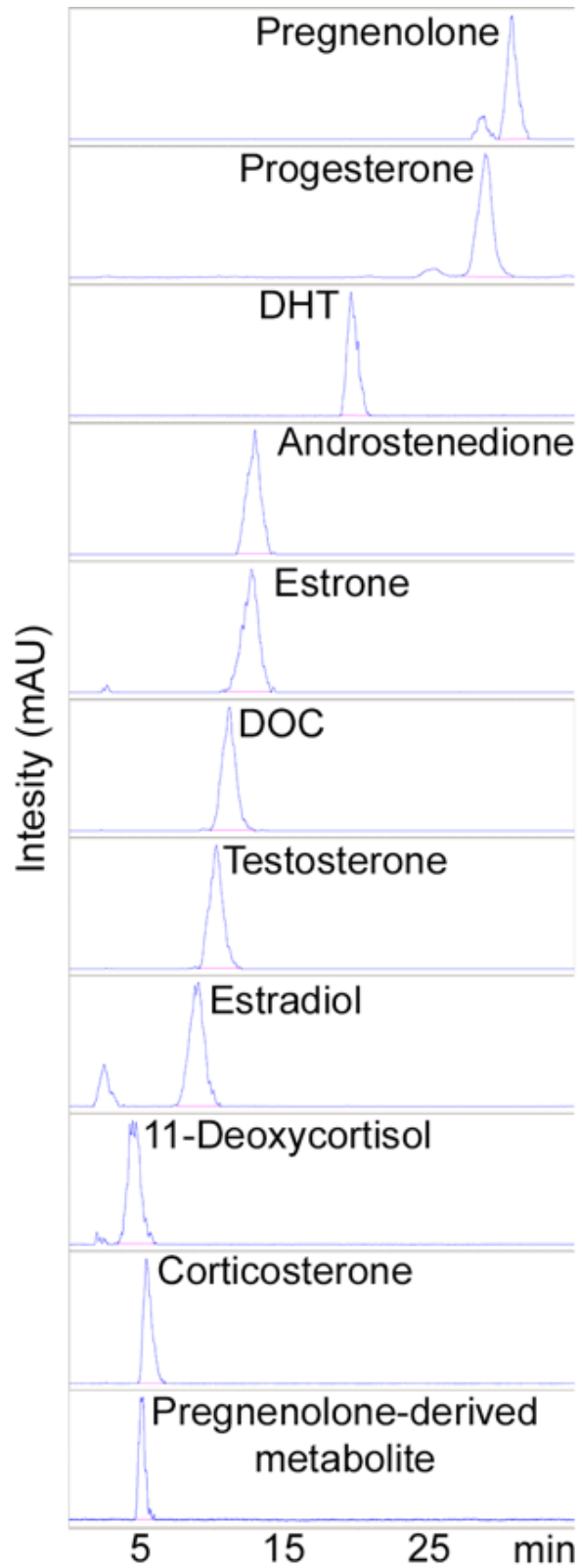


Figure S1. HPLC chromatographic profiles of ^3H -labeled steroid standards and match up to pregnenolone-derived metabolite produced by androgen-responsive cell lines LNCaP, C4.2 and VCaP after 48 h incubation under serum and steroid starvation conditions.

c. HPLC isolation and purification of steroidal compound

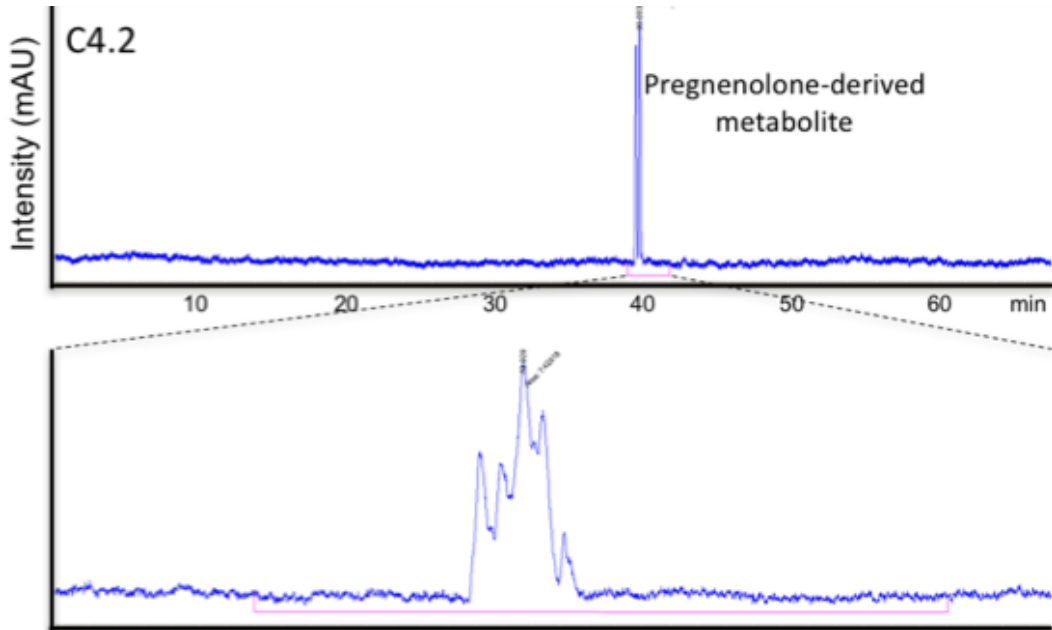


Figure S2. Radio-HPLC chromatogram of [7-³H(N)]-pregnenolone metabolism in C4.2 cultures. Liquid chromatography allowed isolation and further purification of metabolite through sample fractionation (bottom).

APPENDIX

d. HPLC-ESI-ToF-MS – Neurosteroid allopregnanolone metabolism into 5 α -pregnan-3 β ,6 α -diol-20-one

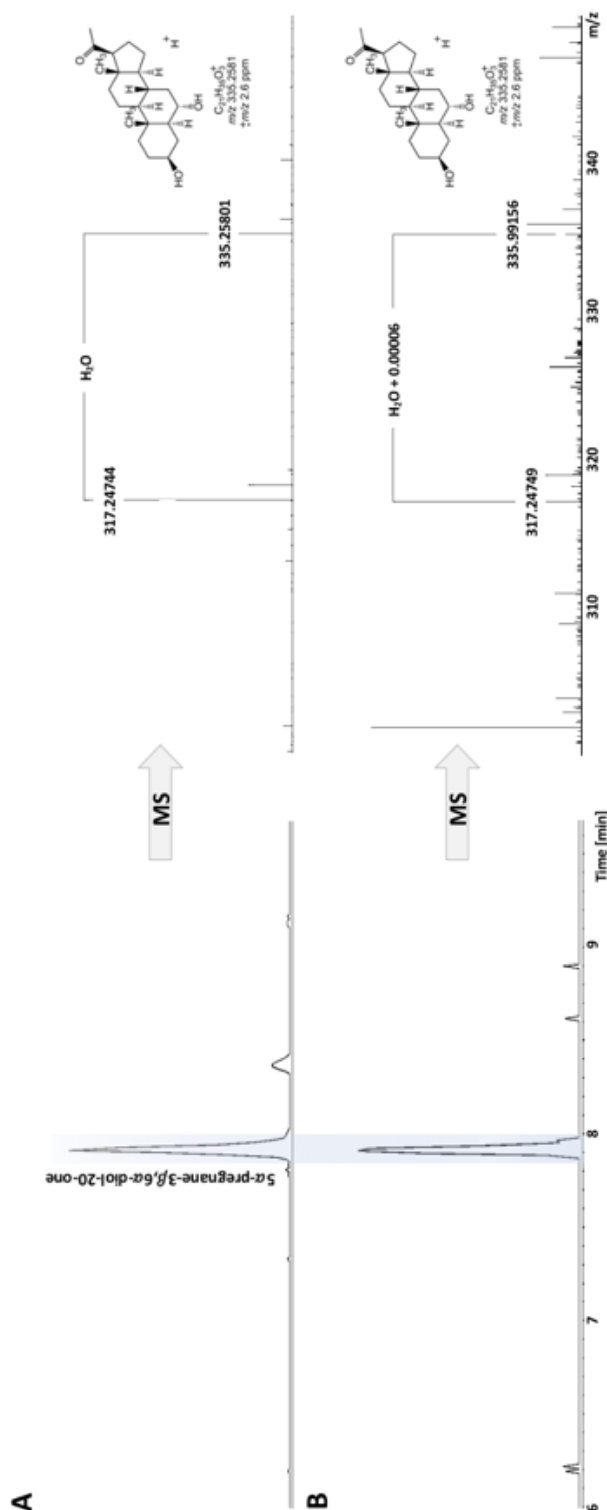


Figure S3. Chromatograms (total ion current, TIC) and mass spectra obtained by HPLC-ESI-ToF-MS analysis of extracted and purified supernatants from C4.2 cell cultures treated with 10 nM pregnenolone (*top*) and 500 nM allopregnanolone (*bottom*). LC graphs (*left*) show the production of 5 α -pregnan-3 β ,6 α -diol-20-one from pregnenolone and allopregnanolone substrates, the latter confirmed by NMR spectra analysis. Inserts show molecular structure of putative metabolic end-product. Chromatograms correspond to the mass spectrometer filter m/z 335.258 \pm 0.002 (protonated molecular ion).

- e. Structural representation of 5α -pregnan- $3\beta,6\alpha$ -diol-20-one

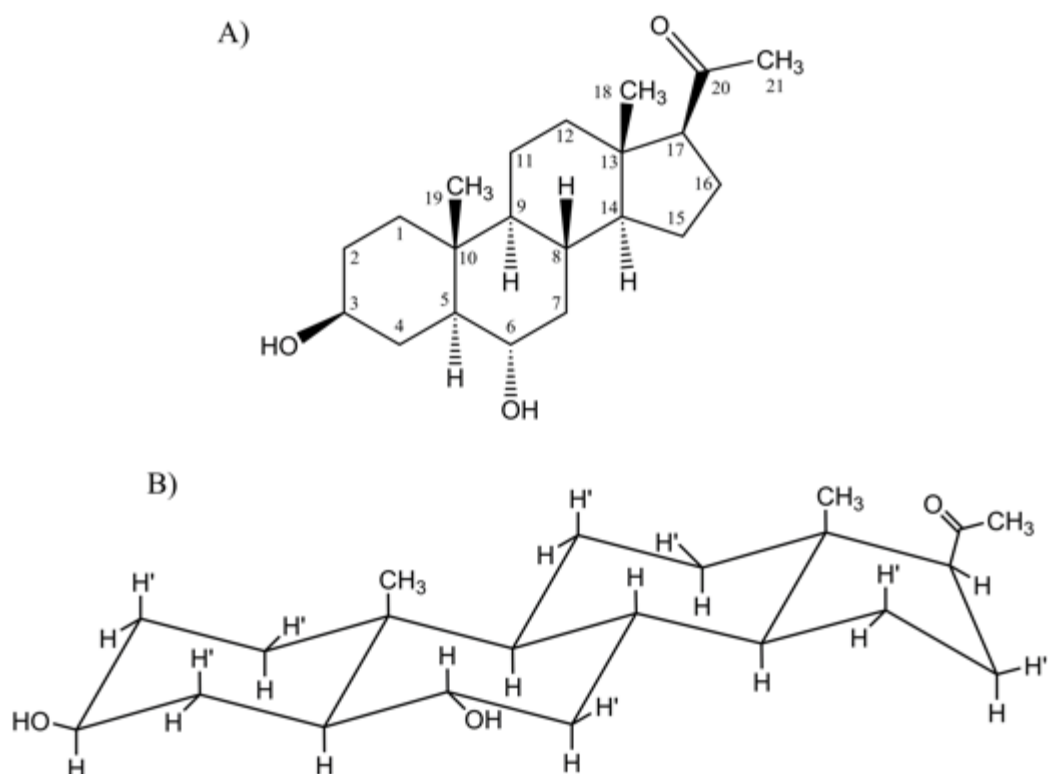


Figure S4. (A) Planar view of the obtained molecule with corresponding carbon enumeration. (B) 3D-view of the metabolic product of early steroid precursors in androgen-responsive cell lines.

II. SUPPLEMENTARY REFERENCES

- 1S. Shingate B B, Hazra B G, Salunke D B, Pore V S, Shirazi F, Deshpande M V. Stereoselective Synthesis and Antimicrobial Activity of Steroidal C-20 Tertiary Alcohols with Thiazole/Pyridine Sidechain. *Eur J Med Chem.* 2011;46:3681–3689.
- 2S. MacNevin C J, Atif F, Sayeed I, Stein D G, Liotta D C. Development and Screening of Water-Soluble Analogues of Progesterone and Allopregnanolone in Models of Brain Injury. *J Med Chem.* 2009; 52; 6012–6023.
- 3S. Pretsch E, Bühlmann P, Badertscher M. Structure Determination of Organic Compounds. Chapter: Tables of Spectral Data. Fourth Ed., Springer-Verlag Berlin Heidelberg. 2009.

11.2 Conference Contributions

POSTER PRESENTATIONS:

Gomes de Mello Martins AG, Haupenthal J, Ohlmann C-H, Thelen P, Stöckle M, Hartmann RW, Unteregger G (2014) The Potentiality of Androgen Synthesis in Prostate Cancer Cell Lines. 6. Symposium – Urologische Forschung der Deutschen Gesellschaft f. Urologie, November 2014, Homburg, Germany

Thomann A, **Gomes de Mello Martins AG**, Brenngel C, Weidel E, Plaza A, Börger C, Empting M, Hartmann RW (2015) Biological Evaluation of a Dual-Target PQS-Quorum Sensing Inhibitor that Hinders Biofilm in *Pseudomonas aeruginosa*. DPhG Jahrestagung, September 2015, Düsseldorf, Germany

Thomann A, **Gomes de Mello Martins AG**, Brenngel C, Empting M, Hartmann RW (2016) Application of Dual Inhibition Concept within Looped Autoregulatory Systems towards Anti-Virulence Agents against *Pseudomonas aeruginosa* Infections. DPhG-Doktorandentagung, March 2016, Aachen, Germany

ORAL PRESENTATIONS:

Gomes de Mello Martins AG, Haupenthal J, Ohlmann C-H, Thelen P, Stöckle M, Hartmann RW, Unteregger G (2015) The Potentiality of Androgen Synthesis in Prostate Cancer Cell Lines. 2. Interdisziplinäres Androgenrezeptor-Meeting, April 2015, Oberding/Notzing, Germany

Thomann A, **Gomes de Mello Martins AG**, Brenngel C, Weidel E, Plaza A, Börger C, Empting M, Hartmann RW (2015) Biological Evaluation of an *In Vivo*-Potent Dual Target PQS-Quorum Sensing Inhibitor that Hinders Biofilm Formation. 4th European Congress on Microbial Biofilms, June 2015, Brno, Czech Republic

Gomes de Mello Martins AG, Allegretta G, Haupenthal J, Eberhard J, van der Zee JA, Unteregger G, Stöckle M, Junker K, Hartmann RW, Ohlmann C-H (2016) The Neurosteroidogenic Potential of Metastatic Prostate Cancer Cell Lines Under Starvation Treatment with Abiraterone. 31st Annual European Association of Urology (EAU), March 2016, Munich, Germany

Thomann A, **Gomes de Mello Martins AG**, Brenngel C, Empting M, Hartmann RW (2016) Application of Dual Inhibition Concept within Looped Autoregulatory Systems toward

Antivirulence Agents against *Pseudomonas aeruginosa* Infections. 6th International HIPS Symposium, June 2016, Saarbrücken, Germany

11.3 Curriculum Vitæ

■ Personal Information

Name: Antonio G. Gomes de Mello Martins
E-Mail: Antonio.Martins@outlook.de
Date/Place of Birth: 08.June 1985, Brasilia/DF - Brazil
Nationality: Brazilian
Marital Status: Married

■ Academic History

02/2014 - to Date **Dr. rer. nat. (Ph.D.)** – Helmholtz Institute for Pharmaceutical Research Saarland & Saarland University, Saarbrücken, Germany. Prof. Dr. Rolf W. Hartmann.

10/2016 - 04/2017 **Visiting Research Fellow** – Harvard Medical School/ Massachusetts General Hospital, Boston, MA, USA. Associate-Prof. Dr. Laurence G. Rahme.

09/2014 – 09/2016 **Master of Business Administration (MBA)** – European Institute for Advanced Behavioural Management, Saarland University, Saarbrücken, Germany. Dissertation: 19/20. Prof. Dr. Andrea Gröppel-Klein.

09/2011 - 01/2014 **Master of Science (M.Sc.)** – Bonn-Rhein-Sieg University of Applied Sciences, Rheinbach, Germany. Dissertation: 1,0. Prof. Dr. med. Oliver Brüstle, Dr. Nadina Stadler.

08/2003 - 11/2007 **Licentia docendi (Lic.)** – University of Brasilia, Brazil (teaching license).

02/2003 - 06/2007 **Bachelor in Science (B.Sc.)** – University of Brasilia, Brasilia, Brazil. Dissertation: 1,0. Prof. Dr. Marlinda Lobo de Souza.

■ Work Experience

02/2014 – to Date **Research Associate** – Helmholtz Centre for Infection Research - Institute for Pharmaceutical Research Saarland. Saarbrücken, Germany

04/2013 – 12/2013 **Research Associate** – Life & Brain GmbH. Bonn, Germany

01/2012 – 10/2012 **Research Assistant** – Bonn-Rhein-Sieg University of Applied Sciences. Departments of Natural and Computer Sciences. Sankt Augustin, Germany

01/2005 – 07/2006 **Laboratory Assistant** – Brazilian Enterprise on Agriculture and Cattle Breeding Research (EMBRAPA). Brasilia, Brazil

■ Awards, Scholarships and Certificates

- 04/2017 **Villa Lessing Europa Prize** – MBA Thesis on the economic strengthening and competition in the EU.
- 09/2016 **DAAD Travel Scholarship** – Research visit at the Harvard Medical School through the GradUS Global initiative of the Saarland University.
- 11/2014 – 11/2016 **Student Scholarship** – StudienStiftungSaar and Deutschlandstipendium.
- 10/2013 **DAAD Outstanding Achievement of a Foreign Student Award.**
- 09/2012 – 03/2013 **Student Scholarship** – Bonn-Rhein-Sieg University of Applied Sciences Studienstiftung.
- 08/2006 – 08/2007 **Student Scholarship** – National Counsel of Technological and Scientific Development (CNPq).
- 12/2004 **Student Talent Award:** *Construction of a Recombinant Baculovirus to Express the Alpha-Amylase BIII Inhibitor.*
EMBRAPA's IX Biotechnology Conference of Young Talents

■ Languages

- Portuguese: Mother tongue
- English: Full professional proficiency
- Spanish
- German

12 ACKNOWLEDGMENTS

First and foremost, I would like to thank Prof. Dr. Rolf W. Hartmann for giving me the unique opportunity of being part of such a prestigious team at the Helmholtz Institute. I will be forever appreciative of his excellent mentoring and the continuous example of an admirable scientist and a kind and humane supervisor.

I am also grateful to my second supervisor, Prof. Dr. Claus-Michael Lehr, for the collegial exchange of scientific advice and support throughout the performance of my projects at the Institute.

I would like to express my deepest appreciation to Dr. Jörg Hauptenthal and Dr. Martin Empting for their immeasurable efforts and consistent help not only on supervising the present work, but also on providing the structure that conveys an exciting academic atmosphere in regard to research and comradeship in the DDOP department.

Certainly, I want to thank all current and former members and colleagues of the Departments of Drug Design and Optimization and Drug Delivery that I had the privilege of working with in an outstanding environment. Particularly, Jeannine Jung and Simone Amann for their untiring efforts in keeping their outstanding work inside and outside the laboratories in a friendly and kind manner. Especially, I thank Ahmed – the Bear – Kamal and Giuseppe – Al Forno – Allegretta with whom I grew as a scientist and a human being. You helped me become who I am today both professionally and personally. You guys rock.

Last but above all, I thank my wife, my mother, and godmother for their unique, unconditional, and uncontested support in a number of ways throughout my studies. You give me the meaning and motivation without which this work would have never been possible.